Performance Issues in Hybrid Fiber Radio Communication Systems due to Nonlinear Distortion Effects in Laser Transmitters

by

Frank Smyth

B Eng , MIEEE

A THESIS SUBMITTED FOR THE DEGREE OF

Master of Engineering

In the School Of Electronic Engineering,

Dublin City University

Research Supervisor

Dr Liam Barry

August 2003

Approval

Name: Frank Smyth

Degree: Master of Engineering

Title of Thesis: Performance Issues in Hybrid Fiber Radio Communication Systems due to Nonlinear Distortion Effects in Laser Transmitters

Examining Committee: Prof Tom Brazil
Dr Pascal Landais

Declaration

I hereby certify that this material, which I now submit for assessment on the programme of study leading to the award of Master of Engineering is entirely my own work and has not been taken from the work of others save an to the extent that such work has been cited and acknowledged within the text of my work.

ID No.: 97633011

Signed: Frank Smyth

Date: 10/1/05

To Mam, Dad and Nic,

Thank you

Acknowledgements

There are two people, without whom this work would never have gotten off the ground The first is my research supervisor, Dr Liam Barry I would like to thank him for his initial faith in me and then for his constant backing and guidance throughout the course of the work The second person, my friend and colleague, Dr Prince Anandarjah deserves a special mention From my very first day in the lab he has been there to offer his assistance and advice It has been much needed and much appreciated

Special thanks must be given to Dr Pascal Landais for his help with the simulation, the maths and the derivations I found this part of the work particularly challenging and his help was invaluable

Some other members of the lab and the school also deserve huge credit Ola Kaszubowska, Paul Maguire, Brendan Kennedy, Damien O'Rourke, Antonia Dantcha, Aisling Clarke and Eoin Kennedy Not only did they help me with my work whenever possible, they also made the lab a pleasant and enjoyable place to work

I would like to thank my girlfriend, Nicola As any research engineer knows, there are times when the work goes well, and times when it doesn't go at all Nic has been there for me through it all and given me constant support throughout

Finally, I would like to thank my parents for their encouragement, throughout the course of this work, and always They instilled in me from an early age, the importance of a good education At this stage, thanks to them, I have one

Abstract

With the increasing demand for broadband services, it is expected that hybrid fiber radio systems may be employed to provide high capacity access networks for both mobile and fixed users In these systems, the radio frequency data signals are modulated onto an optical carrier at a mobile switching centre and then sent over fiber to a number of base stations, before being transmitted over air to the users A possible method of generating the optical radio frequency data signals for distribution over fiber is to directly modulate the electrical signal onto an optical carrier using a laser diode The major problem with this technique is that nonlinearities in electrical-to-optical conversion may seriously degrade the system performance

In this work we initially examined the distribution of a wideband code division multiple access signal (centered around 6 GHz) through an optically fed microwave system Our results show that the adjacent channel leakage ratio is degraded from –52 to –32 dBc after passing through the optical system We then examined the technique of externally injecting light into the directly modulated laser, to extend the bandwidth of the laser diode and hence, increase it's linear region to beyond the frequency of interest With this technique an improvement of over 10 dB in the adjacent channel leakage ratio of the signal was achieved We subsequently went on to examine the distribution of a 5-channel radio frequency signal (each channel carrying 10 Mbit/s) through a hybrid fiber system As in the previous work, we examined how external light injection into the directly modulated laser could be used to improve system performance, and our results show an improvement of up to 5 dB

Finally a model was designed using Matlab, which simulated the 5-channel system mentioned above It used the laser rate equations to mimic the nonlinear effects of the laser diode Good correlation was observed between experimental and simulated results

Table Of Contents

Table Of Tables

Table Of Figures

List of Acronyms

1G	First Generation
2G	Second Generation
3G	Third Generation
4G	Fourth Generation
A/D	Analogue to Digital
ACI	Adjacent Channel Interference
ACLR	Adjacent Channel Leakage Ratio
AM	Amplitude Modulation
AMPS	Advanced Mobile Phone Service
APD	Avalanche Photodiode
ASK	Amplitude Shift Keying
AT&T	American Telephone and Telegraph
BASK	Binary Amplitude Shift Keying
BER	Bit Error Rate
BERT	Bit Error Rate Tester
BPSK	Binary Phase Shift Keyed
BRZ	Bipolar Return to Zero
BS	Base Station
BSC	Base Station Controller
BTS	Base Transceiver Stations
CATV	Cable Television
CCI	Co Channel Interference
CDMA	Code Division Multiple Access
CID	Caller Identification
CLEO	Conference on Lasers and Electro Optics
CN	Core Network
CW	Continuous Wave
DCF	Dispersion Compensated Fiber
DFB	Distributed Feed Back
DH	Double Heterostructure
DSF	Dispersion Shifted Fiber
EAM	Electro Absorption Modulator

ECL	External Cavity Laser
EDA	Electronic Design Automation
EDFA	Erbium Doped Fiber Amplifier
EDGE	Enhanced Data rates for GSM Evolution
EIR	Equipment Identity Register
EMI	Electromagnetic Interference
ESN	Electronic Serial Number
FCC	Federal Communication Commission
FDD	Frequency Division Duplex
FDMA	Frequency Division Multiple Access
FM	Frequency Modulation
FP	Fabry Perot
FSK	Frequency Shift Keying
FWM	Four Wave Mixing
GMSK	Gaussian Minimum Shift Keying
GPRS	General Packet Radio Service
GSM	Global System for Mobile-Communications
HCMTS	High Capacity Mobile Telephone System
HFR	Hybrid Fiber Radio
HLR	Home Location Register
ID	Identification
IEEE	Institute of Electrical and Electronics Engineers
IF	Intermediate Frequency
IM	Intensity Modulation
IMD	Inter Modulation Distortion
IP	Internet Protocol
IR	Infrared
IS-95	Interim Standard 95
ISI	Inter-Symbol Interference
LAN	Local Area Networks
LASER	Light Amplification by Stimulated Emission of Radiation
LED	Light Emitting Diodes
MASER	Microwave Amplification by Stimulated Emission of Radiation

ME	Mobile Equipment
MIN	Mobile Identification Number
MMF	Multi-Mode Fiber
MS	Mobile Station
MSC	Mobile Switching Centre
NAMTS	Nippon Advanced Mobile Telephone Service
NEL	NTT Electronics
NRZ	Non Return to Zero
MT	Mobile Termination
MZM	Mach Zehnder Modulator
NTT	Nippon Telegraph and Telephone Corporation
OOK	On Off Keying
PC	Personal Computer
PCM	Pulse Code Modulation
PI	Power vs Current
PIN	P-type, Intrinsic, N-Type
PSK	Phase Shift Keying
PSTN	Public Switched Telephone Network
QAM	Quadrature Amplitude Modulation
QPSK	Quaternary Phase Shift Keying
R&D	Research and Development
RAF	Remote Antenna Feeding
RF	Radio Frequency
RNC	Radio Network Controller
RNS	Radio Network Subsystem
RZ	Return to Zero
SCM	Sub-Carrier Multiplexing
SID	System Identification
SMSR	Side Mode Suppression Ratio
SNR	Signal to Noise Ratio
SPM	Self Phase Modulation
SMF	Single Mode Fiber
SSMF	Standard Single Mode Fiber

TACS	Total Access Communication System
TDD	Time Division Duplex
TDM	Time Division Multiplexing
TDMA	Time Division Multiple Access
TE	Terminal Equipment
UE	User Equipment
UMTS	Universal Mobile Telecommunications System
USIM	User Services Identity Module
UTRAN	UMTS Terrestrial Radio Access Network
VLR	Visitor Location Register
WAN	Wide Area Networks
WCDMA	Wideband Code Division Multiple Access
WDM	Wavelength Division Multiplexing
WLAN	Wireless Local Area Networks
WWII	World War Two
XPM	Cross Phase Modulation

Thesis Overview

This thesis is divided into six chapters and it's layout is as follows

Chapter 1 gives an introduction to the two types of communication system that we are concerned with, namely optical and radio It gives a brief history of each and describes their advantages and disadvantages To finish it leads into the topic of chapter two – hybrid fiber radio systems

Chapter 2 begins with the mobile station and describes how communication in a hybrid fiber radio system takes place The components at the mobile station, base station and mobile switching centre are described Finally some of the network architectures and topologies available for hybrid fiber radio are detailed

Chapter 3 discusses in some detail, the use of laser diodes in hybrid fiber radio systems The nonlinearity problems associated with these devices are discussed along with what we see as a possible solution to these problems – the use of external light injection This chapter also discusses the model of the laser diode which was designed, based on the laser rate equations

Chapter 4 describes one set of experiments that was carried out within the confines of this work It involved transmitting a WCDMA signal over fiber, and improving the performance by linearising the laser diode This chapter also describes some more work which was done on the simulation A two tone radio over fiber system is set up and external injection is incorporated into it

Chapter 5 describes the second set of experiments These experiments are based on the transmission of a number of subcarrier multiplexed data channels over optical fiber Again external injection is used to improve performance The model is also expanded to allow data to be transmitted rather than simple tones only

Chapter 6 gives a brief summary of the thesis and presents some conclusions Further work which could be performed is also discussed

Chapter 1 – Introduction

This chapter introduces communication in general before going into some detail about the more specific topics of optical communication and mobile communication Finally the reader is given a brief introduction to the primary concern of this thesis – Hybrid Fiber Radio (HFR)

1.1 – Communication

Communication is the transmission of information from one point to another Every communication system follows these six steps

1 Generation of the signal
2 Description of that signal to a measure of precision i e conversion to symbols
3 Encoding of the symbols into a form suitable for transmission
4 The actual transmission across the channel
5 The decoding and reproduction of the symbols
6 The recreation of the original message

Any communication system consists of a transmitter, a channel and a receiver The transmitter is at one point, the receiver at another and the channel is the physical medium connecting them Due to channel imperfections you get distortion of the signal and you also get interference from other signals Therefore the received signal is a corrupted version of the transmitted signal [1]

The following sections describe two common communication systems in use today and a third system, a hybrid of the two, which is beginning to come to the fore

1.2 – Optical Communication

Light has been used as a communication source since the early stages of humanity when fire was used as a warning or distress signal It has been used more recently for sending messages in Morse code Such methods are obviously extremely limited in their maximum data transmission rate Today, light is being used to transmit information at huge data rates and over thousands of kilometres in optical fiber communication networks

1 2 1 – A Brief History of Optical Communication

The two main developments which led to the optical communication systems with which we are familiar today were the laser and the optical fiber waveguide

In 1954 Charles Townes created a device that amplified microwaves He called this device a MASER (an acronym of Microwave Amplification by Stimulated Emission of Radiation) Six years later, an American Physicist Theodore Maiman further developed the Maser to amplify light This device became known as a LASER (for Light Amplification by Stimulated Emission of Radiation) It had a ruby rod as the active medium and a spiral lamp as the power source [2] This was the first coherent source of electromagnetic radiation and it operated at a frequency of 432 THz The development of the semiconductor laser began in 1962 Initial semiconductor lasers only had lifetimes of a few hours, required huge drive currents and could not be operated continuously at room temperature The development of heterojunction and double heterojunction structures around 1969 greatly improved the performance of the injection laser and lowered the currents necessary to drive them [3]

The development of optical waveguides began in 1984 when John Tydnall used total internal reflection to guide a beam of light through a jet of water No further significant work was done using water as a waveguide but in 1956 Kapany built the first optical fiber structure It consisted of a rod of glass with refractive index n_1 coated by another layer of glass with refractive index n_2, where $n_2 < n_1$ and again total internal reflection caused it to guide a beam of light In 1966 Kao and Hockman proposed that a very thin glass fiber could be used in the same way to transmit light Their initial prototypes suffered huge losses (~1000 dB/km) which obviously made them unsuitable for any sort of communication but it marked the beginning of the development of optical fiber [4] and by 1976 the loss in fiber had been reduced to 0 5 dB/km

These two developments allowed the first lightwave communication systems to be put into place in the late 70's Factors such as costs, laser lifetime, attenuation and coupling capacity, however, meant that it would be a long time before these systems could compete commercially with existing copper wire networks

The very first optical systems operated at a wavelength of 850 nm due the fact that source materials used at the time emitted at this wavelength [5] The discovery of a dispersion minimum around 1300 nm caused the industry to begin to develop lasers for use at this wavelength At the time, lasers were operating at relatively low speeds such that dispersion was not actually a very serious factor Loss, on the other hand, was very important, and the desire for longer transmission distances caused the industry to move to the current standard operating wavelength of 1550 nm due to an absorption minimum at this point and to suffer the higher dispersion at this wavelength

The next major development was Dispersion Shifted Fibers (DSFs) By adjusting the core cladding refractive indices and by reducing the core diameter [6], it was found that the dispersion minimum could be tuned over a wide range of wavelengths This allowed the industry the best of both worlds, minimum dispersion and minimum attenuation

Once optical communication systems were in place the main problem was then to find ways to put more and more data onto each fiber, rather than having to lay extra fibers The technique of Wavelength Division Multiplexing (WDM) was one solution to this problem It was known that many wavelength channels could be combined and put onto one fiber thereby significantly increasing data rates The problem was that in optical systems at the time, amplification was still done in the electrical domain This meant that each time you needed to amplify a WDM system you had to demultiplex and amplify each channel individually, before re-multiplexing them and retransmitting them

The development of optical amplifiers changed this and really allowed WDM to take off These amplifiers use optical fiber doped with erbium to boost the power of the signal in the optical domain, allowing all wavelength channels to be amplified simultaneously By adding amplifiers at intervals along the fiber, the need to constantly regenerate the signal is reduced This development provided network operators with increased bandwidth and yet needed less power and maintenance [6]

All of the developments which have been mentioned are used in present optical communication systems The current state of the art systems have hundreds of channels each carrying 40Gbit/s giving total data rates of multi-terabits per second

1.2 2 – Advantages of Optical Systems over Electrical

Enormous potential bandwidth – Coaxial cable has a maximum bandwidth of less than 1 GHz Because the optical carrier frequency is in the range of 25,000 GHz, optical fiber has a far greater potential bandwidth

Small Size and weight – Optical fibers are often no larger in diameter than a human hair and this small size and light weight means less duct congestion in cities and also makes them very useful in aircraft and satellites

Immunity to Electromagnetic Interference (EMI) and crosstalk – Optical fibers are free from EMI They also exhibit no crosstalk when many fibers are used together in one cable

Signal Security – To extract any information from optical fiber it is necessary to break the link and draw light from it This break would be easily detectable

Low Loss – Optical fiber has much lower loss than metallic cabling This is a huge advantage in long haul systems as it reduces the number of repeaters and amplifiers and hence reduces the cost

Potential Low Cost – The raw material of optical fiber is sand which is an extremely plentiful resource when compared to copper for example Although the process of manufacturing ultra pure glass is more complicated and therefore more expensive than the manufacture of copper cable, as optical fiber has become more and more prevalent costs have come down and they will continue to fall [6, 7]

1.2.3 – The Optical Communication System

Like any communication system, an optical communication system has three main parts a transmitter, a channel, and a receiver The transmitter usually consists of a semiconductor laser or LED, modulated by an electrical information source The modulated light from the source is coupled into an optical fiber channel through which it is transmitted It is then detected at the receiver, which consists of a photodetector, and a decision device A generalised optical communication systems is shown in Figure 1 1

Usually the information is converted back to electrical because most signal processing is done in the electrical domain Recently however, huge advances have been made in the field of optical signal processing, and all optical networks will be realised in the near future [8]

The optical carrier can be modulated with either a digital or an analogue signal In analogue modulation the light varies in a continuous manner whereas with digital modulation, pulses are used to form a discrete signal Analogue modulation is simpler but needs a much better signal to noise ratio, and as we will see later can be seriously affected by nonlinearity especially at high modulation frequencies [6]

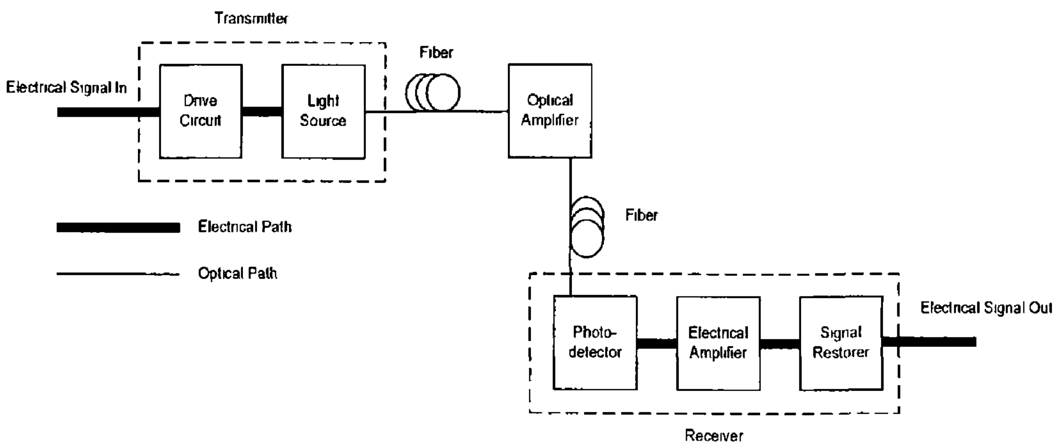

Figure 1 1 – Basic optical communication system

1.3 – Radio Frequency Communication

1 3 1 – A brief history of Radio Communication

Heinrich Hertz first proved the existence of electromagnetic waves in experiments conducted from 1886 to 1888 He recorded their most important characteristics and was the first to broadcast and receive radio waves In 1897 radio transmission over an 18 mile path to a tugboat based on Hertz's work was demonstrated by Marchese Guglielmo Marconi [9] These developments marked the beginning of radio communication

The first experiments in land mobile communication took place around 1921 These were broadcasts made to police cars in Detroit, Michigan in the USA Initial communications were unreliable, unidirectional and the equipment required was costly and bulky They operated in the 2 MHz Radio Frequency (RF) band The first 2-way system was used in Bayonne, New Jersey, USA in the early 1930s The utility of such systems were recognised immediately and demand grew rapidly [10] Up to this time all mobile radio systems used Amplitude Modulation (AM) By 1940, due to propagation problems experienced by AM systems, nearly all police systems in the United States had converted to Frequency Modulation (FM) During the Second World War (WWII) hundreds of thousands of mobile radio systems were built for military use The end of WWII was a huge stimulus to mobile communication and it saw the first mobile radio systems enter the commercial arena Demand was strong and in 1949 the FCC officially recognised mobile radio as a new class of service By 1963 there were 1 4 million mobile radio users In these early days demand grew so rapidly that probability of having a call blocked rose to as high as 65% or more It became obvious that the usefulness of mobile communication was diminishing due to this difficulty of finding an available channel The original FM mobile telephone channels had a channel bandwidth of 120 kHz By the early 1960s that bandwidth had been reduced to 30 kHz Also around this time, multiplexing had been developed Together these steps greatly increased system capacity and spectral efficiency [11]

The cellular concept was initially proposed in the late 1940s This concept involved replacing the current model of a high powered transmitted to cover a wide area with a number of lower powered transmitters each designed to serve only a smaller area, a "cell" The concept of frequency reuse is illustrated in Figure 1 2 Provided there is a certain distance between cells to make interference negligible then the same frequencies can be reused over and over again Another feature of the cellular concept is cell splitting When a cell has reached it's capacity it can be split into a number of smaller cells with even lower powered transmitters Hence the reuse pattern can be repeated on a smaller scale Another important feature of cellular communication is the use of hand-off control Obviously because the users are mobile there is a strong possibility that a call may not be started and completed inside the boundaries of one cell The cellular system has automatic switching capabilities that know when the user is moving from one cell into another and can switch to the new cell without interrupting the call [10, 12]

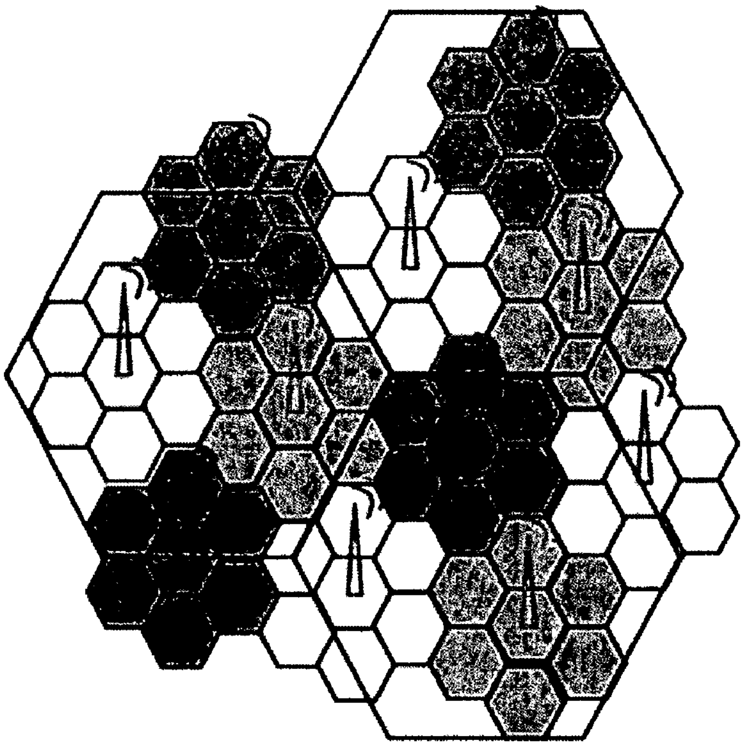

Figure 1 2 – Frequency reuse and cell size reduction

In 1971 American Telephone and Telegraph (AT&T) Bell Laboratories submitted a proposal for a new analogue cellular FM radio system known as the High Capacity Mobile Telephone System (HCMTS) to the FCC It was accepted and allocated 40 MHz of spectrum in the 850 MHz band It was implemented as a developmental system in 1978 and a commercial system in 1983 known as the Advanced Mobile Phone Service (AMPS)

Europe and Japan were also developing similar systems in parallel Japan's was called Nippon Advanced Mobile Telephone Service (NAMTS) and Europe's was called the Total Access Communication System (TACS) These systems were the standard in the 1980s and 1990s Such analogue cellular systems were the so called First Generation (1G) mobile systems These systems all had common features but they were very far from a worldwide standard [13, 14]

1.3.2 – Present and future Wireless Communication

Although the cellular concept promised almost unlimited capacity due to frequency reuse, practical limits were reached in the 1990's with the huge increase in popularity of mobile radio systems Cells were becoming smaller and smaller and hence more and more base stations were needed This meant higher costs and more difficulty in finding locations for base stations These practical limits meant that cellular systems were capped below targets and below market demand Also, incompatible standards worldwide meant that a person could not use the same phone in different countries These things motivated the development of the Second Generation (2G) of mobile communication systems – higher capacity and more compatibility [10]

The transition from analogue to digital was the choice that defined 2G mobile communication Digital systems have several advantages over their analogue counterparts They

- allow greater use of the available spectrum,
- are more robust to interference, they will operate correctly under conditions of much higher co-channel and adjacent channel interference
- exhibit improved efficiency for hand off control
- allow the inclusion of new services such as encryption, data services, authentication

Development of Third Generation (3G) Mobile systems began around 1995 Based on Global System for Mobile-Communications (GSM), Universal Mobile Telecommunications System (UMTS) is one such system It is broadband transmission of text, digital voice, video, and multimedia at data rates up to and possibly above 2 Mbit/s This is a huge leap from the maximum 22 8kbit/s of 2G systems like GSM Another advantage of 3G systems is that they are designed to be fully compatible with 2 & 2 5G[1] systems [15, 16] In 1997 Wideband Code Division Multiple Access (WCDMA) was considered as one of the 3G technologies for UMTS during a workshop conference held in Korea and in 1998 the first call using a Nokia WCDMA terminal in DoCoMo's trial network was completed at Nokia's Research and Development (R&D) unit near Tokyo in Japan Three years later on October 1, 2001 Nippon Telegraph and Telephone Corporation (NTT) DoCoMo launched the first commercial WCDMA 3G mobile network [17]

[1] such as General Packet Radio Service (GPRS) and Enhanced Data Rates for GSM Evolution (EDGE)

1 3.3 – The Cellular Communication System

A cellular telephone system provides a wireless connection to the Public Switched Telephone Network (PSTN) for any user inside the radio range of the system The advantages of such a system have been discussed earlier A cellular system is illustrated in Figure 1 3 It consists of Mobile Stations (MSs), Base Stations (BSs) and a Mobile Switching Centre (MSC)

Each MS communicates with the BS of the cell that it is located in and during a call may be handed off to another BS The MS contains a transmitter and receiver as well as signal processing circuitry and may be vehicle mounted or in a hand held unit BSs can consist of several transmitters and receivers and generally contain a tower which holds many antennae They handle many simultaneous calls and connect to the MSC either by microwave or wired link The MSC connects the entire cellular system to the PSTN and generally coordinates the activities of all of the BSs

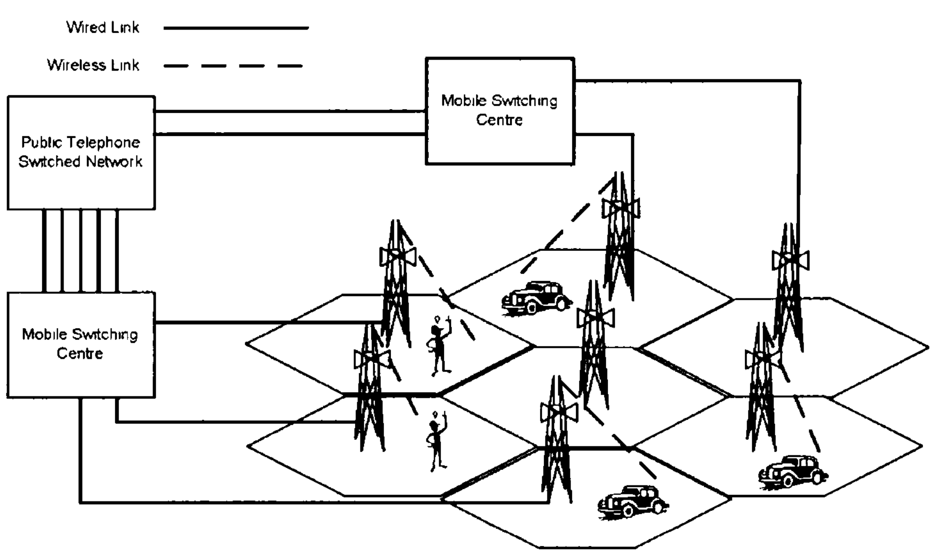

Figure 1 3 – The cellular communication system

While the cellular system illustrated in Figure 1 3 shows an outdoor system employing macrocells[1], the same idea applies (albeit on a much smaller scale) to in-building applications Buildings which traditionally suffered from poor coverage such as office blocks, airport terminals, and shopping centres make extensive use of picocells[2] which transmit low power signals to indoor users

---

[1] Macrocells typically have a radius of 1 – 30 km

[2] Picocells typically have a radius of up to 100 m

1 3 4 – Wireless Networking

Mobile telephony is not the only use of RF technologies Wireless technology is now being used extensively for computer networking both in Local Area Networks (LANs) and Wide Area Networks (WANs) Wireless Local Area Networks (WLANs) offer a flexible alternative to the traditional wired Ethernet solution Due to the scarcity of radio spectrum available, the infrared region of the electromagnetic spectrum was used in initial wireless LANs However infrared requires line of sight making it a rather poor substitute for RF In 1990 the Institute of Electrical and Electronics Engineers (IEEE) formed working group 802 11 to develop a standard to govern WLANs The 802 11 standard was completed in June of 1997 Since then there have been some additions to the standard, namely 802 11a and 802 11b (with 802 11g pending ratification) 802 11b is the most popular version, operating in the 2 4 GHz spectrum with maximum data rates of 11Mbps and a range of about 300 feet 802 11a is much faster than 802 11b at 54Mbps but has a shorter range because of operation in the higher frequency 5 GHz band [18]

Security in WLANs is a very important issue and because signals can pass through walls, it is very difficult to keep information secure 'Hotspots' exist in many cities throughout the world, at which users with a WLAN capable laptop Personal Computer (PC) can tap into networks to use a nearby building's internet connection [19, 20]

Wireless networking does not, in general use the cellular concept Rather it uses traditional computer networking topologies and protocols Computers on a wireless LAN have an Internet Protocol (IP) address while handsets in a cellular telephone network have codes such as their Electronic Serial Number (ESN), Mobile Identification Number (MIN), and System Identification (SID) Code and also their phone number for identification One of the projected aims of Fourth Generation (4G) systems is to have greater integration between all wireless and mobile standards

1.4 – Hybrid Fiber Radio

Because of the low bandwidth of copper wire, signal transmission between BS and MSC in traditional cellular systems must be at relatively low frequencies As systems move to higher operating frequencies, the copper cables between the MSC and BSs will not be able to handle the upconverted signals There are two solutions to this problem available to network operators They can continue to transmit over copper wire and have upconversion and downconversion equipment at the base station or they can convert to a HFR network [11] In a HFR system optical fiber replaces the traditional copper wire The data is modulated onto an optical carrier using a laser diode and transmitted over the fiber Such systems combine the advantages of a fiber system, i e huge bandwidth, high electromagnetic interference (EMI) immunity and low attenuation, with the advantages of a radio system, i e inexpensive mobile and fixed access and long lasting installation process [21]

Provision of the high quality, high bandwidth services that 3G offers requires a high base station density of tens, hundreds or even thousands of base stations per square kilometre Using the HFR concept will reduce the cost in such systems by transferring complicated equipment away from the base stations to a centralised control station Hence the base stations will consist of a photodiode and an RF amplifier in the forward link and a low noise amplifier and laser diode in the reverse link Such systems will make extensive use of microcells and picocells in order to deliver very high bandwidths These systems also solve frequency limitation problems because cell radius can be reduced by installing many base stations, thereby optimising frequency reuse Smaller cells means lower power level thereby reducing costs by eliminating the need for high power amplifiers currently used at base stations Some of the advantages of using HFR in mobile communication networks are outlined below [22]

- Low RF power base stations and user terminals, giving low interference, increased spectrum efficiency, increased battery lifetime, relaxed human health issues
- The high density of BSs means that line of sight operation is often possible which minimises multipath effects It also means that good coverage is available everywhere
- Smaller BSs reduce the environmental impact

- Centralised systems allow simple upgrading and adaptation They reduce maintenance costs and increase reliability
- Optical fiber has lower attenuation than copper wire
- Optical fiber's large bandwidth allows high data rates which are essential for the provision of broadband multimedia applications It also allows the transmission of many services operating at different frequencies simultaneously

Figure 1 4 shows the basic structure of a HFR system Only one BS is shown when in fact there can be up to thousands connected to a single MSC User A transmits his signal which is received at the BS's receiving antenna It is then modulated onto an optical carrier using a laser diode before being transmitted over fiber to the MSC The detector at the MSC receives the signal, performs and necessary operations before reconverting it to an optical signal and relaying it back to the BS The BS's detector converts the signal back to an electrical one before transmitting it to user B over air

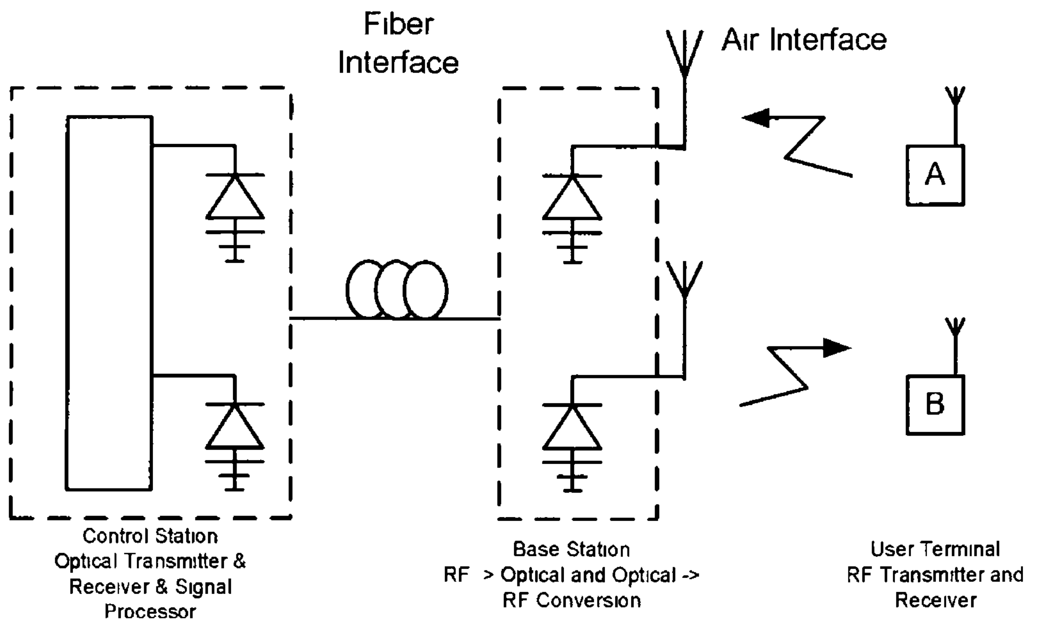

Figure 1 4 – Hybrid fiber radio communication system

1.5 – Conclusion

This chapter has outlined the basics of HFR The next chapter will explain more about the different parts of the network and the components used in each part One of the major drawbacks of HFR systems is laser diode nonlinearity which gives rise to intermodulation distortion and clipping noise and can seriously degrade system performance [23] This effect is one of the primary concerns of this thesis and will be discussed in detail in chapter 3

References

[1] S Haykin, *Communication Systems (3^{rd} Edition)*, Wiley, 1994

[2] G P Agraval, *Semiconductor Lasers, Past, Present and Future,* Springer Verlag, 1995

[3] I H White, "Picosecond Optical Pulse Generation using Semiconductor Lasers", in *Laser Sources and Applications,* by A Miller and D M Finlayson, Institute of Physics Publishing, 1997

[4] J Hecht, *Understanding Fiber Optics (4^{th} Edition)*, Prentice Hall, 1999

[5] D A Ackerman, J E Johnson, L J P Ketelson, L E Eng, P A Kiely, T G B Mason, "Telecommunication Lasers" in *Optical Fiber Telecommunication,* by Ivan Kaminow and Tingye Li, Academic Press, 2002

[6] J Senior, *Optical Fiber Communication Principles and Practice*, Prentice Hall, 1985

[7] T Li, "Optical Fiber Communication-The State of the Art Communication", *IEEE Transactions on Communication*, vol 26, pp 946 – 955, 1978

[8] H -P Nolting, B Sartorius, "Advanced Devices and Their Features for Future Optical Networks", *2000 IEEE/LEOS Annual Meeting Conference Proceedings*, vol 2, pp 627 – 628, 2000

[9] W C Y Lee, *Mobile Communication Engineering Theory and Applications (2^{nd} Edition),*McGraw-Hill Professional, 1997

[10] Dr K Feher, *Wireless Digital Communication Modulation and Spread Spectrum Applications,* Prentice Hall, 1995

[11] Theodore S Rappaport, *Wireless Communication Principles and Practice,* Prentice Hall, 1996

[12] Benny Bing, *Broadband Wireless Access*, Kluwer Academic Publishers, 2000

[13] F G Harrison, P Bishop, "Cellular radio-just ten short years" *International Conference on 100 Years of Radio Conference Proceedings*, pp 193 –198, 1995

[14] D J Goodman, "Trends in cellular and cordless communication", *IEEE Communication Magazine*, vol 29, pp 31 – 40, 1991

[15] T Edwards, *Gigahertz and Terahertz Technology for Broadband Communication*, Artech House, 2000

[16] 3G-Generation, "3G Dive into the Multimedia Wave", http //www 3g-generation com/what_is htm, (06/02/2004)

[17] UMTS World, "UMTS/3G History and Future Milestones", http //www umtsworld com/umts/history htm, (06/02/2004)

[18] R Dettmer, "Local network radio the wireless LAN", *IEE Review*, vol 39 iss 3, pp 127 –131, 1993

[19] K Pahlavan, "Wireless communication for office information networks", *IEEE Communication Magazine*, vol 23, iss 6, pp 19 –27, 1985

[20] E Chien, D Goodman, J Russell,, "Cellular access digital network (CADN) Wireless access to networks of the future", *IEEE Communication Magazine*, vol 25, iss 6, pp 22 –27, 1987

[21] F Smyth, L P Barry, "Effects of Laser Diode Nonlinearities in Hybrid Fiber/Radio Systems", *SPIE Opto Ireland Conference Proceedings*, 2002

[22] H Al-Raweshidy, "HFR for the Next Generation", in *HFR technologies for Mobile Communication Networks* by Hamed Al-Raweshidy, Shozo Komaki, Artech House, 2002

[23] R E Schuh, D Wake, "Distortion of W-CDMA signals over optical fiber links", *International Topical Meeting on Microwave Photonics 1999*, pp 9-12 (supplement), 1999

Chapter 2 – Hybrid Fiber Radio Networks

2.1 – Introduction

The growth of mobile communications over the past decade has been phenomenal At the end of 2002 there were estimated to be more over 1 billion cellular subscribers in over 190 countries worldwide [1] It is clear that the major growth area for the future will be data applications and in the near future, services such as video on demand, interactive multimedia and high speed Internet will be available to mobile devices Existing network infrastructure using coaxial and twisted pair cables will not have enough available bandwidth to support these broadband applications so it will be necessary to replace it with optical fiber [2] A Hybrid Fiber Radio (HFR) transmission system is essentially any system which employs both optical fiber and free space radio as it's transmission paths Such systems are beginning to find an increasing role in telecommunications networks [3] HFR is particularly suited to a role in Remote Antenna Feeding (RAF) RAF is the title given to systems in which the Base Station (BS) or antenna site is kept as simple as possible by moving all of the complex processing equipment needed by the network to a Mobile Switching Centre (MSC) Almost all existing RAF systems use coaxial cable or radio links In 1998 Hunziker and Baechtold [4] showed that in new networks and for link lengths of over 200 m it is more economical to lay optical fiber

2.2 – The Hybrid Fiber Radio System

This section will use the example of a simple voice call to describe the HFR system and the basics of mobile communication Only the uplink i e from the user to the MSC will be discussed in detail because the downlink is essentially a mirror image of it The principles for data transfer are almost identical It should be noted that there are many different architectures used in mobile communication networks and that the following description is a generic one It would be beyond the scope of this thesis to describe specific systems A cellular network consists of three main 'stations' and the terms used for these will be as follows The Mobile Station (MS) is the physical equipment used by a subscriber The BS is the radio equipment which serves a cell The MSC connects the mobile network to the Public Switched Telephone Network (PSTN) and handles all mobile traffic In a HFR system, the link between the MS and the BS is free space radio, and the link between the BS and the

MSC is optical fiber This is an over simplified view of the network but for our purposes, it is sufficient The table below gives a more realistic view of the architectures of two systems in use today

Simplified View	**GSM**	**UMTS**
MS	MS consisting of Mobile Termination (MT) and Terminal Equipment (TE)	User Equipment (UE) consisting of Mobile Equipment (ME) and the User Services Identity Module (USIM)
BS	Base Station Subsystem consisting of Base Transceiver Stations (BTSs) and a Base Station Controller (BSC)	UMTS Terrestrial Radio Access Network (UTRAN) consisting of a number of Radio Network Subsystem (RNSs) which in turn consist of Node Bs and a Radio Network Controller (RNC)
MSC	MSC connecting to Home Location Register (HLR), Visitor Location Register (VLR,) Equipment Identity Register (EIR), Authentication Centre (AuC)	Core Network (CN) consisting of Serving Network Domain, the Home Network Domain and the Transit Network Domain each of which could be further expanded

Table 2 1 – GSM and UMTS architecture overviews

First Generation (1G) mobile systems had all of the complex processing equipment located at the MSC In Second Generation (2G) systems, some of this equipment was moved to the BS to reduce the workload of the MSC Similarly, Third Generation (3G) systems like Universal Mobile Telecommunication System (UMTS) perform some of the processing at the BS [5] However, to increase coverage and allow higher data rates, the number of required BSs rises Thus costs also increase dramatically It is therefore expected that the trend of moving complex and expensive equipment to the BS will be broken Future networks may return to simplified BSs and centralised processing where possible Apart from reducing costs, centralisation of processing equipment also eases maintenance requirements [6] The HFR system described in this section will use this simplified BS architecture

2 2 1 – Mobile Station

The MS is the mobile equipment that the subscriber uses for communication The most common type is a cellular telephone

2 2 1 1 – Initialisation

When the MS is turned on, it must establish communication with a BS To do this it scans several control channels Each control channel carries signals from nearby BSs The MS measures the signal strength from each BS and tunes to the strongest It then decodes the information on this control channel and in doing so obtains information about the cell Data transmitted back to the MSC from the BS on control channels, allow the MSC to know which BS is serving every MS in it's network To make a call the MS transmits a service request message to it's BS This service request contains information about the call such as the number calling and the number to be called The BS relays this request to the MSC which knows the BS of the dialled number It can therefore establish communications between the two BSs Once the link is established the voice signal is processed and transmitted [7]

2 2 1 2 – Processing the Signal

The signal processing which takes place at the MS for a voice call can be broken into three mam sections The first is Analogue to Digital (A/D) conversion, the second is modulation and the third is transmission A/D conversion is necessary due to the fact that speech is analogue and yet we wish to transmit it digitally Modulation converts this digital data into a form suitable for transmission The modulated data is then transmitted over air to the BS

The A/D conversion consists of 3 main stages Sampling, Quantising and Coding Sampling is the measurement of the value of a signal at particular moments in time

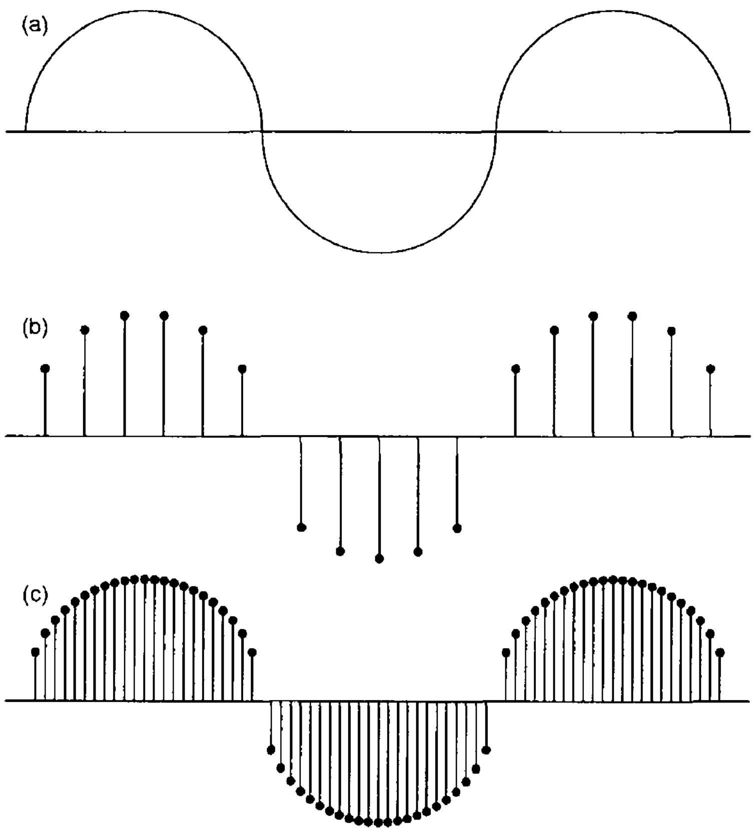

Figure 2 1 – Sampling an analogue waveform (a) analogue waveform (b) sampling at a slow rate (b) increased sampling rate

There are two methods of sampling The first approach is known as Fourier analysis and it is based upon the fact that any waveform can be viewed as the sum of a finite number of sine waves It is computationally complex and used much less widely than the second approach The second approach is known as the Nyquist theorem or the sampling theorem and it is illustrated in Figure 2 1 It is based on the idea that any complex waveform can be reconstructed from an adequate number of discrete samples This adequate number is at least two times the sampling frequency Hence to accurately describe a 4 kHz signal, 8000 samples per second are required [8]

Quantisation is the rounding off of the amplitude of each individual sample to a digital value For example, assume that the difference between the maximum and minimum amplitude is defined This range is then divided into a number of steps The amplitude of each sample is then rounded to its closest step (see Figure 2 2) This allows each step to can be assigned a digital value Obviously because of the rounding off process, a degree of error is introduced The relative magnitude of this error, known as quantisation noise, is determined by the fineness of the scale [9] For example, if the system described above used 80 steps instead of 8 then the quantisation noise would be reduced[1] The error introduced in quantisation cannot be recovered

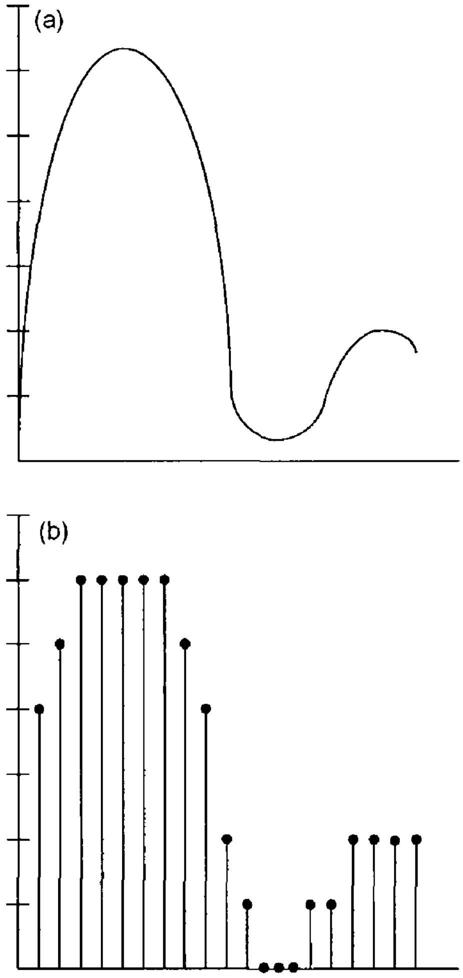

Figure 2 2 – Quantisation (a) initial analogue waveform, (b) sampled and quantised waveform

The next step is coding of the signal There are two extremes in coding An example will illustrate these Assume that a waveform has been sampled and then quantised with 128 levels At one extreme the 128 levels could be each represented by a 1 V change in pulse amplitude This method would be very efficient as it only requires a single pulse per sample The problem with this method is that the receiver must be able to distinguish between a pulse of 126 V and a pulse of 127 V This is a difference of less than 1% and any noise, distortion or attenuation would cause errors in the received signal At the other extreme the 128 levels could each be represented by a 7 bit binary code This method, known as binary coding, is inefficient as each sample requires seven pulses to represent it, however it minimises receiver errors as

[1] The problem of quantisation noise cannot be completely eliminated by increasing the number of intervals indefinitely The more intervals the higher the required bandwidth More intervals can also make the signal more vulnerable to transmission noise It is a design trade off between quantisation noise and bandwidth

the receiver must only distinguish between two levels Pulse Code Modulation (PCM) is a very popular technique for digitising voice It uses binary coding and the term modulation is added because it changes the state of a medium (for example voltage in a circuit) There are a many different binary coding schemes for example Non-Return to Zero (NRZ), Return to Zero (RZ) and Bipolar Return to Zero (BRZ) Each of these are illustrated in Figure 2 3

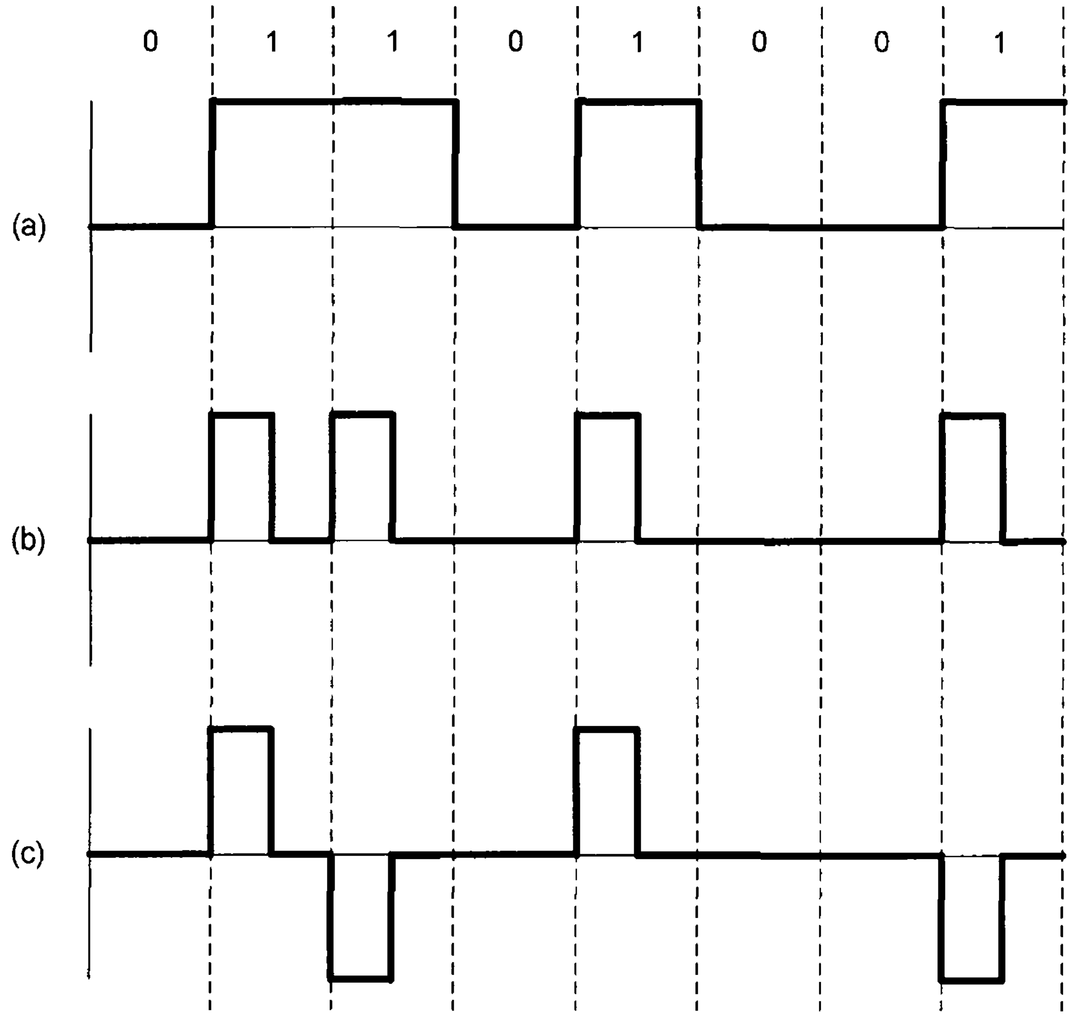

Figure 2 3 – Binary coding schemes (a) NRZ, (b) RZ, (c) BRZ

Once the data is digitised it must be modulated onto the form of energy[1] that is to be used in the circuit The modulation process involves switching the amplitude, frequency or phase of a sinusoidal carrier in some fashion in accordance with the incoming data stream The three basic methods of digital modulation are known as Amplitude Shift Keying (ASK), Frequency Shift Keying (FSK) and Phase Shift Keying (PSK) They are shown in Figure 2 4

[1] Light energy electrical energy or electromagnetic energy

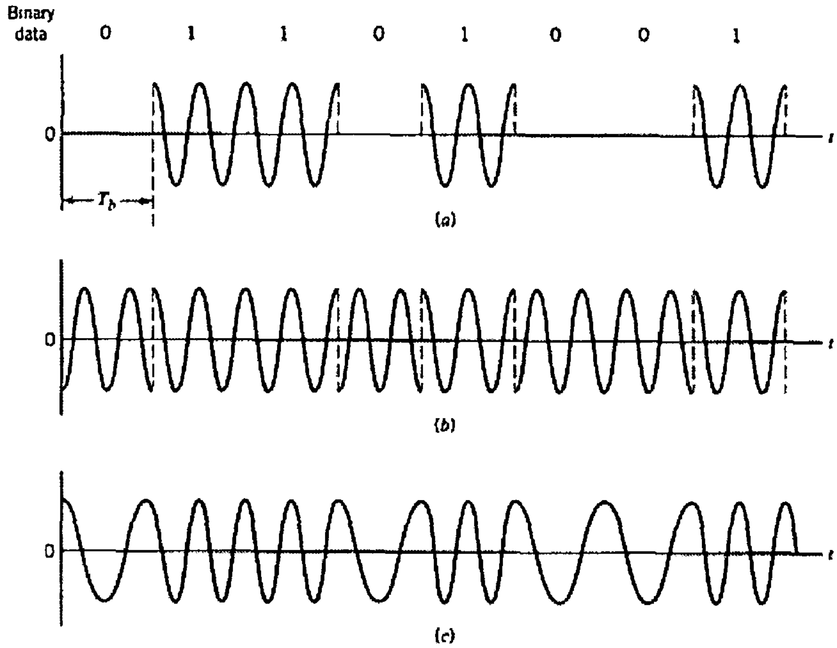

Figure 2 4 – Basic digital modulation schemes (a) ASK, (b) PSK, (c) FSK

In any radio system, bandwidth is a very scarce and therefore precious resource Hence it must be used as efficiently as possible In a wired system more bandwidth is always available (albeit at a price) by simply buying more wires However there is no easy way to "manufacture" additional radio spectrum Digital modulation usually expands the bandwidth required to transmit a signal This means that digital radio is at a distinct disadvantage over analogue, so radio engineers have developed multilevel modulation techniques Essentially this meant that each symbol transmitted could carry more than one bit of data For example Quaternary Phase Shift Keying (QPSK), can transmit two bits of data m each symbol This is clearly shown in Figure 2 5 [8]

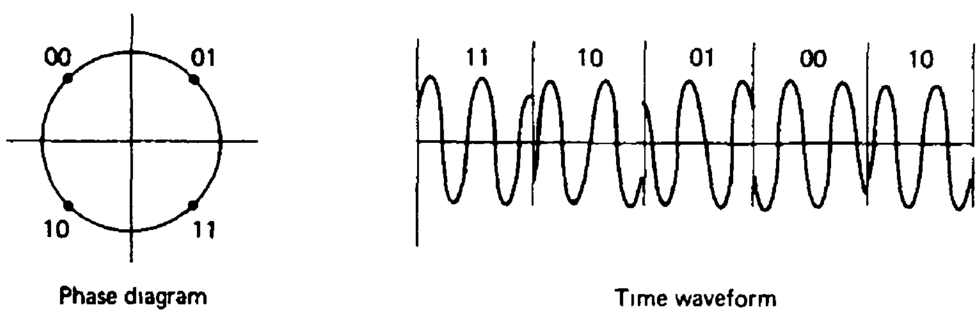

Figure 2 5 – Quaternary phase shift keying

These multilevel digital modulation schemes have made steady progress A common form today is Quadrature Amplitude Modulation (QAM) QAM is like a hybrid between amplitude and phase modulation and has been shown with up to and above 1024 levels [10] This means that over 10 bits can be transmitted with only 1 symbol, thereby greatly reducing the bandwidth required to transmit the entire signal Global System for Mobile-Communication (GSM) and UMTS both use forms of PSK GSM uses Gaussian Minimum Shift Keying (GMSK) and UMTS uses QPSK [11]

MSs contain a radio transmitter, receiver and antenna They transmit the digitised and modulated signal at a frequency which has been assigned to them by the MSC The peak power that a GSM phone can output is 2W, but depending on coverage it can be as little as 2 mW [5] This power is transmitted in all directions because the phone has no idea which direction the BS is Ideally, location and mobility of a user would not be an issue in a wireless communication system but, due to channel impairments we find that they are

2.2.2 – Mobile Station to Base Station Air Link

Unlike a wired channel, a radio channel is random and unpredictable The transmission path can vary from simple line of sight to one obstructed by buildings mountains or foliage Weather also plays a part The main limiting factors in the radio channel are

- Attenuation and Loss
- Multipath
- Noise
- Interference

2 2 2 1 – Free Space Loss

When a signal radiates it's power diminishes as it moves further and further from the transmitter In free space, a transmitted RF ray decreases in power by the inverse of the square of the distance from the transmitter In practical systems the loss is much worse Depending on terrain, atmospheric effects and the existence of reflected waves the path loss may be the cube of the distance or some higher product [12] The attenuation is highly dependant on the frequency due to absorption peaks and troughs at certain frequencies (see Figure 2 6)

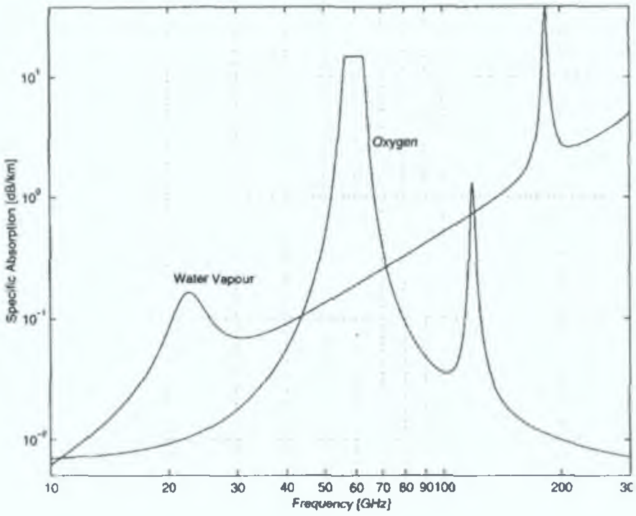

Figure 2.6 – Atmospheric attenuation profile

Generally, lower frequencies have greater penetrating power and will propagate further. For example below 1 GHz rain and atmospheric moisture can almost be neglected. Frequencies above 10 GHz are severely affected and frequencies above 30 GHz are virtually unusable outdoors. Buildings and other large obstacles cause radio 'shadows'. These are locations where there is a large attenuation over a small distance. The type of environment has a large effect on the attenuation. Cities typically show 10 dB worse signal strengths than suburban areas and 30 dB worse than rural areas [8]. Foliage is also important, as one study showed that in summer when the trees were in full leaf, signal strength was over 10 dB less than in the same location in winter [12]. In practise, due to the high complexity of the calculations, there is no exact formula to calculate the power at the receiver. Instead there are models for predicting the propagation loss in the system. Examples of these are the Okumura, Lee method or Hata formulas. Although these are models based on the measurements made in Japanese cities, by using modification factors they can also be applied to other cities or even to the countryside [12-14].

2.2.2.2 – Multipath

A signal travelling across free space diffuses. While some of the signal may reach the receiver directly, other portions will reach it by reflection, diffraction, and scattering [15]. Reflection occurs when the signal impinges on an object which is large in relation to the signal's wavelength like a building for example. This causes the signal to 'bounce' off the object in another direction. Scattering is when the signal is obstructed by objects which are smaller than the wavelength of the signal for example foliage Scattering causes the signal to spread out or diffuse in all directions Diffraction occurs when the signal meets irregular or sharp objects In this case the signal can actually bend around the obstruction Some of these effects are illustrated in Figure 2 7 When portions of the signal take different paths to the receiver they arrive with different time delay, phase and amplitude Depending on it's phase each of the signal portions will interfere either constructively or destructively at the receiver This gives rise to an effect known as multipath or multipath fading[1]

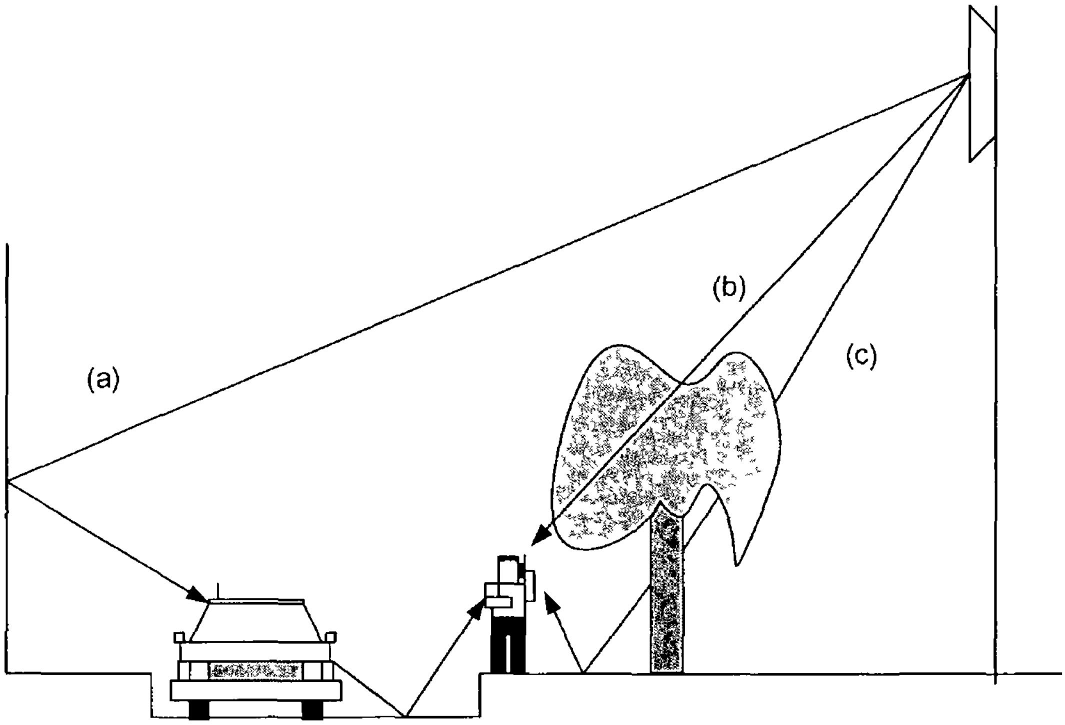

Figure 2 7 – Multipath fading (a) Reflection off building and intermittent blockage by automobiles, (b) Scattering and partial blockage by foliage, (c) clear path behind tree reflection off ground

Multipath fading is affected by the location of the transmitter and receiver as well as movement around them It has three main ill effects Delay spread is the time dispersion of a signal Because the propagation results in a variety of travel times, pulses are broadened as they travel through air If data rates are high, the delay spread can cause Inter-Symbol Interference (ISI) Rayleigh Fading is the second detrimental effect of multipath It is characterised by rapid fluctuations in signal power at the receiver This introduces periods of low Signal to Noise Ratio (SNR) The final effect of multipath fading is known as Doppler Spread Doppler Spread

[1] Also known as fast fading or small scale fading because it represents quick fluctuations in signal power that only occurs over a short period of time

introduces random frequency and phase shifts which cause undesired frequency modulation of the signal It is caused by movement of the MS relative to the BS and also by movement of obstacles [16]

2 2 2 3 – Noise

The term noise is used to describe unwanted signals over which we have no control, that disturb the transmission signals The sources of noise may be external or internal to the system In the environment electromagnetic sources such as lightning and car ignitions add noise [8] Inside the system there are two main types of noise shot noise and thermal noise Shot noise arises because of the random nature of current flow in certain devices For example in a photodetector, current is produced each time a photon falls on the device but photons fall on the devices randomly and at discrete times Thermal noise is electrical noise which arises from the random motion of electrons in a conductor [9] It is inherent in every electrical circuit to some extent Noise in the signal gets amplified at any amplification stages and reduces the signal quality The fundamental measure of signal quality is the SNR This is defined as the ratio of the signal power to the noise power

2 2 2 4 – Interference

In today's cellular networks, the emphasis is on multiple users sharing network resources such as time and frequency As a result of such sharing the system will be subject to interference Interference is caused by other transmitted radio signals impinging on the desired signal and there are two main types Adjacent Channel Interference (ACI) and Co-channel Interference (CCI) Both of these are illustrated in Figure 2 8 ACI is caused by imperfect receivers and filters allowing nearby frequencies in to the passband of the desired channel [17] It can be particularly detrimental when the interfering transmitter is closer to the receiver than the desired transmitter This is known as the near-far effect ACI can be minimised by careful filtering and channel assignments CCI is caused by the fact that more than one cell in the system uses the same set of frequencies simultaneously It occurs when a transmission at the same frequency from another cell, is picked up by the receiver

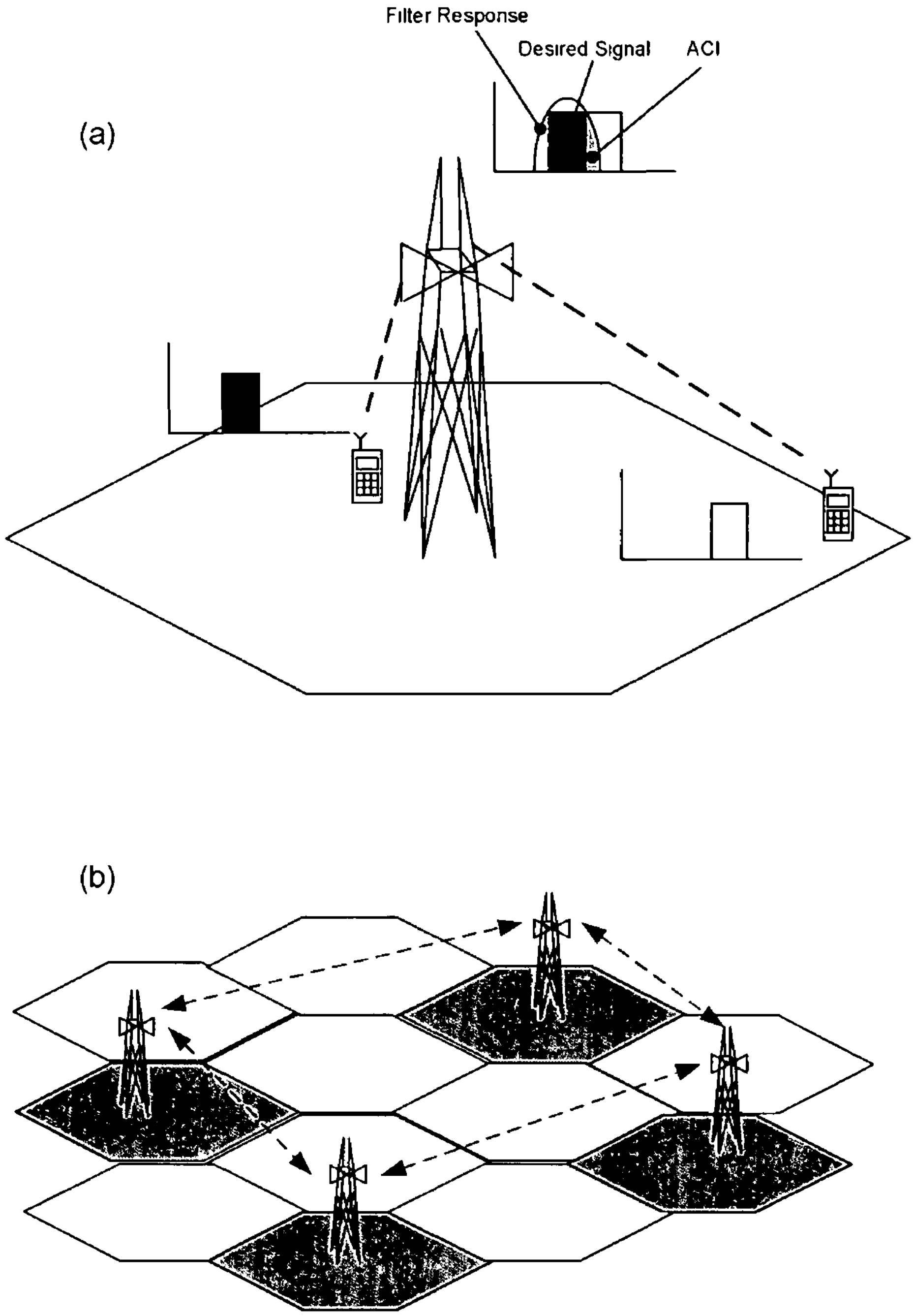

Figure 2 8 – Interference (a) ACI, the two phones transmit in adjacent bands and poor receiver filtration at the BS causes ACI, (b) CCI, each of the shaded cells use identical frequencies therefore each receiver will pick up some undesired components

2 2 3 – Base Station

As was mentioned previously, the BS transmits controls signals from the MSC which allow a MS in it's cell to tune to it When a call is made, the BS receives the service request and relays it on to the MSC The MSC then connects the two communicating MSs and assigns a traffic channel to them [7] Communication between the two can then begin Once the signal has propagated through the air and been subjected to all the detrimental effects mentioned above, it is received at the BS The BS is a transceiver located near the centre of a cell whose primary purpose is to handle all incoming & outgoing calls within the cell In a HFR system the BS relays the MS's signal to the MSC via optical fiber As mobile networks evolve and the number of users grow the number of BSs must also increase As a result equipment, installation and maintenance costs all rise It is therefore, very desirable to have as simple a BS as possible [18] For this reason, we will discuss the BS in this simplified form as it will be in the future mobile networks That is, consisting of an antenna, an electrical amplifier and a laser diode (we are only discussing the uplink) Again our simplified version of the network architecture should be noted Cell radii may range from a small as 20 m (picocell) up to 50 km (macrocell) HFR is suitable for servicing the BSs of cells of any size Obviously, macrocells are going to need very high powered amplifiers to allow their signals to transmit over such a large distance Picocells on the other hand have been developed which require no power at all [19] These are based on an unbiased Electro-Absorption Modulator (EAM) which acts as an optical transceiver

2 2 3 1 – The Antenna

The operation of the wireless system depends strongly on the design and the performance of it's antennae The antenna converts the signals from electromagnetic form into electrical form and vice versa and it's most significant parameter is the directive gain The directive gain of the antenna in a particular direction is the ratio of the power density received or transmitted by it in that direction to the power density that would be received or transmitted by an isotropic antenna[1] with the same input power The shape of the antennas radiation pattern describes it's gain in each direction The direction of maximum power is known as the front lobe[2] The direction exactly opposite to this is called the back lobe with lobes adjacent to the front lobe known as the side lobes In a receiver antenna, it is the side lobes and back lobe that are responsible for absorbing unwanted radiations, leading to interference [9] In a cellular system the BS antennae are generally mounted on a mast so that

[1] An isotropic antenna is an ideal antenna that radiates equally in all direction In practice no antenna is completely isotropic
Also known as the primary beam, or the major lobe

they above the level of most buildings and trees and hence provide the greatest level of coverage possible

2 2 3 2 – Amplification

Electrical amplifiers are used to compensate for loss of signal power incurred in transmission Cost, size, heat dissipation and power consumption of the entire BS are totally dominated by the power amplifiers [20] Depending on the size of the cell, some amplification is generally required before the signal can be used to modulate the laser in the uplink In the downlink, depending on the cell size, amplifiers are needed to increase the power of the output signal so that it is receivable everywhere in the cell Because they are an active component, it is possible that the amplifier will have a nonlinear response at certain frequencies This nonlinear response may introduce additional noise into the system due to a phenomenon known as Inter-Modulation Distortion (IMD) To avoid IMD it is vital to have amplifiers which operate linearly at the frequencies of operation of the network

2 2 3 3– Transmitting the Signal The Laser Diode

Having been amplified, the signal received at the antenna is then used to modulate a laser diode This electro-optic conversion process is the primary concern of this thesis and will be thoroughly dealt with in the next chapter This section on the other hand will discuss the basic concepts behind lasers in communication systems today

Once the optical carrier which is modulated with the radio signal is generated, it is then ready to be transmitted over optical fiber from each of the BSs to the MSC One of the main advantages of HFR systems lies here The antenna can receive signals at a wide range of frequencies This allows many radio services (at different frequencies) to be received at the same time By simply modulating the laser with the signal received at the antenna, all of these radio services can be transmitted simultaneously over the same fiber to the MSC [21, 22]

2 2 3 3 1 – Semiconductor Laser Diodes

Semiconductor laser diodes are used in communication networks for conversion from electrical to optical energy They are operated by applying a bias current which pumps carriers up to the higher level of a two level energy system thereby causing a population inversion These carriers can then be stimulated into falling back down to the lower energy level with the emission of coherent light in a process known as stimulated emission [23] A common semiconductor structure used in laser diodes today is known as a Double Heterostructure (DH) [24] as shown in Figure 2 9(a) The DH laser structure gives good carrier confinement[1] and good optical confinement[2]

Amplification is achieved by introducing mirrors into the device at either end of the active region These mirrors are formed by cleaving or polishing the semiconductor crystal This forms an oscillator called a Fabry-Perot (FP) resonator which has several resonant frequencies[3] [25] Light will be emitted at any of these frequencies where the gain overcomes the optical losses in the cavity resulting in a number of longitudinal modes [26] The structure of a DH FP laser is shown in Figure 2 9 (b)

Long haul, high bandwidth applications require the use of single mode lasers due to their higher tolerance to dispersion For single mode operation a laser must only output light in a single longitudinal mode [27] There are many ways to get a laser to operate in a single mode regime but the most common method is to insert a corrugated optical waveguide inside the laser cavity [28, 29] This waveguide, known as a Bragg Grating, causes periodic variations in the refractive index and induces feedback by Bragg Scattering The wavelength of the light which is fed back into the cavity enhances the mode at that wavelength and suppresses all other modes causing single mode operation Lasers fabricated using this design are known as Distributed Feed-Back (DFB) lasers and are the most common type in use in communication today Figure 2 9 (c) shows a basic schematic of both an FP and a DFB laser In terms of the use of DFB lasers in HFR systems, the modulation response is the most important characteristic This will be discussed in some detail in Chapter 3

---

[1] Carrier confinement is important for increasing quantum efficiency by ensuring a high level of radiative recombination takes place inside the active region

[2] Optical confinement prevents absorption of the radiation in regions around the active region

[3] Lasers fabricated using this design are called FP lasers

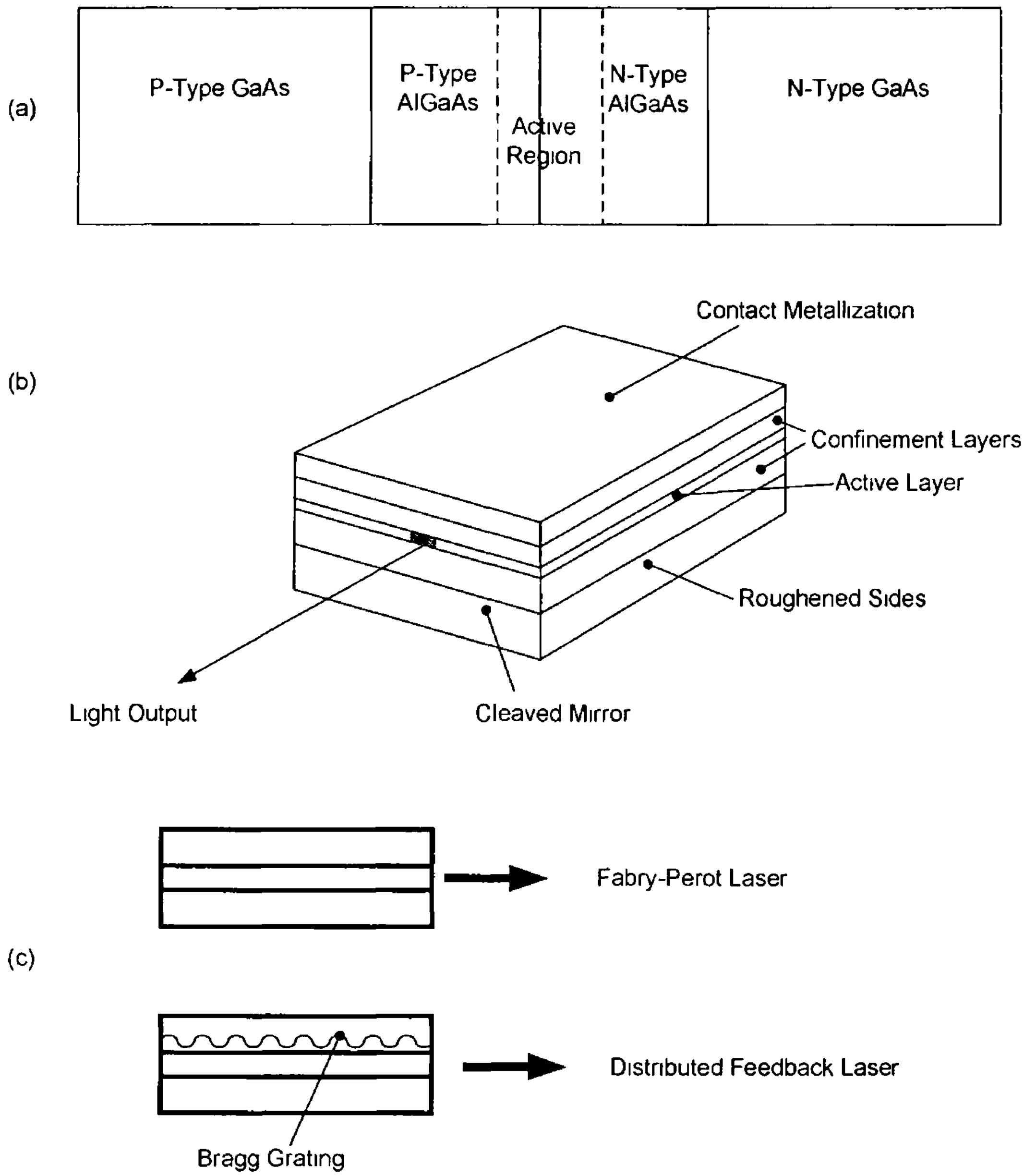

Figure 2 9 – Lasers (a), The DH structure, (b) DH FP laser, (c) schematic of FP and DFB

2.2 4 – Base Station to Mobile Switching Centre: Optical Fiber Link

2 2 4 1 – Optical Fiber

Once radio signals received at the BS have been modulated onto an optical carrier, they may be transmitted over optical fiber to the MSC Optical fiber is usually made of silica glass[1] It consists of a core, surrounded by a cladding which in turn is

[1] Can be made from plastic also

usually coated with a jacket or buffer for protection [30, 31] The refractive index[1] of the cladding is lower than that of the core Thus, light which is incident on the boundary between core and cladding is reflected back into the core This phenomenon is known as total internal reflection, and it gives optical fiber the ability to guide light along it's core [32]

Fiber is generally categorised by two parameters The first is its refractive index profile Step index fiber is the simplest type, it has an abrupt change in refractive index between core and cladding Another type of fiber is known as graded index fiber In graded index fiber the refractive index gradually varies throughout the fiber before reaching its maximum at the centre of the core [33] The second parameter is the number of modes that it can support A mode is a single electromagnetic wave[2] There are two variations available, Single Mode Fiber (SMF) and Multi-Mode Fiber (MMF) Essentially the difference is in core diameter The core in a single mode fiber is very small, so that it can only support one mode Multimode fiber has a wider core[3] and hence can support the propagation of more than one mode Standard Single Mode Fiber (SSMF) is the most common fiber used in communication systems today [33, 34] The main types of optical fiber are illustrated in Figure 2 10

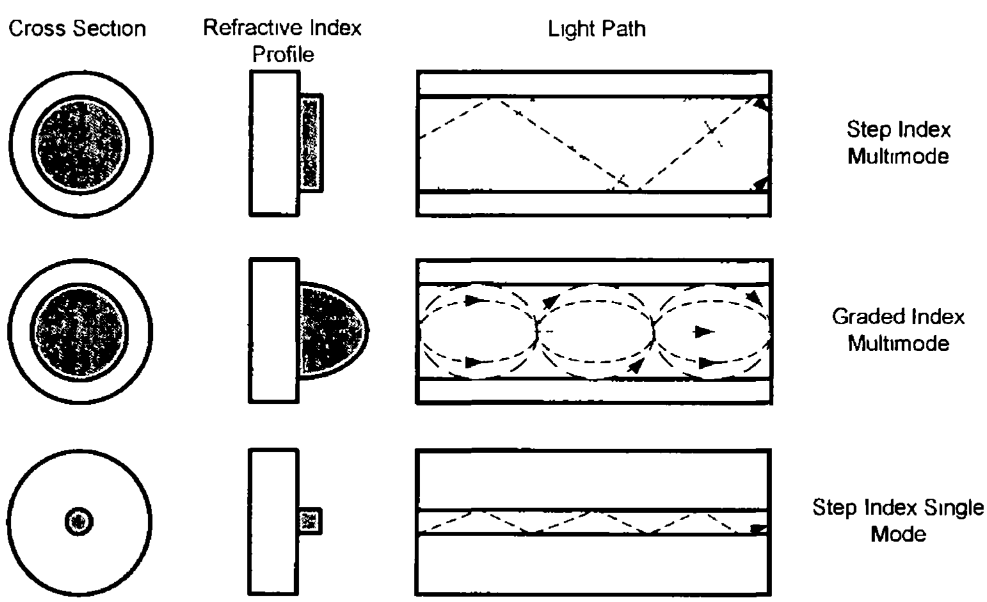

Figure 2 10 – Fiber variants

[1] The refractive index of a material is a ratio of the speed of light in a vacuum to the speed of light as it travels through the material

[2] Electromagnetic modes in fiber should not be confused with the modes of a laser

[3] typical diameter is 62 5 micrometers for MM fiber as opposed to 8 9micrometers for SM

The most important fiber characteristics are attenuation, dispersion and fiber nonlinearity

Attenuation

Optical fiber's low attenuation is one of the main advantages that it has over copper wire At present attenuation is given as 0 2 dB/km in fiber There are 3 mam causes of attenuation [35]

1 Material Absorption – Due to impurities in optical fiber The main impurity is the OH ion (hydroxide) It has an absorption peak around 1370 nm causing traditional fiber to be useless at this wavelength

2 Rayleigh Scattering – An intrinsic loss mechanism caused by the interaction of photons with the molecules of silica itself

3 Bending loss – Introduced by physical stress on the fiber

The attenuation profile of a fiber determines what wavelengths of light can be transmitted with it From the loss profile of standard fiber shown in Figure 2 11 you can see the three main transmission windows that have been used Recently, Lucent Technologies have developed a fiber, known as *Allwave* fiber, which has dramatically reduced the loss peak at 1 37 μm [36] This allows the fiber to be used to transmit over a huge range of frequencies, which dramatically increases the available bandwidth

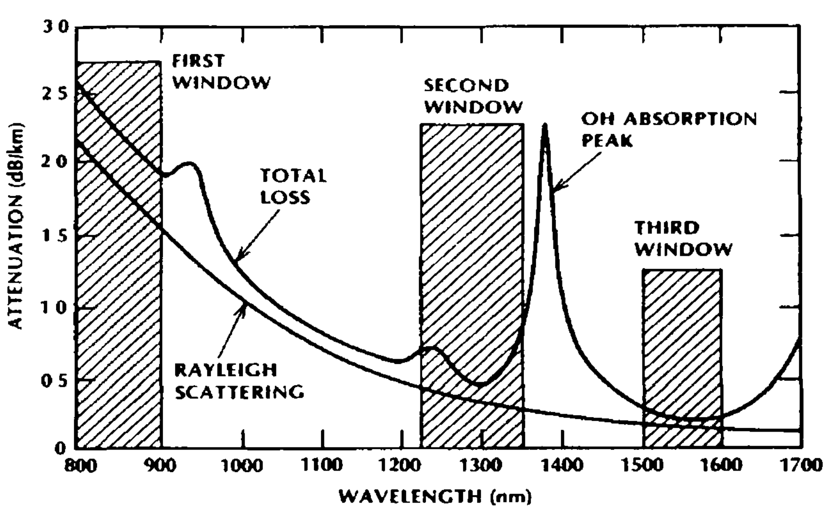

Figure 2 11 – Attenuation profile of standard optical fiber

Dispersion

This factor causes pulse broadening or narrowing[1], as data signal propagates in the fiber, and limits the bandwidth–distance product of optical transmission systems This changing of pulse width in the time domain can cause pulses to overlap resulting in Inter-Symbol Interference (ISI).

There are three types of dispersion [37]:

1. Modal Dispersion – Only present in multimode fiber, modal dispersion is caused by the fact that different modes travel different paths inside the fiber. The result of this is that the different modes reach their destination at slightly different times. Using graded index fiber reduces this effect and using single mode fiber eliminates it completely.
2. Material Dispersion – Due to the fact that refractive index is a function of wavelength, different frequencies travel at different speeds through the fiber. Thus for a data signal with finite bandwidth some parts of the signal will travel faster than others resulting in broadening or narrowing of the signal.
3. Waveguide Dispersion – Not all of the light is completely confined to the core. A small amount may propagate in the cladding and because the core and cladding have different refractive indices, the light travelling in them will travel at different speeds.

The combined effect of material dispersion and waveguide dispersion is known as chromatic dispersion. Material dispersion is due to the glass itself and is an inherent property. On the other hand, waveguide dispersion is structure dependant and can be varied. Figure 2.12 shows a plot of the total dispersion in standard optical fiber. The dispersion zero at 1300 nm can be clearly seen. By altering the refractive index profile and hence the waveguide dispersion curve it is possible to get a chromatic dispersion zero at a desired wavelength [38]. Fibers employing this technique are known as zero Dispersion Shifted Fibers (DSFs) and the first of them had their zero-dispersion shifted to 1550 nm to match their absorption minimum, giving fibers with negligible dispersion and very little loss around the operating wavelength. In the same manner the dispersion parameter of a fiber can be modified to some degree in the manufacturing stage to have an opposite curve to SSMF. Placing this 'Dispersion

[1] depending on whether the dispersion factor of the fiber is negative or positive

Compensated Fiber' (DCF) after the SSMF compensates for dispersion by counteracting the dispersion effects it has caused

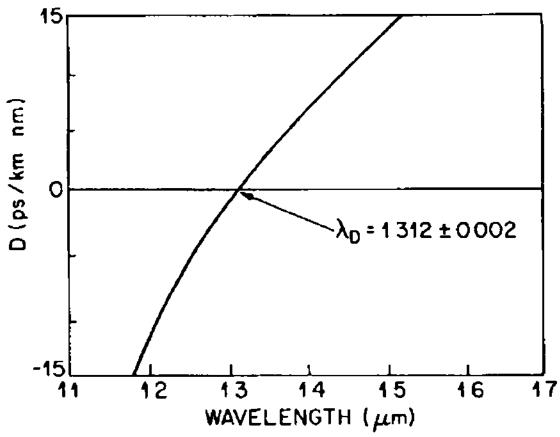

Figure 2 12 – Dispersion in standard optical fibers showing dispersion zero at 1 3μm

Fiber Nonlinearity

When subjected to strong electromagnetic fields the response of silica fiber becomes nonlinear [39] It's refractive index is dependent on intensity and this dependency leads to nonlinear effects The main effects that are considered are self-phase modulation (SPM), cross phase modulation (XPM), and Four Wave Mixing (FWM) [40] Nonlinear effects in systems with long transmission distances or where many channels are propagating (such as WDM) can be quite serious However providing transmission powers are kept quite low then nonlinear effects can be neglected

2 2 4 2 – Optical Amplifiers

Although optical fiber exhibits very low attenuation when compared with copper wire, in a HFR communication system where the BS and MSC are a long distance apart amplification of the optical signal may be necessary Originally in order to achieve amplification of an optical signal it was necessary to convert it to an electrical signal, amplify it electrically, reprocess it[1], and convert it back to an optical signal The network components which performed these functions were called repeaters and regenerators Optical amplifiers have advantages and disadvantages when compared with repeaters and regenerators A distinct advantage is that they allow simultaneous amplification of many channels inside the operating band, whereas repeaters and regenerators require a separate electrical channel for each

[1] Processing included retiming and pulse shaping

optical one They are also much simpler devices However the main disadvantage associated with optical amplifiers is that they amplify noise and distortion effects also The most common optical amplifier is the Erbium Doped Fiber Amplifier (EDFA) and this is the type that was used in this work As the name suggests, EDFAs are based on normal silica fiber which has been doped with erbium They operate in the C band[1] and the L band[2] [41]

2 2.5 – Mobile Switching Centre

The optical signal arrives at the MSC with the Radio Frequency (RF) signal modulated onto it It is coupled into the optical detector, which outputs the RF signal The RF signal then undergoes all of the processing necessary, before being transmitted and essentially beginning the whole process again only in reverse The MSC interacts with the PSTN and it performs administrative duties such as account checking, and Caller Identification (CID) among others It is also responsible for switching, multiplexing, channel assignment, handoff etc

In 1G systems the MSC controlled the entire network GSM, (a 2G system) saw the introduction of Base Station Controllers (BSCs) which perform some of the necessary processing thereby reducing the MSCs workload A single BSC controls a number of BSs 3G systems also perform some processing away from the MSC With the huge number of BSs necessary to provide high data rates to users, it is expected that in future mobile networks, the cost of BSs will be reduced by simplifying them and moving the complexity back to a central location

2 2 5 1 – Detecting the RF Signal Photodiodes

The detector is a crucial part of the HFR system, as it performs the conversion from the optical domain back to electrical domain, where most signal processing is performed There are two forms and these are known as PIN (for p-type, intrinsic, n-type) photodiode and Avalanche Photodiode (APD) More information on the operation of photodiodes is available in references [24, 26, 36, 42] The three most important characteristics of a photodetector for use in a HFR system are it's bandwidth, responsivity and the amount of noise it adds

---

[1] C band stands for conventional and ranges from 1530nm to 1565nm
[2] L band stands for Long and ranges from 1565nm to 1625nm

1 The bandwidth of a photodetector is defined as the frequency at which the output signal has dropped to 3 dB below it's power at a low frequency [36] It puts an upper limit on the frequency that can be used in the system Device geometry, materials used, electrical bias and other factors all combine to determine the bandwidth

2 The responsivity is often the quoted value for the performance of a photodiode It defines how much current is output per watt of light power incident on the device

3 Noise is any unwanted or spurious signal and is added to the desired signal in every detector thereby degrading system performance There are three main types

a) Quantum noise is due to the random nature of photon to electron conversion

b) Thermal noise is due to thermal interaction between electrons and ions in the amplifier circuitry

c) Dark current is current which is generated in the detector even when there is no light incident on it

2 2 5 2 – Processing the Signal

Channel Assignment and Switching

The MSC knows which cell each MS on it's network is in When a service request is transmitted by a MS, it is forwarded on to the MSC by the relevant BS The MSC then transmits a paging request containing the number being called to the BS it desires The BS then transmits the paging request over air to it's users When the MS being paged recognises it's number, it sends a response to it's BS, which again relays this message to the MSC The MSC then knows the BSs of both MSs and hence can set up the traffic channels to allow communication to take place It sets up a channel for each MS In contrast to the control channels which are shared by many MSs, these traffic channels are dedicated to the two communicating MSs The receiving MS sends a message to the MSC to say that it has tuned to the traffic channel The MSC then sends an alert message to the MS which begins to ring When the MS is answered the MSC connects the two traffic channels and communication can begin [7]

Handoff

Cellular technology allows the " hand-off" of subscribers from one cell to another as they travel around This is the key feature which allows the mobility of users A computer constantly tracks mobile subscribers of units within a cell When the signal strength being received at the BS begins to weaken, (as the user reaches the border of a cell), the MSC requests reports of signal strength from several surrounding BSs The MSC will then automatically "hand-off" the call to the BS with the strongest signal and the call is assigned a new channel in a different cell [7, 8, 12]

Multiplexing/Multiple Access

Because all users in a mobile communication network use the one medium there will be constant interference between users To avoid this the medium must be somehow divided Once the MSC knows how the medium is divided, it can then separate the signals and obtain the one it desires In mobile communication networks, there are three methods, which are commonly used to divide up the available spectrum These methods are known as Multiple Access Techniques [8, 16, 43] They are illustrated in Figure 2 13

1 Frequency Division Multiple Access (FDMA) is the term used to describe a system which transmits signals on non overlapping frequency bands Simple band pass filters can then be used to separate the individual signals thereby ensuring that they don't interfere In practice some leakage would occur between adjacent channels so guard bands are used to fully separate channels
2 Time Division Multiple Access (TDMA) is where each user accesses the full frequency channel but for only a fraction of the time and on a periodic basis This means that rather than having a carrier for each user, only one carrier is required To demultiplex the desired signal, the receiver is simply switched on only during the transmission of the desired signal Strong synchronisation is therefore needed between users, BSs, and MSCs Most practical TDMA systems, use FDMA and TDMA together (see Figure 2 13 (b)) i e the entire available bandwidth is not used by a single user, rather it is split into frequency channels which are then each time division multiplexed

3 Code Division Multiple Access[1] (CDMA) is the most complicated method of the three Each user uses all of the bandwidth like TDMA for the whole duration of the call like FDMA The information signal is mixed with a pseudo random spreading code resulting in a "noise" signal containing the information signal If the receiver knows the spreading code then it can extract the information from the signal Because the spreading code is pseudo random, CDMA is very secure

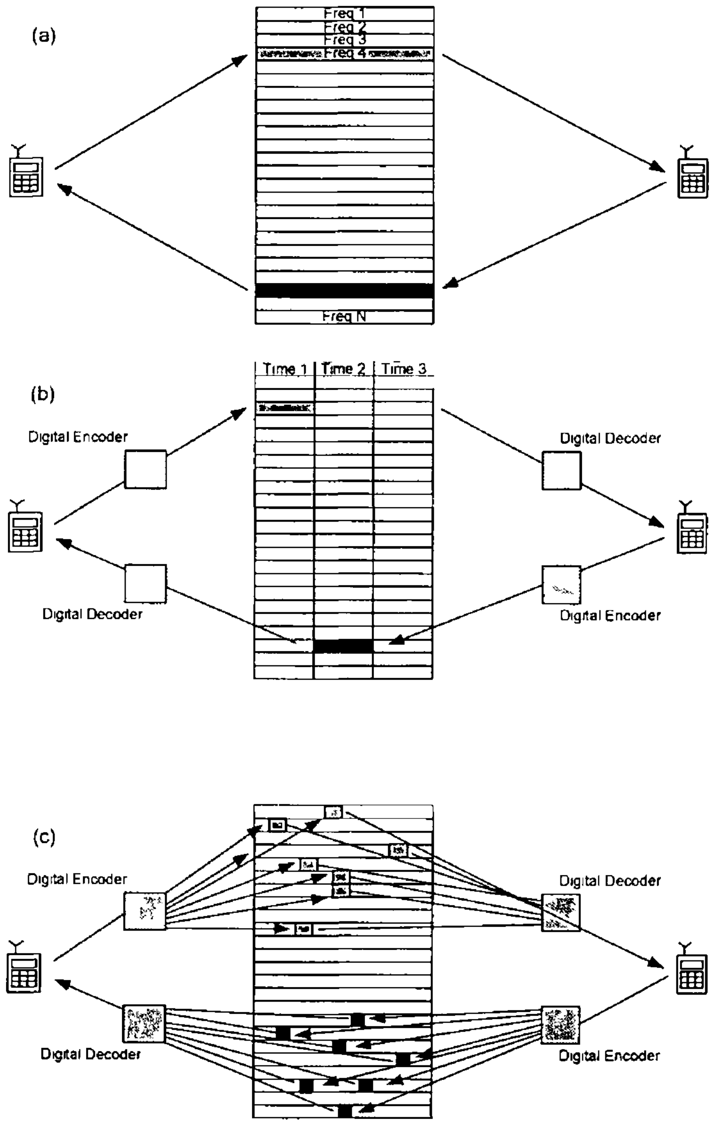

Figure 2 13 – Multiple access techniques (a) FDMA, (b) TDMA, (c) CDMA

[1] Also known as Direct Sequence Spread Spectrum Multiple Access (DS/SSMA)

2 2 6 – The Downlink

The radio signal which has been transmitted is processed at the MSC before being transmitted on the downlink The downlink is basically a mirror image of the uplink which has just been described It begins with the modulation of the data onto a laser located at the MSC The optical carrier is transmitted over optical fiber and arrives at the desired BS The detector at the BS converts the optical signal back to an electrical one which is then fed into the transmitting antenna The signal propagates over air to the desired MS which processes it and outputs it to the user The technique of duplexing allows the data to transfer on the uplink and the downlink simultaneously

2.3 – Network Architectures

Having discussed the different components of the HFR system, it is now apt to describe some of the different network architectures and topologies which have been discussed These include

- Baseband feeder – The baseband data signal is transmitted over fiber and up-converted at the antenna unit [44] This architecture has the most complex BS
- Intermediate Frequency (IF) Feeder – In this architecture some of the complexity is removed from the BS by upconverting to an IF (with a frequency around 1 GHz) at the MSC and then having Intermediate Frequency to Radio Frequency (IF/RF) upconversion at the BS [45]
- Microwave/Millimeter-Wave Feeder – The end signal is generated at a central site with fiber distribution to the cells In the microwave feeder the frequency of operation is less than 10 GHz and hence standard optical components will suffice For mm-wave (frequency of operation > 10 GHz), expensive optical equipment is required [46]

A novel technique which has been proposed for use in picocells, where high signal power is not required is the use of the passive picocell [19] These were first shown by Wake *et al* in 2000 Rather than using standard electro-optical conversion equipment they use a single unbiased Electro-Absorption Modulator (EAM), which provides conversion for both the uplink and downlink Each architecture has it's specific advantages and disadvantages but the Microwave Feeder using standard components is the method we employed due to it's simple BS

Aside from the numerous different architectures which are possible in HFR, there are also a number of network topologies available for use These are usually defined as a combination of two standard topologies split into and optical part and a wireless part For example the most commonly used topology in HFR cellular networks is known as "optical star[1] to radio cellular" [22] This means that the optical part of the network (i e CS to many BSs) uses a star topology and the wireless part of the network uses a cellular topology

2.4 – Conclusion

This chapter has discussed the three stations of the generalised HFR system, and the processing required for transmission The important components at each station were also discussed before giving an overview of some of the HFR system architectures and network topologies which have been proposed While an overview of the laser diode was included in this chapter, the following chapter will discuss in much greater detail, aspects of the laser diode which are of vital importance in a HFR system

[1] Star topology is where a central hub transmits different signals on separate paths

References

[1] J De Vriendt, P Laine, C Lerouge, X Xiaofeng, "Mobile network evolution a revolution on the move", *IEEE Communications Magazine*, vol 40, pp 104 –111, April 2002

[2] S Hunzinker, "Low Cost Fiber Optic Links for Cellular Remote Antenna Feeding", in *HFR Technologies for Mobile Communication Networks,* by Hamed Al-Raweshidy, Shozo Komaki, Artech House, Boston 2002

[3] H S Al-Raweshidy, S O Ampem-Darko, "WCDMA-Based HFR System Performance with Multiple-User Interference in Multiple Service Transmission", IEE 3G Mobile Communication Technologies Conference 2001, pp 152 – 155, 2001

[4] S Hunziker and W Baechtold, "Cellular remote antenna feeding Optical fiber or coaxial cable?", *Electronics Letters,* vol 34, no 11, 1998

[5] R Steele, C -C Lee, P Gould, *GSM, cdmaOne, and 3G Systems,* Wiley, 2001

[6] D Wake, C R Lima, P A Davies, "Optical Generation of Millimeter-Wave Signals for Fiber-Radio Systems Using a Dual-Mode DFB Semiconductor Laser", *IEEE Transactions on Microwave Theory and Techniques,* Vol 43, pp 2270 – 2276, Sept 1995

[7] D J Goodman, *Wireless Personal Communications Systems,* Addison-Wesley, 1997

[8] G Calhoun, *Digital Cellular Radio*, Artech House, 1998

[9] S Haykin, *Communication Systems (4^{th} Edition),* Wiley, 2001

[10] K Feher, "1024-QAM and 256-QAM Coded Modems for Microwave and Cable System Applications" *IEEE Journal on Selected Areas in Communication,* Vol , No 3 , April 1987

[11] E Dahlman, B Gudmundson, M Nilsson, A Skold, "UMTS/IMT-2000 based on wideband CDMA", *IEEE Communications Magazine*, vol 36 , pp 70 –80, Sept 1998

[12] T S Rappaport, *Wireless Communications - principles and practice*, Prentice Hall PTR, New Jersey 1996

[13] W C Y Lee, *Mobile Cellular Telecommunications – analogue and digital systems*, McGraw-Hill, 1995

[14] V K Garg *et al* "Wireless and Personal Communications Systems", Prentice Hall PTR, Upper Saddle River 1996

[15] B Sklar, "Rayleigh Fading Channels", in *The Mobile Communications Handbook (2nd Edition)*, by Jerry D Gibson, CRC Press, 1999

[16] R Steele, "Introduction to Digital Cellular Radio", in *Mobile Radio Communications (2nd Edition)* by Raymond Steele and Lajos Hanzo, Wiley, 1999

[17] M D Yacoub, "Cell Design Principles", in *The Mobile Communications Handbook (2nd Edition)*, by Jerry D Gibson, CRC Press, 1999

[18] R E Schuh, C Schuler, M Mateescu, "An Architecture for Radio-Independent Wireless Access Networks", *Proceedings 49th IEEE Annual International Vehicular Technology Conference, VTC'99*, vol 2, pp 1227 - 1231, May 1999

[19] D Wake, D Johansson, D G Moodie, "Passive picocell a new concept in wireless network infrastructure" *Electronics Letters*, vol 33 no 5, pp 404 –406, 1997

[20] P B Kenington, "Linearised transmitters an enabling technology for software defined radio", *IEEE Communications Magazine,* vol 40, pp 156 – 162, Feb 2002

[21] R Steele, "Microcellular Radio Communications", in *Mobile Radio Communications (2nd Edition)* by Raymond Steele and Lajos Hanzo, Wiley, 1999

[22] Eurescom Project P816-PF, Implementation Frameworks for integrated Wireless-Optical Access Networks, Deliverable 4
http //www eurescom de/public/projects/P800-series/p816/

[23] A Rogers, *Understanding Optical Fiber Communication*, Artech House, 2001

[24] G Keiser, *Optical Fiber Communication (2nd Edition),* McGraw-Hill, 1991

[25] W Culshaw, "Further Considerations on Fabry-Perot Type Resonators", *IEEE Transactions on Microwave Theory and Techniques,* vol 10, pp 331 –339, Sept 1962

[26] T Nakagami, T Sakurai, "Optical and Optoelectronic Devices For Optical Fiber Transmission Systems", *IEEE Communication Magazine*, vol 26, pp 28 –33, Jan 1988

[27] J Gowar, *Optical Communication Systems,* Prentice Hall, 1984

[28] T P Lee, C -E Zah, "Wavelength-tunable and single-frequency semiconductor lasers for photonic communication networks", *IEEE Communication Magazine*, vol 27, pp 42 –52, Oct 1989

[29] G Morthier, P Vankwikelbergre, *Handbook of Distributed Feedback Laser Diodes*, Artech House, 1997

[30] S Personick, , "Fiber optic communication - A technology coming of age", *IEEE Communication Magazine*, vol 16, pp 12 –20, Mar 1978

[31] D Keck, , "Fundamentals of optical waveguide fibers", *IEEE Communication Magazine*, vol 23, pp 17 –22, May 1985

[32] H D Young, *University Physics (9th Edition)*, Addison-Wesly, 1997

[33] S Nagel, , "Optical fiber – The expanding medium", IEEE Communication Magazine, vol 25, pp 33 –43, Apr 1987

[34] J Senior, *Optical Fiber Communication Principles and Practice*, Prentice Hall 1985

[35] J Midwinter, "Optical fiber communication systems development in the UK", *IEEE Communication Magazine*, vol 20, pp 6 -11, Jan 1982

[36] J Hecht, *Understanding Fiber Optics (4th Edition)*, Prentice Hall, 1999

[37] R Guenther, *Modern Optics*, Wiley, 1990

[38] G P Agrawal, *Nonlinear Fiber Optics*, Academic Press, 1989

[39] F Zernike, J Midwinter, *Applied Nonlinear Optics*, Wiley, 1973

[40] R Boyd, *Nonlinear Optics*, Academic Press, 1992

[41] S Bourgeois, "Fiber-based Components Meet EDFA demands", *WDM Solutions*, March 2001

[42] P E Green, Jr , *Fiber Optic Networks*, Prentice Hall, 1993

[43] B P Paris, "Access Methods", in *The Mobile Communications Handbook (2nd Edition)*, by Jerry D Gibson, CRC Press, 1999

[44] K Kojucharow, M Sauer, H Kaluzni, D Sommer, and C Schaeffer, Experimental investigation of WDM channel spacing in simultaneous upconversion millimetre-wave fiber transmission system at 60 GHz band, IEEE MTT-S International Microwave Symposium, Boston, Digest pp 1011-1014, June 2000

[45] R E Schuh, D Wake, B Verri, M Mateescu, "Hybrid Fiber Radio Access A Network Operators Approach and Requirements", *Proceedings of the 10th Microcoll Conference, Microcoll '99*, pp 211 – 214, 1999

[46] R E Schuh, "Hybrid Fiber Radio for Second and Third Generation Wireless Systems", *International Topical Meeting on Microwave Photonics 1999, MWP'99*, post deadline papers, pp 9-12, 1999

Chapter 3 – Directly Modulated Laser Diodes for Hybrid Fiber Radio Systems

3.1 – Modulation of a Laser Diode

There are essentially only four parameters of light that can be modulated They are the power, frequency, phase and polarisation [1] All of these can have analogue or digital data modulated onto them This work involves modulating the power (or amplitude) of the optical signal Generally for analogue data, the term "modulation" is added to the parameter to name the type of modulation With digital data, it is common practice to use the term "shift keying" For example, using analogue data to modulate the frequency of the light is known as Frequency Modulation (FM), and using digital data to modulate the phase of the signal is known as Phase Shift Keying (PSK)

3 1 1 – External Modulation

In general, there are two techniques which can be used to modulate the optical output from a laser The first method is called external modulation This is where the laser is driven by a direct current (dc) only and therefore emits continuous wave (CW) light This CW light is then modulated by the data signal using a device called an external modulator The most common form of external modulators are known as intensity modulators In an external intensity modulator the light is split into two paths of different length By applying an external voltage source to one of the paths, the refractive index of the path can be changed which causes a phase shift in the propagating light Variation of the phase can be used to cause either constructive or destructive interference between the two paths and hence can be used to modulate the light There are a few different types of external modulator available but the most common is the Mach Zehnder Modulator (MZM)

3 1 2 – Direct Modulation

The second method of modulation is known as direct modulation In direct modulation the data signal is superimposed on the dc bias current using a device known as a bias tee This means that the driving current and hence the output light, varies with the input data [2]

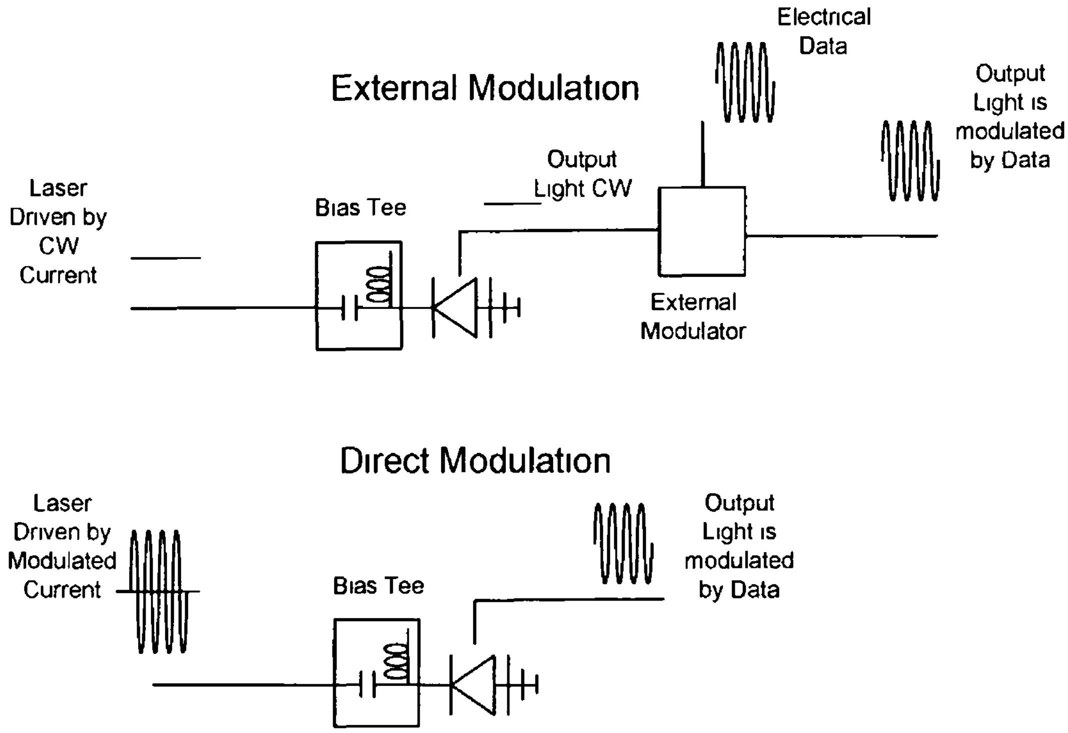

Figure 3 1 – Direct and external modulation

3.2– Laser Characterisation

The characteristics of a laser diode are extremely important as they decide what applications the device is suitable for and there are two main groups The static characteristics include any characteristic which is taken while the laser is being driven with a dc current only Examples include the light-current curve, the optical spectrum of the laser, temperature dependence and noise characteristics Dynamic characteristics on the other hand include any characteristic which involves modulation of the laser Examples are turn-on delay, rise-time, overshoot and the intensity modulation response Some of these characteristics are more important to this work than others and they will be discussed in further detail below

3 2 1 – Optical Power vs. Current Curve

The Power vs Current (PI) curve essentially describes how much light power is emitted from the laser for a given bias current As can be seen from the figure below, for low currents the laser does not emit much light and an increase in current only gives rise to a small increase in output power The light that is emitted is due to spontaneous emission Once the current reaches a certain threshold level, stimulated emission starts to dominate and amplification begins in the cavity At bias currents above threshold a small increase in current gives rise to a large increase in power [3] The threshold current of a laser is typically somewhere between 10 mA and 30 mA The linearity of the PI curve is extremely important when using direct modulation This linearity will be discussed in section 3 3

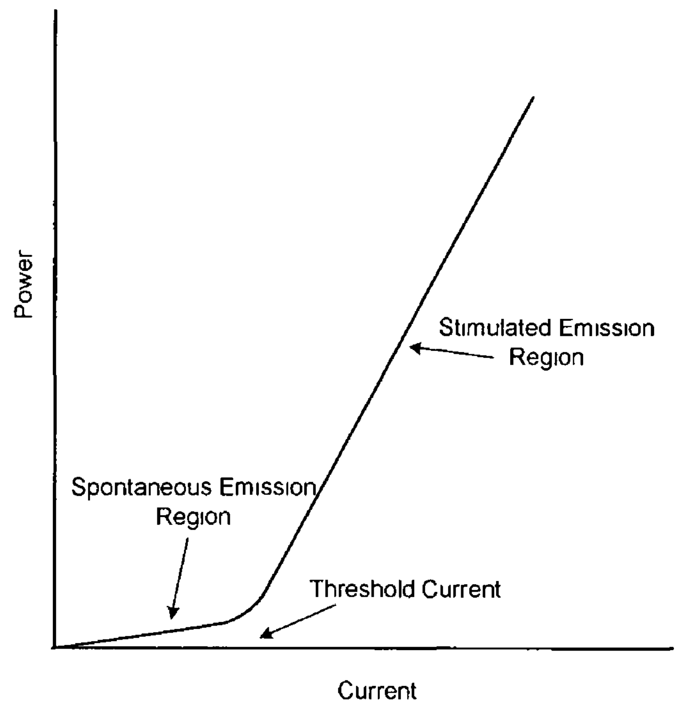

Figure 3 2 – A generalised PI curve

When using direct digital modulation, the laser is biased at a value such that a logical '0' reduces the drive current close to threshold, hence the power in the output light will be low Conversely a logical '1' will increase the bias current into the stimulated emission region of the PI curve meaning that a much higher power of light will be output Direct analogue modulation requires a bias current which ensures that the current stays above threshold for the entire period of the signal If sufficient bias is not used, clipping of the data signal occurs, causing serious distortion of the signal Clipping is where the peaks of the signal are cut off due to the laser being driven below threshold and is illustrated in Figure 3 3c

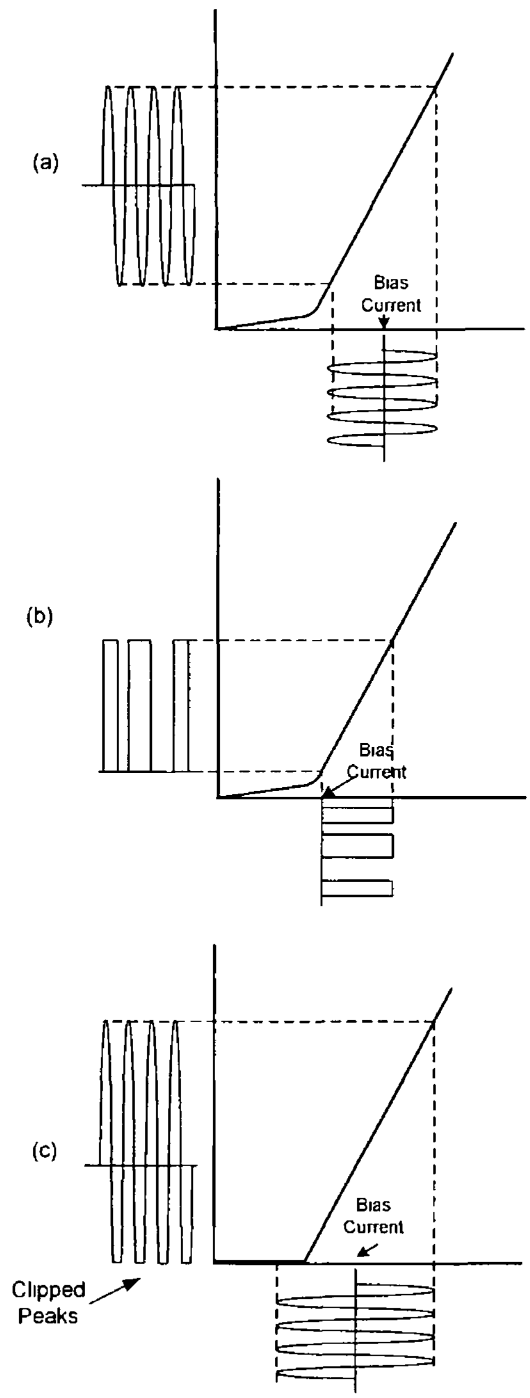

Figure 3 3 – PI Curves with (a) analogue and (b) digital modulation (c) shows the clipping of an analogue signal

3 2.2 – Optical Spectrum

The optical spectrum shows how the output power is distributed in the frequency (wavelength) domain Generally for a standard Fabry Perot (FP) laser there may be a number of 'lines' present in the spectrum which correspond to multiple longitudinal modes The shape of the spectrum depends on the gain curve of the laser and the width of this gain curve is known as the spectral width of the laser [3]

In contrast with a standard multimode FP laser, a Distributed Feed-Back (DFB) laser has a single mode spectrum The dominant mode is referred to as the lasing mode and all others are referred to as side modes The Side Mode Suppression Ratio (SMSR) is the ratio of the output power emitted in the lasing mode to the power in the second strongest mode An SMSR of 30 dB is generally required for optimal single mode operation

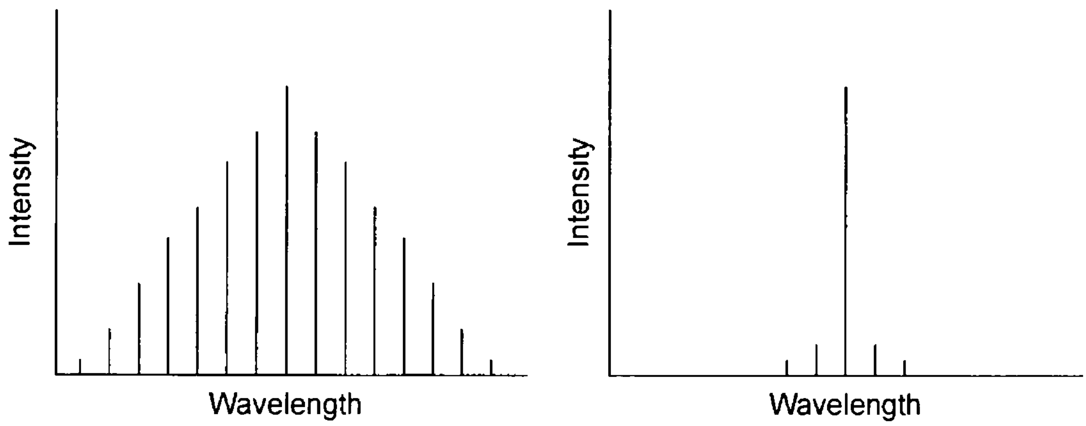

Figure 3 4 – Typical spectra for FP laser (left) and DFB laser (right)

Figure 3 5 shows the optical spectrum of one of the lasers used in this work The laser used was a 1450 nm DFB laser As can be seen it had a SMSR of approximately 45 dBm

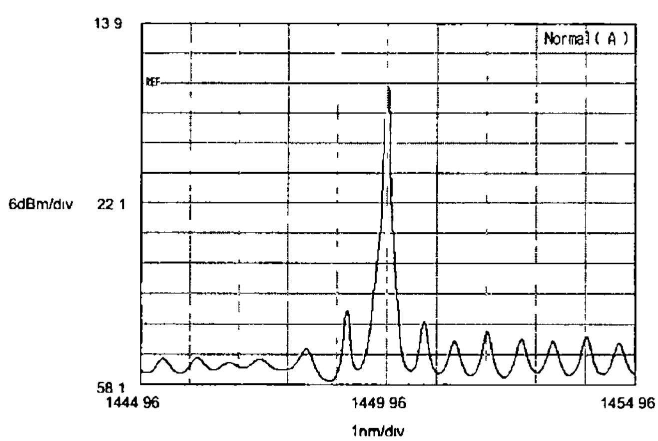

Figure 3 5 – Optical Spectrum of a 1450nm DFB laser

3.2 3 – Intensity Modulation Response

When a laser is directly modulated, the modulated optical power is not the same at all frequencies It is usually fairly constant at low frequencies and then rises to a peak before falling off rapidly The peak is due to resonance caused by interactions between the optical power density and the excess carrier density in the cavity and is known as the resonance peak [3, 4]

The resonance frequency (and hence the modulation bandwidth) increases with increasing bias current according to the following equation [5]

$$f_r = \frac{1}{2\pi}\sqrt{\frac{1}{\tau_p \tau_n}\left(\frac{J}{J_{th}} - 1\right)} \tag{3 1}$$

where J is the driving current density, J_{th} is the threshold current density, and τ_p and τ_n are the photon and electron lifetimes respectively

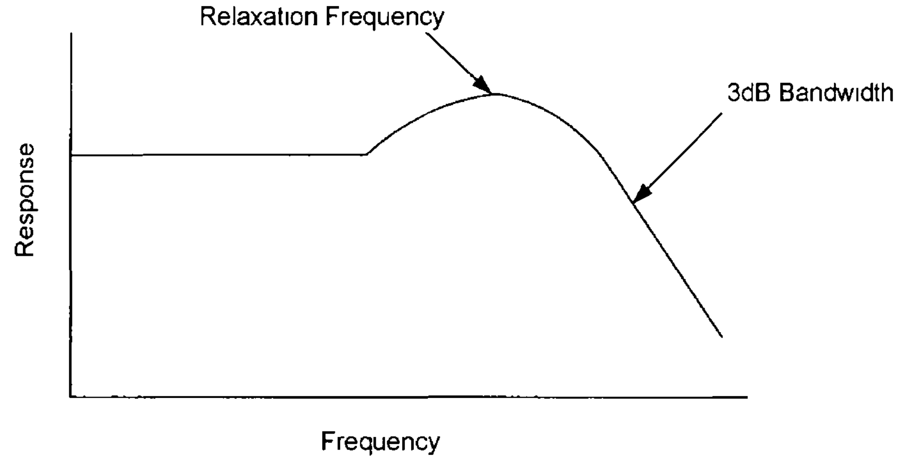

Figure 3 6 – Generalised intensity modulation response of a standard laser

The most important parameter that can be derived from the modulation response is the 3 dB bandwidth which is defined as the frequency at which the amplitude of the modulated signal drops by 3 dB when compared with it's dc value

The measurement of the modulation response of a laser is relatively straightforward and the setup used is shown in Figure 3 7 A network analyser[1] is used which consists of a spectrum analyser and an s-parameter test set The laser under test is

[1] In our case a Agilent 8510B

driven by a −10 dBm tone[1] oscillating around a dc bias A photodetector is then used to detect the output from the laser to and send the captured modulation signal back to the network analyser Test set S_{21} is used to measure the intensity modulation response The network analyser performs a sweep of a range of frequencies and at each frequency it divides the power of the detected electrical signal by the power of the input electrical signal[2] and plots the result

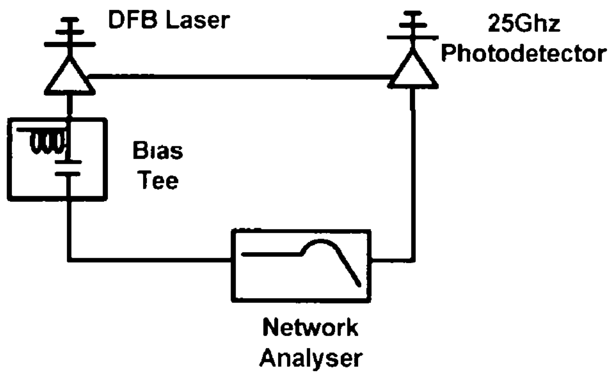

Figure 3 7 – Experimental setup for Intensity Modulation (IM) response measurement

Figure 3 8 shows the response of an actual laser using such a setup The laser used was a 1550 nm DFB laser As can be seen it had a 3 dB bandwidth of approximately 8 GHz when biased at 40 mA

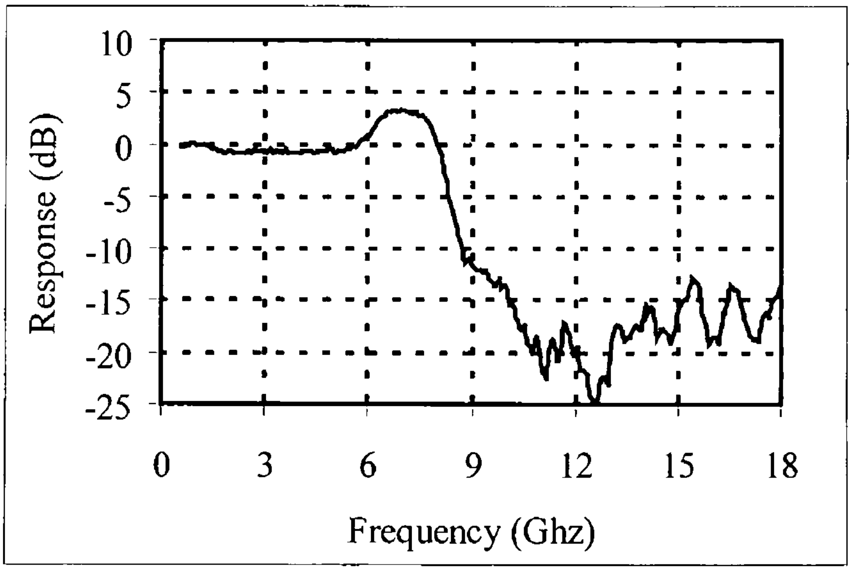

Figure 3 8 – Actual Modulation Response of 1550 nm DFB laser biased at 40 mA

---

[1] from the S parameter test set

[2] which is usually constant at all frequencies

3.3 – Nonlinearities in Laser Diodes

The performance of an analogue optical communication system depends highly on the linearity of the system Nonlinearities in the system result in distortions of the signal and reduce the quality of the received data [6] Many components in an optical system have associated nonlinearities but this work is mainly concerned with laser diode nonlinearity and it is that which will be discussed in detail There are two main types of nonlinearity associated with laser diodes Static nonlinearity refers to the nonlinear relationship between applied current and light output Dynamic nonlinearity refers to the nonlinear response of a laser under modulation Two of the most important effects of these nonlinearities are harmonic distortion and Inter-Modulation Distortion (IMD) These are unwanted products of the transmitted frequencies and can cause serious problems in Hybrid Fiber Radio (HFR) systems

3.3.1 – Static Nonlinearity

As mentioned above, static nonlinearity refers to the nonlinear relationship between applied current and light output Essentially this means that the PI curve is not exactly linear even in the stimulated emission region

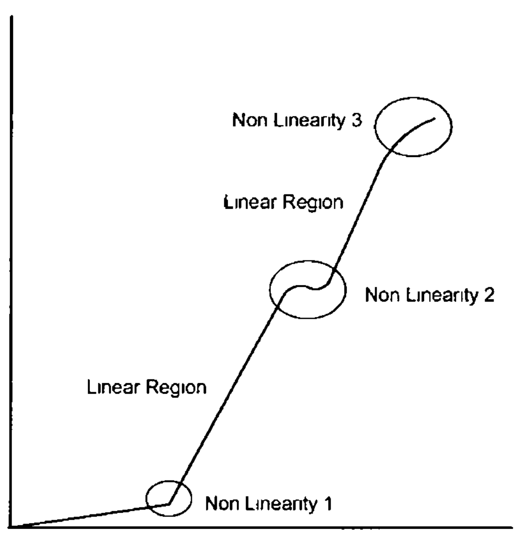

Figure 3 9 – Static nonlinearities

The different types of static nonlinearity are illustrated in Figure 3 9 Nonlinearity 1 is at the point where stimulated emission begins to become more prevalent over spontaneous emission If the applied signal causes the current to enter this region then clipping of the output signal will occur as was shown in Figure 3 3(c) Nonlinearity 2 is a kink in the PI curve The causes of such a nonlinearity in laser diodes are leakage currents [7], gain suppression [8], spatial hole burning [9], and other effects in the active region of the device [3] Nonlinearity 3 is power saturation This can happen at high powers due to the heating of the active layer [10, 11]

Thanks to constantly improving technology, modern lasers do not generally have kinks in their PI curve This means that static nonlinearity is relatively easy to overcome Given that the maximum power to be directly modulated onto the laser is known, then by simply biasing with the correct current, it can be ensured that the drive current neither enters the power saturation region at it's maximum nor the spontaneous emission region at it's minimum [12]

Static nonlinearity is the main nonlinearity that is encountered in low frequency modulation applications such as Cable Television (CATV) In broadband systems however which operate in the microwave range near the relaxation oscillation of the laser diode, dynamic nonlinearity comes to the fore [13]

3 3 2 – Dynamic Nonlinearity

Dynamic nonlinearity is caused by nonlinear interactions between photons and carriers in the laser cavity The nonlinear interactions also result in a peak in the response of the laser diode at modulation frequencies close to its bandwidth [4] The response of the laser depends strongly on the bias current and generally as the bias current increases the relaxation frequency increases hence the linear region is made wider Figure 3 10 shows the generalised response of a laser As can be seen, the laser operates linearly over low frequencies As the frequency of modulation increases however, the response becomes nonlinear as it reaches it's relaxation oscillation frequency If a laser is to be operated at frequencies which lie in the nonlinear region of the laser response, then serious distortion can be introduced into the system, reducing the performance considerably [14, 15]

In the paragraph above and throughout the remainder of this work we have in essence equated the nonlinearity of the device and the nonlinearity of it's modulation response It is important to note that such an equation is not strictly correct For example an RF amplifier with a perfectly flat modulation response can still suffer from IMD With a laser, the intrinsic nonlinearity (from which the IMD products originate), is caused by the interaction of the carriers and electrons in the laser cavity It so happens that this interaction is what also causes the relaxation oscillation peak in the laser's modulation response So the worst intermodulation products occur at the relaxation frequency of the modulation response and are reduced when the relaxation peak is reduced It therefore simplifies the description of the situation to say that by linearising the modulation response, we reduce the intermodulation distortion

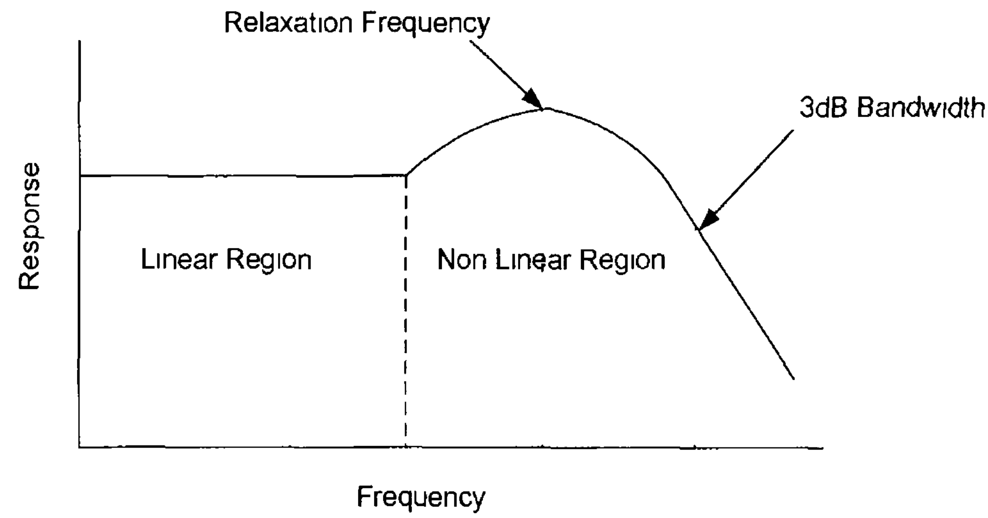

Figure 3 10 – Generalised modulation response of a laser diode showing linear and nonlinear regions

3 3 3 – Harmonic and Intermodulation Distortion

Distortion is classified as either linear or nonlinear Linear distortion includes processes that may change the level or phase of a signal or its individual frequency components, but not add any new components In multiple carrier systems such as Sub-Carrier Multiplexing (SCM), the nonlinearities mentioned in the previous section cause the generation of frequency components at undesirable locations in the frequency spectrum Harmonic distortion is where the unwanted frequency components are generated at integer multiples of the transmitted components Generally, at high modulation frequencies, these multiples occur out of the frequency band of interest so they can usually be ignored or easily filtered out [16, 17] IMD on the other hand, is not harmonically related to the input signal It is where new frequency components are generated at the sum and difference of integer multiples of the transmitted frequencies As can be clearly seen from Figure 3 11 below, these components lie in-band and will interfere with adjacent channels [13, 16, 18, 19]

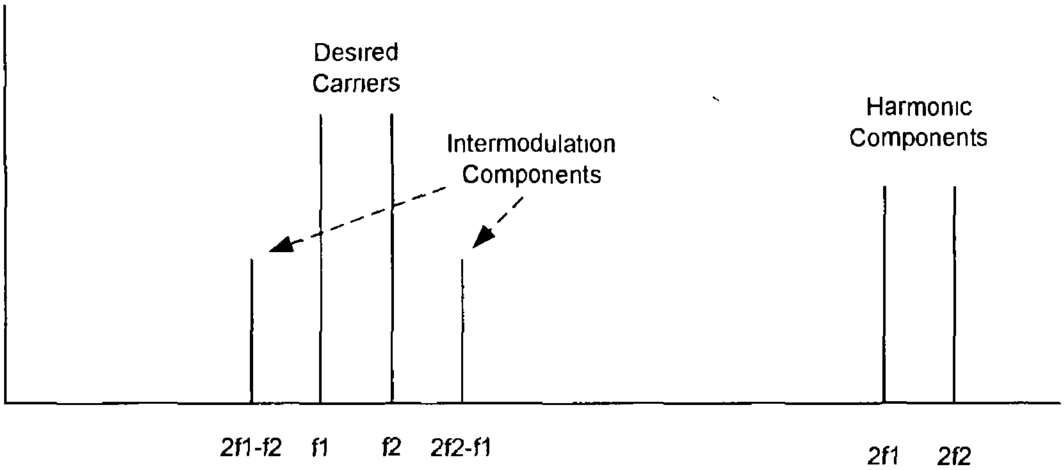

Figure 3 11 – Harmonic and intermodulation distortion

Distortion or mixing between two frequency components, f_1 and f_2, occurs at $|mf_1 \pm nf_2|$ where m and n are non negative integers Hence, these products will be harmonic components where either m or n are equal to zero, and intermodulation components otherwise Generally only odd-order IMD components are considered This is because, like harmonic components, even-order IMD components generally lie out of band In Figure 3 11 the intermodulation components are 3rd order components 5th order components would lie either side of these and so on

There are many ways to characterise the linearity and distortion characteristics of a device but two tone IMD measurement is the most common In this technique two sine waves are applied to the Device Under Test (DUT) The ratio (in dB) of either input tone to the worst third-order (or higher) intermodulation product is an indication of the linearity of the device at that frequency It is not yet known to any degree of certainty how the performance of a device under test using two sine waves, correlates to it's performance when complicated digital signals are employed [20]

3.4– Improving Linearity

The simplest and most cost efficient technique of opto-electrical conversion is the direct modulation of the laser However due to the nonlinearities mentioned above, systems using direct analogue modulation of the laser at frequencies around the resonance peak of a laser diode can suffer serious degradation In particular, SCM systems experience interference between channels due to IMD Looking at Figure 3 10 it can be seen that at frequencies which approach the bandwidth limit of the laser it's modulation response becomes nonlinear It stands to reason then that if it is possible to increase the bandwidth of the laser, then the linear region will also be increased

Much effort has been made to enlarge the intrinsic modulation bandwidth including sophisticated fabrication techniques and broadband matching techniques However, this results in an increase of cost and complexity of the lasers As was mentioned previously, increasing the bias current driving the laser increases the relaxation frequency and hence the bandwidth of the laser Theoretically they could be increased indefinitely However high bias currents cause facet damage and faster obsolescence of the source and so this technique is not very suitable Another method of increasing the bandwidth is to use a technique known as external light injection

3 4 1 – Light Injection

By coupling light from an external laser (known as the master) back into the cavity of the laser under modulation (known as the slave), it is possible to increase the bandwidth significantly and hence increase the frequency up to which the laser operates linearly [21] While the master laser can be a fixed wavelength laser, the development of the tunable laser really allowed this technique to take off The difference between the wavelength of the slave and master laser is known as the detuned wavelength The ideal detuned wavelength for optimum bandwidth enhancement varies for each specific laser It usually lies inside a range of few gigahertz either side of the slave laser's operating wavelength The physical reason for the increase in modulation bandwidth has not yet been fully investigated It has been suggested, however that it may be related to the coherent coupling of the two optical fields inside the laser cavity

The first work in the area of external light injection began in the late '70s and early '80s It was noted that by coupling light from an external source back into the cavity that the static and dynamic characteristics of the laser could be changed [22, 23] Since then there has been detailed work done on each of the different effects of light injection for example linewidth narrowing effects [24], frequency chirping effects [25], and noise effects [26, 27] From 1991 onwards many groups began to report simulations which predicted large increases in modulation bandwidth [30-32] by coupling light from an external source into the device, but it was not until 1998 that Meng *et al* showed the first experimental demonstrations and achieved a bandwidth enhancement of almost 4 times using external light injection [31]

3 4.2 – Experimental Work on External Light Injection

In our work we were not concerned so much with increasing the bandwidth to very high frequencies but rather with linearising the response at frequencies which would be nonlinear using a free running directly modulated laser diode In Figure 3 12 you can see the experimental set up that was used to examine the enhancement of modulation bandwidth using external injection

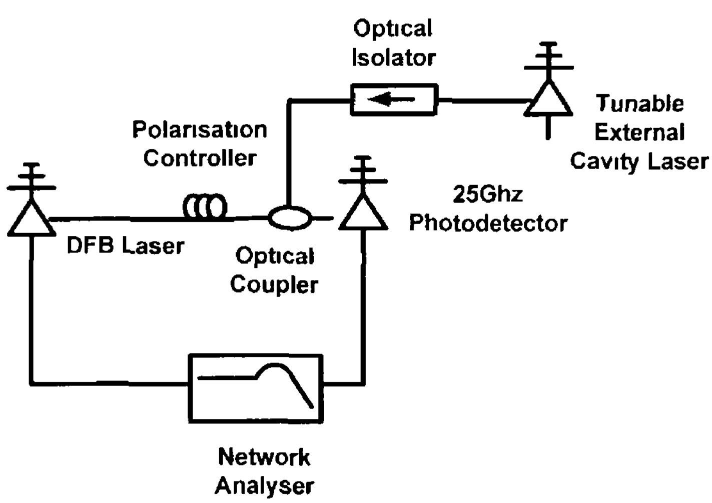

Figure 3 12 – Experimental setup for bandwidth enhancement

As far as the measurement of the modulation response is concerned the setup is very similar that used in section 3 2 3 In this case the extra components which are needed for external injection are added Two different DFB lasers from NTT Electronics

(NEL) were examined as slave lasers The first (KELD1451CCC) had a central lasing wavelength of 1450 nm and a threshold current of approximately 10 mA It had an intrinsic bandwidth of about 7 GHz when biased at 30 mA The second laser (KELD1551CCC) had a central lasing wavelength of 1553 nm and a threshold current of 26 mA It had an intrinsic bandwidth of about 8 GHz when biased at 40 mA The slave laser is directly modulated with a sine wave from the network analyser Again, the network analyser used was a Hewlett Packard 8510C

The master laser used in this work was a tunable External Cavity Laser (ECL) from Agilent[1] It had a wavelength tuning range from 1400 nm to 1600 nm over which it's maximum output power was 7 dBm ECLs usually have a simple FP laser as their active section, and have a resonant cavity external to this FP lasers are multimode devices and as was discussed previously, some form of feedback can force them into single mode operation Tuning is provided by a mechanically tunable diffraction grating which also acts as one of the cavity mirrors When the mirror is rotated it changes the wavelength of the light reflected back into the cavity as well as the cavity length and this changes the wavelength of the single mode output [32]

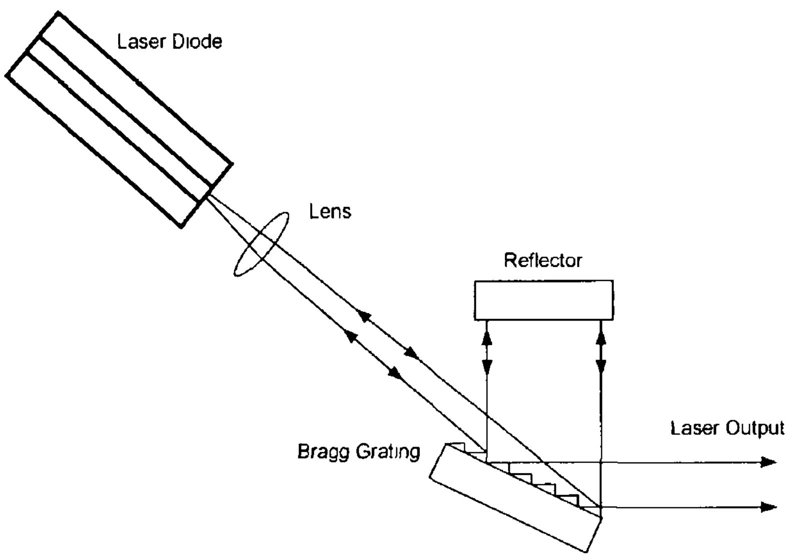

Figure 3 13 – External Cavity Laser

The ECL is used to channel light back into the slave laser's cavity through one arm of a 50 50 optical coupler The optical isolator prevents back reflections and scattered light from reaching the ECL and the polarisation controller is used to

[1] Agilent 8168F Tunable laser source

optimise the coupling by varying the polarisation of the injected light The propagated optical signal is detected using a 25 GHz New Focus photodetector with a responsivity of 0 4 A/W and received signal is then fed back into the network analyser

Figure 3 14 below shows the optical spectrum of the 1450 nm laser under external injection It is clearly seen that the laser remains in single mode operation even under these conditions This fact becomes important in the simulation work described in later sections, as the model for a single mode laser is significantly different from that of a multimode laser

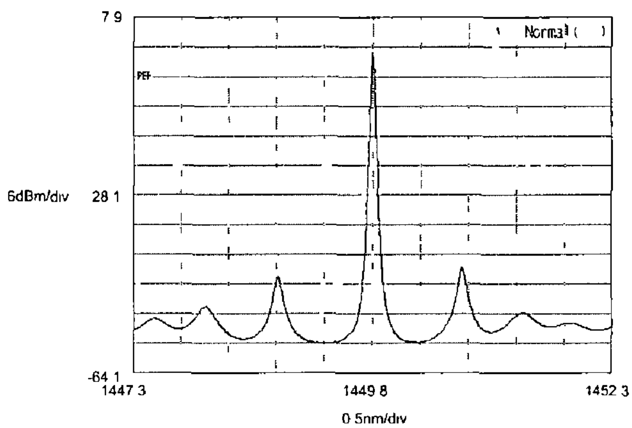

Figure 3 14 – The optical spectrum of the 1450nm laser subject to external injection

Figure 3 15 and Figure 3 16 show the results of the linearisation using external injection of the 1450 nm and 1553 nm DFB lasers respectively In Figure 3 15, it can be seen that the 3 dB bandwidth has been increased from approximately 6 5 GHz to around 9 5 GHz with an injection level of 3 mW from the ECL More importantly the linearity of the response in the frequency range from 4 to 8 GHz has improved drastically This linearisation is the basis for the experiments detailed in Chapter 4 In Figure 3 16, it can be seen that the 3 dB bandwidth has been increased from approximately 8 GHz to around 11 GHz and again the linearity of the response has improved drastically This plot is the basis for the work detailed in Chapter 5 It will be shown that improving the linearity around the operating frequency gives rise to improved performance in SCM systems

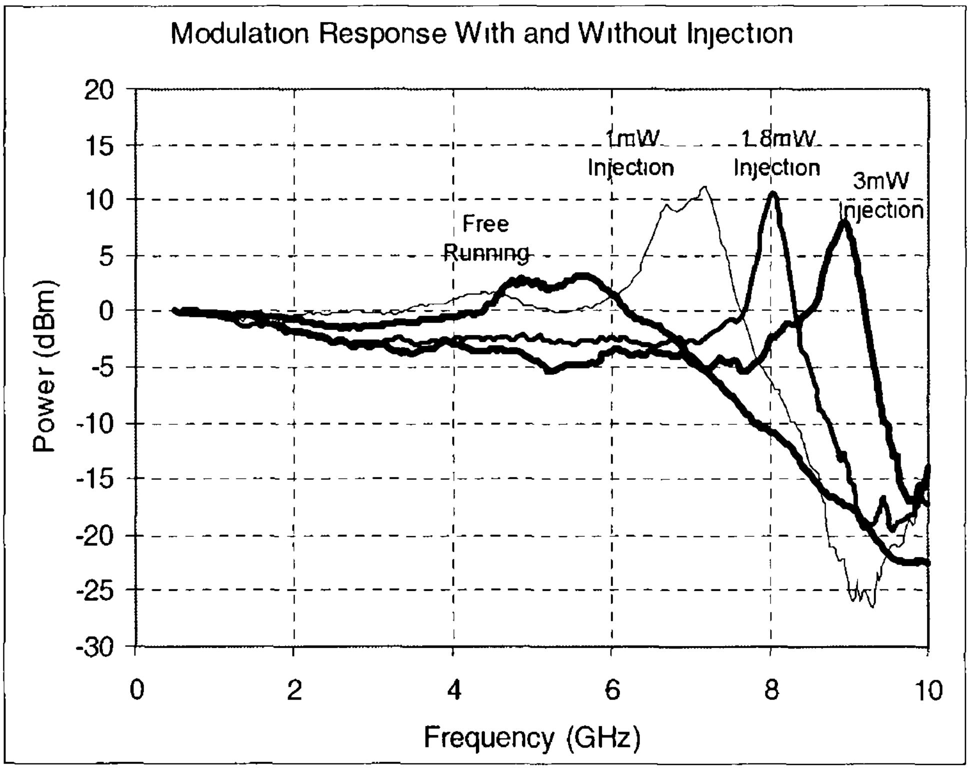

Figure 3 15 – Plot showing experimental bandwidth enhancement of a 1450 nm DFB laser

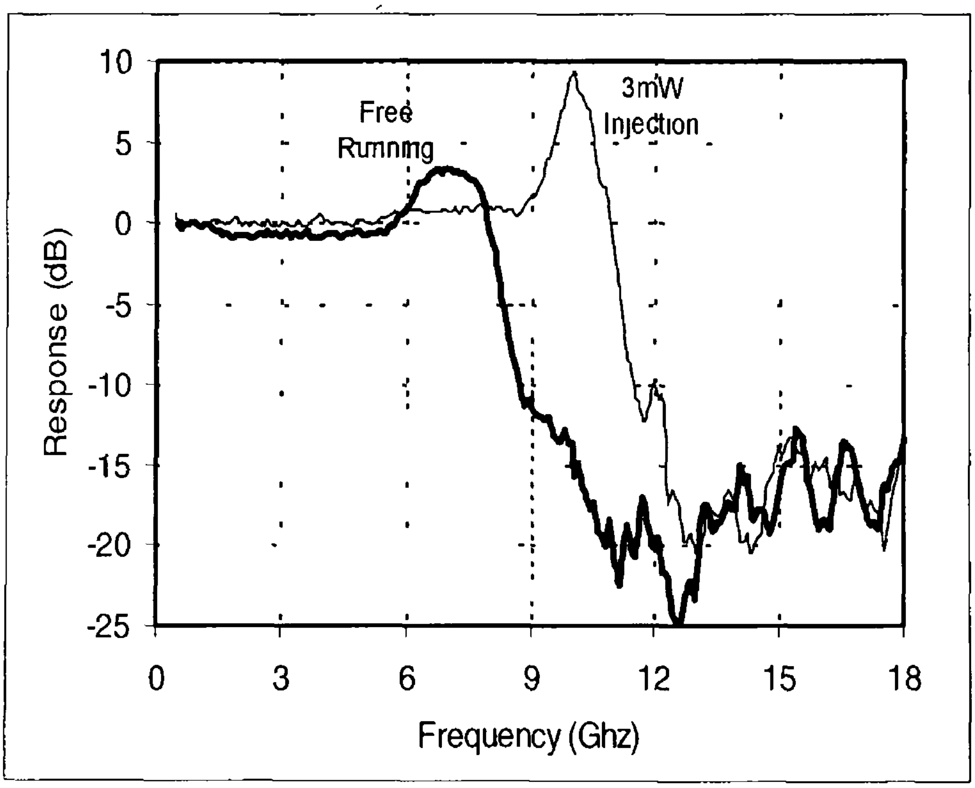

Figure 3 16 – Plot showing experimental bandwidth enhancement of a 1550 nm DFB laser

3.5 – Matlab Model

Due to the number of variables which must be assessed when designing a HFR system, it is vital to use simulations both before and after the actual experimentation [33] This work employed Matlab, a program which is widely used in Electronic Design Automation (EDA) Using Matlab, a model was designed to simulate the laser diode described above and to verify the results obtained It used the laser rate equations to describe the operation of the laser One major advantage of doing a simulation was that the laser parameters could be manipulated which enabled accurate tuning of the modulation response The performance could then be measured with a number of different responses which were easily obtained

3.5.1 – The Free Running Laser Rate Equations

There are many different forms of the rate equations and almost every work has some slight differences The form we used for our free running laser was very similar to those used before normalisation by Le Bihan and Yabre in [13] In an expansion of this paper Yabre neglects the gain compression factor, ε, by assuming that the optical power is moderate enough to allow the approximation $(\varepsilon S << 1)$ and hence $(1-\varepsilon S) \approx 1$ For simplification purposes we also this approximation [30] Many versions of the laser rate equations include noise parameters Again for simplification and because thermal noise in the detector is the dominant noise source in our system, noise in the rate equations is ignored

The single mode rate equations for the free running laser with photon density $S(t)$, corresponding phase $\phi(t)$ and carrier density $N(t)$ used in the model are as follows

$$\frac{dN(t)}{dt} = \frac{I(t)}{qV} - \frac{N(t)}{\tau_n} - g_0\left(N(t) - N_{om}\right)S(t) \tag{3 2}$$

$$\frac{dS(t)}{dt} = \Gamma g_0\left(N(t) - N_{om}\right)S(t) - \frac{S(t)}{\tau_p} + \Gamma\beta\frac{N(t)}{\tau_n} \tag{3 3}$$

$$\frac{d\phi(t)}{dt} = \frac{\alpha}{2}\left(\Gamma g_0 (N(t) - N_{om}) - \frac{1}{\tau_p}\right) - \Delta\omega \tag{3 4}$$

where g_0 is the gain coefficient, τ_p is the photon lifetime, $I(t)$ is the injection current, τ_n is the carrier lifetime, N_{om} is the transparency carrier density, α is the linewidth enhancement factor, q is the electron charge, $\Delta\omega$ is the detuning frequency, V is the volume of the active region, Γ is the optical confinement factor and β is the spontaneous emission factor

3 5 2 – The Laser Rate Equations with External Light Injection

For the injection locked case we added the following terms [29]

$2K_c\sqrt{S_{inj}S(t)}Cos(\phi(t))$ was added to equation (3 3)

$-K_c\sqrt{\frac{S_{inj}}{S(t)}}Sin(\phi(t))$ was added to equation (3 4)

These terms describe the amplitude and the phase of the injected light

Therefore the complete single mode rate equations for injection locked lasers with photon density $S(t)$, corresponding phase $\phi(t)$ and carrier density $N(t)$ used in the model are as follows

$$\frac{dN(t)}{dt}=\frac{I(t)}{qV}-\frac{N(t)}{\tau_n}-g_0(N(t)-N_{om})S(t) \qquad (3\ 5)$$

$$\frac{dS(t)}{dt}=\Gamma g_0(N(t)-N_{om})S(t)-\frac{S(t)}{\tau_p}+\Gamma\beta\frac{N(t)}{\tau_n}+2K_c\sqrt{S_{inj}S(t)}Cos(\phi(t)) \qquad (3\ 6)$$

$$\frac{d\phi(t)}{dt}=\frac{\alpha}{2}\left(\Gamma g_0(N(t)-N_{om})-\frac{1}{\tau_p}\right)-\Delta\omega-K_c\sqrt{\frac{S_{inj}}{S(t)}}Sin(\phi(t)) \qquad (3\ 7)$$

where k_c is the coupling coefficient for the injected light, and S_{inj} is the photon density of the injected light Clearly, by simply setting S_{inj} to zero the equations revert back to the free running case This meant that the same model could be used for the systems employing both free running and injection locked laser

3.5.3 – Rate Equations Explained

The origins of each of the terms in equations (3 5), (3 6), and (3 7) are now investigated in order to obtain an understanding of how each of the terms fit into the overall equations and how the equations help to build up a detailed model of the dynamics of the laser

3 5 3 1 – *Carrier Density Equation*

$$\frac{dN(t)}{dt} = \frac{I(t)}{qV} - \frac{N(t)}{\tau_n} - g_0\left(N(t) - N_{om}\right)S(t)$$

This equation comes about by considering the transitions between higher and lower energy states according to generation and recombination in the cavity

- The $\frac{I(t)}{qV}$ term describes the carrier pumping rate from the fundamental state to the excited state per unit volume This rate increases as the injection current in the active zone is increased and for smaller volumes of the active area due to the higher carrier concentration and confinement achieved
- The $-\frac{N(t)}{\tau_n}$ term accounts for the decrease in carriers in the conduction band due to spontaneous emission
- The $-g_o(N(t) - N_{om})S(t)$ term accounts for the stimulated recombination rate Because it depends both on N(t) itself and S(t), it gives rise to the nonlinear behaviour of the laser The N(t) and N_{om} terms ensure that it only comes into use at and above transparency[1]

3 5 3 2 – *Photon Density Equation*

$$\frac{dS(t)}{dt} = \Gamma g_0\left(N(t) - N_{om}\right)S(t) - \frac{S(t)}{\tau_p} + \Gamma\beta\frac{N(t)}{\tau_n} + 2K_c\sqrt{S_{inj}S(t)}Cos\left(\phi(t)\right)$$

This equation relates photon generation resulting from stimulated and spontaneous decay processes to photon loss resulting from absorption and scattering along the active media and facet coupling to the external media

- The $\Gamma g_0\left(N(t) - N_{om}\right)S(t)$ term accounts for the growth in the photon rate resulting from stimulated emission It is similar to the stimulated emission term from the carrier density equation except for the sign change and the inclusion of the optical confinement factor The sign is changed due to the fact that photons are produced by stimulated emission while carriers on the other hand are lost

---

[1] When the gains equal the losses

- The $-\frac{S(t)}{\tau_p}$ term describes photons which are lost from the cavity These losses result from absorption, scattering and external coupling

- The $\Gamma\beta\frac{N(t)}{\tau_n}$ term is a fraction of the total spontaneous emission term given in the carrier density equation These rate equations are for a single mode laser, but because spontaneous emission occurs in all directions, we denote the amount of spontaneous decay that yields a photon in this mode by assigning a fraction β to the photon equation

- The $2K_c\sqrt{S_{inj}S(t)}Cos(\phi(t))$ term essentially describes how much of the injected light will be coupled into the cavity K_c represents is the coupling coefficient and the rest of the term describes the intensity and phase of the light [23]

3 5 3 3 – The Phase Equation

$$\frac{d\phi(t)}{dt}=\frac{\alpha}{2}\left(\Gamma g_0(N(t)-N_{om})-\frac{1}{\tau_p}\right)-\Delta\omega-K_c\sqrt{\frac{S_{inj}}{S(t)}}Sin(\phi(t))$$

The third rate equation expresses the change in phase of the optical signal as a result of the change in excited state carriers This equation is not necessary if one is restricted to consider amplitude modulation alone, however, it is necessary when the influence of optical feedback or injection is considered as this causes phase modulation also

- The $\frac{\alpha}{2}\left(\Gamma g_0(N(t)-N_{om})-\frac{1}{\tau_p}\right)$ part of the phase equation comes about due to the fact that changes in carrier density change the optical gain This in turn causes changes in the refractive index causing an amount of phase modulation [34]

- The $-\Delta\omega$ term is called the detuning parameter and represents the difference in frequency between the slave laser and the master laser

- The $-K_c\sqrt{\frac{S_{inj}}{S(t)}}Sin(\phi(t))$ term describes the phase and intensity of the injected light Multiplication by $\sqrt{\frac{S(t)}{S(t)}}$ yields $-\frac{K_c}{S(t)}\sqrt{S_{inj}S(t)}Sin(\phi(t))$ which is very similar to the final term in the photon density equation The main difference is due to the separation of the real and imaginary parts which results in the *Sin(φ(t))* in this equation where we had *Cos(φ(t))* in the photon density equation

3.5.4 – Laser Characterisation

The parameters used for the laser model are given in the table below

g_0	1e-12	Δf	-1 1e9
N_{om}	1 4e23	$\Delta\omega$	$2\pi\Delta f$
V	1 1e-17	S_{inj}	varied
τ_p	2e-11	k_c	2 5e11
τ_n	0 3e-9	Ar	03e-12 m^2
Γ	0 35	c	3e8 ms^{-1}
β	0 0	n	3 63
q	1 6e-19	h	6 625e-34
α	6 8	f	1 935e14 Hz
$I(t)$	70e-3	R	0 32

Table 3 1 – Laser Model Parameters

3 5 4 1 – The PI Curve

The first step in the design of the full system model was the characterisation of the Light Current curve Because this is a static characteristic, only dc values are required

I_0 is a known constant which represents the bias current The dc values of photon density, current density and phase can be obtained by letting the left hand side of equations (3 5), (3 6), (3 7) above equal zero Using the relationship,

$Cos^2 A + Sin^2 A = 1$, adding manipulated versions of (3 6) and (3 7), yields the following

$$K_c^2 \frac{S_{inj}}{S_0} = \frac{1}{4}\left[\left(\Gamma g_0(N_0 - N_{om}) - \frac{1}{\tau_p}\right) + \frac{\Gamma\beta N_0}{S_0 \tau_n}\right]^2 + \left[\frac{\alpha}{2}\left(\Gamma g_0(N_0 - N_{om}) - \frac{1}{\tau_p}\right) - \Delta\omega\right]^2 \tag{3 8}$$

Letting the left hand side of Equation (3 5) equal zero and rearranging gives

$$\frac{\frac{I_0}{qV} - \frac{N_0}{\tau_n}}{g_0(N_0 - N_{om})} = S_0 \tag{3 9}$$

Substituting for S_0 in Equation (3 8) yields a quartic equation in N_0 which Matlab can easily solve, giving the dc value for carrier density From this S_0 can then be obtained using Equation (3 9) and ϕ_0 can be obtained from equation (3 6) or (3 7) Once S_0 is known then the power can be found and hence the PI curve can be plotted The full derivation of these equations are given in Appendix B

The equation used to convert photon density into optical power is as follows

$$Pout = \left(\frac{S_0 A_r c}{2\Gamma n}\right) hv(1\text{-}r) \tag{3 10}$$

where S_0 is the steady state photon density, Ar is the area of the active region, c is the speed of light, Γ is the optical confinement factor, n is the refractive index, h is Planck's constant, f is the frequency of the light and R is the reflectivity of the facet

The results of the steady state simulation are shown below Figure 3 17 shows the PI curve of the modelled laser It had a threshold current of approximately 17 mA This will be important in later parts of the simulation work, where it is necessary to ensure that the applied signal did not clip the laser The external quantum efficiency, η_D of a laser diode is defined as the ratio of the increase in photon output rate for a given increase in the number of injected electrons This is essentially the slope of the PI curve The operational efficiency of our simulated laser diode was 0 18 W/A

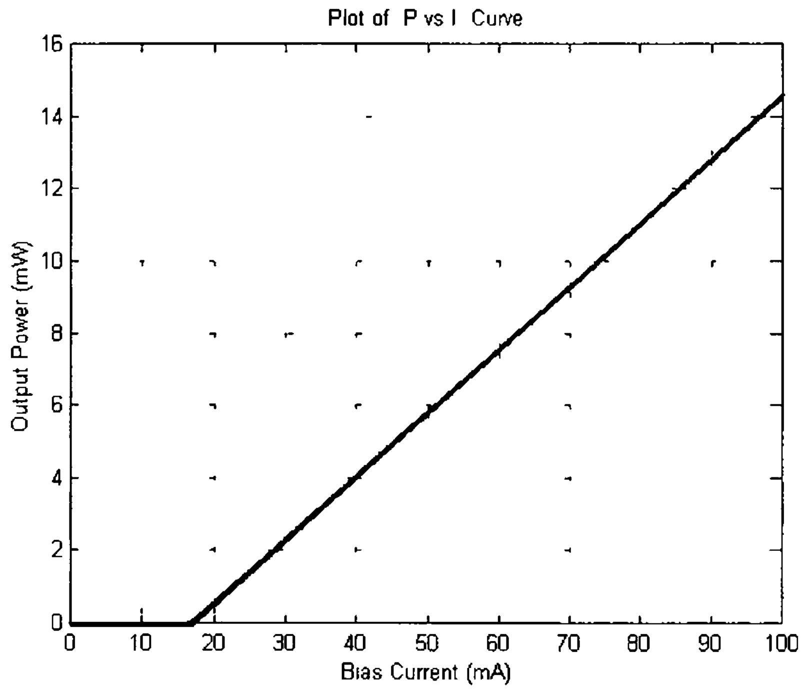

Figure 3 17 – Simulated PI curve

Figure 3 18 shows how the PI curve varies with external injection The *injection ratio* is the ratio of the steady state photon density of the slave laser to the photon density of the injected light It is used as to quantify the external injection throughout the simulation The injection causes the threshold current to decrease and also the operational efficiency to increase With an injection ratio of 0 012 the threshold had reduced to approximately 4 mA and the operational efficiency had increased to 0 4 W/A The reason for the change in threshold is that, due to the extra photons injected into the cavity, less additional photons are needed to overcome losses thereby reducing the threshold An increase in bias current means that there are more free carriers available for recombination The change in operational efficiency comes about because the 'resident' photons in the cavity *and* the injected photons can stimulate these free carriers This means that for the same increase in bias current more light will be emitted in a laser under external injection than in a free running laser

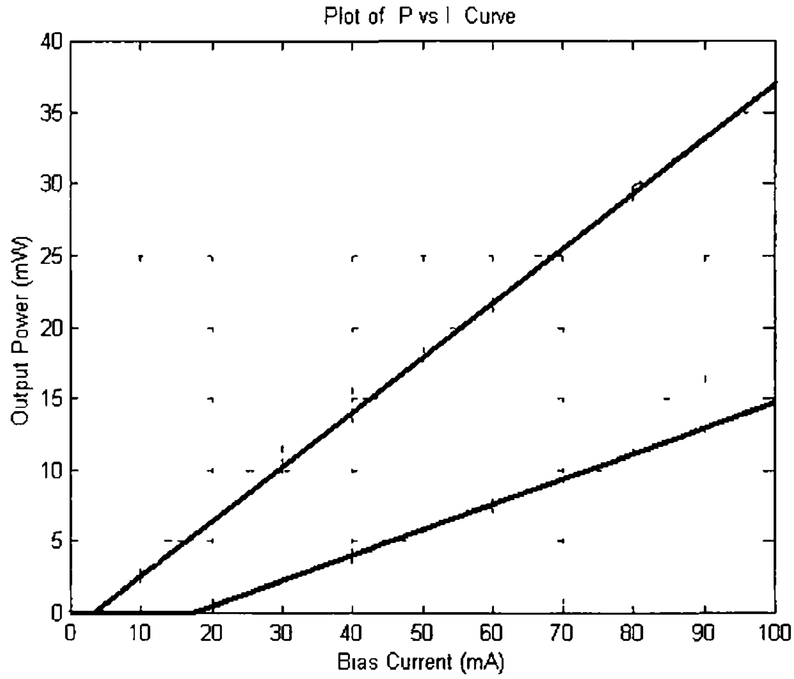

Figure 3 18 – Simulated PI curve with injection

3 5 4 2 – Modulation Response

The next characteristic to be obtained was the intensity modulation response of the laser diode This was obtained using small signal analysis In small signal analysis, time varying components are considered to have a dc part and an ac part The following were substituted into (3 5), (3 6) and (3 7) above

$I(t) = I_0 + \delta I$

$S(t) = S_0 + \delta S$

$N(t) = N_0 + \delta N$

$$\phi(t) = \phi_0 + \delta\phi \qquad (3\ 11)$$

where I_0, S_0, N_0, ϕ_0 are the dc parts, and $\delta I, \delta S, \delta N, \delta\phi$ are the ac parts of the current, photon density, carrier density, and phase, respectively Ignoring the steady state solution and higher order terms yields a set of linearised equations for the ac components of $S(t)$, $N(t)$ and, $\phi(t)$

$$\begin{pmatrix} j\omega + a_{11} & a_{12} & a_{13} \\ a_{21} & j\omega + a_{22} & a_{23} \\ a_{31} & a_{32} & j\omega + a_{33} \end{pmatrix} \begin{pmatrix} \delta N \\ \delta S \\ \delta\phi \end{pmatrix} = \begin{pmatrix} \delta I/qV \\ 0 \\ 0 \end{pmatrix} \qquad (3\ 12)$$

where

$a_{11} = \frac{1}{\tau_n} + g_0 S_0$	$a_{12} = \frac{1}{\Gamma \tau_p} - \frac{X}{\Gamma S_0}$	$a_{13} = 0$
$a_{21} = -\Gamma g_0 S_0$	$a_{22} = \frac{X}{2S_0}$	$a_{23} = 2S_0 Y$
$a_{31} = -\frac{\alpha}{2}\Gamma g_0$	$a_{32} = \frac{-Y}{2S_0}$	$a_{33} = \frac{X}{2S_0}$
$X = 2K_c\sqrt{S_{inj}S_0}Cos(\phi_0)$	$Y = K_c\sqrt{\frac{S_{inj}}{S_0}}Sin(\phi_0)$	

Table 3 2 – Coefficients of the linearised rate equations

All of the steady state values are known and hence the modulation response is then given as $\frac{\delta S}{\delta I}$ Again, the full derivation of these equations are given in Appendix B

Figure 3 19 shows the modulation response of the free running laser with four different dc bias currents As was predicted in section 3 2 3 the relaxation oscillation and hence modulation bandwidth increases with increasing bias It can be clearly seen that the response also reduces Clearly, the bias current could be continually increased to linearise the device In practical systems this is not possible as we have discussed previously 70 mA was found to be the most suitable bias current for our simulation as it gave a similar response to that of the experimental measurements and it also ensured that the laser would not be clipped when modulated

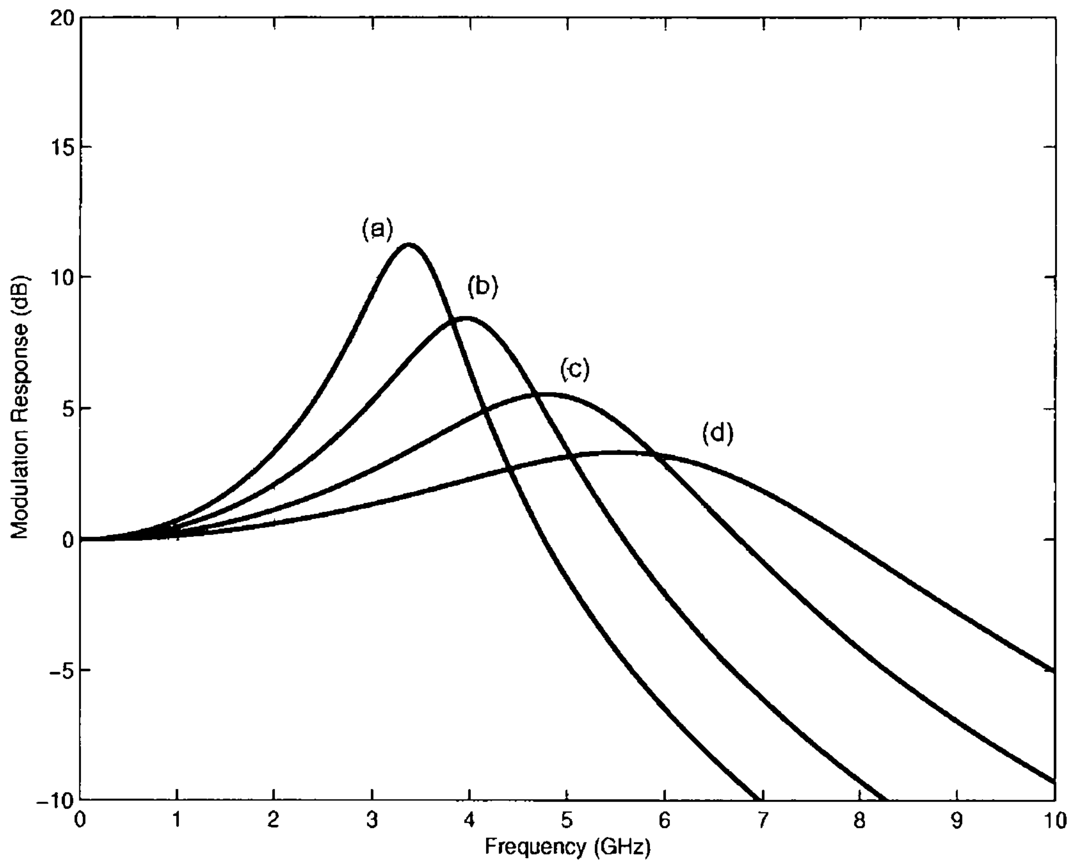

Figure 3 19 – Modulation Response of the laser under different bias conditions (a) 40 mA, (b) 50 mA, (c) 70 mA, (d) 100 mA

Figure 3 20 shows the modulation response of the laser under free running conditions and under three different levels of external light injection The injection ratios in Figure 3 20 were 0 017, 0 025 and 0 045 The free running simulated laser has a 3 dB bandwidth of about 7 GHz It's response is rather nonlinear at frequencies above 2 GHz It can be seen that as the level of external injection is increased the response increases and also becomes more linear at lower frequencies An injection ratio of 0 045 increases the 3 dB bandwidth to almost 16 GHz and in doing so linearises the laser at frequencies up to about 7 GHz The usefulness of this linearisation will be shown in simulated results in chapters 4 and 5

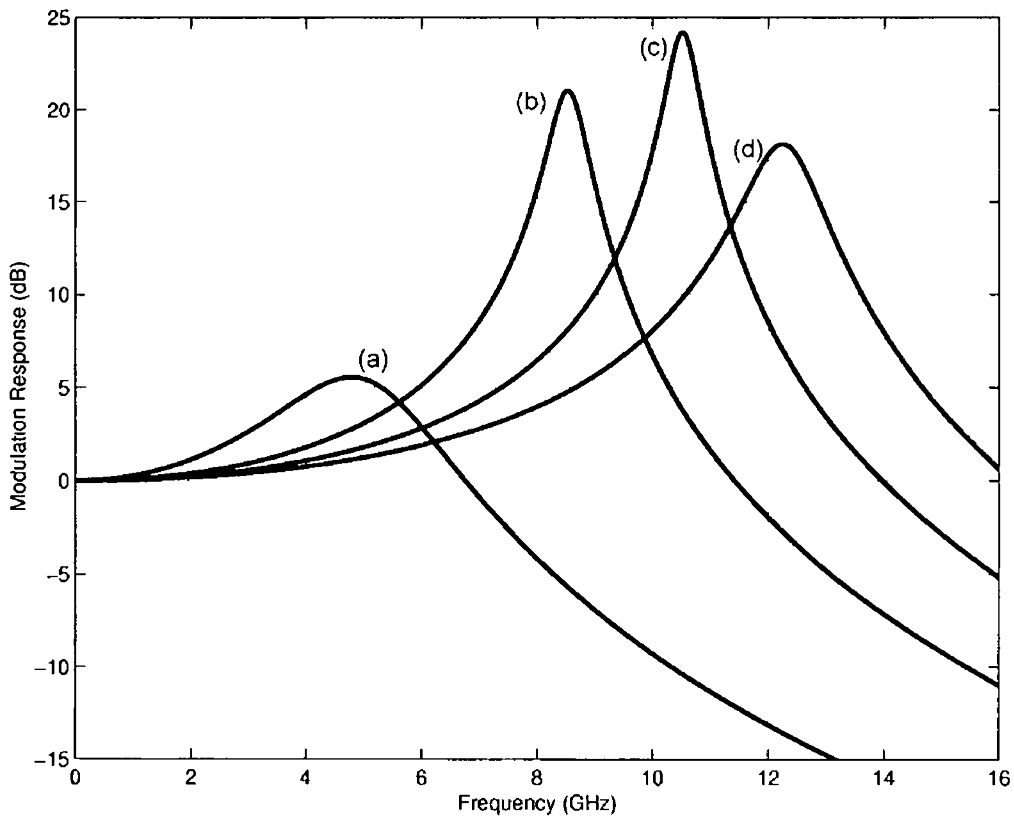

Figure 3 20 – Modulation Response of the simulated laser under free running conditions (a) and with injection ratios of 0 01 (b), 0 025 (c), 0 045 (d) In all cases the bias current was 70 mA

3.6 – Conclusion

This chapter has discussed the use of directly modulated laser diodes in HFR systems Much attention was paid to the linearity problems which are encountered when using these devices The technique of external light injection was described and it was shown that it can be used to increase the bandwidth of a laser and also to linearise the laser at certain frequencies The model of the laser, designed using Matlab was also discussed The next chapter will detail some more experimental work which was carried out This work investigates the problems introduced by the nonlinearity and also attempts to improve the performance by linearising the device using external injection It also includes some expansion work which was carried out on the simulation This involved including the modelled laser described above in a full system model

References

[1] P E Green, Jr , *Fiber Optic Networks*, Prentice Hall, 1993

[2] J Hecht, *Understanding Fiber Optics (4th Edition)*, Prentice Hall, 1999

[3] G Keiser, *Optical Fiber Communication (2nd Edition)*, McGraw-Hill, 1991

[4] G Morthier, P Vankwikelbergre, *Handbook of Distributed Feedback Laser Diodes*, Artech House, 1997

[5] K Y Lau, A Yariv, "Ultra High-Speed Semiconductor Lasers", *IEEE Journal of Quantum Electronics*, vol 21, no 2, 1985

[6] J Senior, *Optical Fiber Communication Principles and Practice,* Prentice Hall 1985

[7] N Dutta, D Wilt, R Nelson, "Analysis of leakage currents in 1 3-μm InGaAsP real-index-guided lasers", Journal of Lightwave Technology, vol 2 no 3, pp 201 – 208, 1984

[8] M Willatzen, A Uskov, J Mork, H Olesen, B Tromborg, A -P Jauho, "Nonlinear gain suppression in semiconductor lasers due to carrier heating", *IEEE Photonics Technology Letters*, vol 3, no 7, pp 606 –609, July 1991

[9] W S Rabinovich,, B J Feldman,, "Spatial hole burning effects in distributed feedback lasers", *IEEE Journal of Quantum Electronics*, vol 25 no 1, pp 20 –30, Jan 1989

[10] A Rogers, *Understanding Optical Fiber Communication*, Artech House, 2001

[11] J Chen, R J Ram, R Helkey, "Linearity and third-order intermodulation distortion in DFB semiconductor lasers", *IEEE Journal of Quantum Electronics,* vol 35, pp 1231-1237, 1999

[12] F Smyth, L P Barry, "Effects of Laser Diode Nonlinearities in Hybrid Fiber/Radio Systems", *SPIE Opto Ireland Conference Proceedings*, 2002

[13] J Le Bihan, G Yabre, "IM and FM intermodulation distortion in directly modulated single-mode semiconductor lasers" *IEEE Journal of Quantum Electronics*, vol 30, pp 899-904, 1994

[14] S J Wang, N K Dutta, "Intermodulation and harmonic distortion in GaInAsP distributed feedback lasers", *Electronics Letters*, vol 25, pp 850 –852, 1989

[15] Ralf E Schuh and David Wake, "Distortion of W-CDMA Signals over Optical Fiber Links", *IEEE International Conference on Third Generation Wireless Communication Conference Proceedings*, 2000

[16] T E Darcie, R S Tucker, and G J Sullivan, "Intermodulation and harmonic distortion in InGaAsP lasers," *Electronics Letters*, vol 21, pp 665–666, 1985

[17] Morthier, G , "Harmonic Distortion in Semiconductor Lasers for Analogue Transmission", *CLEO, Europe '96 Conference Proceedings*, pp 80 –80, 1996

[18] X J Meng, T Chau, M C Wu, "Suppression of intermodulation distortion in DFB lasers by external optical injection locking", *OFC/IOOC '99 Technical Digest*, vol 3, pp 335 –337, 1999

[19] M A Madureira, H M Salgado, "Analysis of External Optical Feedback Effects in the Non-linear Semicondutor Laser Response Considering Second Order Intermodulation Products", *University College London Communication Symposium Conference Proceedings*, September 2000

[20] K Barkley, "Two-Tone IMD Measurement Techniques", *RF Design,* August 2001

[21] G Yabre, J Le Bihan, "Reduction of nonlinear distortion in directly modulated semiconductor laser by coherent light injection", *IEEE Journal of Quantum Electronics,* vol 33, pp 1132-1140, 1997

[22] T Kanada, K Nawata, "Injection laser characteristics due to reflected optical power", *IEEE Journal of Quantum Electronics*, vol 15, pp 559 – 565, 1979

[23] R Lang, K Kobayashi, "External Optical Feedback Effects on Semiconductor Injection Laser Properties", *IEEE Journal of Quantum Electronics,* vol 16, pp 347-355, 1980

[24] G P Agrawal, "Line Narrowing in a Single Mode Injection Laser Due to External Optical Feedback", *IEEE Journal of Quantum Electronics,* vol 20, pp 468-471, 1984

[25] S Piazzolla, P Spano, M Tamburrini, "Small Signal Analysis of Frequency Chirping in Injection Locked Semiconductor Lasers", *IEEE Journal of Quantum Electronics,* vol 22, pp 2219-2223, 1986

[26] G Yabre, H De Waardt, H P A van den Boom, G -D Khoe, "Noise characteristics of single-mode semiconductor lasers under external light injection" *IEEE Journal of Quantum Electronics*, vol 36, pp 385 –393, March 2000

[27] Nikolaus Schunk and Klaus Petermann, Noise Analysis of Injection Locked Semiconductor Injection Lasers *IEEE Journal of Quantum Electronics,* vol 22 pp 642-650, 1986

[28] O Lidoyne, P B Gallion, D Erasme, "Modulation Properties of an Injection-Locked Semiconductor Laser", *IEEE Journal of Quantum Electronics*, vol 27, pp 344 – 851, March 1991

[29] J Wang, M K Haldar, L Li, F V C Mendis, "Enhancement of Modulation Bandwidth of Laser Diodes by Injection Locking", *IEEE Photonics Technology Letters*, vol 8, pp 34-36, 1996

[30] G Yabre, "Effect of Relatively Strong Light Injection on the Chirp-to-Power Ratio and the 3dB bandwidth of Directly Modulated Semiconductor Lasers", *Journal of Lightwave Technolgy*, vol 14, pp 2367-2373, Oct 1996

[31] X J Meng, T Chau, M C Wu, "Experimental demonstration of modulation bandwidth enhancement in distributed feedback lasers with external light injection" *Electronics Letters*, vol 34, pp 2031-2032, 1998

[32] J Hecht, Tuning In to Tunable Lasers, *WDM solutions*, Vol 4 No 3 March 2002

[33] A Lowery, O Lenzmann, I Koltchanov, R Moosburger, R Freund, A Richter, S Georgi, D Breuer and H Hamster, "Multiple Signal Representation Simulation of Photonic Devices, Systems and Networks," *IEEE Journal of Selected Topics in Quantum Electron* , vol 6, pp 282-296, 2000

[34] G P Agrawal, *Fiber-Optic Communication Systems (3rd Edition),* Wiley, 2002

Chapter 4 – Distribution of WCDMA Signals over Optical Fiber

As was mentioned previously, the increasing demand for broadband services, will mean that Hybrid Fiber Radio (HFR) systems will be employed in high capacity access networks for both mobile and fixed users [1] To make these future generation systems commercially viable it is important to keep costs as low as possible The use of HFR in a cellular system allows the Base Station (BS) complexity (and hence costs) to be kept to a minimum, as the only tasks performed at the BS are opto-electronic and electro-optic conversion [2-4] Direct modulation of a laser diode with the Radio Frequency (RF) data signals is the simplest and most cost effective solution for generating the optical RF data signals for distribution over fiber The major problem with this technique is that nonlinearities in electro-optical and opto-electrical conversions, around the electrical transmission frequencies, may seriously degrade the system performance [5, 6] This aspect has already been discussed in Chapter 3 In this chapter we study the transmission of a Wideband Code Division Multiple Access (WCDMA) signal over optical fiber The detrimental effects of the laser diode nonlinearity are examined and external injection is used in an attempt to overcome these effects

4.1- WCDMA for UMTS

Code Division Multiple Access (CDMA) was introduced in Chapter 2 It is one of a number of access techniques used in mobile communication systems today, to share the transmission medium of air It is a spread spectrum technique which means that each message bit with a logical value of 1 is replaced by a spreading code made up of chips These chips are short pulses of data with a value of ±1 If the data bit is zero then the code is inverted Because the spreading code is faster than the data, the coded signal requires a much higher bandwidth, hence the name spread spectrum Each user has a unique spreading code known only by itself and the MSC, therefore, even though all of the combined signals will appear as noise they can be decoded by the MSC

Some Second Generation (2G) systems employ CDMA and have a carrier bandwidth of about 1 MHz These systems are known as narrowband CDMA systems WCDMA is the multiple access technique used in Universal Mobile Telecommunication System (UMTS), a Third Generation (3G) mobile communication system The carrier bandwidth of WCDMA is approximately 5 MHz The wide bandwidth of WCDMA offers performance benefits such as higher resistance to multipath effects and the support of high user data rates [7] 3G systems offer data rates of up to 2 Mbit/s which allow broadband services such as streaming video to the mobile user There are two main modes of operation for WCDMA in UMTS Frequency Division Duplex (FDD) and Time Division Duplex (TDD) Duplexing allows data transfer in both directions simultaneously In FDD, a separate 5 MHz carrier is used for the uplink and the downlink and in TDD the same channel is shared over time between the uplink and the downlink [8]

The Adjacent Channel Leakage Ratio (ACLR)[1] is one of the most important specifications for the transmitter in WCDMA systems It is defined as the ratio of the power in the adjacent channel to the power in the desired channel The reason the ACLR is so important is due to the fact that the radio spectrum allocated for UMTS is so limited In most countries two 60 MHz bands have been allocated and seeing as each channel's bandwidth is over 4 MHz, channels must be closely packed, leaving little or no guard band between them Hence any leakage will lie directly in an adjacent channel's band

In this chapter we examine the distribution of WCDMA signals through a HFR system using direct modulation of a laser diode Wake *et al* first demonstrated this technique in 2000 [9] They observed distortion of the WCDMA signal due to frequency chirp, fiber dispersion and laser nonlinearity Other groups expanded on the work concerning the linearity of the laser [10, 11] WCDMA has emerged as the most widely adopted 3G air interface, and looking forward to future mobile systems it is likely that they will employ similar access techniques but at higher electrical frequencies in order to accommodate higher bit rates For this reason, in our work we centered the WCDMA signal around 6 GHz We demonstrate that by using external

[1] Also known as Adjacent Channel Power Leakage Ratio or Adjacent Channel Power Ratio

light injection into the laser, we can significantly reduce the dynamic nonlinearity of the laser in the employed RF region [12, 13], and thus greatly improve the ACLR of WCDMA signal after transmission through the HFR setup

The set of experiments consisted of three main sections First a WCDMA signal was passed through a HFR link to examine the predicted degradation Then, bandwidth enhancement using external injection was performed on the laser Finally these two sections were combined to improve the performance of the WCDMA signal using external light injection

4.2 – WCDMA over Fiber Experimental Work

4 2.1 – Experimental Setup

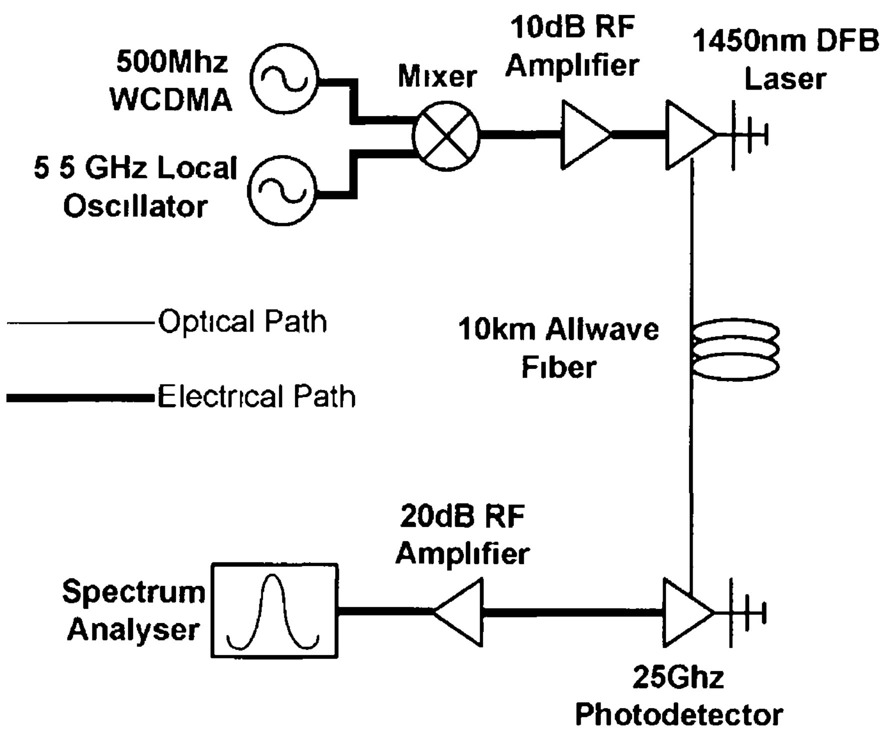

Figure 4 1 – Experimental setup for WCDMA over fiber

Figure 4 1 shows the initial setup used to send a WCDMA signal over optical fiber It used a –7 dBm WCDMA signal at 500 MHz from a Hewlett Packard E4437B signal generator, mixed with a 5 5 GHz local oscillator signal at a power of 10 dBm

This resulted in an output which was a WCDMA signal up-converted to an RF band centered around 6 GHz This upconverted signal was then amplified using an RF amplifier with 10 dB gain[1] To ensure that the amplifier was not being saturated, an oscilloscope was used to measure the power in the signal The amplified signal was then used to directly modulate a single mode laser diode operating at a wavelength of 1450 nm The laser, which had a threshold current of 11 mA, was biased at 30 mA This bias was sufficient to ensure that clipping of the applied RF signal, as mentioned in section 3 3 1, did not occur Hence, only dynamic nonlinearity of the laser would affect the system performance The resulting optical signal was then transmitted through 10 km of *Allwave* optical fiber which, unlike standard fiber allows transmission in the 1450 nm region It should be noted that the 1450 nm laser was chosen simply to demonstrate that HFR systems can operate at 1450 nm with the use of *Allwave* fiber We could have equally used 1310 or 1550 nm diodes for this set of experiments The propagated optical signal was then detected using a 25 GHz New Focus photo-detector with a responsivity of 0 4 A/W, before being amplified and then examined using an Anritsu MS2668C electrical spectrum analyzer

4 2 2 – Experimental Results

Figure 4 2 displays the electrical spectrum of the WCDMA signal applied to the laser diode, and the detected signal after passing through the optical link It can be seen from the plots in Figure 4 2, that the ACLR of the signal before the laser was almost –52 dBc, but after passing through the optical link, the ACLR was degraded to only –32 dBc We knew that the dynamic nonlinearity of the laser diode caused degradation in the ACLR of the signal but it was also possible that some nonlinearity in the electrical amplifier that is used after the optical detector was adding to the signal degradation

[1] Picosecond Pulselabs Model number 5824

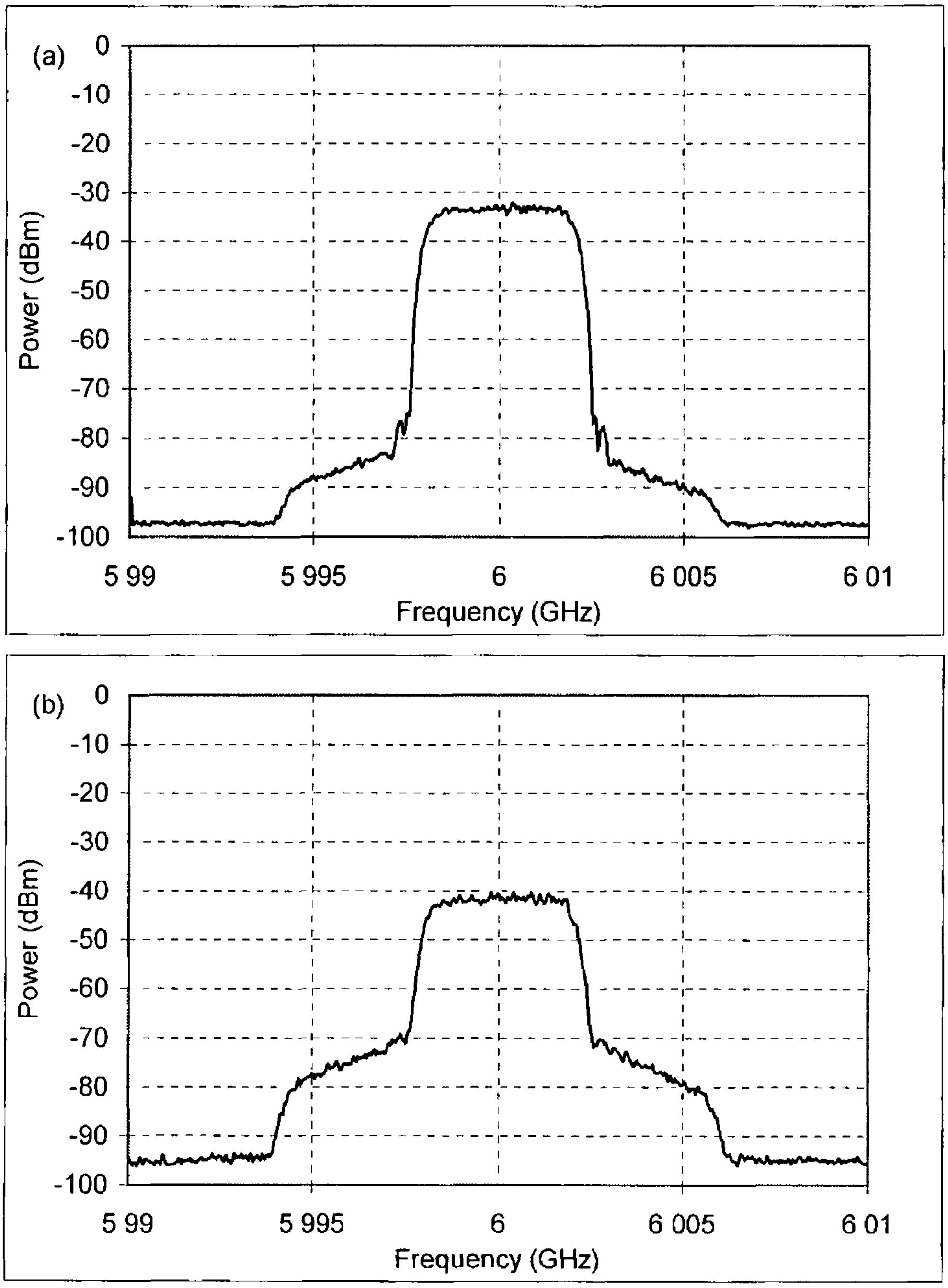

Figure 4 2 – Degradation in ACLR due to nonlinear distortions in the laser (a) WCDMA signal used to modulate the laser, (b) received WCDMA signal having passed through the optical link

Using two tone analysis, we were able to confirm that the nonlinearity introduced by the RF amplifier was negligible Tones from two signal generators were combined using an RF power coupler before being used to modulate the laser The detected signal was viewed on a spectrum analyser and the difference between the fundamental frequency and the Inter-Modulation Distortion (IMD) products was measured for a number of different RF power levels The 20 dB amplifier was then added to the system and the same measurements were taken again Although the power of the both the fundamental frequencies and the IMD products increased, the difference between them remained the same This allowed us to conclude that the amplifier was causing minimal distortion and this fact is illustrated by Figure 4 3

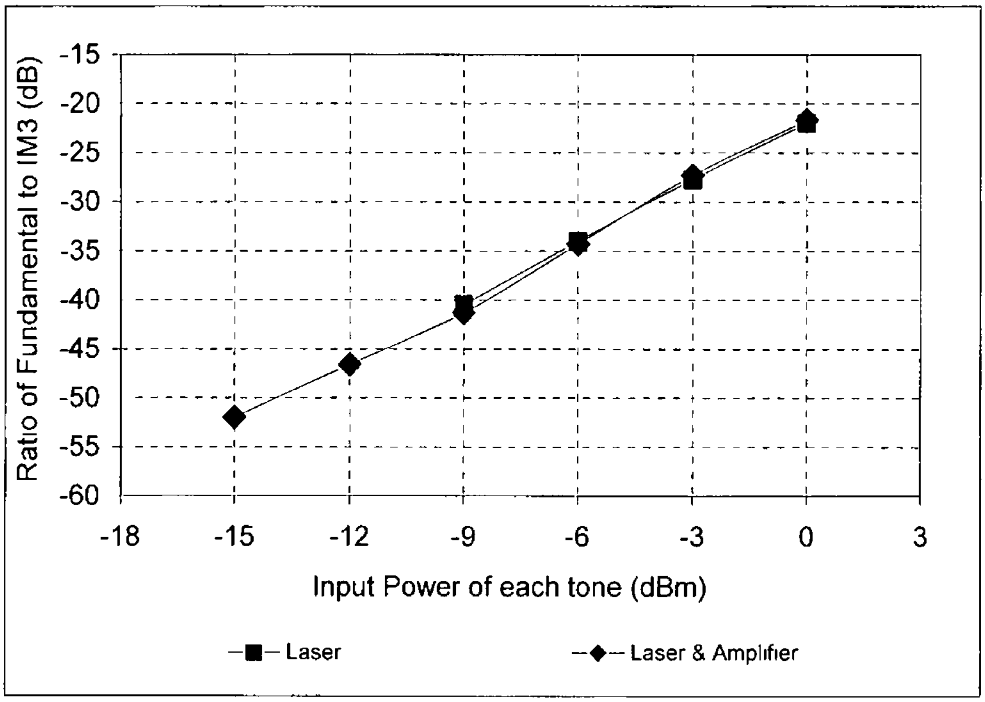

Figure 4 3 – Two-tone amplifier linearity testing

Once we had proven that the laser alone was causing serious distortion in the system the next step was to find a solution to this problem One possible solution would be to employ a laser diode with a relaxation frequency well beyond 6 GHz, such that its modulation response is more linear in the RF band around 6 GHz Such high speed devices, however, can be difficult to fabricate and expensive to purchase Another possibility would be to bias the laser at very high currents thus pushing the nonlinear part of the response past 6 GHz Reasons were given in Chapter 3 as to why this method is unsuitable In this work we have thus focused on improving the dynamic nonlinearity of the laser by using the external injection technique as outlined in section 3 4 With this technique we can increase the relaxation frequency of the laser diode, and in so doing reduce the dynamic nonlinearity of the laser in the RF band that we are using for the WCDMA transmission

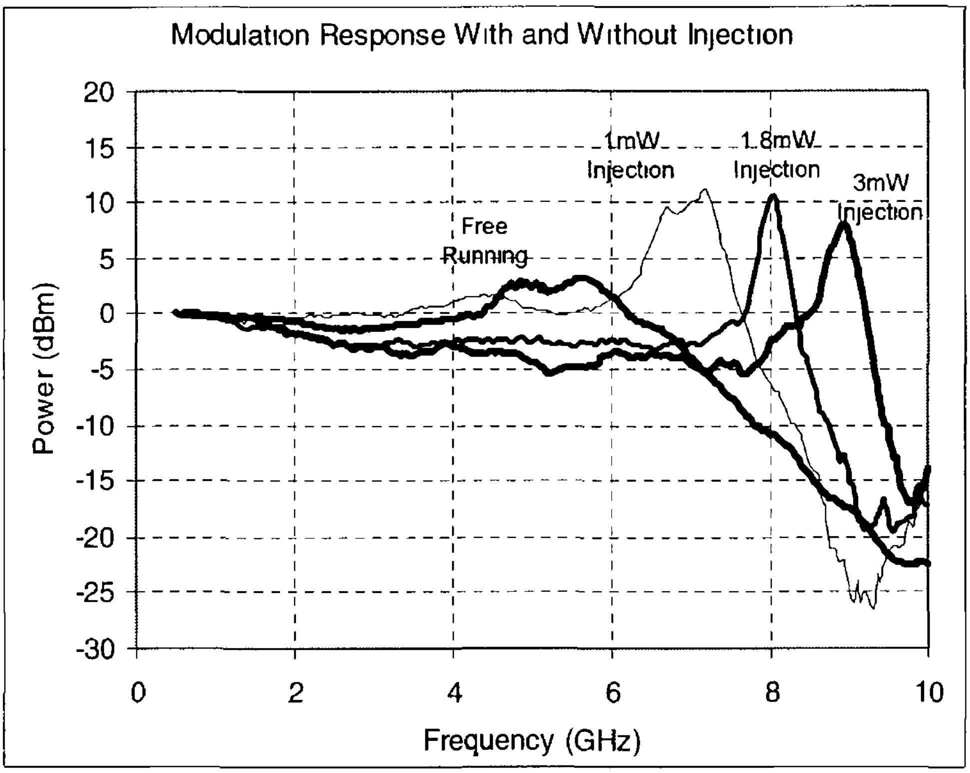

Figure 4 4 – Modulation bandwidth enhancement showing free running laser and laser under the influence of different powers of injection

To implement the external injection technique we again used the wavelength tunable ECL to inject light into the 1450 nm diode The wavelength of the tunable laser was varied in order to obtain maximum enhancement in the modulation response of the 1450 nm Distributed Feed-Back (DFB) laser, as measured using a network analyzer Figure 4 4 shows how the external light injection alters the modulation response of the laser diode biased at 30 mA It can be seen that it is essentially flat in the RF region being employed, when we inject a power level of 1 8 mW from the tunable laser into the DFB cavity It is impossible to know the exact power of the light which gets into the cavity but, taking into account optical losses between the ECL and DFB laser, we estimate this level to be around 100 μW The modulation response does show a large peak around 8 GHz, but this does not influence the transmission of the RF data signal around 6 GHz

We subsequently used the external injection technique to examine how it may be beneficial for the transmission of WCDMA signals over a HFR system The complete experimental setup that was employed is shown in Figure 4 5 As before, a 5 5 GHz Local Oscillator was mixed with a 500 MHz WCDMA RF data signal at

-7 dBm The up-converted WCDMA signal was then amplified before being used to modulate the laser As in chapter 3, the external injection setup consisted of the ECL, in conjunction with an optical coupler and a polarisation controller The ECL was used to inject light into the 1450 nm DFB laser cavity The output optical signal from the modulated laser was then passed through 10 km of optical fiber, detected and amplified, before being examined using an electrical spectrum analyzer The transmission fiber used in the experiment again was *Allwave* fiber

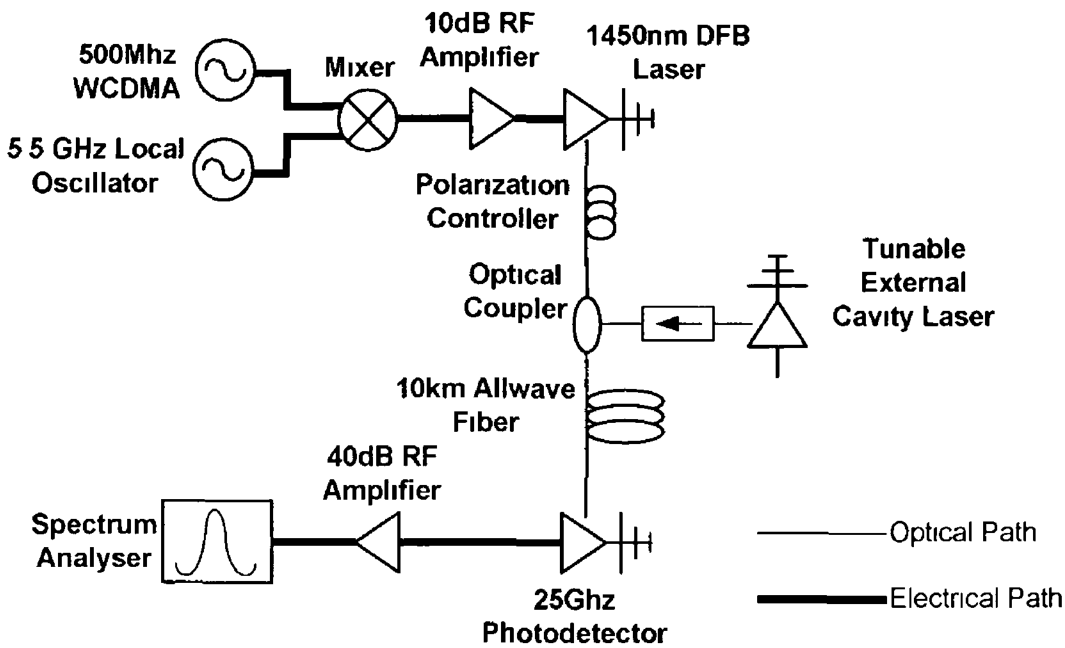

Figure 4 5 – WCDMA over fiber employing external injection experimental setup

Figure 4 6 shows the ACLR improvement achieved by using external injection in our system The injection level from the tunable laser was 1 8 mW, and with this level of external injection the improvement in the modulation response of the laser is sufficient to obtain an improvement in the ACLR of over 10 dB (from -31 dBc to -41 dBc)

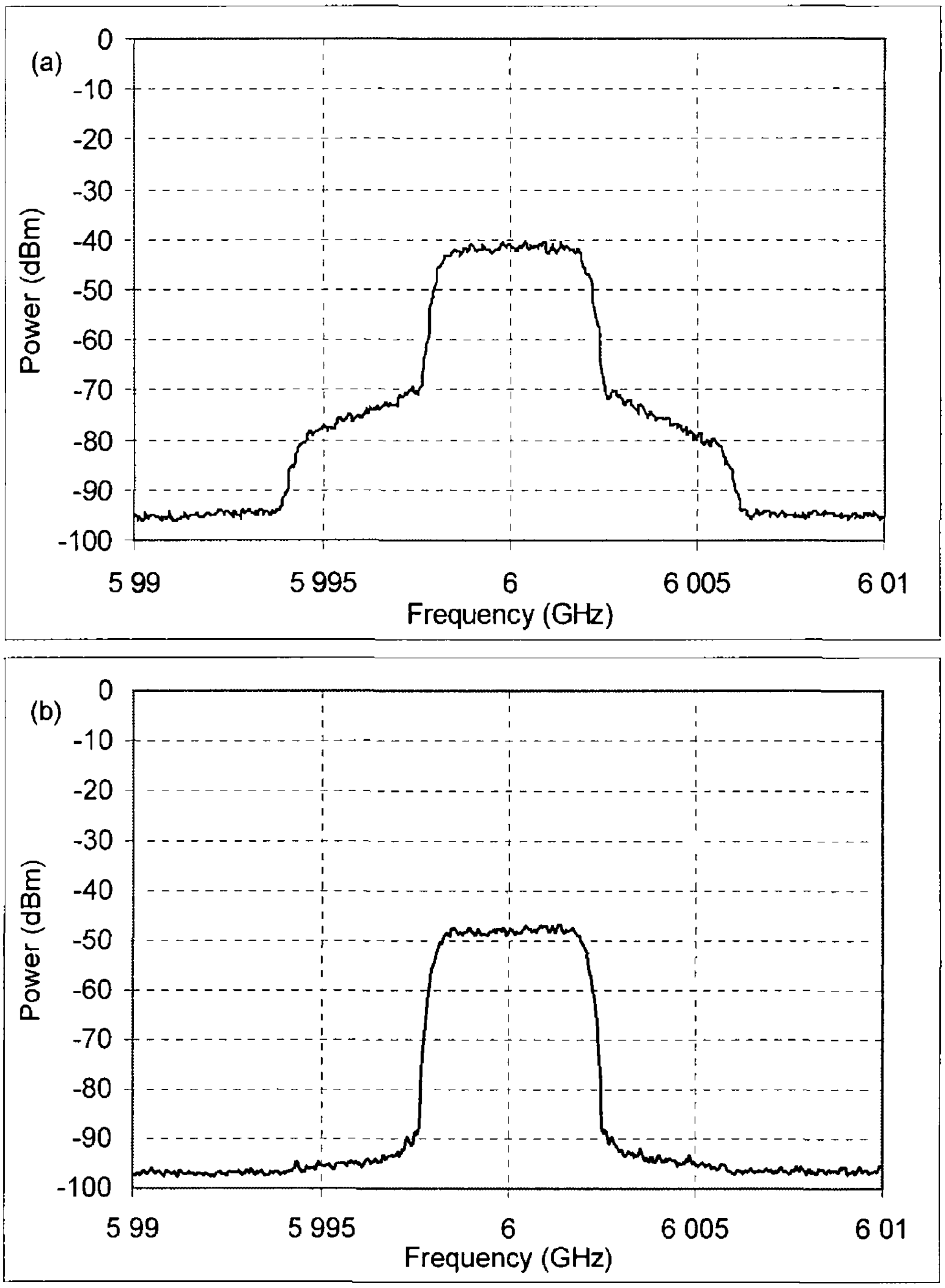

Figure 4.6 – Improvement in ACLR due to external light injection into the laser (a) received WCDMA signal from free running laser, (b) received WCDMA signal from externally injected laser

We consider a 10 dB improvement to be quite substantial and it brings the ACLR from below both of the standards set by the 3G Partnership Project (3GPP) for radio transmission, to above the downlink requirement of -33 dBc and close to the uplink requirement of -45 dBc [14]. However, as can be seen from the electrical spectrum of the received signal (Figure 4.6 (b)), when external injection is employed the ACLR measurement is limited by the dynamic range of our electrical measurement system To confirm this point we have measured the ACLR value as a function of RF power from the vector signal generator This plot is shown in Figure 4 7

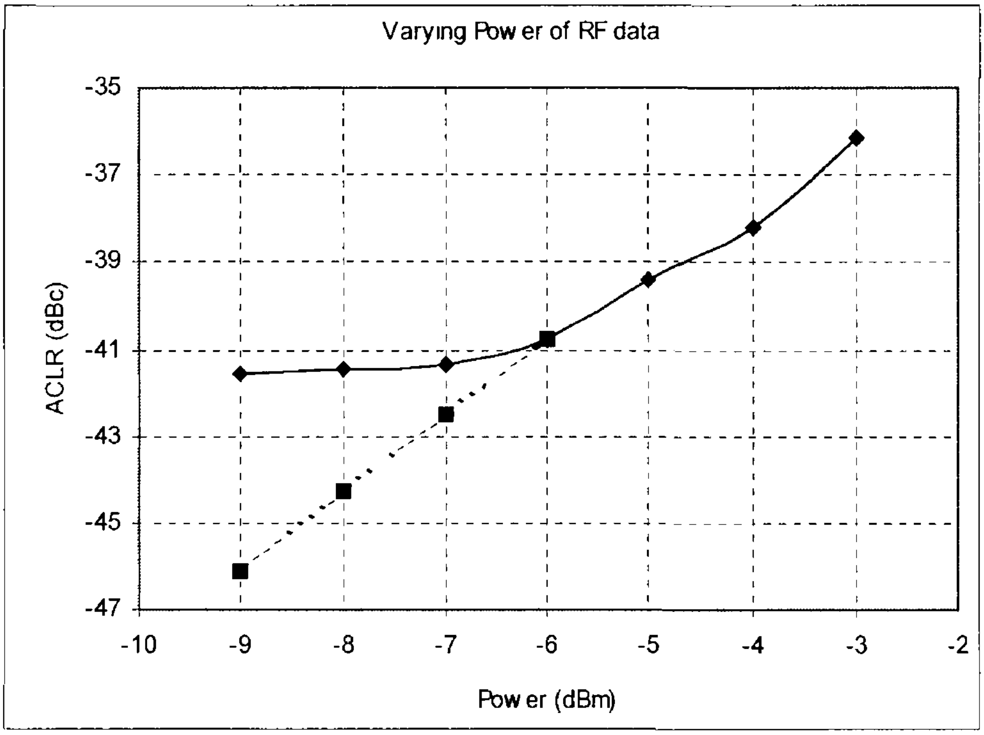

Figure 4 7 – Plot of ACLR with varying input signal power

The worsening of the ACLR with increasing RF data power is caused by increasing power leakage into adjacent channels due to 3rd order IMD caused by the dynamic nonlinearity of the laser It may seem that the slope of Figure 4 7 should be 3 due to the fact that it plots 3rd Order IMD This is not in fact the case The plot is of the ACLR which is actually the difference between the desired carrier and the 3rd order products, hence the slope of 2 As can be seen the ACLR value tends towards -41 5 dBc, as this is the lowest value that can be measured using our current setup By extrapolation of the nonlinear part of this curve we can see that the actual ACLR that could be achieved with an RF power of -9 dBm from the vector signal generator is -46 dB, which is better than is needed for 3G transmission

The next part of our experimental work involved measuring the ACLR as a function of the external optical injection power into the DFB laser diode The results of this work are plotted in Figure 4 8 It can be clearly seen, that at low injection power levels the ACLR value actually increases before it drops off to the maximum ACLR value that can be measured using the current setup

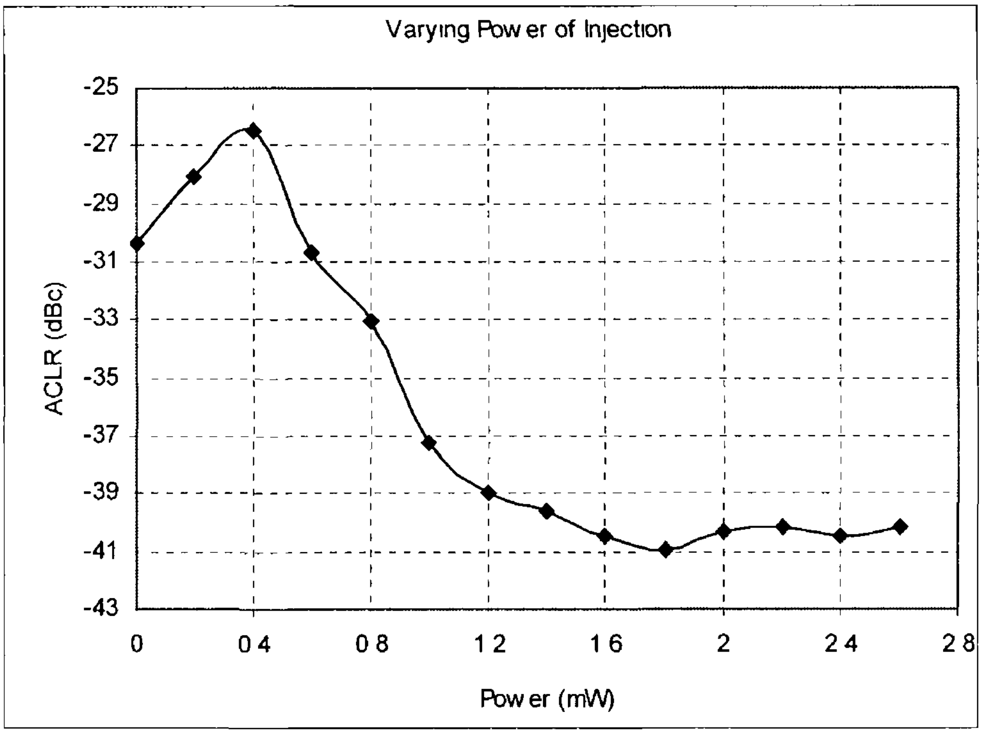

Figure 4 8 – Plot of ACLR with variation in intensity of injected light

This initial increase in the ACLR value can be explained by considering the modulation response of the laser without external light injection In this case the relaxation frequency of the laser (around 5 2 GHz) is slightly lower than the RF band used for the WCDMA transmission When the external light injection is initiated and gradually increased, the relaxation frequency of the device also begins to increase When the injection level reaches 0 4 mW, the response at the RF band being used for WCDMA transmission is at it's most nonlinear, thus the IMDs are maximised and the ACLR is at it's most degraded level of -26 5 dBc As the injection level is further increased, the relaxation frequency moves out beyond the RF band being used, and hence the 6 GHz region becomes more and more linear This causes a dramatic improvement in ACLR As with our previous measurements, the optimum ACLR value that we can achieve is limited by the dynamic range of our setup, thus it is difficult to determine by how much the distortions may be reduced by continually increasing the external injection level

4.3– Computer Model

In order to simulate and thus verify the experimental work carried out in this section we developed a simulation based on the laser modeled in chapter 3 To do this it was necessary to add a time domain analysis to the model This is done by using a function of Matlab known as ODE45 ODE45 solves ordinary differential equations over time It would have been beyond the scope of this project to write the code to model a WCDMA signal using Matlab Instead, simple two tone analysis is used to investigate similar properties as those discussed directly above, i e how distortion changes with variations in external light injection and RF signal power

4.3 1 – Components

The different components of this new part of the model will be discussed below

4 3 1 1 – Local Oscillator

The computer model of the local oscillator was designed to generate a tone at a certain frequency and with a desired amplitude, according to the equation of a sine wave, $A_c Cos(2\pi f_c t)$, where A_c is the amplitude of the wave, f_c is it's frequency and t is time The amplitude is defined to ensure the composite input signal will not clip the laser Figure 4 9 shows an output from one of the tone generators in both the time and the frequency domain The frequency response is obtained by performing a 2^{19} point Fast Fourier Transform on the signal A time of 200ns was chosen but the time domain plot only shows a few nanoseconds of this The frequency domain plot is on a logarithmic scale

4 3 1 2 – The Power Coupler

The power combiner is modelled by simply adding each of the generated tones together This gives the composite signal which will modulate the laser Figure 4 10 shows two tones coupled together in both time and frequency domain

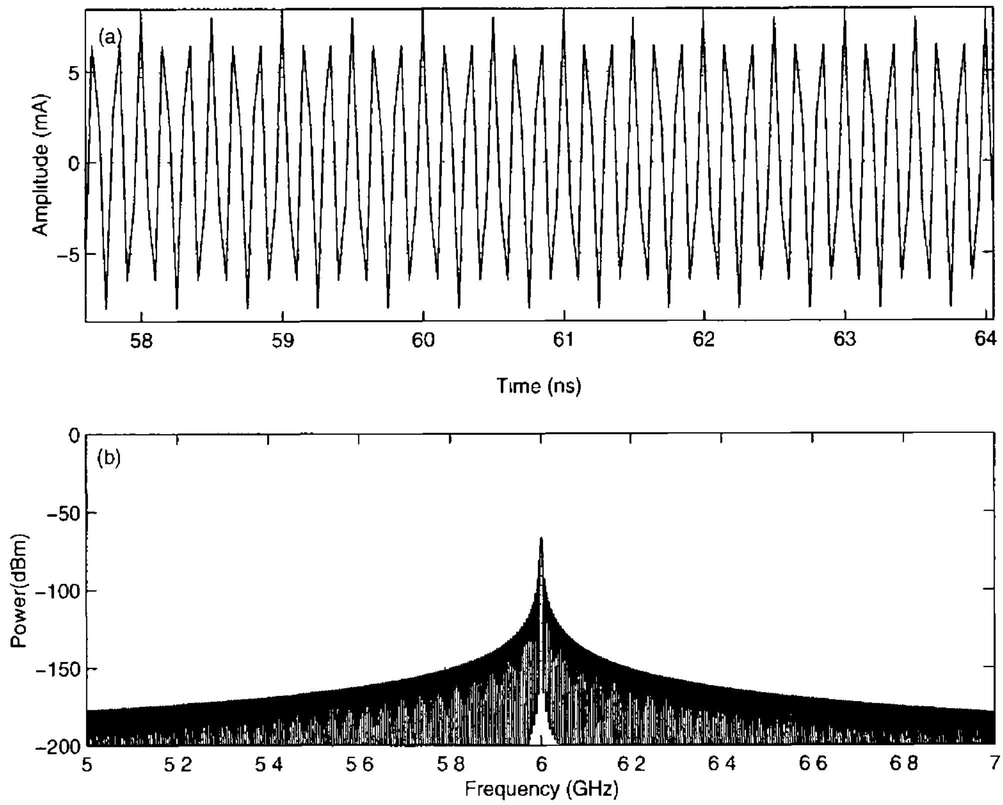

Figure 4 9 – Generated tone in the time (a), and log scale frequency (b) domains

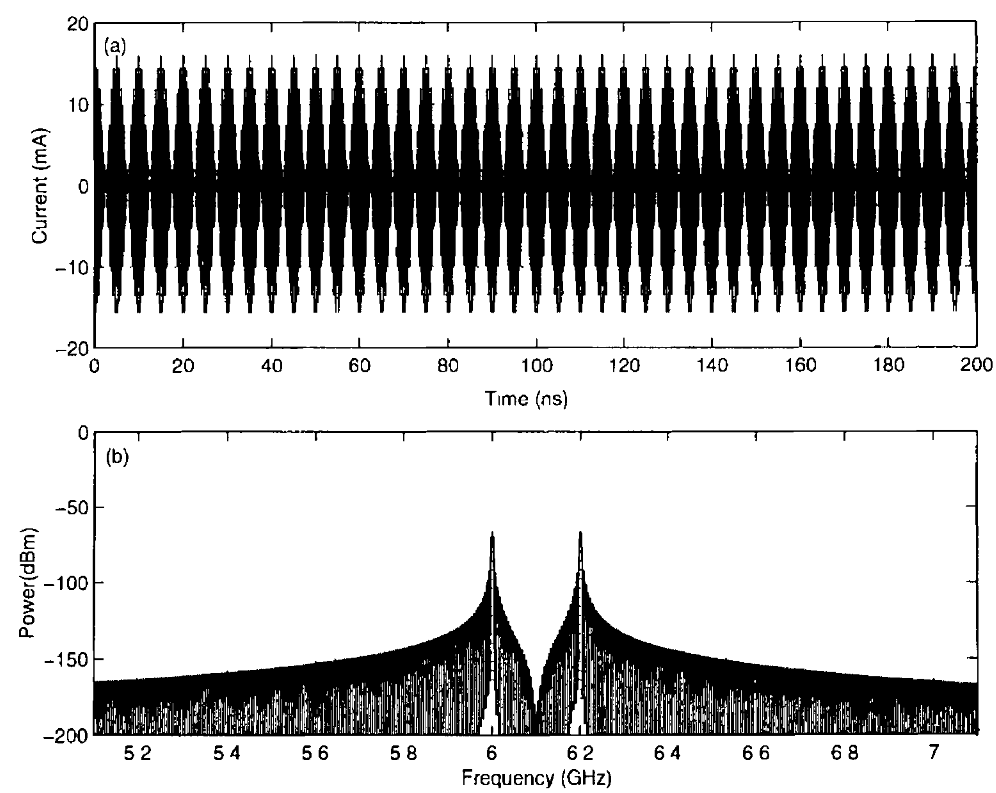

Figure 4 10 – Two coupled tones in the time (a), and log scales frequency (b) domains

4 3 1 3 – Bias Tee

The bias tee simply adds the combined tones to a user defined bias current In this case the bias current was 70 mA and hence the two tone input signal oscillates around the 70 mA point as can be seen in Figure 4 11 below

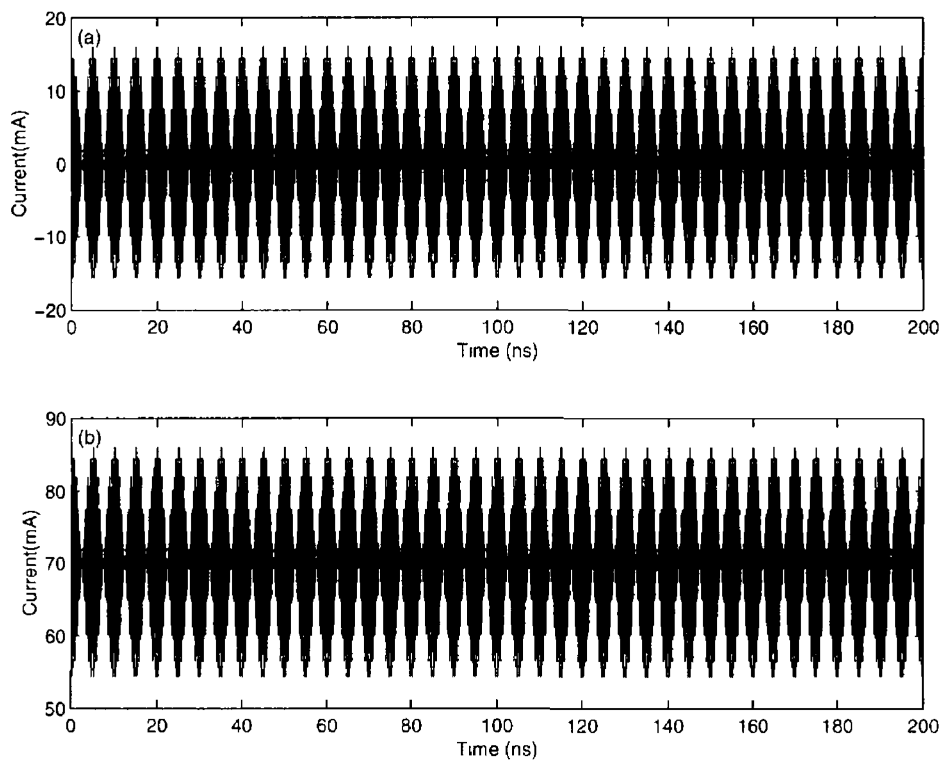

Figure 4 11 – Output from power coupler (a), output from bias tee (b)

4 3 1 4 – Laser Diode

To model the response of the laser to a time varying signal, a Matlab function named ODE45[1] is used This function accepts parameters such as time range, initial conditions and the differential equations to be solved It then uses the Runge-Kutta method [15] to solve the coupled rate equations for the different values of the modulating current From this we obtain corresponding values of carrier and photon density and associated phase

[1] ODE stands for ordinary differential equations

The photon density which is returned is then converted into optical power according to the following equation (refer to section 3 5 4 for details)

$$P = \left(\frac{SA_r c}{2\Gamma n}\right) hv(1\text{-}R)$$

This light output is modulated with the two tones Figure 4 12 and Figure 4 13 show the input and output signals of the laser in both the time and frequency domain It is clearly seen in the time domain that a bias current of 70 mA corresponds to an output power of approximately 9 mW This corresponds to the simulated Power vs Current (PI) curve from Chapter 3 In the frequency domain plot of Figure 4 13 the distortion being introduced by the laser is evident

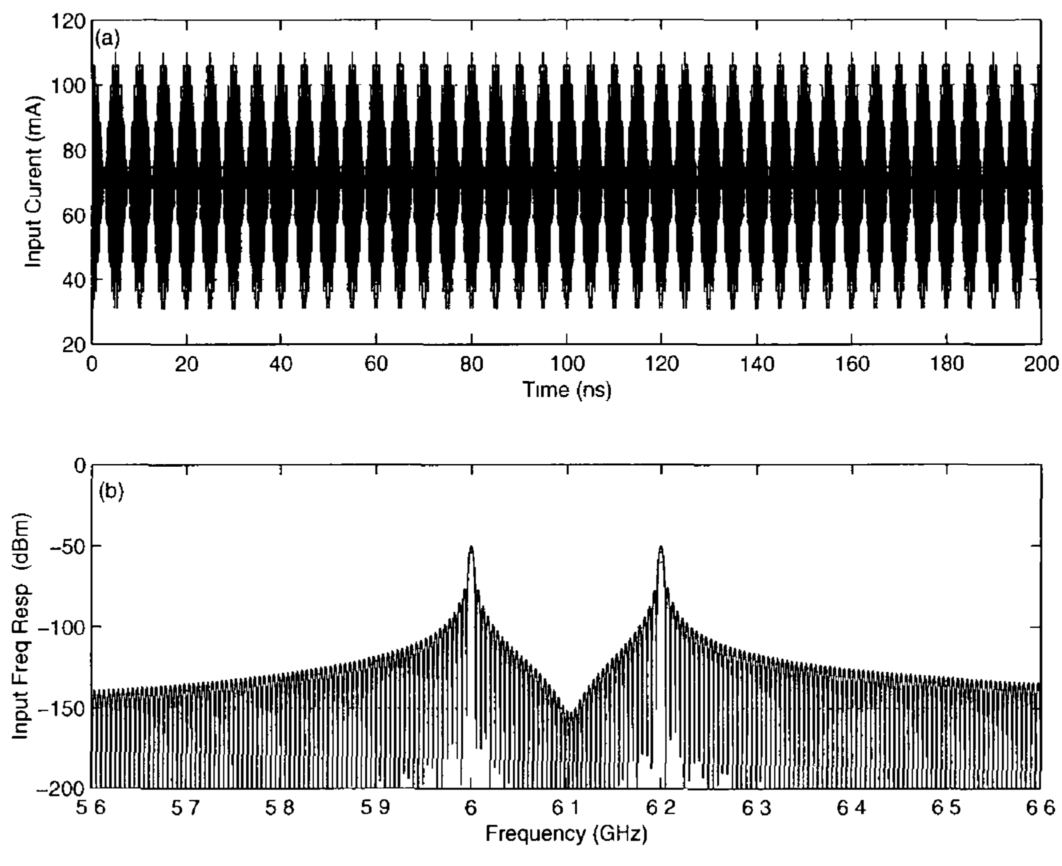

Figure 4 12 - Input to laser in time (a) and frequency (b) domains

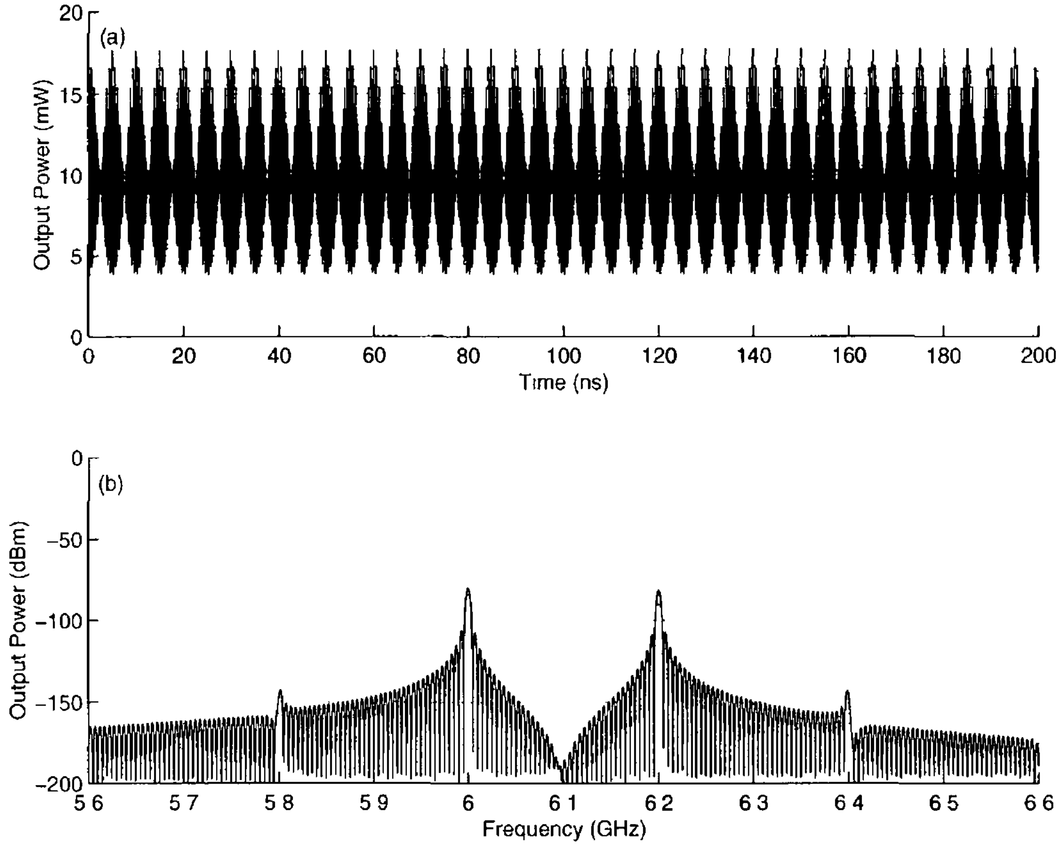

Figure 4 13 – Detected output from laser in time (a), and frequency (b) domains

4 3 2 – Simulation Results

Figure 4 16 shows the modeled two tone setup used It consists of a pair of local oscillators emitting tones at 6 & 6 2 GHz These are then combined using a power coupler and used to modulate the laser There is no specific piece of code written to simulate the external laser and optical coupler Instead these components are included using the modifications to the rate equations which were mentioned in the previous chapter The optical signal modulated with the two tones then falls on the detector which converts it back to an electrical signal

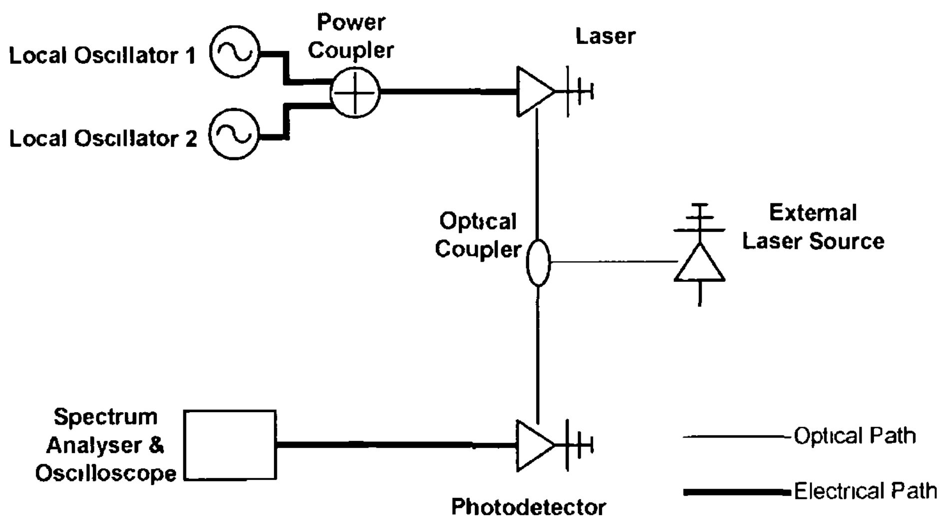

Figure 4 14 – Simulated two tone setup

This simulation work consisted of two parts The first involved modulating the free running laser with a pair of sine waves of identical amplitude and measuring the difference between the desired tones and the undesired intermodulation products generated This difference is then plotted for different amplitudes of the sine waves Figure 4 15 plots the results of these measurements As can be seen this plot correlates closely to the experimental results (see Figure 4 7) Again at high powers it has a slope of 2 but this slope reduces gradually as you reach simulation limitations introduced by the fourier transform

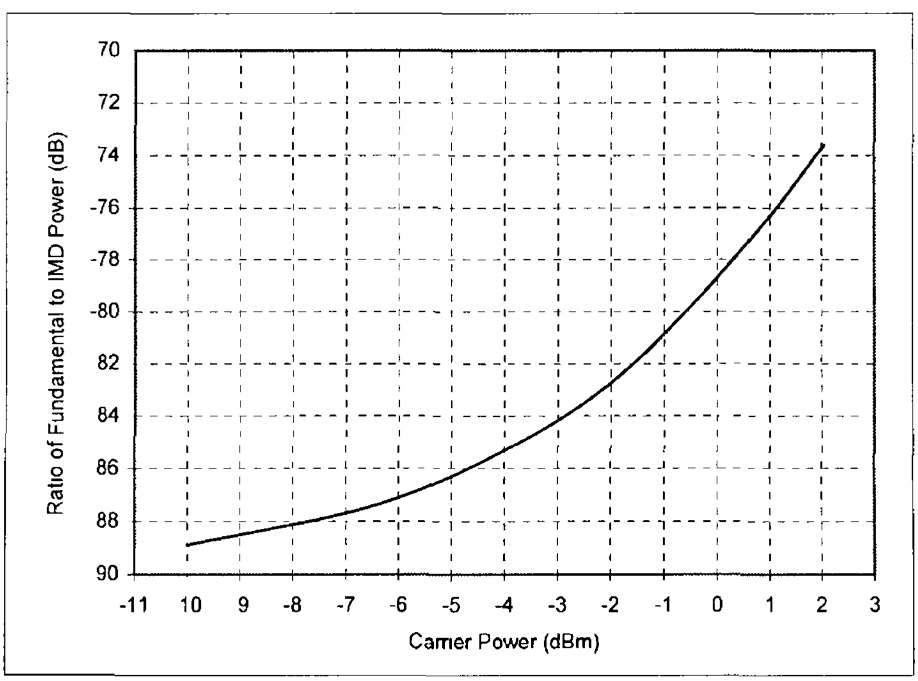

Figure 4 15 – Two-tone measurements with varying RF power

In contrast, the second part of the two tone linearity measurements involved keeping the RF power constant and varying the level of injection Figure 4 16 plots some of these measurements The effects of the linearisation by external injection can be clearly seen in the levels of the IMD products Plot (a) of Figure 4 16 corresponds to the free running laser It can be seen from Figure 4 17 that as the injection level begins to rise, the relaxation peak begins to move to higher frequencies and the linearity actually worsens, causing an increase in IMD products This corresponds to plot (b) of Figure 4 16 As the peak relaxation frequency continues to rise, the RF band around 6 GHz begins to linearise and hence the IMD products reduce, thereby improving the ratio of the fundamental to IMD products This corresponds to plot (c) in Figure 4 16

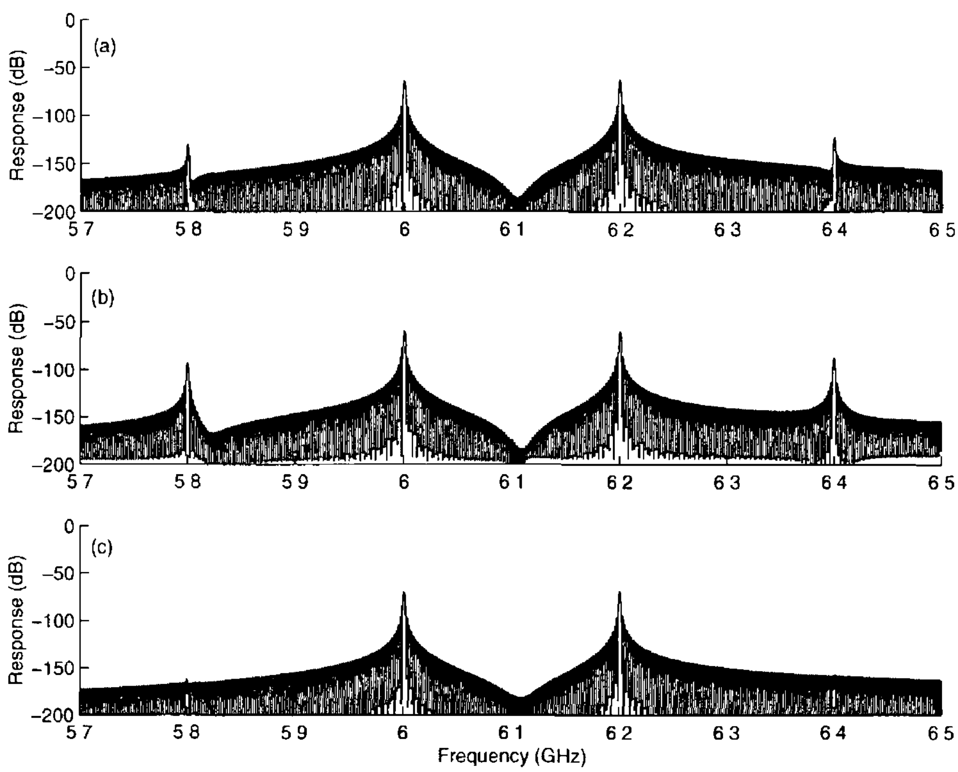

Figure 4 16 – Received electrical spectra for two-tone measurements using different levels of injection free running (a), injection ratio 0 01 (b), injection ratio 0 045 (c)

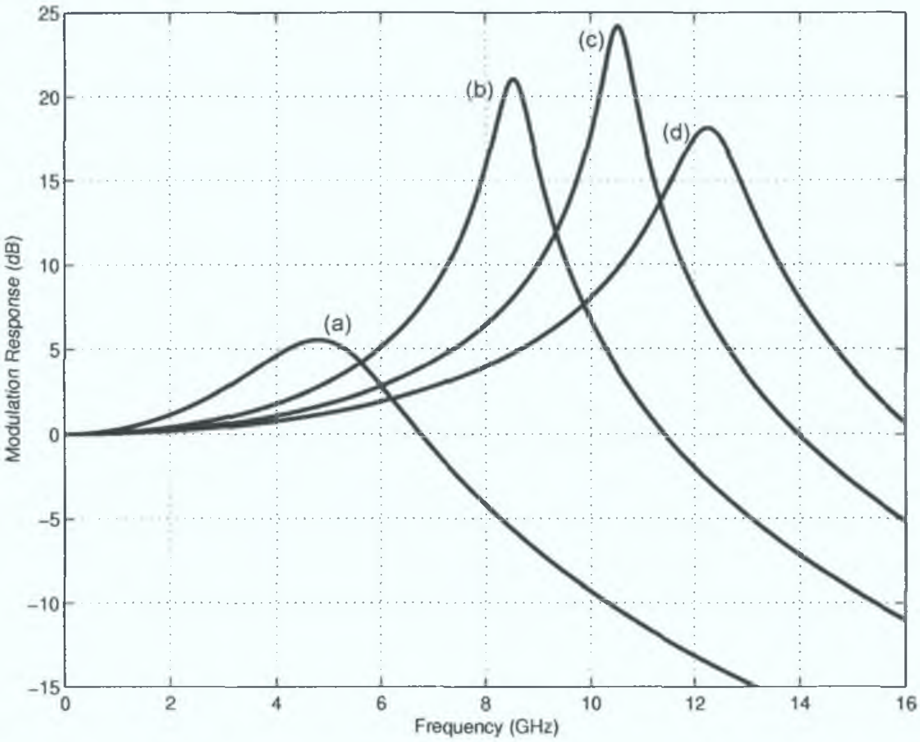

Figure 4.17 – Modulation Response of the simulated laser under free running conditions (a) and with injection ratios of 0.01 (b), 0.025 (c), 0.045 (d). In all cases the bias current was 70 mA

Figure 4.18 plots the difference between the fundamental frequency and the IMD products for a number of different injection levels and again, close correlation is seen between the experimental and simulated results (see Figure 4.8).

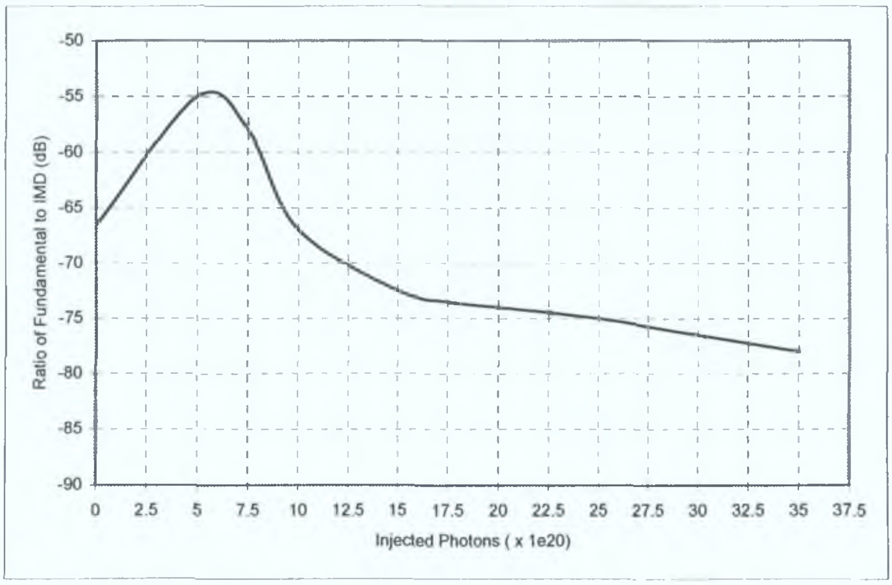

Figure 4.18 – Two Tone Measurement with varying levels of injection

4.4 – Conclusion

This chapter looked at the effect of laser diode nonlinearity on a single WCDMA channel Passing through the optical link caused a degradation in ACLR of approximately 20 dB However by employing the technique of external light injection almost 10 dB was regained The model was expanded to include modulation of the laser diode and external injection in the simulation showed similar trends to the experimental work

The operators of future mobile communications networks may use the technique of Sub-Carrier Multiplexing (SCM) to transmit multiple WCDMA channels over the very limited spectrum available to them Any leakage between channels therefore, will cause serious interference problems The next chapter goes on to look at a multi-channel HFR system Again the technique of external light injection is used to linearise the laser and to minimize IMD effects This is shown to increase system performance significantly

References

[1] D Wake, "HFR Systems for Mobile Applications", in *HFR Technologies for Mobile Communication Networks,* by Hamed Al- Raweshidy, Shozo Komaki, Artech House, Boston 2002

[2] R P Braun, G Grosskopf, H Heidrich, C von Helmolt, R Kaiser, K Kruger, U Kruger, D Rohde, F Schmidt, R Stenzel, D Trommer "Optical Microwave Generation and Transmission Experiments in the 12- and 60-GHz Region for Wireless Communications", *IEEE Transactions on Microwave Theory and Techniques,* vol 46 pp 320-330, 1998

[3] G H Smith, "A millimeter-wave full-duplex fiber-radio star-tree architecture incorporating WDM and SCM", *IEEE Photonics Technology Letters* vol 10 pp 1650-1652, 1998

[4] W I Way, "Subcarrier Multiplexed Lightwave System Design Considerations for Subscriber Loop Applications", *IEEE Journal of Lightwave Technology* vol 7, pp 1806- 1818, 1989

[5] J Chen, R J Ram, R Helkey, "Linearity and third-order intermodulation distortion in DFB semiconductor lasers", *IEEE Journal of Quantum Electron,* vol 35, pp 1231-1237, 1999

[6] T Ohno, H Fukano, Y Muramoto, T Ishibashi, T Yoshimatsu, Y Doi, "Measurement of Intermodulation Distortion in a Unitraveling-Carrier Refracting-Facet Photodiode and a p-i-n Refracting-Facet Photodiode", *IEEE Photonics Technology Letters,* vol 14, pp 375-377, 2002

[7] H Holma, A Toskala, U Lappalainen, "Introduction", in *WCDMA for UMTS – Radio Access for Third Generation Communications, by* Harri Holma, Antti Toskala, Wiley, 2001

[8] O Lehtinen, A Toskala, H Holma, H Vaataja, "UTRA TDD Mode" in *WCDMA for UMTS – Radio Access for Third Generation Communications, by* Harri Holma, Antti Toskala, Wiley, 2001

[9] D Wake, R E Schuh, "Measurement and simulation of W-CDMA signal transmission over optical fiber links", *Electronics Letters*, vol 36, pp 901-902, 2000

[10] R Yaqub, N Massao, "Inter and intrasystem nonlinearity compensation for radio on fiber considering wideband CDMA air-interface", *VTC 1999 - Fall* vol 5, pp 2800 -2804, 1999

[11] H Pretl, L Maurer, W Schelmbauer, R Weigel, B Adler, J Fenk, T Perkins, "Linearity Considerations of WCDMA front ends for UMTS" *2000 IEEE MTT-S International Microwave Symposium Digest,* vol 1, pp 433-436, 2000

[12] G Yabre, J Le Bihan, "Reduction of nonlinear distortion in directly modulated semiconductor laser by coherent light injection", *IEEE Journal of Quantum Electronics,* vol 33, pp 1132-1140, 1997

[13] X J Meng, T Chau, M C Wu, "Experimental demonstration of modulation bandwidth enhancement in distributed feedback lasers with external light injection", *Electronics Letters*, vol 34, pp 2031-2032, 1998

[14] 3GPP TSG RAN WG4 documents TS 25 104, Radio Transmission and Reception, and TS 25 101, UE Radio Transmission and Reception

[15] K A Stroud, *Further Engineering Mathematics 3rd Edition*, Macmillan Press, 1996

Chapter 5 – Subcarrier Multiplexing in Hybrid Fiber Radio Systems

5.1– Subcarrier Multiplexing

It is expected that broadband network operators will divide the available Radio Frequency (RF) spectrum into a number of separate channels for broadcast This use of multiple carrier distribution is known as Sub-Carrier Multiplexing (SCM) In SCM, data from each channel or user is modulated onto a separate microwave frequency subcarrier Each of these subcarriers are then frequency division multiplexed using a power coupler and the combined signal is then modulated onto an even higher frequency carrier for transmission In the most common application of SCM, the high frequency carrier is an optical carrier from a laser diode The photodiode then detects all subcarrier channels but only the desired one must be demodulated [1, 2]

The fundamental reason for using SCM in Hybrid Fiber Radio (HFR) networks is to increase capacity SCM systems are not limited by baseband electronic switching speeds, but rather by the response speeds of optical sources and detectors There are also other advantages to using SCM in a HFR network For one, it allows many different types of traffic to be transmitted simultaneously, simply by allocating different subcarriers to each The fact that each channel is continuously available and independent of other channels is also beneficial This is in contrast to Time Division Multiplexing (TDM), where channel synchronisation is necessary

We have looked at the effects of laser diode nonlinearity on a single Wideband Code Division Multiple Access (WCDMA) channel This chapter describes work which was carried out to investigate performance issues in multichannel systems [3] While Third Generation (3G) network operators would place multiple WCDMA signals side by side, we had no way of obtaining accurate system performance measurements using multichannel WCDMA Rather, we used 5 simple Binary Phase Shift Keyed (BPSK) channels with a data rate of 10 Mbit/s from an Anritsu MU163220A pattern generator Then using an Anritsu Bit Error Rate Tester (BERT)

(MU163240A) we were able to obtain accurate system performance measurements While a BPSK Signal is very different from a WCDMA signal the underlying fact remains that Inter-Modulation Distortion (IMD) from adjacent channels will cause interference and hence performance degradation Again the linearity of the laser is going to affect system performance and again we will show that external light injection can be used to improve it Under external injection conditions the relaxation frequency of the laser may be increased significantly [4-8], and the modulation response at lower frequencies can be made significantly more linear than that without external injection [9] The exact alteration in the modulation response of the laser under external injection conditions is dependent on both the injected power and the detuning between the master and slave laser, and by varying these two parameters it is feasible to optimise the lasers modulation response for different applications [10]

The use of SCM in HFR systems was initially proposed and demonstrated experimentally by Darcie *et al* in 1986 [1, 11] and since then groups have built upon this work demonstrating the use of SCM in Global System for Mobile-Communications (GSM) systems [12] and spread spectrum systems [13] Smith *et al* demonstrated the use of frequency multiplexing in both the electrical and the optical domain in a Hybrid Wavelength Division Multiplexing/Sub-Carrier Multiplexing (WDM/SCM) system [14]

In terms of the use of external injection in SCM systems, in 1998 Meng *et al* showed that the technique of external injection could be used to improve performance in an experimental data system with a *single* data channel [15] Kaszubowska *et al* expanded this work to incorporate SCM [16] In both of these cases the greatly improved system performance is due simply to the enhanced modulation response of the laser at the RF band employed in the hybrid system However the nonlinear response of the laser with external injection may still cause problems for multicarrier HFR systems [17] To our knowledge there has been no work undertaken to examine how external light injection may be used to improve the performance of a practical multi-carrier HFR system by linearising the laser's modulation response around the operating RF band

It is important to note that the experimental work is set up such that the relative modulation response of the laser with and without external injection is the same, thus the measured improvement in system performance is simply due to the improved linearity of the directly modulated laser transmitter and not due the any increase in the modulation response caused by external injection

5.2 – SCM in HFR Experimental Work

5 2.1 – Experimental Setup

The laser used in this work was an NTT Electronics (NEL) 1550 nm Distributed Feed-Back (DFB) laser It had a threshold current of 26 mA and an intrinsic modulation bandwidth of around 8 GHz when biased at 40 mA Using the technique of external injection this bandwidth can be quite significantly increased With an external injection level of 3 mW from the tuneable laser into the 1550 nm device a bandwidth of over 11 GHz was achieved (see Figure 5 1) More importantly for our work, it can be seen that the response of the laser has been well linearised at the operating frequency of 6 GHz It was also important for this work that we could obtain responses that were equal in magnitude with and without injection This would allow us to determine how much of the performance was due to improved response and how much was due to improved linearity

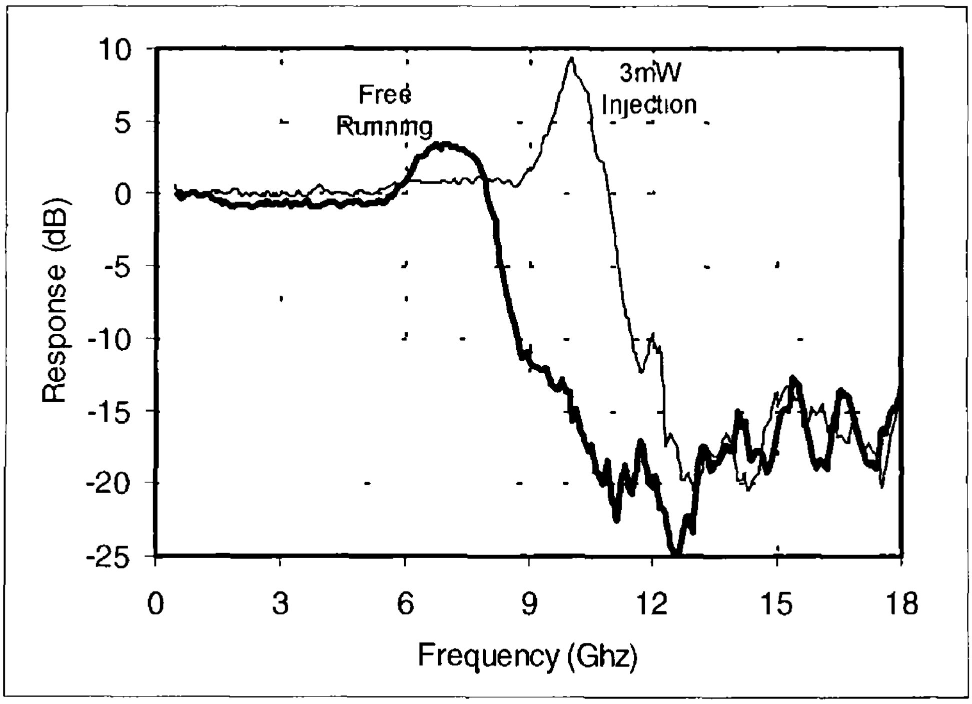

Figure 5 1 – Modulation response of the 1550 nm DFB with and without external injection

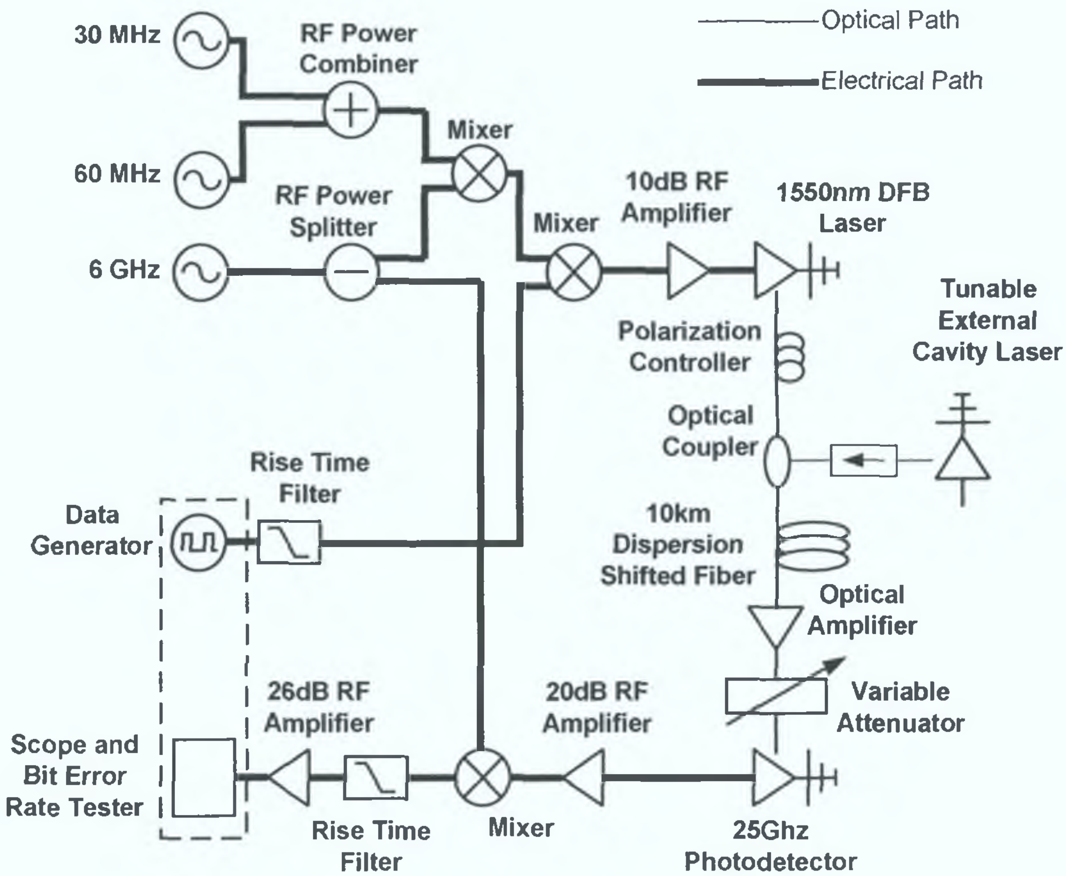

Figure 5.2 – The experimental setup for multichannel HFR system with external light injection.

Figure 5.2 shows our experimental setup. We first combined a 30 MHz carrier and a 60 MHz carrier in an RF power coupler. This composite signal was then mixed with a local oscillator at 6 GHz to give five carriers spaced by 30 MHz and centred at 6 GHz. The number of carriers was chosen to suit equipment limitations in the laboratory[1]. A 10 Mbit/s Non-Return to Zero (NRZ) data stream from an Anritsu pattern generator was passed through a low pass filter with a bandwidth of 10.7 MHz to minimise the bandwidth occupied by it, and the resulting data signal was then mixed with the five carriers to give the five data channels required. 30 MHz spacing was chosen by observing on an oscilloscope the minimum spacing at which cross channel interference between the five RF data channels was negligible. The signal was then amplified before being added to the bias current and used to modulate the laser. In the free running setup the resulting optical microwave signal was then optically amplified before being detected using a 25 GHz photodetector from New

[1] In most UMTS systems, both bands will contain twelve 5 MHz channels with minimal spacing.

Focus The received signal was electrically amplified and then downconverted by mixing it again with the 6 GHz local oscillator Note that only the central channel of the five RF data channels was downconverted It was then low pass filtered to ensure that only the baseband signal was examined by the oscilloscope A 20 dB RF amplifier was added, so that the signal level was sufficient for the error analyser In the externally injected system a tunable External Cavity Laser (ECL), in conjunction with an optical coupler and a polarisation controller, was used to inject light into the slave laser cavity With this setup, the laser can be operated in the free running regime by simply switching the external source off

As was mentioned, there are two characteristics of the laser diode response that will affect the performance of a HFR system Firstly consider the magnitude of the modulation response of the laser diode This magnitude is directly related to the amount of electrical power in the received signal Hence the higher the magnitude of the modulation response at the frequency of operation, the more electrical power will be received The second characteristic is the linearity of the response at the frequency of interest If we are operating in a linear portion of the modulation response, IMD is kept to a minimum, however at frequencies around the relaxation frequency the response tends to be quite nonlinear It has been shown in previous sections that external injection can improve the performance of HFR systems This work set out to examine how the intermodulation products lying at the same frequency affected the performance of our transmitted channels

5.2 2 – Experimental Results

Figure 5 3 shows the electrical spectra of our five channel system Spectrum (a) is the signal used to modulate the laser Spectrum (b) shows the received signal from the system with the free running laser (see Figure 5 1) From the new frequency components generated, it is clear that the nonlinearity of the device at 6 GHz has led to signal distortion The IMD products which can be seen on the spectrum, lying outside of the five channels have corresponding IMD products which lie beneath our transmitted data channels These will cause distortion of our data channels as will be seen in Figure 5 4 Finally Spectrum (c) is that of the system with increased linearity due to external light injection and the reduction in IMD is clearly evident

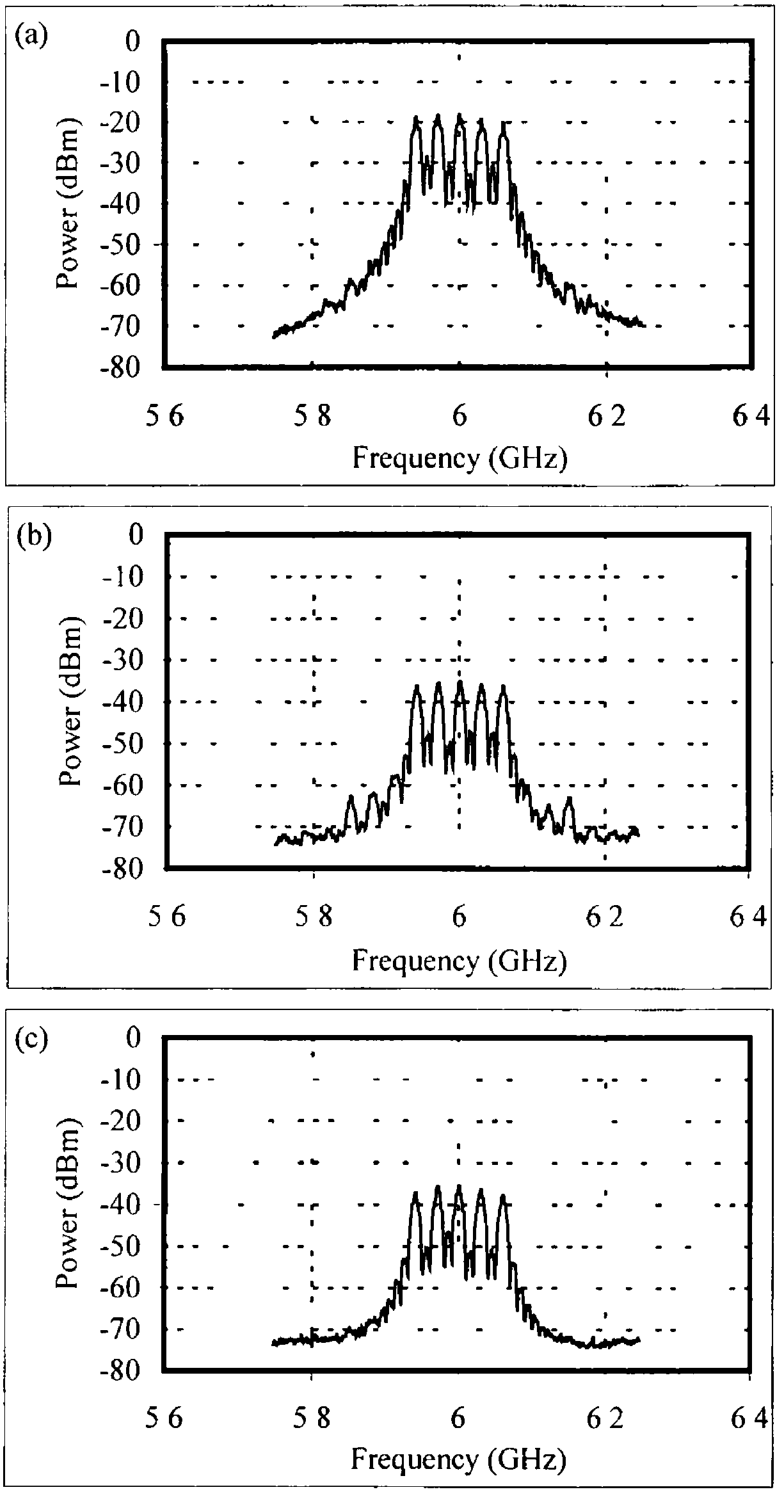

Figure 5 3 – Electrical Spectra of the five 10 Mbit/s data channels (a) input signal to laser, (b) received signal, free running laser, (c), received signal, externally injected laser

The spectra above show us that the nonlinearity in the free running laser is introducing signal distortion at 6 GHz To calculate how this nonlinearity affected the performance it was necessary to ensure that the magnitude of the modulation response of the laser remained the same even though the linearity was improved by increasing the modulation bandwidth Figure 5 1 shows the modulation response with both the free running and the externally injected laser At 6 GHz the level of the response is identical but clearly the injected laser has a more linear response

To examine the system performance it is necessary to look at the received eye diagrams and the Bit Error Rate (BER) of the signals after passing though the HFR link Figure 5 4 shows these received eye diagrams with and without external injection This figure shows the fact that the response magnitude is identical because the amplitude of the received signal is identical in both the injected and the free running regime It can also be seen that the opening of the eye in the system using the free running DFB laser (Figure 5 4 (a)) is quite poor when compared to the system employing external injection (Figure 5 4 (b)) The difference in quality of the two eyes is due to the IMD products (observed in Figure 5 3) which lie beneath the desired channels These unwanted IMD products result in added noise on the received data signal resulting in a reduction in the size of the eye opening

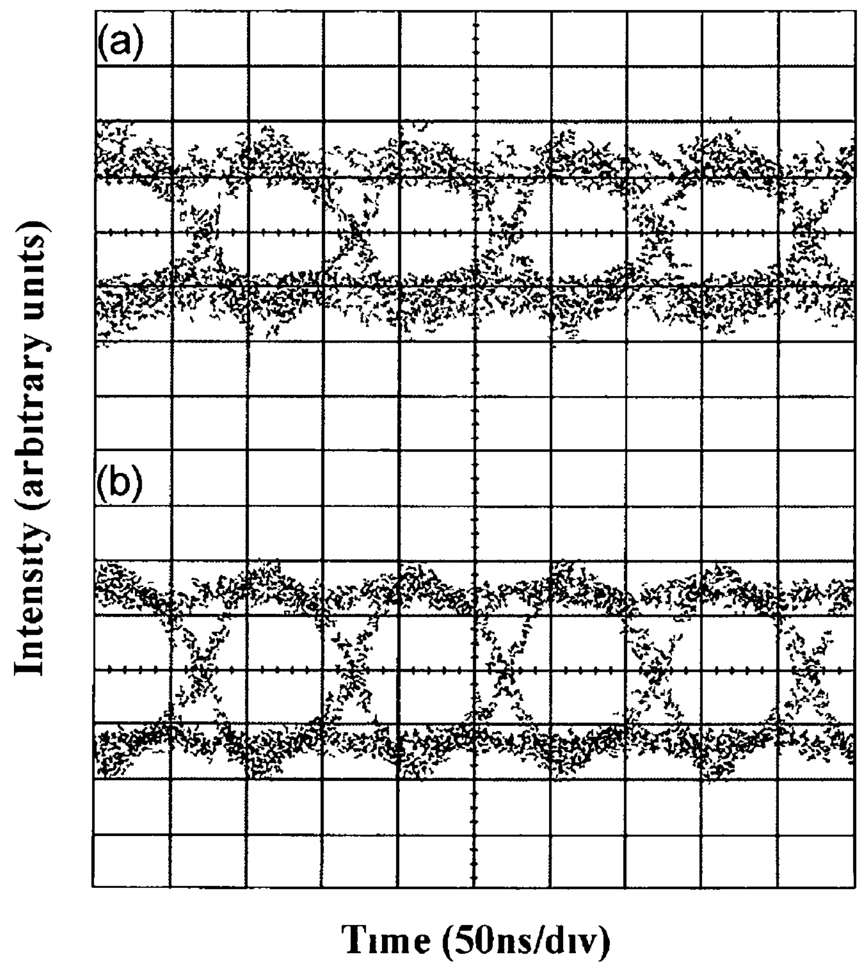

Figure 5 4 – Received eye diagrams using (a) free running laser, (b) external injection laser giving improved linearity and identical response

An optical attenuator was used to vary the received optical power, and the BER was measured for a number of different powers Figure 5 5 plots the BER against different received powers and shows that a 2 dB improvement at a BER of $1x10^{7}$ was achieved by using external light injection As the magnitude of the response is identical in both the free running and externally injected case it can be concluded that this improvement is solely due to the increased linearity of the system

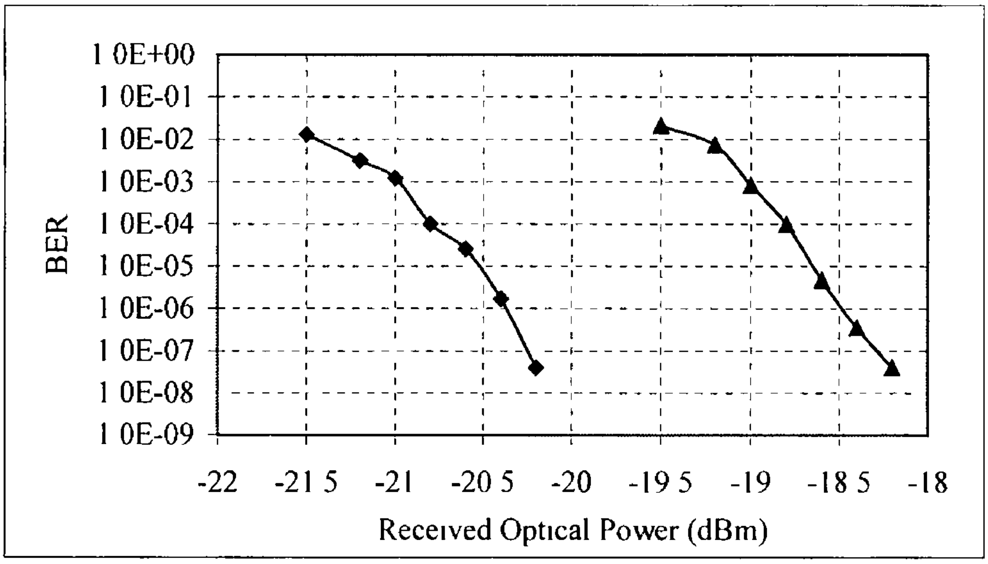

Figure 5 5 – BER versus received optical power for the central RF data channel using directly modulated laser with (●) and without (▲) external injection

Externally injected lasers are highly sensitive to changes in the power, wavelength or polarisation of the light which is injected back into the DFB laser cavity Small variations of any of these parameters can significantly change the modulation response of the slave laser This allows the response to be tuned to achieve maximum performance Figure 5 6 shows a plot of the further improvement which can be gained by optimising the tuning For the same optical power used in Figure 5 4, a performance improvement of 5 dB at a BER of $1x10^{7}$ was achieved (see Figure 5 7) when the response was tuned so that the response at 6 GHz was not only more linear due to external injection but it also had a higher magnitude The simulation work at the end of this chapter illustrates this well

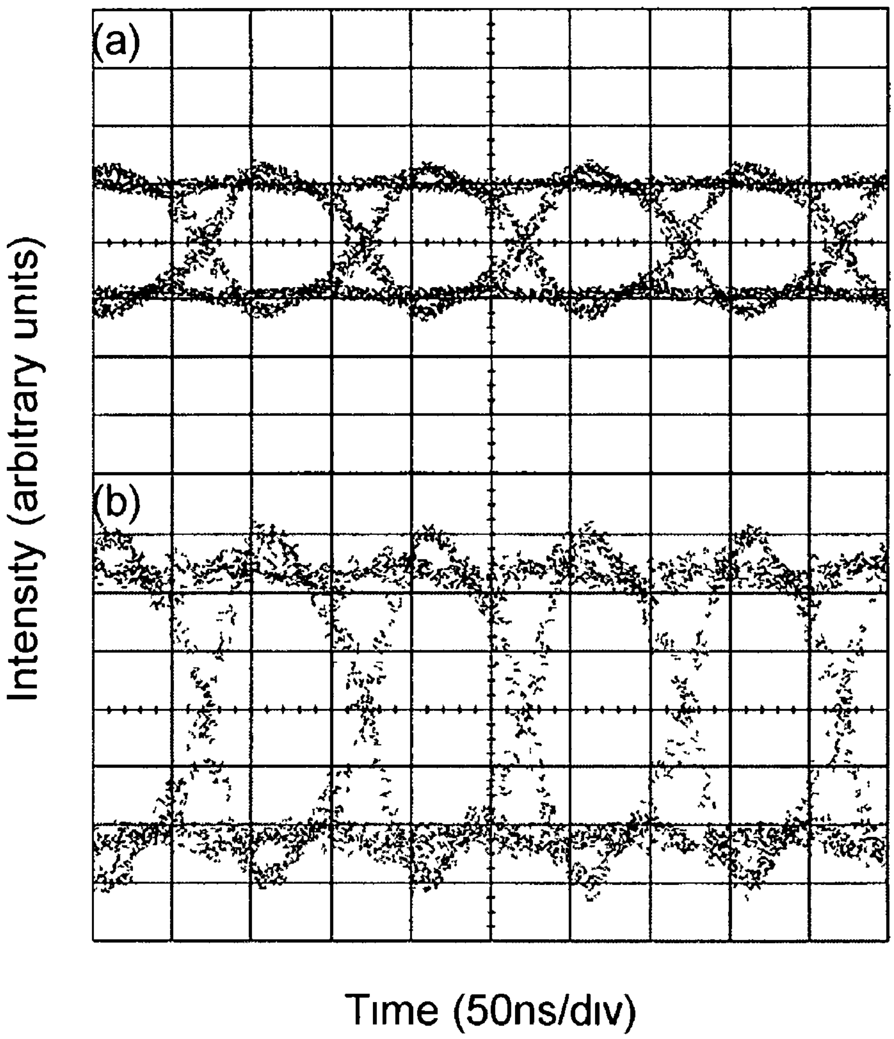

Figure 5 6 – Received eye diagrams using (a) free running laser, (b) external injection laser giving improved response and improved linearity

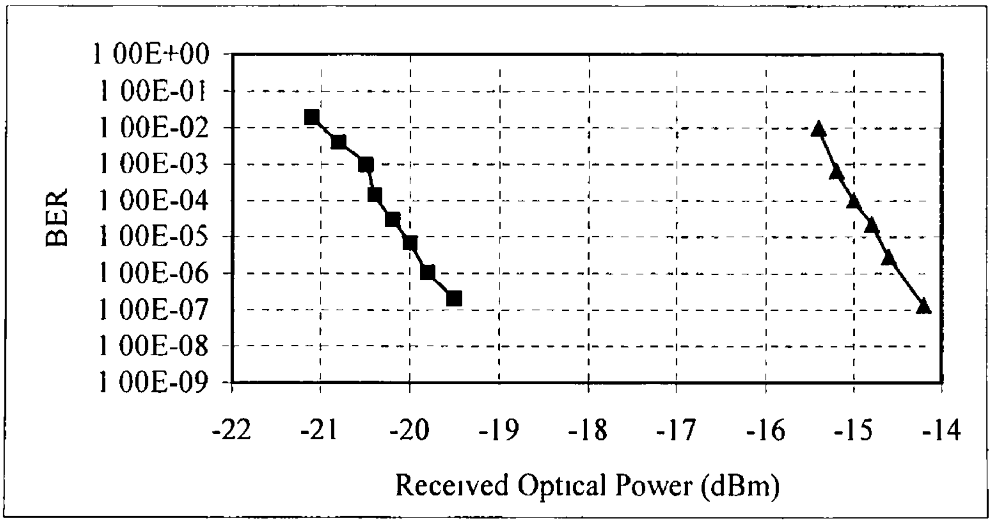

Figure 5 7 – BER versus received optical power for the central RF data channel using directly modulated laser with (●) and without (▲) external injection

5.3 – Computer Model

Most of the simulation work in this area to date has been on the laser alone [4-8] and there has been no work reported at all which simulates a full communication system This work builds upon the simulation work described in the previous chapter by adding data onto the carriers It is quite an accurate model of the actual experimental system The entire system comprised of a data source, rise time filter, local oscillator, mixer, power combiner, laser, detector, receiver filter, demodulator, BERT and oscilloscope Simulation allows a much more ideal filter to be employed and hence we used a channel spacing of 20 MHz between the RF carriers rather than the 30 MHz of the experimental system

5.3.1 – Components

5 3 1 1 – Data Source

The computer model could be programmed to output a random bit pattern or a fixed one The number of bits in the pattern and the bit rate were also variable To correlate as closely as possible with the experiment, a data rate of 10 Mbit/s was chosen It output NRZ data and again this matched the experimental data source The figure below shows a random bit pattern generated by the program

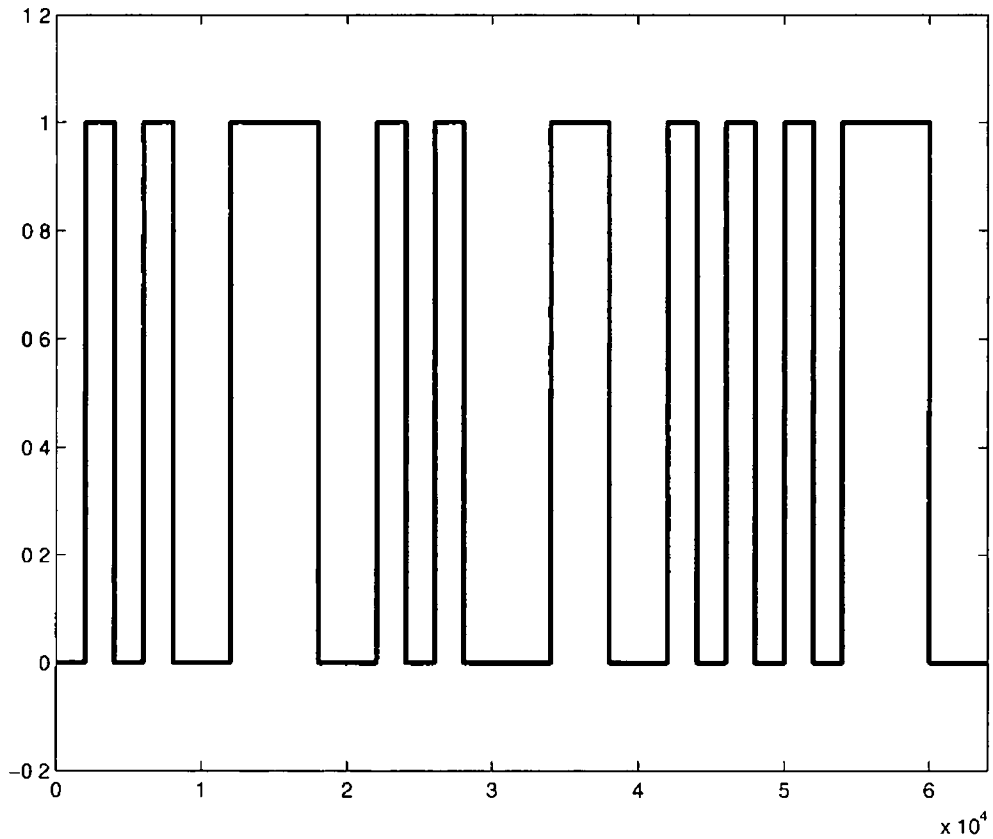

Figure 5 8 – Data pattern generated by the computer model

A modulation rate of 10 Mbit/s corresponds to a bit period of 100ns and because a sampling frequency of 20 GHz was used this in turn corresponded to 2000 samples per bit This can be verified from Figure 5 8 above which shows a sample 32-bit pattern which was generated

*5 3 1 2 – **Rise Time Filter***

A rise time filter was added to reduce the bandwidth occupied by the data signal It was a 5th Order Chebyshev Type II digital filter with a cutoff frequency of 7 MHz and a stopband attenuation of 70 dB Figure 5 9 shows the same bit pattern as before having passed through the filter

Figure 5 10 shows the result of low pass filtering the baseband input data signal to minimise the bandwidth occupied by it The plot only shows the frequency spectrum up to 100 MHz In fact in the unfiltered plot, (a), the ripple continues at approximately the same level out to several gigahertz It is clearly seen in (b), that the occupied bandwidth is significantly reduced when filtering is used

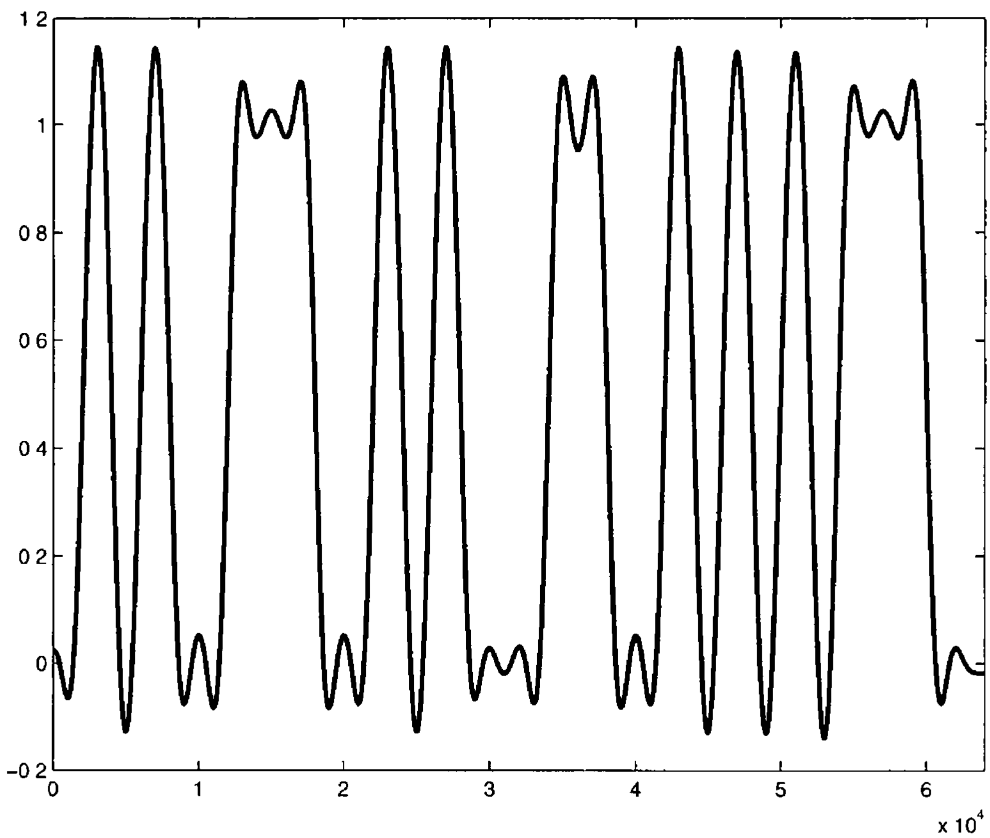

Figure 5 9 – Low pass filtered input data pattern

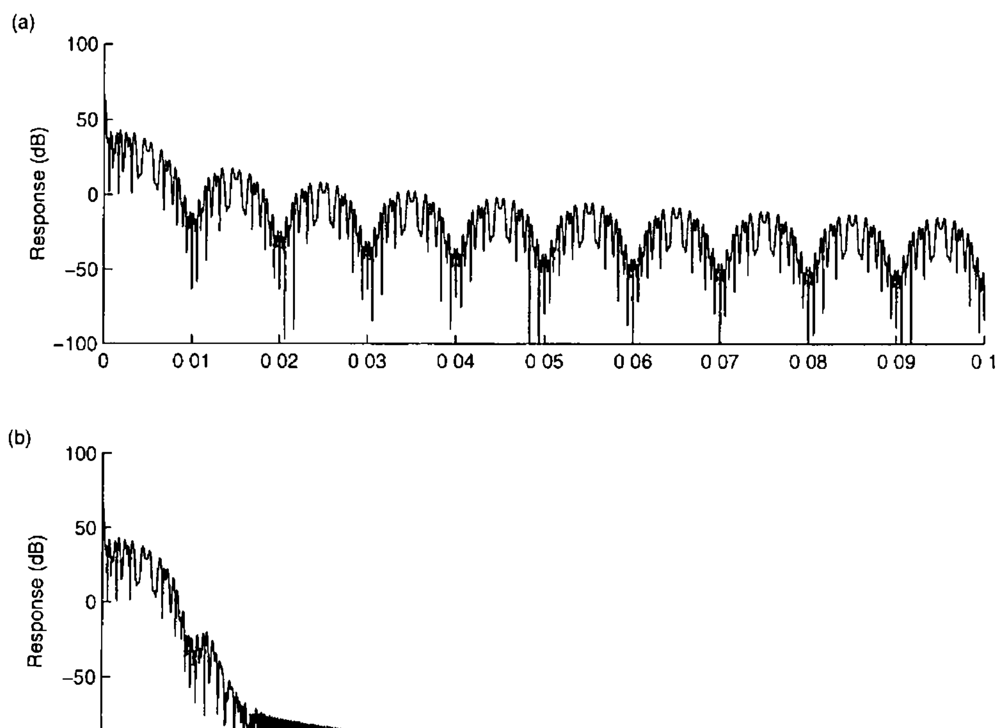

Figure 5 10 – Occupied bandwidth minimisation by low pass filtering the baseband signal (a) pre filtration, (b) post filtration

5 3 1 3 – Local Oscillator

The local oscillator is identical to the tone generator described in the previous chapter It is used here for data upconversion

5 3 1 4 – The Mixer

The mixer performs the modulation of each carrier by it's associated data channel The modulation scheme being used is Binary Amplitude Shift Keying (BASK) so when the data signal is a 1 the carrier is multiplied by 1 giving itself and when the data signal is 0 the carrier is multiplied by 0 giving no signal Simple multiplication of the carrier by the data signal results in a BASK signal, hence the equation used is $A_c m(t) Cos(2\pi f_c t)$ where m(t) is either 1 or 0 depending on the data bit

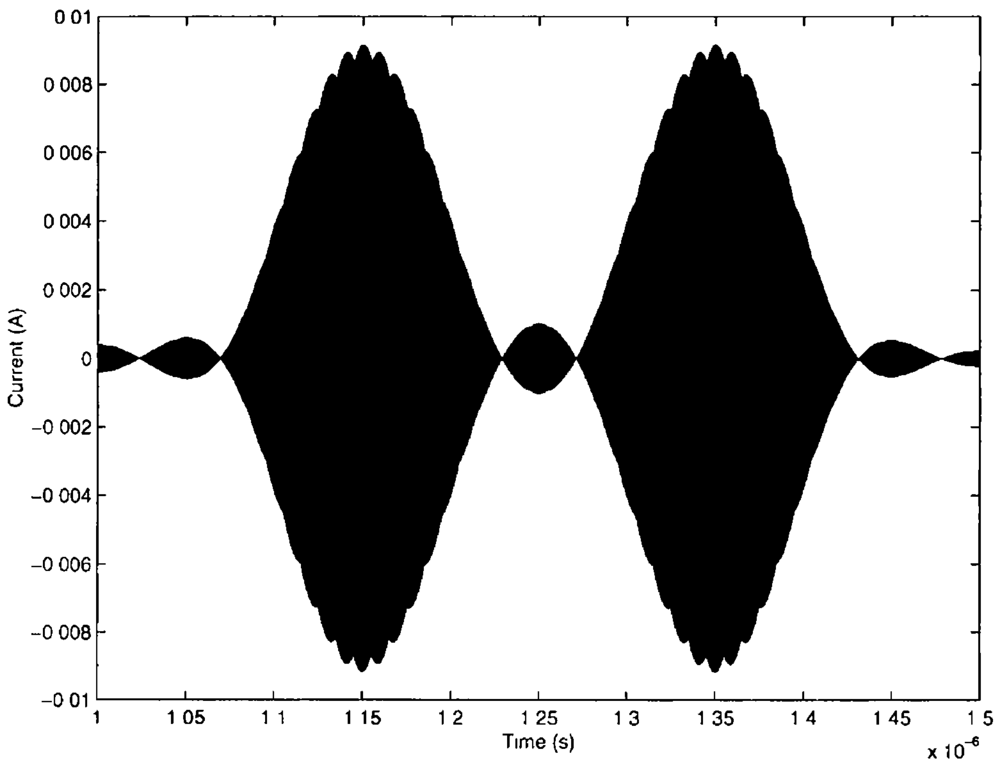

Figure 5 11 – 6 GHz Carrier Modulated with '01010' bit stream

Figure 5 11 shows 0 5μs of the modulated carrier signal This plot corresponds to a bit pattern of '01010' modulated onto the 6 GHz carrier Viewing the plot over an even shorter time range, would allow us to see the underlying sine wave

5 3 1 5 – The Power Coupler and Bias Tee

The power coupler is used to combine a number of RF data channels, with which we can then modulate the laser This combined signal is then coupled to the dc bias current and used to modulate the laser In this case, five RF data channels were used and the bias current was 70 mA Hence the input signal oscillates around the 70 mA point as can be seen in Figure 5 12 below

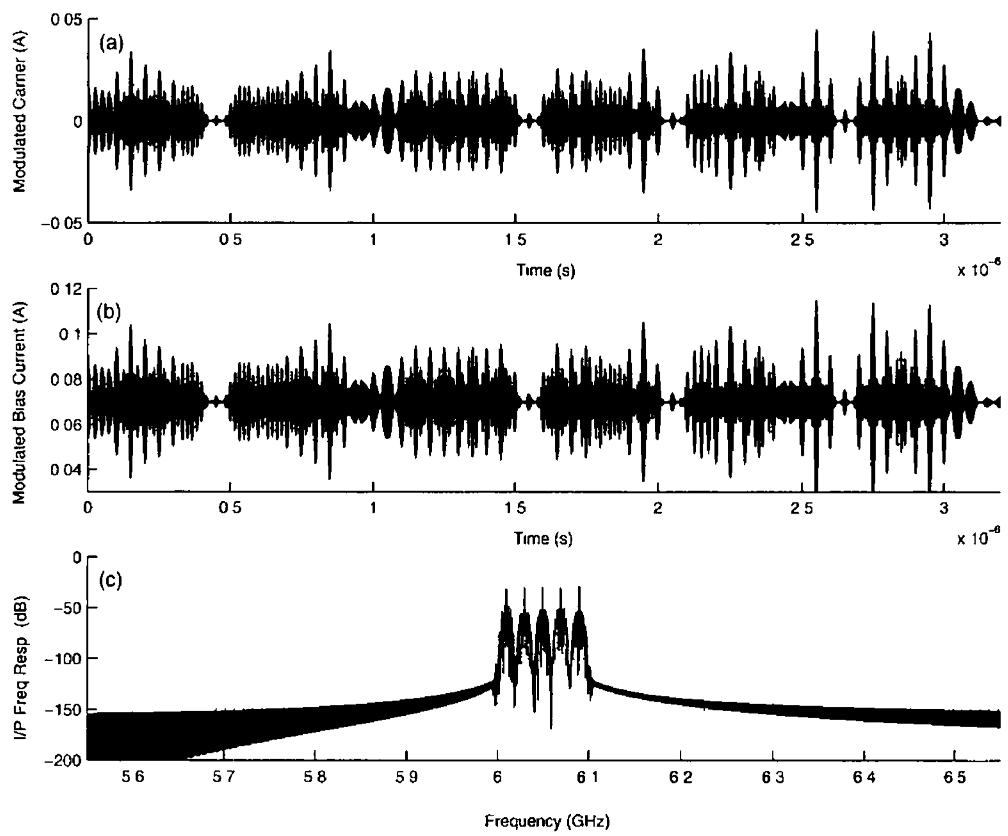

Figure 5 12 – Coupled data signals (a), combined data signals coupled with dc bias of 70 mA in the time (b) and frequency (c) domain

5 3 1 6 – Laser Diode

The model for the laser is identical to that of the two tone case described in the previous chapter Figure 5 12 (b & c) show the RF signal which is used to modulate the laser in both the time and the frequency domain

5 3 1 7 – Optical Fiber

For simplicity, the link between the laser and the photodetector was not included It could also be said the link consisted of ideal optical fiber[1] We were mainly interested in the nonlinear response of the laser In a real system, fiber nonlinearities could be neglected by keeping the optical powers low Loss and dispersion could be

[1] zero loss zero dispersion and perfect linearity

assumed negligible or could be overcome using optical amplifiers and Dispersion Compensating Fiber (DCF), respectively

5 3 1 8 – Variable Attenuator

A variable attenuator was added to the system to allow the BER to be measured at a number of different optical powers To model it, the output power of the laser was simply divided by a user defined value The effect of increasing the attenuation will be shown in Figure 5 15 By reducing the optical power into the receiver, the electrical power it outputs is also reduced Thus the Signal to Noise Ratio (SNR) of the resulting signal is degraded

5 3 1 9 – Photodiode

The photodiode was modelled as a simple optoelectronic conversion with the addition of noise For simplicity, thermal noise was considered but shot noise was ignored The equation for thermal noise is given as

$$\sigma_{th}^{2} = \frac{4kTf_0}{R}$$

where k is Boltzmann's constant, T is the temperature in degrees Kelvin, R is the receiver impedance, and f_0 is the receiver bandwidth Noise is random in nature so it cannot be predicted what it will do to the signal To model the noise in this system the following assumptions were made

- The noise had zero mean,
- The noise had a Gaussian distribution,

These assumptions allows the noise model to be greatly simplified

A responsivity of 0 6 A/W was used The Light Current (PI) curve in Chapter 3 (Figure 3 17) shows that a bias current of 70 mA corresponds to an optical power of approximately 6 65 mW Detection of this optical signal centred around 6 65 mW with a 0 6 A/W responsivity should yield a received signal oscillating around approximately 4 mA and this is confirmed in Figure 5 13, which shows the detected optical signal in both the time and frequency domain Comparison of Figure 5 12 and Figure 5 13 shows the distortion (caused by the nonlinearity of the laser diode) which has been added in the optical link While the distortion is not evident in the time domain it can be clearly seen in the frequency domain by the generation of new undesired frequency components

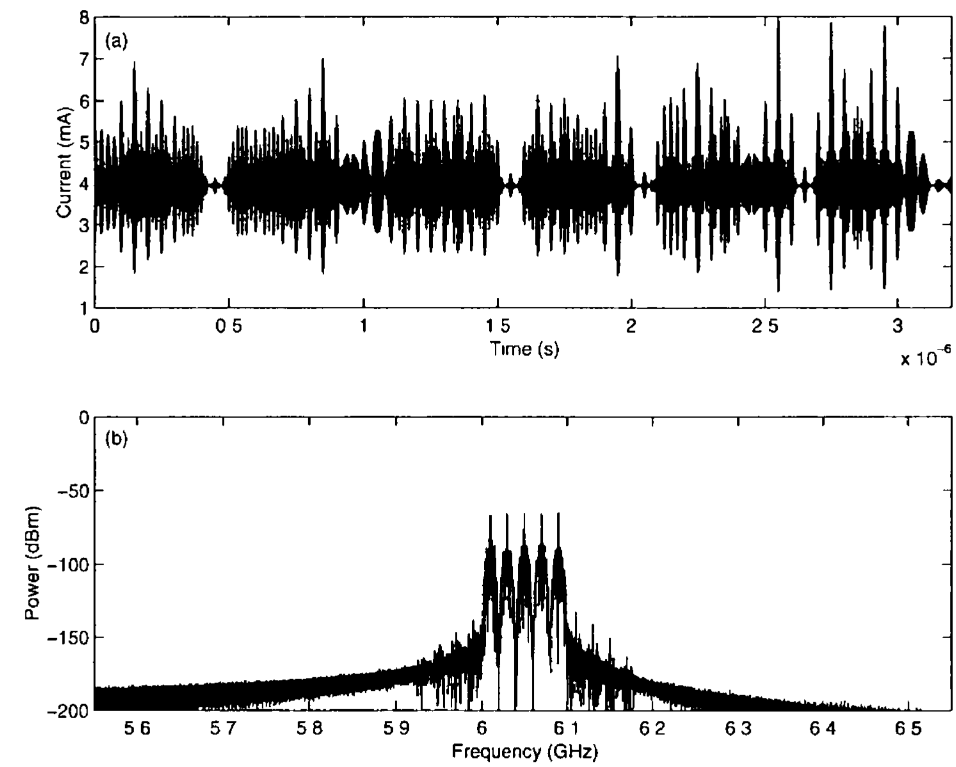

Figure 5 13 – Received signal from the laser in the time (a), and frequency (b) domains

5 3 1 10 – Downconversion and Filtering

After the detector each of the signals are mixed with their respective local oscillators to extract the baseband signal from the carrier Figure 5 14 is a plot of the result of downconversion of the central channel of the five RF data signals This is done by mixing the received signal with the 6 05 GHz local oscillator Clearly it has brought the central channel to baseband The data is then filtered out using another lowpass filter Again it was a 5th Order Chebyshev Type II digital filter with a cutoff frequency of 7 MHz and a stopband attenuation of 70 dB It is vital to choose a suitable filter bandwidth to avoid interference from adjacent channels

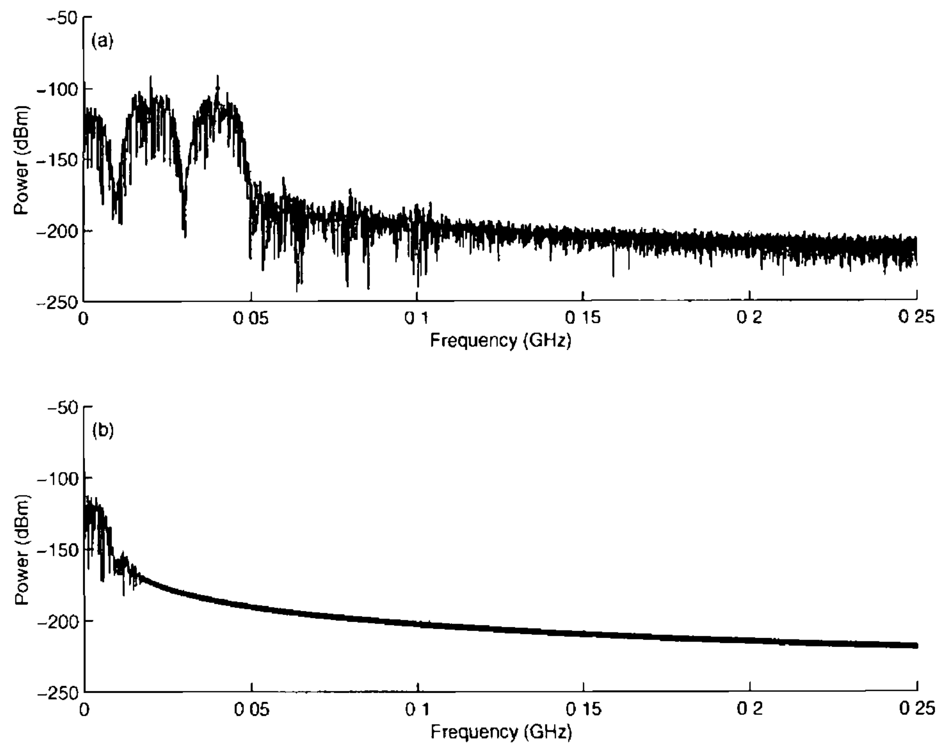

Figure 5 14 – Received signal in the frequency domain showing the downconverted central channel (a) and the filtered baseband signal (b)

Figure 5 15 shows the initial data signal and the recovered received signal In this case attenuation of 25 dB was added to the system It is clear that the attenuation had reduced the SNR of the signal

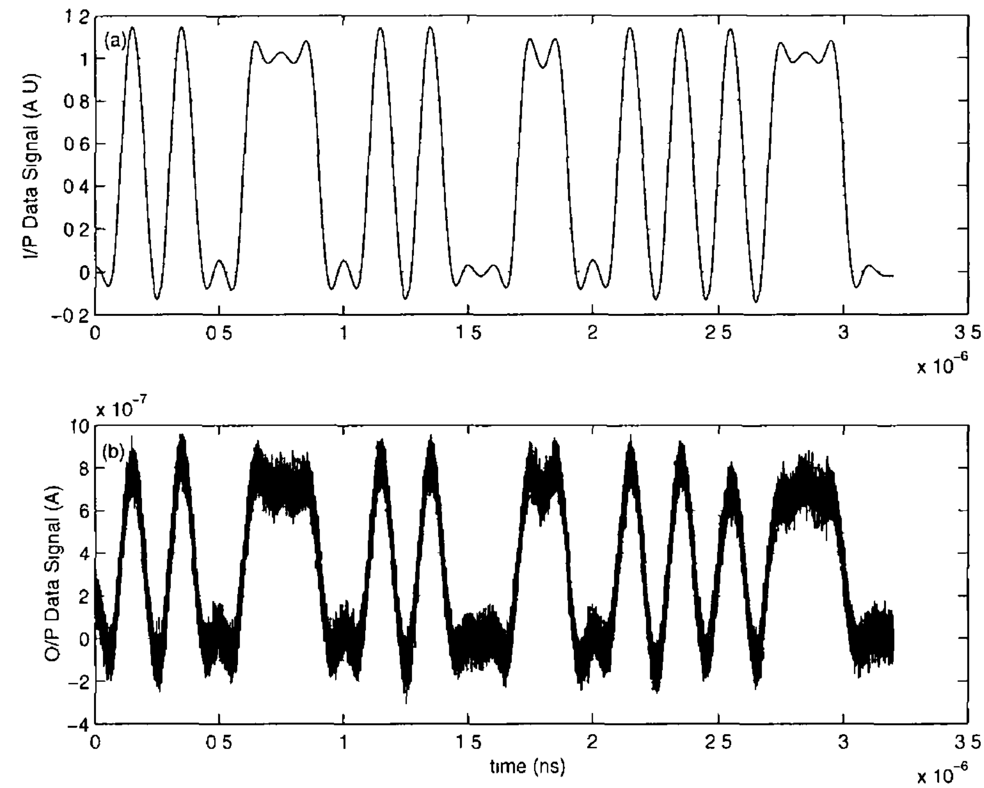

Figure 5 15 – Input data signal (a) and recovered data signal having passed through the simulated system with 25 dB attenuation (b)

5 3 1 11 – Bit Error Rate Tester and Oscilloscope

The eye diagram, is a visual aid for approximating system performance It is defined as the synchronised superposition of all the possible realisations of the signal of interest viewed within a particular signaling interval [18] In simpler terms, an eye diagram is a plot of all of the bit transitions, superimposed onto each other The width of the opening of the eye, defines the time interval over which the signal can be sampled without error from intersymbol interference The height of the eye defines the noise margin of the system The slope of the transitions gives information about the sensitivity of the system to timing errors Figure 5 16 shows an example of an eye diagram which was generated using the simulation

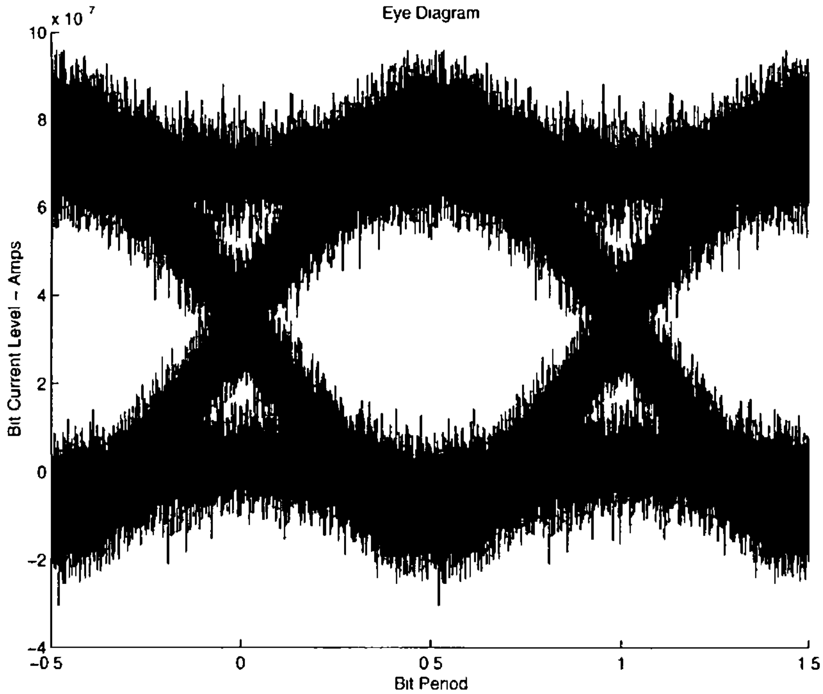

Figure 5 16 – Example of Generated Eye Diagram

A numerical value for system performance is given as it's BER The BER simply tells us how many errors were in the received signal given that the transmitted signal is known It is a telecommunication standard to have a BER of 10^{9} in systems Therefore any system that has more than 1 error per billion is sub-standard For a system where the noise on a 1 is equal to the noise on a 0, the threshold or decision point is taken to be exactly half way between the mean "1" level and the mean "0" level That is

$I_D = \dfrac{\overline{I_{(1)}} - \overline{I_{(0)}}}{2}$ This is the case in our model because we are only using thermal noise which has the same noise level for both high and low If the model included shot noise then the following equation would have to be used because shot noise is current dependent and hence a 1 will have more shot noise than a 0 So if $\sigma_1 \neq \sigma_0$

$I_D = \dfrac{\sigma_0 \overline{I_{(1)}} - \sigma_1 \overline{I_{(0)}}}{\sigma_1 + \sigma_0}$ is the equation which must be used

The equation used to calculate the BER in the model was

$$BER = \frac{1}{4}\left[erfc\left(\frac{\overline{I_{(1)}} - I_D}{\sqrt{2}\sigma_1} \right) + erfc\left(\frac{I_D - \overline{I_{(0)}}}{\sqrt{2}\sigma_0} \right) \right]$$

where,

$\overline{I_{(1)}}$ is the mean of the current when the signal is high

$\overline{I_{(0)}}$ is the mean of the current when the signal is high low

σ_1 is the standard deviation of the current when the signal is high

σ_0 is the standard deviation of the current when the signal is low

5 3.2 – Simulation Results

Figure 5 17 shows the complete setup that was used in the simulation It consisted of five NRZ data sources which were low pass filtered and mixed with five carriers at frequencies from 6 01 to 6 09 GHz and with a carrier spacing of 20 MHz These five channels were then coupled together using a power coupler before being combined with a dc bias current of 70 mA and used to modulate a laser External injection into the laser is achieved by setting the injected photon density to a positive number Conversely to use the free running regime, this value is simply set to zero The optical signal is passed through a variable attenuator, before being received by the detector which converts the optical signal back to an electrical one Downconversion of each channel is then achieved by mixing the received signal with the respective local oscillators This results in a signal containing both the baseband signal and the respective carrier Low pass filtering this signal removes any unwanted components and leaves the received data channel, which is subsequently passed into the oscilloscope and BERT

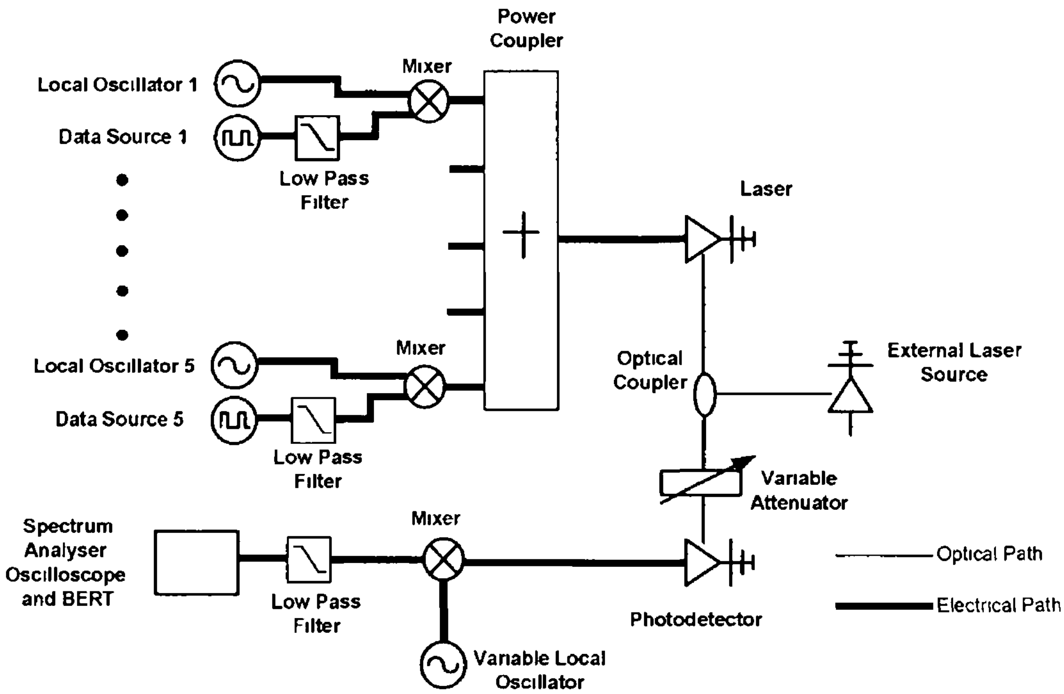

Figure 5 17 – Simulation setup for SCM over fiber

Figure 5 18 plots the response of the modelled laser used in the simulation It can be used as a free running laser or under the influence of external injection Reference will be made to this plot in describing the results obtained in this section

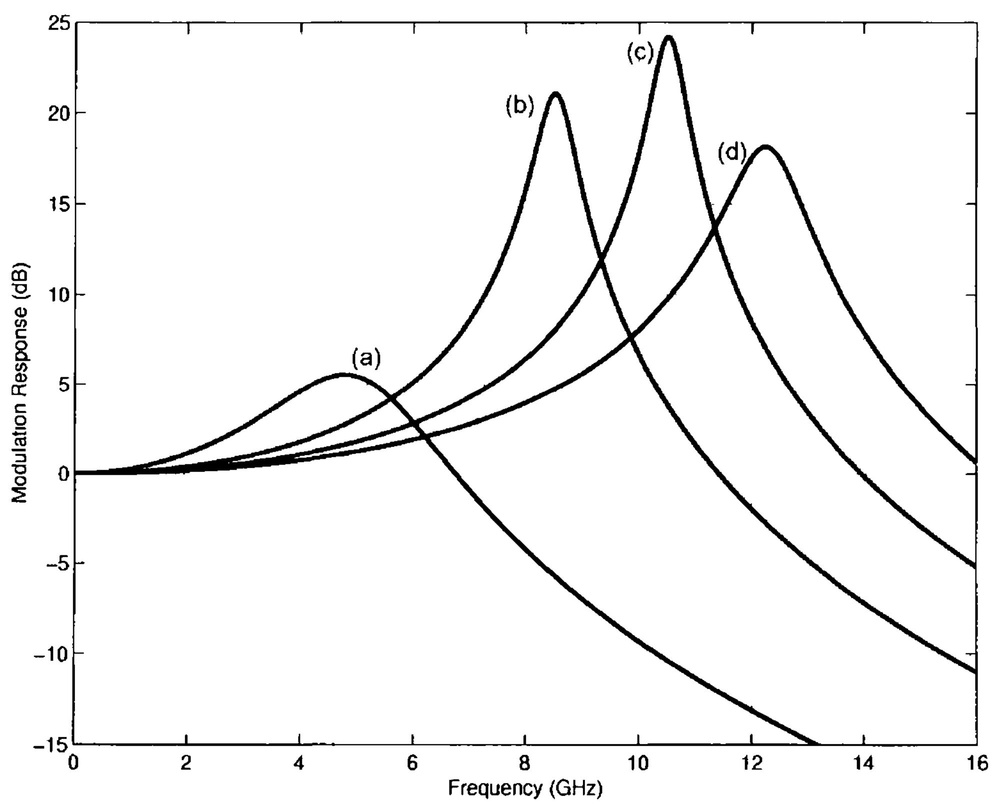

Figure 5 18 – Modulation Response of the simulated laser under free running conditions (a) and with injection ratios of 0 01 (b), 0 025 (c), 0 045 (d). In all cases the bias current was 70 mA

Figure 5 19 shows the eye diagrams of the two 10 Mbit/s data signals from the optically fed microwave system using (a) free running laser diode and (b) laser diode with the external injection ratio of 0 025 The received optical power (before photodiode) was –18 23 dB in both cases Seeing as the only change made to the simulation when taking these results was to change the injection from off to on, it is clear that using the technique of external injection has improved the performance in the simulated system The amplitude of both eyes are identical which implies that the modulation response in each case was the same This shows that the improvement in performance is solely due to the linearisation of the laser diode's response at 6 GHz and not down

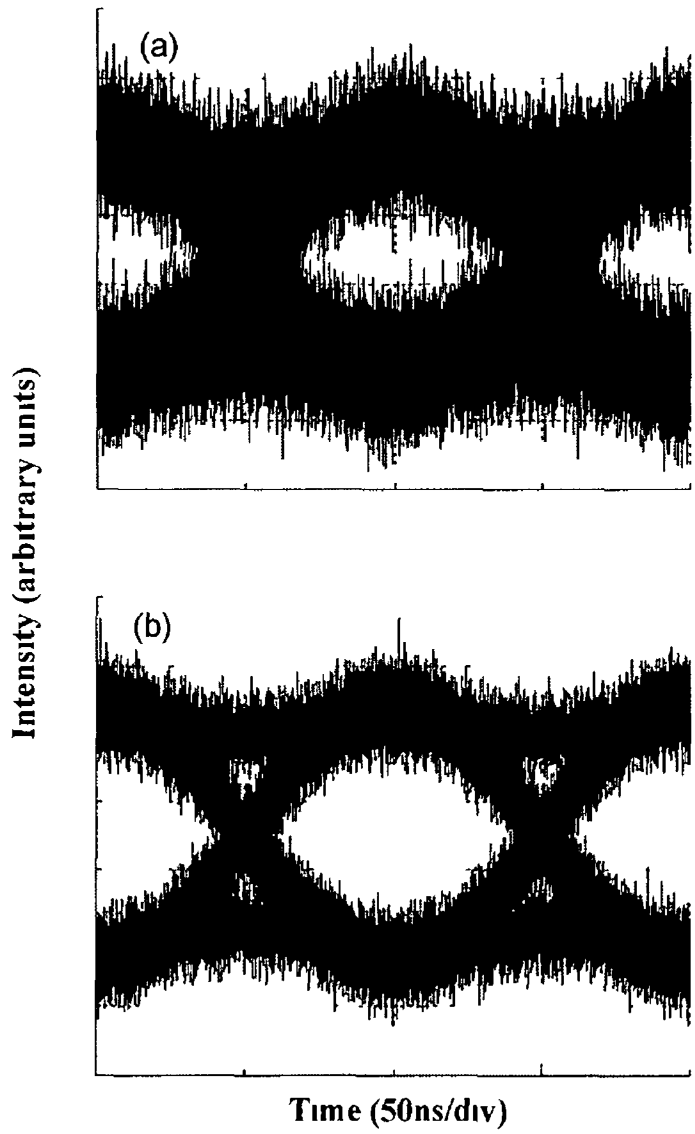

Figure 5 19 – Simulated eye diagrams with free running laser (a) and laser under external injection (b) showing improvement due to linearity alone

In the experimental results section we showed that by tuning the power and wavelength of the injected light the response could be optimised so that the level of the response could be improved as well as it's linearity This would cause even greater performance enhancements

The four eye diagrams shown in Figure 5 20 represent the four different levels of injection shown in Figure 5 18 The power at the receiver was kept constant for each of them Plots (a) and (b) correspond to the free running laser and injection ratio 0 025 respectively and as can be seen, their equal amplitudes match the equal responses seen in Figure 5 18 When the injection ratio is increased to 0 045, we can see that although it becomes more linear, it's response drops by approximately 1 5 dB This drop corresponds to a reduction in received signal amplitude which can be seen clearly in plot (c) Conversely, reducing the level of injection decreases the linearity around 6 GHz but it increases the response The higher amplitude seen in eye (d), corresponds well to this

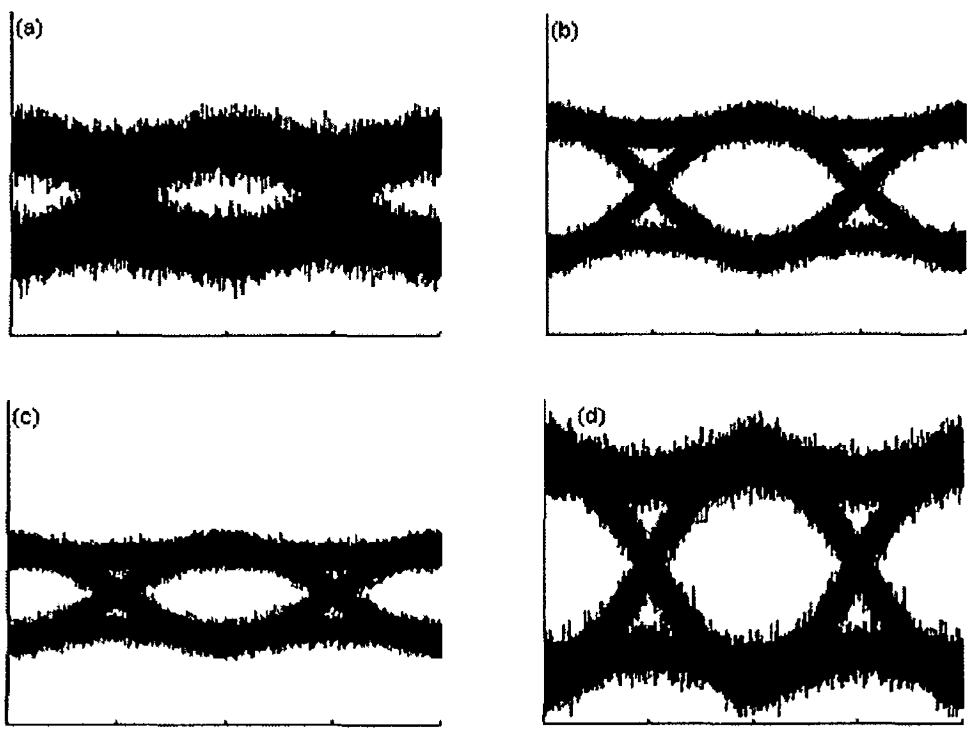

Figure 5 20 – Eye Diagrams corresponding to different levels of injection (a) free running, (b) injection level 0 025, (c) injection level 0 045, (d) injection level 0.017.

To obtain an accurate measurement of the performance we measured the BER for a number of different received optical powers Figure 5 21 below shows quite clearly the different effects on performance that the linearity and the magnitude of the response have Each of the curves in this figure correspond to one of the eye diagrams in Figure 5 20 By turning on injection, and having the responses equal but the linearity improved (injection ratio 0 025 (■)), performance was improved by over 3 5 dB at a BER of 1×10^{9} This 3 5 dB is solely due to the improved linearity For injection ratios less than 0 025 (i e 0 017 (▲)) the modulation response has linearised slightly and the magnitude of the response is also increased Both of these changes in the modulation response add together to give an overall improvement in system response of greater than 4 dB However as you inject more light, the response becomes flatter but you also get less power in your electrical signal Hence the slight worsening performance with an injection ratio of 0 045 (×)

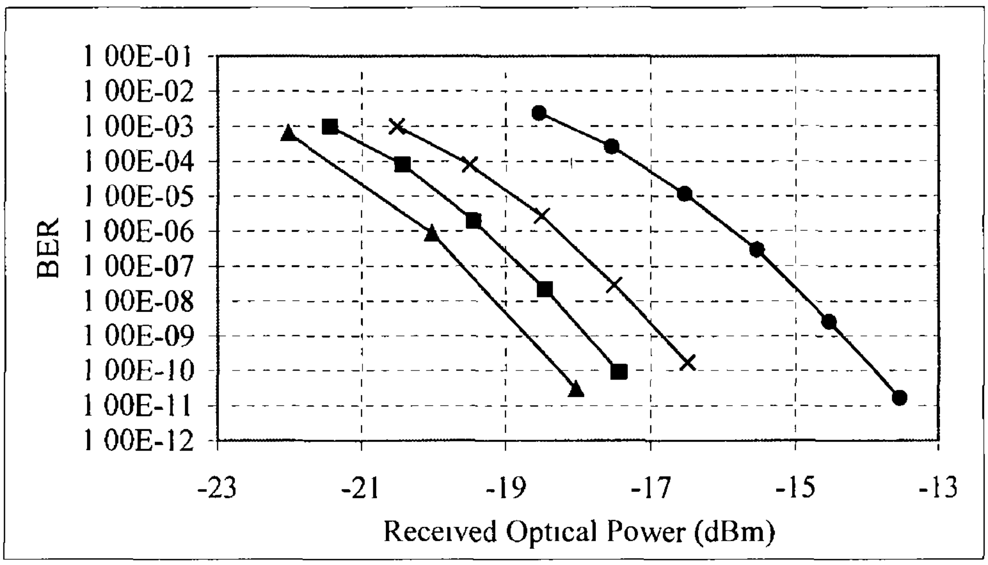

Figure 5 21 – BER versus received optical power different levels of injection

By experimenting further with the tuning it is expected that even greater performance improvements could be achieved in the linear portion of the laser's response While it is possible to operate in the high response peak which is caused by the external injection, the strong nonlinearity near the peak means that the advantage of having the high response is cancelled out

5.4 – Conclusion

We have shown in this chapter, that the performance of SCM data channels in a HFR system can be improved using the technique of external light injection into the laser diode Systems like this may be employed by mobile communication networks in order to transport channels between the BSs and the MSC simultaneously The system model was expanded to allow the subcarrier multiplexing of data channels and the results correlated well with experimental ones

References

[1] T E Darcie, "Subcarrier Multiplexing for Multiple Access Lightwave Networks", *Journal of Lightwave Technology,* vol 5, pp 1103 – 1110, August 1987

[2] P A Davies, N J Gomes, "Subcarrier Multiplexing in Optical Communication Networks" in *Analogue Optical Fiber Communications,* by B Wilson, Z Ghassemlooy, I Darwazeh, IEE, 1995

[3] J Yu, Y Kim, M Lee, K Lee, J Park, "Analysis of Nonlinear Effects in Subcarrier-Multiplexed Fiber Optic Links for CDMA RF Signal Transmissions", *Microwave Optical Technology Letters*, vol 29, pp 37-40, 2001

[4] C L Tang, H Statz, "Phase-locking of laser oscillators by injected signal," *Journal of Applied Physics*, vol 38, pp 323-324, 1967

[5] K Otsuka, S Tarucha, "Theoretical studies on injection locking and injection-induced modulation of laser diodes," *IEEE Journal of Quantum Electronics*, vol 7, pp 1515-1521, 1981

[6] X J Meng, T Chau, M C Wu, "Experimental demonstration of modulation bandwidth enhancement in distributed feedback lasers with external light injection" *Electronics Letters*, Vol 34, pp 2031-2032, 1998

[7] R Lang, K Kobayashi, "External Optical Feedback Effects on Semiconductor Injection Laser Properties", *IEEE Journal of Quantum Electronics*, Vol 16, pp 347 – 355, 1980

[8] J Wang, M K Haldar, L Li, F V C Mendis, "Enhancement of Modulation Bandwidth of Laser Diodes by Injection Locking", *IEEE Photonics Technology Letters*, Vol 8, pp 34-36, 1996

[9] F Smyth, L P Barry, "Overcoming distortion limitations in hybrid radio/photonic systems for the distribution of WCDMA signals", *Springer Journal of Electrical Engineering*, accepted for publication April 2003, due for press September 2003

[10] C -H Chang, L Chrostowski, C Chang-Hasnain, "Frequency Response Enhancement of Injection Locked Lasers", *Technical Digest Summary of Papers Presented at Conference on Lasers and Electro-Optics 2003, CLEO '03*, 2003

[11] T E Darcie, M E Dixon, B L Kasper, C A Burns, "Lightwave System Demonstration of Subcarrier Multiplexing", *Electronics Letters*, vol 22, no 15, pp 774-775, 1986

[12] H S Al-Raweshıdy, D Galbrıth, R Prasad, "Performance of radıo on fiber for mıcrocellular GSM networks" *48th IEEE Vehıcular Technology Conference, 1998 VTC 98*, vol 1 , pp 392 –396, 1998

[13] B J Koshy, P M Shankar, "Spread-spectrum technıques for fiber-fed mıcrocellular networks", *IEEE Transactıons on Vehıcular Technology*, vol 48, pp 847 –857, 1999

[14] G H Smıth, D Novak, C Lım, "A mıllımeter-wave full-duplex WDM/SCM fiber-radıo access network", *Technıcal Dıgest of the Optıcal Fıber Communıcatıon Conference and Exhıbıt, 1998 OFC '98*, vol 1, pp 18 –19, 1998

[15] X J Meng, D T K Tong, T Chau, M C Wu, "Demonstratıon of an Analogue Fıber-Optıc Lınk Employıng a Dırectly Modulated Semıconductor Laser wıth External Lıght Inȷectıon", *IEEE Photonıcs Technology Letters*, vol 10, pp 1620 – 1622, 1998

[16] A Kaszubowska, P Anandaraȷah, L P Barry, "Enhanced Performance of an Optıcally Fed Mıcrowave Communıcatıon System Usıng a Dırectly Modulated Laser Transmıtter wıth External Inȷectıon", *2001 IEEE/LEOS Annual Meetıng, LEOS 2001*, vol 1, pp 314-315, 2001

[17]G Yabre, J Le Bıhan, "Reductıon of nonlınear dıstortıon ın dırectly modulated semıconductor laser by coherent lıght ınȷectıon", *IEEE Journal of Quantum Electronıcs*, vol 33, pp 1132-1140, 1997

[18] S Haykın, Communıcatıon Systems (3rd Edıtıon), Wıley, 1994

Chapter 6 – Conclusion

The growth in mobile communication has been phenomenal The second generation of mobile communication included systems such as Global System for Mobile Communications (GSM) and Interim Standard 95 (IS-95) and at the end of 2002 there were estimated to be more over one billion cellular subscribers in over 190 countries worldwide [1] In the future systems such as Third Generation (3G) systems which are already operational in places and Fourth Generation (4G) systems which are being developed will offer broadband packet based data services as well as simple voice Services such as mobile video conferencing, and music/video on demand will become commonplace Such services however, due to their high bandwidth requirements, force the network operators to seek ways to increase the capacity of their telecommunication system The integration of wireless and optical networks is one potential solution for increasing both capacity and mobility Such hybrid networks benefit from the advantages of both systems Optical fiber provides a high capacity medium with electromagnetic interference immunity and low attenuation, while radio will enable broadband data to be delivered to the end-users in a quick, flexible and inexpensive manner Hybrid Fiber Radio (HFR) also has added benefit of reducing costs in the access network by allowing centralisation of the complex processing equipment and thereby simplifying the many base stations which must be deployed There are also many other advantages associated with HFR including its ability to allow many radio services over the same fiber to some remote antenna site, in order to utilise the full spectrum of the optical fiber and the fact that it allows simple upgrade to further upcoming radio standards, e g from GSM to Universal Mobile Telecommunications System (UMTS)

A number of network architectures have been proposed, ranging from end signal generation at a central site with fiber distribution to the cells [2], to baseband data signal distribution over fiber and up-conversion at the antenna unit [3] with many intermediate concepts Each architecture has it's specific advantages and disadvantages The architecture we chose was a microwave feeder using conventional opto-electric conversion at the Base Station (BS) In this architecture, the only functions performed at the BS are electro-optic and opto-electric conversion, and perhaps amplification It was chosen for the simplicity of it's BSs, which, as has been mentioned, will be paramount in the commercial success of future mobile networks

The two main techniques that can be employed at the transmitter of HFR systems are direct modulation of the laser with the Radio Frequency (RF) signal, and external modulation of a Continuous Wave (CW) optical signal with the RF data External modulators are expensive and this makes them unsuitable for use in HFR networks in which cost must be kept to a minimum Direct modulation also has the advantage of being far simpler due to the fact that you simply superimpose the data signal onto the bias current There are no additional components to power, configure and maintain For these reasons direct modulation is the method considered in this thesis There are however, disadvantages to direct modulation also Firstly the bandwidth available is considerably less than in systems which employ external modulation Another major limitation in systems that employ direct modulation of a laser diode with the RF data signal, is the serious distortion introduced due to the dynamic nonlinearity of the laser at frequencies around it's oscillation frequency This is one of the primary concerns of this thesis

It is expected that the operating frequencies of future mobile networks will lie in the microwave region (3-30 GHz) to make use of the uncluttered radio spectrum The maximum frequency of operation of a directly modulated laser, however is limited by it's inherent bandwidth In general, this bandwidth is less than 10 GHz[1] and linear operating frequencies are usually even lower It has been previously shown that the injection of light from an external source into a laser under modulation can improve it's bandwidth, to over three times it's inherent bandwidth [4] The laser's linearity and response can also be improved by tuning the power, wavelength and polarisation of the injected light [5] A thorough examination of the effects of external injection into the laser diodes to be used in the work was performed It was observed that the modulation bandwidth of one of our lasers could be increased from around 8 GHz to around 11 GHz The linearity could also be improved by pushing the nonlinear oscillation peak out to higher frequencies By varying the power and wavelength of

---

[1] While lasers are available with bandwidths up to around 20GHz these devices are extremely expensive and hence are not suitable for use in HFR networks

the injected light it was possible to both linearise the device and increase it's modulation response over a wide range of frequencies While, much work has been done in the area of external light injection, it's use in HFR networks brings an aspect of novelty to this work

In chapter 4 we discussed the transmission of Wideband Code Division Multiple Access (WCDMA) signals at 6 GHz through a HFR system The initial experimental stages of this work began by examining the simple transmission of WCDMA signals over fiber Degradation of approximately 20 dBc in the Adjacent Channel Leakage Ratio (ACLR) of the transmitted WCDMA signal was observed when it was passed through the system, thereby verifying the predicted effect of the laser nonlinearity This reduced the ACLR to below the requirements set by the 3GPP for WCDMA transmission The technique of external injection was then integrated into the WCDMA over fiber setup and used in an attempt to improve system performance Using external injection the ACLR was improved by 10 dBc to –41 dBc which almost comes in line with the 3GPP requirements These results were limited by the dynamic range of our measurement systems and we believe that in a commercial system the requirements could be easily complied with

Having looked at the effect of laser diode nonlinearity in a single WCDMA channel, we then went on to look at a multi carrier HFR system We multiplexed together five Binary Phase Shift Keyed (BPSK) data channels, each with a data rate of 10 Mbit/s The improvement in system performance that can be achieved in such a multi-channel HFR communication system, by using external injection at the laser transmitter is shown in chapter 5 Improvement in system performance of greater than 2 dB was achieved at a Bit Error Rate (BER) of 1×10^{-7} This improvement in system performance is solely due to the enhanced linearity of the device around the operating RF band, as the relative response of the laser is kept equal for the free running and externally injected case It was also shown that by varying the properties of the externally injected light that the modulation response can be tuned to not only improve the linearity at the frequency of operation but also the magnitude of the response By optimising the modulation response a performance improvement of 5 dB was achieved

Due to the number of variables which must be assessed when designing a HFR system, it is vital to use simulations both before and after the actual experimentation [6] Beforehand, they reduce the need for initial experimentation, and help new ideas to become established and built upon Afterwards simulations are used to verify experimental work and expand upon it where equipment and time limitations do not allow This work employed Matlab, a program which is widely used in Electronic Design Automation (EDA) In our work, an initial model was written to simulate the single mode laser diode alone It was based on the steady state and dynamic responses of the single mode laser diode rate equations External injection was then added to this model By varying the power and wavelength of the injected light the model could be tuned to give modulation responses which matched closely with those of our physical lasers Subsequently the model was expanded to include the entire optical part of a HFR system This was done by adding a time domain analysis to the model using Matlab's ODE45 function This allowed simulations to be carried out in which the laser could be modulated both with tones and with data As mentioned in the simulation sections, the performance trends observed in the experimental work matched closely with their simulated counterparts

Judging by the results presented in this thesis it is clear that laser transmitters based on external light injection may be very suitable sources for HFR systems due to their improved linearity Indeed for practical systems applications it will be more suitable to integrate the slave and master laser into a single chip that exhibits the type of linearity required for next generation multi-carrier RF systems Such a single chip device was first demonstrated at the Conference on Lasers and Electro-Optics (CLEO) 2003 [7]

Further development in HFR systems may see the introduction of Wavelength Division Multiplexing (WDM) techniques [8] To make systems commercially viable for the operators of future mobile networks, costs must be kept to an absolute minimum The sharing of network infrastructure by operators has been discussed to keep costs down and this is one potential use for WDM in a Sub-Carrier Multiplexing (SCM) HFR system Each network operator must transmit several channels which he could multiplex onto a number of subcarriers By using separate optical wavelengths then, each operator's data could be wavelength division multiplexed onto a single fiber In doing so all of the channels for all of the operators can be transmitted to a base station where only a single detector is needed and filters can be used to extract the necessary optical channels

The demand for bandwidth is growing constantly, forcing the carriers to look for new ways to increase the capacity of the networks Many experts believe that radio is capable of delivering almost an infinite bandwidth, providing that cell sites can be engineered cheaply enough to enable operators to install thousands of them Laser diode linearity was the primary concern of this thesis Hence, we have only examined the optical part of the HFR system An extremely interesting extension to this work would be to include the air link A low power or passive picocell could easily be set up in the laboratory and hence downlink and uplink could be achieved This would allow us to verify that the improved performances in the optical link is carried through to the whole system

References

[1] J De Vriendt, P Laine, C Lerouge, X Xiaofeng, "Mobile network evolution a revolution on the move", *IEEE Communications Magazine*, vol 40, pp 104 –111, April 2002

[2] D Wake, D Johansson, D G Moodie, "Passive picocell a new concept in wireless network infrastructure" *Electronics Letters*, vol 33 no 5, pp 404 –406, 1997

[3] K Kojucharow, M Sauer, H Kaluzni, D Sommer, and Ch Schaeffer, Experimental investigation of WDM channel spacing in simultaneous upconversion millimetre -wave fiber transmission system at 60 GHz band, IEEE MTT-S International Microwave Symposium, Boston, Digest pp 1011-1014, June 2000

[4] X J Meng, T Chau, M C Wu, "Experimental demonstration of modulation bandwidth enhancement in distributed feedback lasers with external light injection" *Electronics Letters*, vol 34, pp 2031-2032, 1998

[5] C -H Chang, L Christowski, C Chang-Hasnain, "Frequency Response Enhancement of Injection Locked Lasers", *Technical Digest Summary of Papers Presented at Conference on Lasers and Electro-Optics 2003, CLEO '03* , 2003

[6] A Lowery, O Lenzmann, I Koltchanov, R Moosburger, R Freund, A Richter, S Georgi, D Breuer and H Hamster, "Multiple Signal Representation Simulation of Photonic Devices, Systems and Networks," *IEEE Journal of Selected Topics in Quantum Electron* , vol 6, pp 282-296, 2000

[7] T Jung , H -K Sung, M Wu, D Tishinin, T Tanbun-Ek, K Y Liou, W T Tsang, Technical Digest Summary of Papers Presented at Lasers and Electro-Optics 2003, CLEO '03

[8] S C Liew, "A multivendor multiservice local network based on wavelength-division multiplexing and subcarrier multiplexing" *Conference Digest of LEOS Summer Topical on Broadband Analogue Optoelectronics Devices and Systems, 1990*, pp 13 -14 July 1990

Appendix A – Laser Characterisation

A.1 – NEL 1450 nm DFB Laser: PI Curve

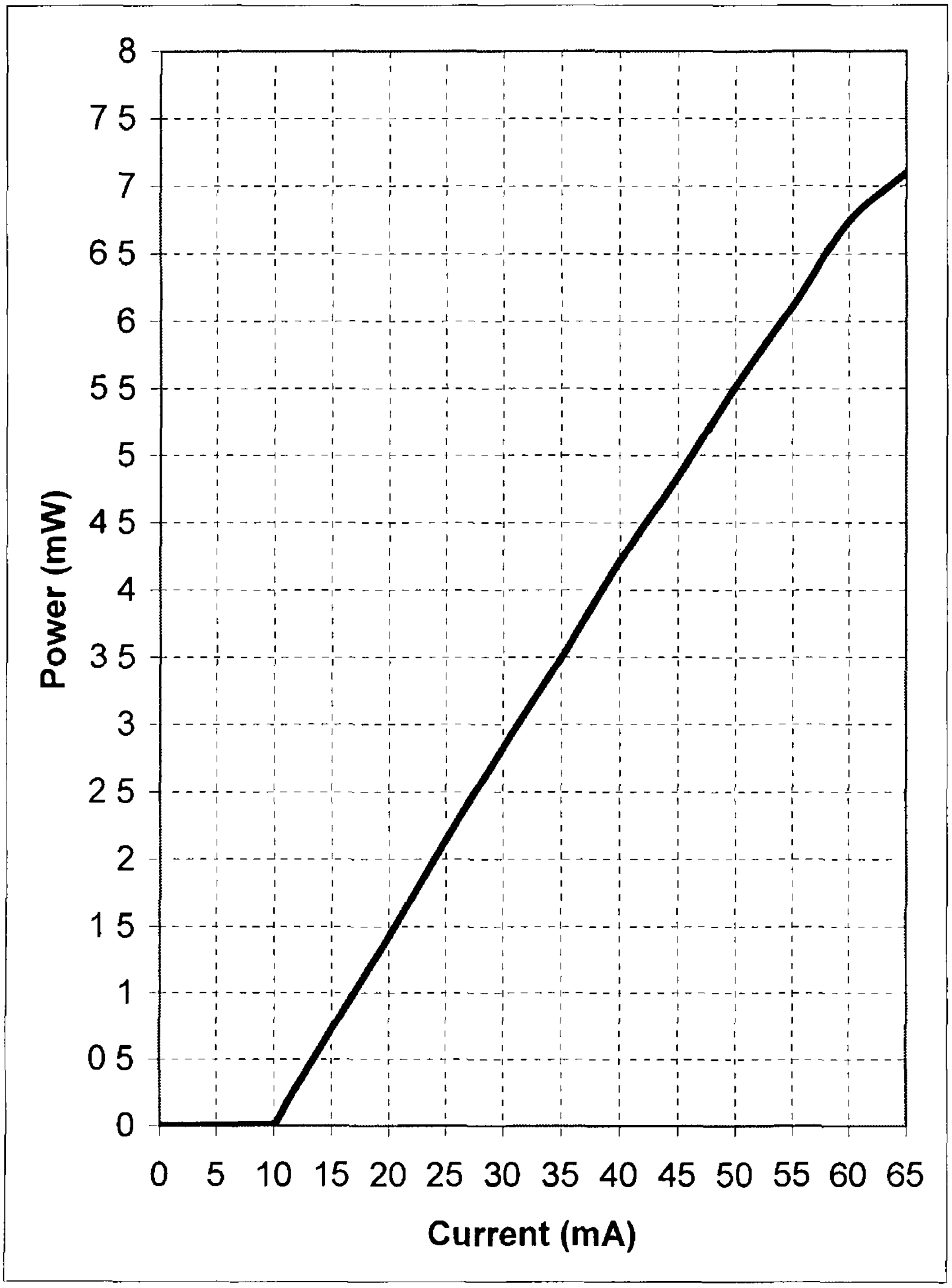

A.2 – NEL 1450 nm DFB Laser: Optical Spectrum

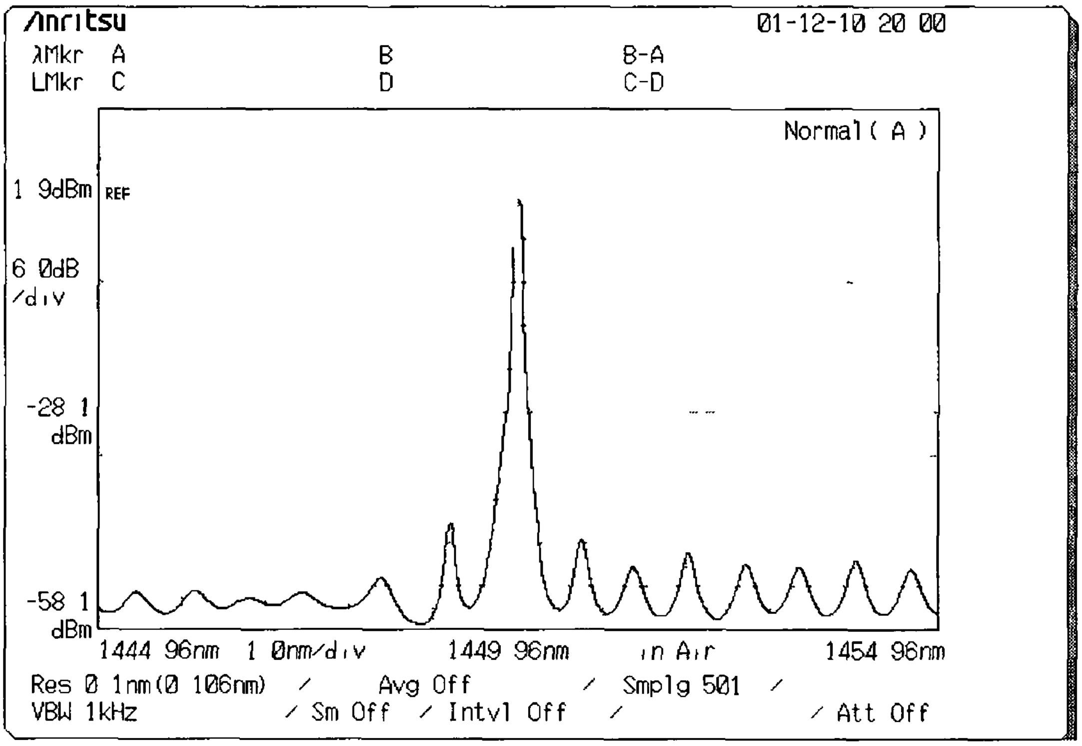

A.3 – NEL 1450 nm DFB Laser Modulation Response: 30 mA

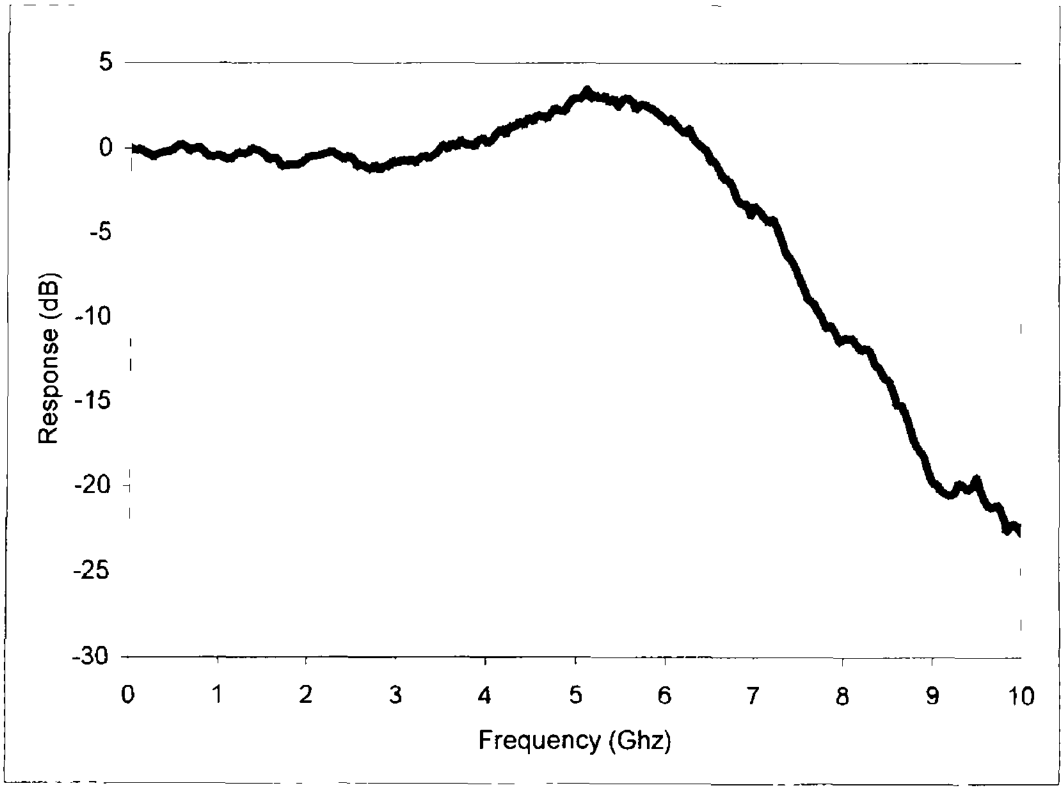

A.4 – NEL 1550 nm DFB Laser: PI Curve

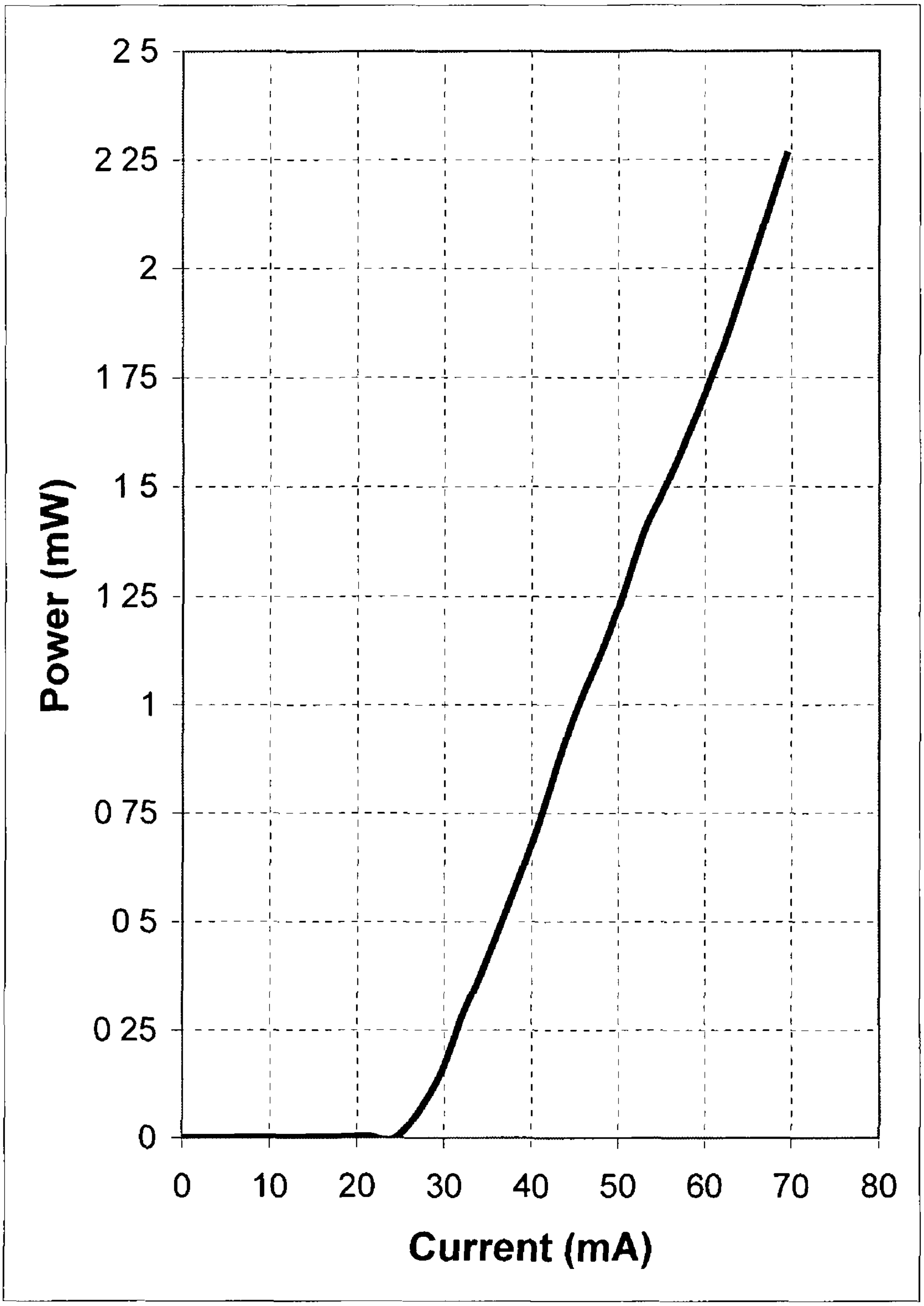

A.5 – NEL 1550 nm DFB Laser: Optical Spectrum

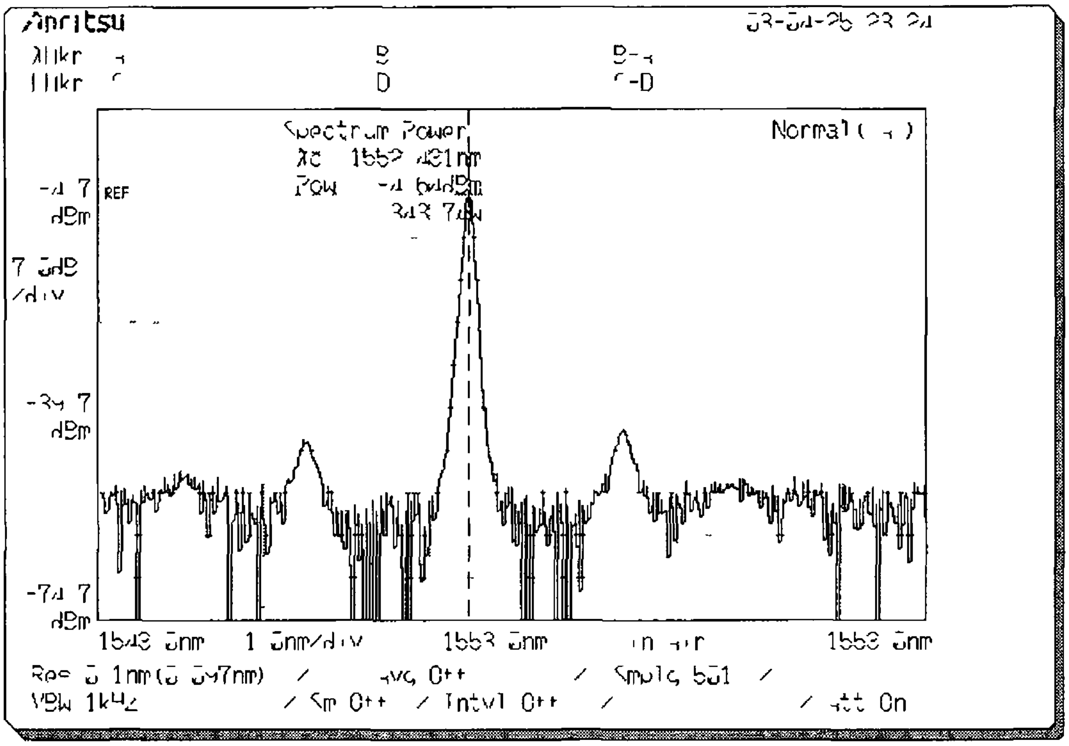

A.6 – NEL 1550 nm DFB Laser: Modulation Response 40 mA

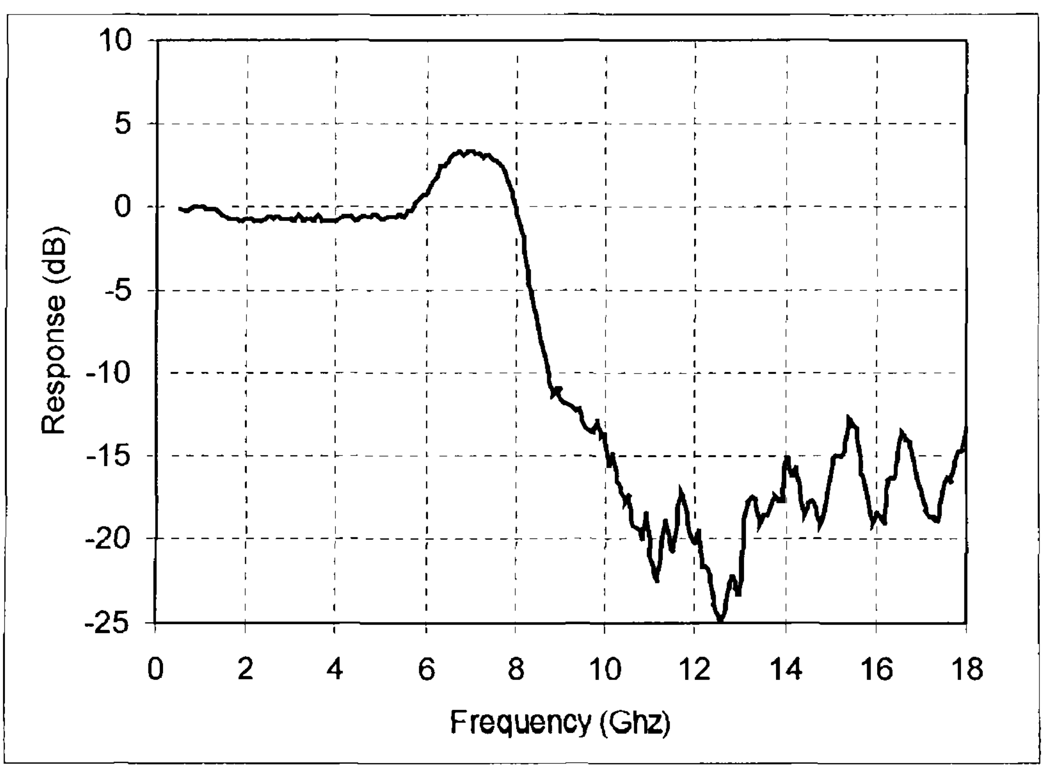

Appendix B – Rate Equations

B.1 – Steady State Solution

The rate equations for a single mode laser diode with injection are as follows By simply setting the external injection term S_{inj} to zero the equations revert back to the free running form

$$\frac{dN(t)}{dt} = \frac{I(t)}{qV} - \frac{N(t)}{\tau_n} - g_0\left(N(t) - N_{om}\right)S(t) \qquad \text{(A 1)}$$

$$\frac{dS(t)}{dt} = \Gamma g_0\left(N(t) - N_{om}\right)S(t) - \frac{S(t)}{\tau_p} + \Gamma\beta\frac{N(t)}{\tau_n} + 2K_c\sqrt{S_{inj}S(t)}Cos(\phi(t)) \qquad \text{(A 2)}$$

$$\frac{d\phi(t)}{dt} = \frac{\alpha}{2}\left(\Gamma g_0(N(t) - N_{om}) - \frac{1}{\tau_p}\right) - \Delta\omega - K_c\sqrt{\frac{S_{inj}}{S(t)}}Sin(\phi(t)) \qquad \text{(A 3)}$$

For the steady state the left hand side of each of the equations (A 1), (A 2), (A 3) can be set to zero

$$0 = \frac{I_0}{qV} - \frac{N_0}{\tau_n} - g_0\left(N_0 - N_{om}\right)S_0 \qquad \text{(A 4)}$$

$$0 = \Gamma g_0\left(N_0 - N_{om}\right)S_0 - \frac{S_0}{\tau_p} + \Gamma\beta\frac{N_0}{\tau_n} + 2K_c\sqrt{S_{inj}S_0}Cos\left(\phi_0\right) \qquad \text{(A 5)}$$

$$0 = \frac{\alpha}{2}\left(\Gamma g_0(N_0 - N_{om}) - \frac{1}{\tau_p}\right) - \Delta\omega - K_c\sqrt{\frac{S_{inj}}{S_0}}Sin\left(\phi_0\right) \qquad \text{(A 6)}$$

Taking (A 6) and manipulating

$$K_c\sqrt{\frac{S_{inj}}{S_0}}Sin(\phi_0)=\frac{\alpha}{2}\left(\Gamma g_0(N_0-N_{om})-\frac{1}{\tau_p}\right)-\Delta\omega \tag{A 7}$$

squaring both sides

$$K_c^{\,2}\frac{S_{inj}}{S_0}\sin^2\phi_0=\left[\left(\frac{\alpha\Gamma g_0(N_0-N_{om})}{2}-\frac{\alpha}{2\tau_p}\right)-\Delta\omega\right]^2 \tag{A 8}$$

Taking (A 5) and manipulating

$$2K_c\sqrt{S_{inj}S_0}Cos(\phi_0)=\frac{S_0}{\tau_p}-\Gamma g_0(N_0-N_{om})S_0-\Gamma\beta\frac{N_0}{\tau_n} \tag{A 9}$$

Multiply by $\frac{\sqrt{S_0}}{\sqrt{S_0}}=1$

$$2K_c\sqrt{S_{inj}S_0}\frac{\sqrt{S_0}}{\sqrt{S_0}}Cos(\phi_0)=\frac{S_0}{\tau_p}-\Gamma g_0(N_0-N_{om})S_0-\Gamma\beta\frac{N_0}{\tau_n} \tag{A 10}$$

$$\Rightarrow 2K_cS_0\frac{\sqrt{S_{inj}}}{\sqrt{S_0}}Cos(\phi_0)=\frac{S_0}{\tau_p}-\Gamma g_0(N_0-N_{om})S_0-\Gamma\beta\frac{N_0}{\tau_n} \tag{A 11}$$

Dividing across by S_0

$$2K_c\frac{\sqrt{S_{inj}}}{\sqrt{S_0}}Cos(\phi_0)=\frac{1}{\tau_p}-\Gamma g_0(N_0-N_{om})-\Gamma\beta\frac{N_0}{S_0\tau_n} \tag{A 12}$$

Squaring both sides

$$4K_c^{\,2}\frac{S_{inj}}{S_0}Cos^2\phi_0=\left[\frac{1}{\tau_p}-\Gamma g_0(N_0-N_{om})-\Gamma\beta\frac{N_0}{S_0\tau_n}\right]^2 \tag{A 13}$$

$$\Rightarrow K_c^{\,2}\frac{S_{inj}}{S_0}Cos^2\phi_0=\frac{1}{4}\left[\frac{1}{\tau_p}-\Gamma g_0(N_0-N_{om})-\Gamma\beta\frac{N_0}{S_0\tau_n}\right]^2 \tag{A 14}$$

Adding (A 14) and (A 8) gives

$$K_c^2 \frac{S_{inj}}{S_0} \sin^2 \phi_0 + K_c^2 \frac{S_{inj}}{S_0} Cos^2 \phi_0 =$$

$$\left[\left(\frac{\alpha \Gamma g_0 (N_0 - N_{om})}{2} - \frac{\alpha}{2\tau_p} \right) - \Delta\omega \right]^2 + \frac{1}{4} \left[\frac{1}{\tau_p} - \Gamma g_0 \left(N_0 - N_{om} \right) - \Gamma \beta \frac{N_0}{S_0 \tau_n} \right]^2 \quad \text{(A 15)}$$

$$K_c^2 \frac{S_{inj}}{S_0} \left(\sin^2 \phi_0 + \cos^2 \phi_0 \right) =$$

$$\left[\left(\frac{\alpha \Gamma g_0 (N_0 - N_{om})}{2} - \frac{\alpha}{2\tau_p} \right) - \Delta\omega \right]^2 + \frac{1}{4} \left[\frac{1}{\tau_p} - \Gamma g_0 \left(N_0 - N_{om} \right) - \Gamma \beta \frac{N_0}{S_0 \tau_n} \right]^2 \quad \text{(A 16)}$$

Using the relationship $\cos^2 \theta + \sin^2 \theta = 1$ gives

$$K_c^2 \frac{S_{inj}}{S_0} = \frac{1}{4} \left[\left(\Gamma g_0 (N_0 - N_{om}) - \frac{1}{\tau_p} \right) + \frac{\Gamma \beta N_0}{S_0 \tau_n} \right]^2 + \left[\frac{\alpha}{2} \left(\Gamma g_0 (N_0 - N_{om}) - \frac{1}{\tau_p} \right) - \Delta\omega \right]^2 \quad \text{(A 17)}$$

Manipulation of (A 4) yields an expression for S_0 as follows

$$\frac{\frac{I_0}{qV} - \frac{N_0}{\tau_n}}{g_0 \left(N_0 - N_{om} \right)} = S_0 \quad \text{(A 18)}$$

Substituting the expression for S_o from (A 18) into (A 17) yields after much manipulation, a quartic expression in N_o which can be solved very simply in Matlab The manipulation used to get from (A 17) to this quartic equation was carried out using the mathematics software, Derive 5 0, and is shown next

#1 $$\frac{NO^2\ OCF^2\ \tau p^2\ (SO^2\ g0^2\ \tau n^2\ (\alpha^2 + 1) + 2\ SO\ \beta\ g0\ \tau n + \beta^2) - 2\ NO\ OCF \sim}{}$$

$$\frac{SO\ \tau n\ \tau p\ (Nom\ OCF\ g0\ \tau p\ (SO\ g0\ \tau n + \beta) + Nth\ OCF\ SO\ \alpha^2\ g0^2\ \tau n\ \tau p + \sim}{}$$

$$\frac{SO\ g0\ \tau n\ (\alpha^2 + 2\ \alpha\ \Delta w\ \tau p + 1) + \beta) + Nom^2\ OCF^2\ SO^2\ g0^2\ \tau n^2\ \tau p^2 + \sim}{4\ SO^2\ \tau n^2\ \tau p^2}$$

$$\frac{2\ Nom\ OCF\ SO^2\ g0\ \tau n^2\ \tau p + SO^2\ \tau n^2\ (Nth^2\ OCF^2\ \alpha^2\ g0^2\ \tau p^2 + 2\ Nth\ OC\sim}{}$$

$$\frac{F\ \alpha\ g0\ \tau p\ (\alpha + 2\ \Delta w\ \tau p) + \alpha^2 + 4\ \alpha\ \Delta w\ \tau p + 4\ \Delta w^2\ \tau p^2 + 1)}{} =$$

$$\frac{Kc^2\ Sinj}{SO}$$

The line above is simply an expanded version of Equation A 17

#2 $$\frac{IO}{e\ V} - \frac{NO}{\tau n} - g0\ (NO - Nom)\ SO = 0$$

#3 $$\frac{IO}{V\ e} - \frac{NO}{\tau n} = SO\ g0\ (NO - Nom)$$

#4 $$\frac{IO\ \tau n - NO\ V\ e}{V\ e\ g0\ \tau n\ (NO - Nom)} = SO$$

The three lines above manipulate the carrier density equation A 4 to get it in terms of SO

#5 $$\frac{NO^2\ OCF^2\ \tau p^2\ (SO^2\ g0^2\ \tau n^2\ (\alpha^2 + 1) + 2\ SO\ \beta\ g0\ \tau n + \beta^2) - 2\ NO\ OCF \sim}{}$$

```
                                                                   2   2              ~
        S0 τn τp (Nom OCF g0 τp (S0 g0 τn + β) + Nth OCF S0 α   g0  τn τp +~
        ------------------------------------------------------------------~
                                                                          ~
                                                                          ~

                 2                           2    2    2    2    2    2   ~
         S0 g0 τn (α  + 2 α Δw τp + 1) + β) + Nom  OCF  S0  g0  τn  τp  + ~
        ------------------------------------------------------------------~
                                       2   2   2                          ~
                                   4 S0  τn  τp                           ~

                 2      2        2   2      2    2  2   2   2             ~
        2 Nom OCF S0  g0 τn  τp + S0  τn  (Nth  OCF  α  g0  τp  + 2 Nth OC~
        ------------------------------------------------------------------~
                                                                          ~
                                                                          ~

                                       2                   2   2
        F α g0 τp (α + 2 Δw τp) + α  + 4 α Δw τp + 4 Δw  τp  + 1)
        ----------------------------------------------------------  -



           2
         Kc  Sinj
        ---------- = 0
            S0
```

The Right hand side of #1 above is subtracted from both sides of the equation

```
              2   2    2    2    2   2    2                                ~
            I0  τn  (N0  OCF  g0  τp  (α  + 1) - 2 N0 OCF g0 τp (Nom OCF g0 τp ~
#6        --------------------------------------------------------------------~
                                                                          ~
                                                                          ~

                    2           2                        2    2    2    2     ~
        + Nth OCF α  g0 τp + α  + 2 α Δw τp + 1) + Nom  OCF  g0  τp  + 2 N~
        ------------------------------------------------------------------~
                                                                          ~
                                                                          ~

                          2    2  2    2    2                             ~
        om OCF g0 τp + Nth  OCF  α  g0  τp  + 2 Nth OCF α g0 τp (α + 2 Δw ~
        ------------------------------------------------------------------~
                                                                          ~
                                                                          ~

              2                   2   2                            2      ~
        τp) + α  + 4 α Δw τp + 4 Δw  τp  + 1) - 2 I0 V e τn (2 Kc  Sinj g0~
        ------------------------------------------------------------------~
                                                                          ~
                                                                          ~
```

$$\tau n \, \tau p^{2} \, (N0 - Nom) + N0 \, (N0^{2} \, OCF^{2} \, g0^{2} \, \tau p^{2} \, (\alpha^{2} - \beta + 1) + N0 \, OCF \, g0 \sim$$

$$\tau p \, (2 \, Nom \, OCF \, g0 \, \tau p \, (\beta - 1) - 2 \, Nth \, OCF \, \alpha^{2} \, g0 \, \tau p - 2 \, \alpha^{2} - 4 \, \alpha \, \Delta w \sim$$

$$\tau p + \beta - 2) + Nom^{2} \, OCF^{2} \, g0^{2} \, \tau p^{2} \, (1 - \beta) + Nom \, OCF \, g0 \, \tau p \, (2 - \beta) + \sim$$

$$4 \, \tau p^{2} \, (I0 \, \tau n - N0 \, V \, e)^{2}$$

$$Nth^{2} \, OCF^{2} \, \alpha^{2} \, g0^{2} \, \tau p^{2} + 2 \, Nth \, OCF \, \alpha \, g0 \, \tau p \, (\alpha + 2 \, \Delta w \, \tau p) + \alpha^{2} + 4 \, \alpha \sim$$

$$\Delta w \, \tau p + 4 \, \Delta w^{2} \, \tau p^{2} + 1)) + N0 \, V^{2} \, e^{2} \, (4 \, Kc \, Sinj \, g0 \, \tau n \, \tau p^{2} \, (N0 - Nom \sim$$

$$) + N0 \, (N0^{2} \, OCF^{2} \, g0^{2} \, \tau p^{2} \, (\alpha^{2} + \beta^{2} - 2 \, \beta + 1) - 2 \, N0 \, OCF \, g0 \, \tau p \, (Nom \sim$$

$$OCF \, g0 \, \tau p \, (\beta - 1)^{2} + Nth \, OCF \, \alpha^{2} \, g0 \, \tau p + \alpha^{2} + 2 \, \alpha \, \Delta w \, \tau p - \beta + 1) + \sim$$

$$Nom^{2} \, OCF^{2} \, g0^{2} \, \tau p^{2} \, (\beta^{2} - 2 \, \beta + 1) + 2 \, Nom \, OCF \, g0 \, \tau p \, (1 - \beta) + Nth^{2} \sim$$

$$OCF^{2} \, \alpha^{2} \, g0^{2} \, \tau p^{2} + 2 \, Nth \, OCF \, \alpha \, g0 \, \tau p \, (\alpha + 2 \, \Delta w \, \tau p) + \alpha^{2} + 4 \, \alpha \, \Delta w \, \tau \sim$$

$$p + 4 \, \Delta w^{2} \, \tau p^{2} + 1)) = 0$$

S0 is substituted in

#7 $I0^2\ \tau n^2\ (N0^2\ OCF^2\ g0^2\ \tau p^2\ (\alpha^2 + 1) - 2\ N0\ OCF\ g0\ \tau p\ (Nom\ OCF\ g0\ \tau p +$

$Nth\ OCF\ \alpha^2\ g0\ \tau p + \alpha^2 + 2\ \alpha\ \Delta w\ \tau p + 1) + Nom^2\ OCF^2\ g0^2\ \tau p^2 +$

$2\ Nom\ OCF\ g0\ \tau p + Nth^2\ OCF^2\ \alpha^2\ g0^2\ \tau p^2 + 2\ Nth\ OCF\ \alpha\ g0\ \tau p\ (\alpha +$

$2\ \Delta w\ \tau p) + \alpha^2 + 4\ \alpha\ \Delta w\ \tau p + 4\ \Delta w^2\ \tau p^2 + 1) -$

$2\ I0\ V\ e\ \tau n\ (2\ Kc^2\ Sinj\ g0\ \tau n\ \tau p^2\ (N0 - Nom) +$

$N0\ (N0^2\ OCF^2\ g0^2\ \tau p^2\ (\alpha^2 - \beta + 1) +$

$N0\ OCF\ g0\ \tau p\ (2\ Nom\ OCF\ g0\ \tau p\ (\beta - 1) - 2\ Nth\ OCF\ \alpha^2\ g0\ \tau p - 2\ \alpha^2$

$- 4\ \alpha\ \Delta w\ \tau p + \beta - 2) + Nom^2\ OCF^2\ g0^2\ \tau p^2\ (1 - \beta) +$

$Nom\ OCF\ g0\ \tau p\ (2 - \beta) + Nth^2\ OCF^2\ \alpha^2\ g0^2\ \tau p^2 +$

$2\ Nth\ OCF\ \alpha\ g0\ \tau p\ (\alpha + 2\ \Delta w\ \tau p) + \alpha^2 + 4\ \alpha\ \Delta w\ \tau p + 4\ \Delta w^2\ \tau p^2 + 1))$

$+ N0\ V^2\ e^2\ (4\ Kc^2\ Sinj\ g0\ \tau n\ \tau p^2\ (N0 - Nom) +$

$N0\ (N0^2\ OCF^2\ g0^2\ \tau p^2\ (\alpha^2 + \beta^2 - 2\ \beta + 1) -$

$2\ N0\ OCF\ g0\ \tau p\ (Nom\ OCF\ g0\ \tau p\ (\beta - 1)^2 + Nth\ OCF\ \alpha^2\ g0\ \tau p + \alpha^2 +$

$2\ \alpha\ \Delta w\ \tau p - \beta + 1) + Nom^2\ OCF^2\ g0^2\ \tau p^2\ (\beta^2 - 2\ \beta + 1) +$

$2\ Nom\ OCF\ g0\ \tau p\ (1 - \beta) + Nth^2\ OCF^2\ \alpha^2\ g0^2\ \tau p^2 +$

$2\ Nth\ OCF\ \alpha\ g0\ \tau p\ (\alpha + 2\ \Delta w\ \tau p) + \alpha^2 + 4\ \alpha\ \Delta w\ \tau p + 4\ \Delta w^2\ \tau p^2 + 1))$

$= 0$

Both sides are multiplied by the denominator to get the equation all on a single line

#8 $N0^4\ OCF^2\ V^2\ e^2\ g0^2\ \tau p^2\ (\alpha^2 + \beta^2 - 2\ \beta + 1) -$

$2\ N0^3\ OCF\ V\ e\ g0\ \tau p\ (I0 \cdot OCF \cdot g0 \cdot \tau n \cdot \tau p \cdot (\alpha^2 - \beta + 1) +$

$$V\,e\,(\mathrm{Nom}\,\mathrm{OCF}\,g0\,\tau p\,(\beta - 1)^2 + \mathrm{Nth}\,\mathrm{OCF}\,\alpha^2\,g0\,\tau p + \alpha^2 + 2\,\alpha\,\Delta w\,\tau p -$$

$$\beta + 1)) + N0^2\,(I0^2\,\mathrm{OCF}^2\,g0^2\,\tau n^2\,\tau p^2\,(\alpha^2 + 1) -$$

$$2\,I0\,\mathrm{OCF}\,V\,e\,g0\,\tau n\,\tau p\,(2\,\mathrm{Nom}\,\mathrm{OCF}\,g0\,\tau p\,(\beta - 1) -$$

$$2\,\mathrm{Nth}\,\mathrm{OCF}\,\alpha^2\,g0\,\tau p - 2\,\alpha^2 - 4\,\alpha\,\Delta w\,\tau p + \beta - 2) +$$

$$V^2\,e^2\,(4\,Kc^2\,\mathrm{Sinj}\,g0\,\tau n\,\tau p^2 + \mathrm{Nom}^2\,\mathrm{OCF}^2\,g0^2\,\tau p^2\,(\beta^2 - 2\,\beta + 1) +$$

$$2\,\mathrm{Nom}\,\mathrm{OCF}\,g0\,\tau p\,(1 - \beta) + \mathrm{Nth}^2\,\mathrm{OCF}^2\,\alpha^2\,g0^2\,\tau p^2 +$$

$$2\,\mathrm{Nth}\,\mathrm{OCF}\,\alpha\,g0\,\tau p\,(\alpha + 2\,\Delta w\,\tau p) + \alpha^2 + 4\,\alpha\,\Delta w\,\tau p + 4\,\Delta w^2\,\tau p^2 + 1))$$

$$-\,2\,N0\,\tau n\,(I0^2\,\mathrm{OCF}\,g0\,\tau n\,\tau p\,(\mathrm{Nom}\,\mathrm{OCF}\,g0\,\tau p + \mathrm{Nth}\,\mathrm{OCF}\,\alpha^2\,g0\,\tau p + \alpha^2$$

$$+\,2\,\alpha\,\Delta w\,\tau p + 1) + I0\,V\,e\,(2\,Kc^2\,\mathrm{Sinj}\,g0\,\tau n\,\tau p^2 +$$

$$\mathrm{Nom}^2\,\mathrm{OCF}^2\,g0^2\,\tau p^2\,(1 - \beta) + \mathrm{Nom}\,\mathrm{OCF}\,g0\,\tau p\,(2 - \beta) +$$

$$\mathrm{Nth}^2\,\mathrm{OCF}^2\,\alpha^2\,g0^2\,\tau p^2 + 2\,\mathrm{Nth}\,\mathrm{OCF}\,\alpha\,g0\,\tau p\,(\alpha + 2\,\Delta w\,\tau p) + \alpha^2 +$$

$$4\,\alpha\,\Delta w\,\tau p + 4\,\Delta w^2\,\tau p^2 + 1) + 2\,Kc^2\,\mathrm{Nom}\,\mathrm{Sinj}\,V^2\,e^2\,g0\,\tau p^2) +$$

$$I0^2\,\tau n^2\,(\mathrm{Nom}^2\,\mathrm{OCF}^2\,g0^2\,\tau p^2 + 2\,\mathrm{Nom}\,\mathrm{OCF}\,g0\,\tau p +$$

$$\mathrm{Nth}^2\,\mathrm{OCF}^2\,\alpha^2\,g0^2\,\tau p^2 + 2\,\mathrm{Nth}\,\mathrm{OCF}\,\alpha\,g0\,\tau p\,(\alpha + 2\,\Delta w\,\tau p) + \alpha^2 +$$

$$4\,\alpha\,\Delta w\,\tau p + 4\,\Delta w^2\,\tau p^2 + 1) + 4\,I0\,Kc^2\,\mathrm{Nom}\,\mathrm{Sinj}\,V\,e\,g0\,\tau n^2\,\tau p^2 = 0$$

Expanded to get in terms of N0 rather than I0

#9 $$I0^2\,\tau n^2\,(N0^2\,\mathrm{OCF}^2\,g0^2\,\tau p^2\,(\alpha^2 + 1) -$$

$$2\,N0\,\mathrm{OCF}\,g0\,\tau p\,(\mathrm{Nom}\,\mathrm{OCF}\,g0\,\tau p\,(\alpha^2 + 1) + \alpha^2 + 2\,\alpha\,\Delta w\,\tau p + 1) +$$

$$\mathrm{Nom}^2\,\mathrm{OCF}^2\,g0^2\,\tau p^2\,(\alpha^2 + 1) + 2\,\mathrm{Nom}\,\mathrm{OCF}\,g0\,\tau p\,(\alpha^2 + 2\,\alpha\,\Delta w\,\tau p + 1)$$

$$+\,\alpha^2 + 4\,\alpha\,\Delta w\,\tau p + 4\,\Delta w^2\,\tau p^2 + 1) -$$

$$2\,I0\,V\,e\,\tau n\,(2\,Kc^2\,\mathrm{Sinj}\,g0\,\tau n\,\tau p^2\,(N0 - \mathrm{Nom}) +$$

$$\mathrm{NO}\,(\mathrm{NO}^2\,\mathrm{OCF}^2\,g0^2\,\tau p^2\,(\alpha^2 - \beta + 1) -$$

$$\mathrm{NO}\,\mathrm{OCF}\,g0\,\tau p\,(2\,\mathrm{Nom}\,\mathrm{OCF}\,g0\,\tau p\,(\alpha^2 - \beta + 1) + 2\,\alpha^2 + 4\,\alpha\,\Delta w\,\tau p - \beta$$

$$+ 2) + \mathrm{Nom}^2\,\mathrm{OCF}^2\,g0^2\,\tau p^2\,(\alpha^2 - \beta + 1) + \mathrm{Nom}\,\mathrm{OCF}\,g0\,\tau p\,(2\,\alpha^2 +$$

$$4\,\alpha\,\Delta w\,\tau p - \beta + 2) + \alpha^2 + 4\,\alpha\,\Delta w\,\tau p + 4\,\Delta w^2\,\tau p^2 + 1)) +$$

$$\mathrm{NO}\,V^2\,e^2\,(4\,\mathrm{Kc}^2\,\mathrm{Sinj}\,g0\,\tau n\,\tau p^2\,(\mathrm{NO} - \mathrm{Nom}) + \mathrm{NO}^3\,\mathrm{OCF}^2\,g0^2\,\tau p^2\,(\alpha^2 +$$

$$\beta^2 - 2\,\beta + 1) - 2\,\mathrm{NO}^2\,\mathrm{OCF}\,g0\,\tau p\,(\mathrm{Nom}\,\mathrm{OCF}\,g0\,\tau p\,(\alpha^2 + (\beta - 1)^2) +$$

$$\alpha^2 + 2\,\alpha\,\Delta w\,\tau p - \beta + 1) + \mathrm{NO}\,(\mathrm{Nom}^2\,\mathrm{OCF}^2\,g0^2\,\tau p^2\,(\alpha^2 + \beta^2 - 2\,\beta +$$

$$1) + 2\,\mathrm{Nom}\,\mathrm{OCF}\,g0\,\tau p\,(\alpha^2 + 2\,\alpha\,\Delta w\,\tau p - \beta + 1) + \alpha^2 + 4\,\alpha\,\Delta w\,\tau p +$$

$$4\,\Delta w^2\,\tau p^2 + 1)) = 0$$

The term Nth is taken to be equal to Nom so it is Subbed in an simplified

#10 $$\mathrm{NO}^4\,\mathrm{OCF}^2\,V^2\,e^2\,g0^2\,\tau p^2\,(\alpha^2 + \beta^2 - 2\,\beta + 1) -$$

$$2\,\mathrm{NO}^3\,\mathrm{OCF}\,V\,e\,g0\,\tau p\,(\mathrm{I0}\,\mathrm{OCF}\,g0\,\tau n\,\tau p\,(\alpha^2 - \beta + 1) +$$

$$V\,e\,(\mathrm{Nom}\,\mathrm{OCF}\,g0\,\tau p\,(\alpha^2 + (\beta - 1)^2) + \alpha^2 + 2\,\alpha\,\Delta w\,\tau p - \beta + 1)) +$$

$$\mathrm{NO}^2\,(\mathrm{I0}^2\,\mathrm{OCF}^2\,g0^2\,\tau n^2\,\tau p^2\,(\alpha^2 + 1) +$$

$$2\,\mathrm{I0}\,\mathrm{OCF}\,V\,e\,g0\,\tau n\,\tau p\,(2\,\mathrm{Nom}\,\mathrm{OCF}\,g0\,\tau p\,(\alpha^2 - \beta + 1) + 2\,\alpha^2 +$$

$$4\,\alpha\,\Delta w\,\tau p - \beta + 2) + V^2\,e^2\,(4\,\mathrm{Kc}^2\,\mathrm{Sinj}\,g0\,\tau n\,\tau p^2 +$$

$$\mathrm{Nom}^2\,\mathrm{OCF}^2\,g0^2\,\tau p^2\,(\alpha^2 + \beta^2 - 2\,\beta + 1) + 2\,\mathrm{Nom}\,\mathrm{OCF}\,g0\,\tau p\,(\alpha^2 +$$

$$2\,\alpha\,\Delta w\,\tau p - \beta + 1) + \alpha^2 + 4\,\alpha\,\Delta w\,\tau p + 4\,\Delta w^2\,\tau p^2 + 1)) -$$

$$2\,\mathrm{NO}\,\tau n\,(\mathrm{I0}^2\,\mathrm{OCF}\,g0\,\tau n\,\tau p\,(\mathrm{Nom}\,\mathrm{OCF}\,g0\,\tau p\,(\alpha^2 + 1) + \alpha^2 + 2\,\alpha\,\Delta w\,\tau p$$

$$+ 1) + \mathrm{I0}\,V\,e\,(2\,\mathrm{Kc}^2\,\mathrm{Sinj}\,g0\,\tau n\,\tau p^2 + \mathrm{Nom}^2\,\mathrm{OCF}^2\,g0^2\,\tau p^2\,(\alpha^2 - \beta +$$

$$1) + Nom\ OCF\ g0\ \tau p\ (2\ \alpha^2 + 4\ \alpha\ \Delta w\ \tau p - \beta + 2) + \alpha^2 + 4\ \alpha\ \Delta w\ \tau p +$$

$$4\ \Delta w^2\ \tau p^2 + 1) + 2\ Kc^2\ Nom\ Sinj\ V^2\ e^2\ g0\ \tau p^2) +$$

$$I0^2\ \tau n^2\ (Nom^2\ OCF^2\ g0^2\ \tau p^2\ (\alpha^2 + 1) + 2\ Nom\ OCF\ g0\ \tau p\ (\alpha^2 +$$

$$2\ \alpha\ \Delta w\ \tau p + 1) + \alpha^2 + 4\ \alpha\ \Delta w\ \tau p + 4\ \Delta w^2\ \tau p^2 + 1) +$$

$$4\ I0\ Kc^2\ Nom\ Sinj\ V\ e\ g0\ \tau n^2\ \tau p^2 = 0$$

Expanding again in terms of N0 yields the quartic equation used in Matlab to get the steady state carrier density

In Matlab the value for the steady state carrier density is obtained using the above quartic equation as follows

```
%the coefficients for a quartic equation in N0 to determine the steady
 state carrier density
% a_var  4 + _var* 3 + _va_* ^2 + d_var*  e_var = 0
a_var = OCF^2*V^2*q^2*g0^2*tp^2*(alpha^2 + B^2 - 2*B + 1)
b_var = OCF*V*q*g0*tp*(I_bias*OCF*g0*tn*tp*(alpha^2 - B + 1)
      + V*q*(Nom*OCF*g0*tp*(alpha^2 + (B-1)^2) + alpha^2
        + alpha*2*tp*deltaw -B + 1))
c_var = (I_bias^2*OCF^2*g0^2*tn^2*tp^2*(alpha^2 + 1)
        + 2*I_bias*OCF*V*q*g0*tn*tp*(2*Nom*OCF*g0*tp*(alpha^2 - B + 1) + 2*alpha^2
        + 4*alpha*tp*deltaw - B + 2) + V^2*q^2*(4*Kc^2*Si*g0*tn*tp^2
        + Nom^2*OCF^2*g0^2*tp^2*(alpha^2 + B^2 - 2*B + 1)
        + 2*Nom*OCF*g0*tp*(alpha^2 + 2*alpha*tp*deltaw - B + 1) + alpha^2
        + 4*alpha*tp*deltaw + 4*deltaw^2*tp^2 + 1))
d_var = tn*(I_bias^2*OCF*g0*tn*tp*(Nom*OCF*g0*tp*(alpha^2 + 1) + alpha^2
        + 2*alpha*tp*deltaw + 1) + I_bias*V*q*(2*Kc^2*Si*g0*tn*tp^2
        + Nom^2*OCF^2*g0^2*tp^2*(alpha^2 - B + 1)
        + Nom*OCF*g0*tp*(2*alpha^2 + 4*alpha*tp*deltaw - B + 2)
        + alpha^2 + 4*alpha*tp*deltaw + 4*deltaw^2*tp^2 + 1)
        + 2*Kc^2*Nom*Si*V^2*q^2*g0*tp^2)
e_var = I_bias^2*tn^2*(Nom^2*OCF^2*g0^2*tp^2*(alpha^2 + 1)
        + 2*Nom*OCF*g0*tp*(alpha^2 + 2*alpha*tp*deltaw +1) + alpha^2
        + 4*alpha*tp*deltaw + 4*deltaw^2*tp^2 + 1)
      + 4*I_bias*Kc^2*Nom*Si*V*q*g0*tn^2*tp^2

%Get the roots of the above equation
N0_eq = [a_var -2*b_var c_var -2*d_var e_var]
N0_Roots = roots(N0_eq)
N0 = N0_Roots(4)     N0  the steady state carrier density
```

Once a value has been obtained for the steady state carrier density, all of the values in (A 18) are known and hence the steady state photon density can be calculated

Finally the steady state phase value can be obtained using either of the following manipulations of (A 5) and (A 6)

From (A 5)

$$2K_c\sqrt{S_{inj}S_0}Cos(\phi_0) = \frac{S_0}{\tau_p} - \Gamma g_0\left(N_0 - N_{om}\right)S_0 - \Gamma\beta\frac{N_0}{\tau_n} \qquad \text{(A 19)}$$

$$Cos(\phi_0) = \frac{\frac{S_0}{\tau_p} - \Gamma g_0 (N_0 - N_{om}) S_0 - \Gamma \beta \frac{N_0}{\tau_n}}{2K_c \sqrt{S_{inj} S_0}} \quad \text{(A 20)}$$

$$(\phi_0) = \cos^{-1}\left(\frac{\frac{S_0}{\tau_p} - \Gamma g_0 (N_0 - N_{om}) S_0 - \Gamma \beta \frac{N_0}{\tau_n}}{2K_c \sqrt{S_{inj} S_0}} \right) \quad \text{(A 21)}$$

From (A 6)

$$K_c \sqrt{\frac{S_{inj}}{S_0}} Sin(\phi_0) = \frac{\alpha}{2}\left(\Gamma g_0 (N_0 - N_{om}) - \frac{1}{\tau_p} \right) - \Delta\omega \quad \text{(A 22)}$$

$$Sin(\phi_0) = \left(\frac{\frac{\alpha}{2}\left(\Gamma g_0 (N_0 - N_{om}) - \frac{1}{\tau_p} \right) - \Delta\omega}{K_c \sqrt{\frac{S_{inj}}{S_0}}} \right) \quad \text{(A 23)}$$

$$(\phi_0) = \sin^{-1}\left(\frac{\frac{\alpha}{2}\left(\Gamma g_0 (N_0 - N_{om}) - \frac{1}{\tau_p} \right) - \Delta\omega}{K_c \sqrt{\frac{S_{inj}}{S_0}}} \right) \quad \text{(A 24)}$$

B.2 – Dynamic Solution

Again the rate equations for a single mode laser diode with injection are as follows By simply setting the external injection term S_{inj} to zero the equations revert back to the free running form

$$\frac{dN(t)}{dt} = \frac{I(t)}{qV} - \frac{N(t)}{\tau_n} - g_0\big(N(t) - N_{om}\big)S(t) \tag{A 25}$$

$$\frac{dS(t)}{dt} = \Gamma g_0\big(N(t) - N_{om}\big)S(t) - \frac{S(t)}{\tau_p} + \Gamma\beta\frac{N(t)}{\tau_n} + 2K_c\sqrt{S_{inj}S(t)}Cos\big(\phi(t)\big) \tag{A 26}$$

$$\frac{d\phi(t)}{dt} = \frac{\alpha}{2}\left(\Gamma g_0(N(t) - N_{om}) - \frac{1}{\tau_p}\right) - \Delta\omega - K_c\sqrt{\frac{S_{inj}}{S(t)}}Sin\big(\phi(t)\big) \tag{A 27}$$

The modulation response of the laser is obtained using small signal analysis in which the each of the time varying components are split into their dc and ac parts as follows

$$\begin{aligned}
I(t) &= I_0 + \Delta I \\
S(t) &= S_0 + \Delta S \\
N(t) &= N_0 + \Delta N \\
\phi(t) &= \phi_0 + \Delta\phi
\end{aligned} \tag{A 28}$$

Substituting the above into (A 25) the carrier density rate equation yields the following

$$\frac{d(N_0 + \Delta N)}{dt} = \frac{I_0 + \Delta I}{qV} - \frac{N_0 + \Delta N}{\tau_n} - g_0\big(N_0 + \Delta N - N_{om}\big)\big(S_0 + \Delta S\big) \tag{A 29}$$

$$\begin{aligned}
\frac{d(N_0)}{dt} + \frac{d(\Delta N)}{dt} = \frac{I_0}{qV} + \frac{\Delta I}{qV} - \frac{N_0}{\tau_n} - \frac{\Delta N}{\tau_n} - g_0\left(N_0 - N_{om}\right)S_0 \\
-g_0\left(N_0 - N_{om}\right)\Delta S - g_0\Delta N S_0 - g_0\Delta N\Delta S
\end{aligned} \tag{A 30}$$

The Steady state solution to the carrier density rate equation is

$$\frac{dN_0}{dt}=\frac{I_0}{qV}-\frac{N_0}{\tau_n}-g_0\left(N_0-N_{om}\right)S_0 \tag{A 31}$$

Removing the steady state solution and higher order products from (A 30) leaves

$$\frac{d(\Delta N)}{dt}=\frac{\Delta I}{qV}-\frac{\Delta N}{\tau_n}-g_0\left(N_0-N_{om}\right)\Delta S-g_0\Delta N S_0 \tag{A 32}$$

Each small signal term is actually an ac term and so could be written as $Xe^{j\omega_m t}$ where X is the time varying term Because every term in (A 32) has one of these ac terms we can divide across to eliminate them The differential of the small signal term however must still be considered as follows

$$\frac{d(N_1 e^{j\omega_m t})}{dt}=j\omega_m N_1 e^{j\omega t}$$

Applying this to (A 32) yields the following

$$j\omega\Delta N=\frac{\Delta I}{qV}-\frac{\Delta N}{\tau_n}-g_0\left(N_0-N_{om}\right)\Delta S-g_0\Delta N S_0 \tag{A 33}$$

It is desirable to remove the $g_0\left(N_0-N_{om}\right)$ terms so by getting the steady state version of (A 26) above and neglecting the spontaneous emission term we obtain the following relationship

$$g_0\left(N_0-N_{om}\right)=\frac{1}{\Gamma\tau_p}-2K_c\frac{\sqrt{S_{inj}S_0}}{\Gamma S_0}\cos\phi_0 \tag{A 34}$$

Substituting (A 34) into (A 33) yields

$$j\omega\Delta N=\frac{\Delta I}{qV}-\frac{\Delta N}{\tau_n}-\frac{\Delta S}{\Gamma\tau_p}+2K_c\frac{\sqrt{S_{inj}S_0}}{\Gamma S_0}\cos\phi_0\Delta S-g_0\Delta N S_0 \tag{A 35}$$

Similarly for the Photon Density Equation, substituting (A 28) into (A 26) yields

$$\frac{d(S_0+\Delta S)}{dt}=\Gamma g_0\left(N_0+\Delta N-N_{om}\right)(S_0+\Delta S)-\frac{(S_0+\Delta S)}{\tau_p}+\Gamma\beta\frac{N_0+\Delta N}{\tau_n}$$
$$+2K_c\sqrt{S_{inj}(S_0+\Delta S)}\cos\left(\phi_0+\Delta\phi\right) \qquad \text{(A 36)}$$

Expansion of the final term in (A 36) is done as follows

$$\cos\left(\phi_0+\Delta\phi\right)=\left(\cos\phi_0\cos\Delta\phi-\sin\phi_0\sin\Delta\phi\right)$$

Because the cos of a small term is approximately equal to one and the sin of a small value is approximately equal to that value

$$\left(\cos\phi_0\cos\Delta\phi-\sin\phi_0\sin\Delta\phi\right)\approx\left(\cos\phi_0\,1-\sin\phi_0\Delta\phi\right)$$

$$\Rightarrow 2K_c(\cos\phi_0-\sin\phi_0\Delta\phi)\sqrt{S_{inj}S_0+S_{inj}\Delta S}$$

Now

$$\sqrt{S_{inj}S_0+S_{inj}\Delta S}=\sqrt{S_{inj}S_0}\times\sqrt{1+\frac{S_{inj}\Delta S}{S_{inj}S_0}}\approx\sqrt{S_{inj}S_0}\times\left(1+\frac{\Delta S}{2S_0}\right)=\sqrt{S_{inj}S_0}+\left(\frac{\sqrt{S_{inj}S_0}\Delta S}{2S_0}\right)$$

Hence the final term in (A 36) can also be written as

$$\left(2K_c\cos\phi_0-2K_c\sin\phi_0\Delta\phi\right)\times\left[\sqrt{S_{inj}S_0}+\left(\frac{\sqrt{S_{inj}S_0}\Delta S}{2S_0}\right)\right]$$

which expands out as

$$2K_c\sqrt{S_{inj}S_0}\cos\phi_0 + 2K_c\frac{\sqrt{S_{inj}S_0}\Delta S}{2S_0}\cos\phi - 2K_c\sin\phi_0\Delta\phi\sqrt{S_{inj}S_0}$$
$$-2K_c\sin\phi_0\Delta\phi\frac{\sqrt{S_{inj}S_0}\Delta S}{2S_0}$$

The full expansion of (A 36) then is as follows

$$\begin{aligned}\frac{d(S_0)}{dt}+\frac{d(\Delta S)}{dt} &= \Gamma g_0\left(N_0-N_{om}\right)S_0+\Gamma g_0\left(N_0-N_{om}\right)\Delta S\\ &+\Gamma g_0\Delta N(S_0)+\Gamma g_0\Delta N\Delta S-\frac{S_0}{\tau_p}-\frac{\Delta S}{\tau_p}\\ &+\frac{\Gamma\beta N_0}{\tau_n}+\frac{\Gamma\beta\Delta N}{\tau_n}+2K_c\sqrt{S_{inj}S_0}\cos\phi_0+\frac{\sqrt{S_{inj}S_0}}{2S_0}\cos\phi_0\Delta S\\ &-2K_c\sin\phi_0\Delta\phi\sqrt{S_{inj}S_0}-2K_c\sin\phi_0\Delta\phi\frac{\sqrt{S_{inj}S_0}}{2S_0}\Delta S\end{aligned} \qquad \text{(A 37)}$$

The steady state response is as follows

$$\frac{dS_0}{dt}=\Gamma g_0\left(N_0-N_{om}\right)S_0-\frac{S_0}{\tau_p}+\Gamma\beta\frac{N_0}{\tau_n}+2K_c\sqrt{S_{inj}S_0}\cos\left(\phi_0\right) \qquad \text{(A 38)}$$

Removing the steady state solution and higher order products from (A 37) leaves

$$\begin{aligned}\frac{d(\Delta S)}{dt} &= \Gamma g_0\left(N_0-N_{om}\right)\Delta S+\Gamma g_0\Delta NS_0-\frac{\Delta S}{\tau_p}+\frac{\Gamma\beta\Delta N}{\tau_n}\\ &+2K_c\frac{\sqrt{S_{inj}S_0}}{2S_0}\cos\phi_0\Delta S-2K_c\sin\phi_0\sqrt{S_{inj}S_0}\Delta\phi\end{aligned} \qquad \text{(A 39)}$$

Because we are operating well above threshold the spontaneous emission term can be assumed to be negligible

$$\begin{aligned}\frac{d(\Delta S)}{dt} &= \Gamma g_0\left(N_0-N_{om}\right)\Delta S+\Gamma g_0\Delta NS_0-\frac{\Delta S}{\tau_p}+2K_c\frac{\sqrt{S_{inj}S_0}}{2S_0}\cos\phi_0\Delta S\\ &-2K_c\sin\phi_0\sqrt{S_{inj}S_0}\Delta\phi\end{aligned} \qquad \text{(A 40)}$$

Again to remove the $g_0(N_0 - N_{om})$ term we use the following relationship

$$g_0(N_0 - N_{om}) = \frac{1}{\Gamma\tau_p} - 2K_c\frac{\sqrt{S_{inj}S_0}}{\Gamma S_0}\cos\phi_0$$

Substituting it into (A 40) yields

$$\begin{aligned} j\omega\Delta S &= \left(\frac{1}{\Gamma\tau_p} - 2K_c\frac{\sqrt{S_{inj}S_0}}{\Gamma S_0}\cos\phi_0\right)\Gamma\Delta S + \Gamma g_0\Delta NS_0 - \frac{\Delta S}{\tau_p} \\ &+2K_c\frac{\sqrt{S_{inj}S_0}}{2S_0}\cos\phi_0\Delta S - 2K_c\sin\phi_0\sqrt{S_{inj}S_0}\Delta\phi \end{aligned} \qquad \text{(A 41)}$$

$$\begin{aligned} j\omega\Delta S &= \frac{\Delta S}{\tau_p} - 2K_c\frac{\sqrt{S_{inj}S_0}}{S_0}\cos\phi_0\Delta S + \Gamma g_0\Delta NS_0 - \frac{\Delta S}{\tau_p} \\ &+2K_c\frac{\sqrt{S_{inj}S_0}}{2S_0}\cos\phi_0\Delta S - 2K_c\sin\phi_0\sqrt{S_{inj}S_0}\Delta\phi \end{aligned} \qquad \text{(A 42)}$$

Cancelling the $\frac{\Delta S}{\tau_p}$ terms and multiplying $-2K_c\frac{\sqrt{S_{inj}S_0}}{S_0}$ by $\frac{2}{2}$ yields

$$\begin{aligned} j\omega\Delta S &= -4K_c\frac{\sqrt{S_{inj}S_0}}{2S_0}\cos\phi_0\Delta S + \Gamma g_0\Delta NS_0 + 2K_c\frac{\sqrt{S_{inj}S_0}}{2S_0}\cos\phi_0\Delta S \\ &-2K_c\sin\phi_0\sqrt{S_{inj}S_0}\Delta\phi \end{aligned} \qquad \text{(A 43)}$$

Addition yields

$$j\omega\Delta S = \Gamma g_0\Delta NS_0 - 2K_c\frac{\sqrt{S_{inj}S_0}}{2S_0}\cos\phi_0\Delta S - 2K_c\sin\phi_0\sqrt{S_{inj}S_0}\Delta\phi \qquad \text{(A 44)}$$

And again for the Phase Equation, substituting (A 28) into (A 27) yields

$$\frac{d(\phi_0+\Delta\phi)}{dt}=\frac{\alpha}{2}\left(\Gamma g_0(N_0+\Delta N-N_{om})-\frac{1}{\tau_p}\right)-\Delta\omega-K_c\sqrt{\frac{S_{inj}}{S_0+\Delta S}}Sin(\phi_0+\Delta\phi) \quad \text{(A 45)}$$

Expanding the final term in a similar manner to that described for the Photon Density equation

$$\sin(\phi_0+\Delta\phi)=(\sin\phi_0\cos\Delta\phi+\cos\phi_0\sin\Delta\phi)\approx(\sin\phi_0\ 1+\cos\phi_0\Delta\phi)$$

$$\sqrt{\frac{S_{inj}}{S_0+\Delta S}}=\frac{\sqrt{S_{inj}}}{\sqrt{S_0+\Delta S}}=S_{inj}^{\frac{1}{2}}\times(S_0+\Delta S)^{-\frac{1}{2}}=S_{inj}^{\frac{1}{2}}\times\left(S_0^{-\frac{1}{2}}-\frac{1}{2}S_0^{-\frac{3}{2}}\Delta S\right)$$
$$=\sqrt{S_{inj}}\times\left(\frac{1}{\sqrt{S_0}}-\frac{1}{2\sqrt{S_0^3}}\Delta S\right)=\left(\frac{\sqrt{S_{inj}}}{\sqrt{S_0}}-\frac{\sqrt{S_{inj}}}{2\sqrt{S_0^3}}\Delta S\right)$$

Hence the final term in (A 45) can also be written as

$$(-K_c\sin\phi_0-K_c\cos\phi_0\Delta\phi)\left(\frac{\sqrt{S_{inj}}}{\sqrt{S_0}}-\frac{\sqrt{S_{inj}}}{2\sqrt{S_0^3}}\Delta S\right)$$

which expands out to

$$-K_c\sin\phi_0\frac{\sqrt{S_{inj}}}{\sqrt{S_0}}+K_c\sin\phi_0\frac{\sqrt{S_{inj}}}{2\sqrt{S_0^3}}\Delta S-K_c\cos\phi_0\Delta\phi\frac{\sqrt{S_{inj}}}{\sqrt{S_0}}+K_c\cos\phi_0\Delta\phi\frac{\sqrt{S_{inj}}}{2\sqrt{S_0^3}}\Delta S$$

The full expansion of (A 45) then is

$$\begin{aligned}\frac{d(\phi_0)}{dt}+\frac{d(\Delta\phi)}{dt}&=\frac{\alpha}{2}(\Gamma g_0(N_0-N_{om}))+\frac{\alpha}{2}(\Gamma g_0(\Delta N))-\frac{\alpha}{2\tau_p}-\Delta\omega\\&\quad-K_c\sin\phi_0\frac{\sqrt{S_{inj}}}{\sqrt{S_0}}+K_c\sin\phi_0\frac{\sqrt{S_{inj}}}{2\sqrt{S_0^3}}\Delta S \qquad \text{(A 46)}\\&\quad-K_c\cos\phi_0\Delta\phi\frac{\sqrt{S_{inj}}}{\sqrt{S_0}}+K_c\cos\phi_0\Delta\phi\frac{\sqrt{S_{inj}}}{2\sqrt{S_0^3}}\Delta S\end{aligned}$$

The steady state solution is

$$\frac{d(\phi_0)}{dt} = \frac{\alpha}{2}\left(\Gamma g_0(N_0 - N_{om}) - \frac{1}{\tau_p}\right) - \Delta\omega - K_c\sqrt{\frac{S_{inj}}{S_0}}Sin(\phi_0) \tag{A 47}$$

and removing this and higher order products yields

$$\frac{d(\Delta\phi)}{dt} = \frac{\alpha}{2}\left(\Gamma g_0(\Delta N)\right) + K_c\frac{\sqrt{S_{inj}}}{\sqrt{4S_0^3}}\sin\phi_0\Delta S - K_c\frac{\sqrt{S_{inj}}}{\sqrt{S_0}}\cos\phi_0\Delta\phi \tag{A 48}$$

So this leaves us with three linearised equations

$$j\omega\Delta N = \frac{\Delta I}{qV} - \frac{\Delta N}{\tau_n} - \frac{\Delta S}{\Gamma\tau_p} + 2K_c\frac{\sqrt{S_{inj}S_0}}{\Gamma S_0}\cos\phi_0\Delta S - g_0\Delta NS_0 \tag{A 49}$$

$$j\omega\Delta S = \Gamma g_0\Delta NS_0 - 2K_c\frac{\sqrt{S_{inj}S_0}}{2S_0}\cos\phi_0\Delta S - 2K_c\sin\phi_0\sqrt{S_{inj}S_0}\Delta\phi \tag{A 50}$$

$$j\omega\Delta\phi = \frac{\alpha}{2}\Gamma g_0\Delta N + K_c\frac{\sqrt{S_{inj}}}{\sqrt{4S_0^3}}\sin\phi_0\Delta S - K_c\frac{\sqrt{S_{inj}}}{\sqrt{S_0}}\cos\phi_0\Delta\phi \tag{A 51}$$

Letting $X = 2K_c\sqrt{S_{inj}S_0}\cos\phi_0$ and $Y = K_c\sqrt{\frac{S_{inj}}{S_0}}\sin\phi_0$

$$j\omega\Delta N = \frac{\Delta I}{qV} - \frac{\Delta N}{\tau_n} - \frac{\Delta S}{\Gamma\tau_p} + \frac{X}{\Gamma S_0}\Delta S - g_0\Delta NS_0 \tag{A 52}$$

$$j\omega\Delta S = \Gamma g_0S_0\Delta N - \frac{X}{2S_0}\Delta S - 2K_c\sqrt{S_{inj}S_0}\sin\phi_0\Delta\phi$$

$$\Rightarrow j\omega\Delta S = \Gamma g_0S_0\Delta N - \frac{X}{2S_0}\Delta S - 2K_c\sqrt{S_{inj}S_0}\frac{\sqrt{S_0}}{\sqrt{S_0}}\sin\phi_0\Delta\phi$$

$$\Rightarrow j\omega\Delta S = \Gamma g_0 S_0 \Delta N - \frac{X}{2S_0}\Delta S - 2K_c S_0\sqrt{\frac{S_{inj}}{S_0}}\sin\phi_0\Delta\phi$$

$$\Rightarrow j\omega\Delta S = \Gamma g_0 S_0 \Delta N - \frac{X}{2S_0}\Delta S - 2S_0 Y\Delta\phi \tag{A 53}$$

$$j\omega\Delta\phi = \frac{\alpha}{2}\Gamma g_0\Delta N + K_c\frac{\sqrt{S_{inj}}}{\sqrt{4S_0^3}}\sin\phi_0\Delta S - K_c\frac{\sqrt{S_{inj}}}{\sqrt{S_0}}\cos\phi_0\Delta\phi$$

$$\Rightarrow j\omega\Delta\phi = \frac{\alpha}{2}\Gamma g_0\Delta N + K_c\frac{\sqrt{S_{inj}}}{\sqrt{S_0}}\frac{\sqrt{1}}{\sqrt{4S_0^2}}\sin\phi_0\Delta S - K_c\frac{\sqrt{S_{inj}}}{\sqrt{S_0}}\frac{\sqrt{S_0}}{\sqrt{S_0}}\cos\phi_0\Delta\phi$$

$$\Rightarrow j\omega\Delta\phi = \frac{\alpha}{2}\Gamma g_0\Delta N + \frac{K_c}{2S_0}\frac{\sqrt{S_{inj}}}{\sqrt{S_0}}\sin\phi_0\Delta S - K_c\frac{\sqrt{S_{inj}S_0}}{S_0}\cos\phi_0\Delta\phi$$

$$\Rightarrow j\omega\Delta\phi = \frac{\alpha}{2}\Gamma g_0\Delta N + \frac{1}{2S_0}K_c\frac{\sqrt{S_{inj}}}{\sqrt{S_0}}\sin\phi_0\Delta S - 2K_c\frac{\sqrt{S_{inj}S_0}}{2S_0}\cos\phi_0\Delta\phi$$

$$\Rightarrow j\omega\Delta\phi = \frac{\alpha}{2}\Gamma g_0\Delta N + \frac{Y}{2S_0}\Delta S - \frac{X}{2S_0}\Delta\phi \tag{A 54}$$

Tidying (A 52), (A 53), and (A 54)

$$\left[j\omega + \frac{1}{\tau_n} + g_0 S_0\right]\Delta N + \left[\frac{1}{\Gamma\tau_p} - \frac{X}{\Gamma S_0}\right]\Delta S + [0]\Delta\phi = \frac{\Delta I}{qV} \tag{A 55}$$

$$[-\Gamma g_0 S_0]\Delta N + \left[j\omega + \frac{X}{2S_0}\right]\Delta S + [2S_0 Y]\Delta\phi = 0 \tag{A 56}$$

$$\left[-\frac{\alpha}{2}\Gamma g_0\right]\Delta N + \left[-\frac{Y}{2S_0}\right]\Delta S + \left[j\omega + \frac{X}{2S_0}\right]\Delta\phi = 0 \tag{A 57}$$

Putting into matrix form yields the following

$$\begin{pmatrix} j\omega + a_{11} & a_{12} & a_{13} \\ a_{21} & j\omega + a_{22} & a_{23} \\ a_{31} & a_{32} & j\omega + a_{33} \end{pmatrix}\begin{pmatrix} \Delta N \\ \Delta S \\ \Delta\phi \end{pmatrix} = \begin{pmatrix} \Delta I/qV \\ 0 \\ 0 \end{pmatrix} \qquad \text{(A 58)}$$

where

$$a_{11} = \frac{1}{\tau_n} + g_0 S_0 \quad a_{12} = \frac{1}{\Gamma\tau_p} - \frac{X}{\Gamma S_0} \quad a_{13} = 0$$

$$a_{21} = -\Gamma g_0 S_0 \qquad a_{22} = \frac{X}{2S_0} \qquad a_{23} = 2S_0 Y$$

$$a_{31} = -\frac{\alpha}{2}\Gamma g_0 \qquad a_{32} = \frac{-Y}{2S_0} \qquad a_{33} = \frac{X}{2S_0}$$

and

$$X = 2K_c\sqrt{S_{inj}S_0}\,Cos(\phi_0)$$

$$Y = K_c\sqrt{\frac{S_{inj}}{S_0}}\,Sin(\phi_0)$$

The frequency response is $\frac{\Delta S}{\Delta I}$ and to obtain this we must eliminate the other two time varying components from the set of equations We will use (A 56) as our main equation and remove the two terms for it by substitution

So to remove $\Delta\phi$ we take (A 57)

$$\left[j\omega + \frac{X}{2S_0}\right]\Delta\phi = \left[\frac{Y}{2S_0}\right]\Delta S + \left[\frac{\alpha}{2}\Gamma g_0\right]\Delta N$$

Letting $O = j\omega + \dfrac{X}{2S_0}$ we obtain

$$\Delta\phi = \frac{\dfrac{Y\Delta S}{2S_0} + \dfrac{\alpha}{2}\Gamma g_0 \Delta N}{O} \qquad \text{(A 59)}$$

Subbing (A 59) into (A 56) then gives

$$[-\Gamma g_0 S_0]\Delta N+\left[j\omega+\frac{X}{2S_0}\right]\Delta S+[2S_0 Y]\left[\frac{\frac{Y\Delta S}{2S_0}+\frac{\alpha}{2}\Gamma g_0\Delta N}{O}\right]=0 \qquad \text{(A 60)}$$

$$[-\Gamma g_0 S_0]\Delta N+\left[j\omega+\frac{X}{2S_0}\right]\Delta S+\left[\frac{Y^2\Delta S}{O}+\frac{S_0 Y\alpha\Gamma g_0\Delta N}{O}\right]=0 \qquad \text{(A 61)}$$

Regrouping terms yields an expression in ΔS without $\Delta\phi$

$$\left[-\Gamma g_0 S_0+\frac{S_0 Y\alpha\Gamma g_0}{O}\right]\Delta N+\left[j\omega+\frac{X}{2S_0}+\frac{Y^2}{O}\right]\Delta S=0 \qquad \text{(A 62)}$$

We now need to eliminate ΔN from (A 62) so taking (A 55)

$$\left[j\omega+\frac{1}{\tau_n}+g_0 S_0\right]\Delta N=\frac{\Delta I}{qV}+\left[-\frac{1}{\Gamma\tau_p}+\frac{X}{\Gamma S_0}\right]\Delta S \qquad \text{(A 63)}$$

Letting $P=j\omega+\frac{1}{\tau_n}+g_0 S_0$ we obtain

$$\Delta N=\frac{\frac{\Delta I}{qV}+\left[-\frac{1}{\Gamma\tau_p}+\frac{X}{\Gamma S_0}\right]\Delta S}{P} \qquad \text{(A 64)}$$

Substituting (A 64) into (A 62) yields

$$\left[-\Gamma g_0 S_0+\frac{S_0 Y\alpha\Gamma g_0}{O}\right]\left[\frac{\frac{\Delta I}{qV}+-\frac{\Delta S}{\Gamma\tau_p}+\frac{X\Delta S}{\Gamma S_0}}{P}\right]+\left[j\omega+\frac{X}{2S_0}+\frac{Y^2}{O}\right]\Delta S=0 \qquad \text{(A 65)}$$

Multiplying out

$$0=\left[j\omega+\frac{X}{2S_0}+\frac{Y^2}{O}\right]\Delta S+\frac{S_0 Y\alpha\Gamma g_0\Delta I}{PqVO}-\frac{S_0 Y\alpha g_0\Delta S}{OP\tau_p}+\frac{Y\alpha g_0 X\Delta S}{PO}$$
$$-\frac{\Delta I\Gamma g_0 S_0}{PqV}+\frac{\Delta S g_0 S_0}{P\tau_p}-\frac{X\Delta S g_0}{P} \qquad \text{(A 66)}$$

Grouping all ΔS terms

$$\left[j\omega+\frac{X}{2S_0}+\frac{Y^2}{O}-\frac{S_0 Y\alpha g_0\Delta S}{OP\tau_p}+\frac{Y\alpha g_0 X\Delta S}{PO}+\frac{\Delta S g_0 S_0}{P\tau_p}-\frac{X\Delta S g_0}{P}\right]\Delta S=$$
$$\frac{\Delta I\Gamma g_0 S_0}{PqV}-\frac{S_0 Y\alpha\Gamma g_0\Delta I}{PqVO} \qquad \text{(A 67)}$$

Dividing both sides by the coefficient of ΔS yields

$$\Delta S=\frac{\dfrac{\Delta I\Gamma g_0 S_0}{PqV}-\dfrac{S_0 Y\alpha\Gamma g_0\Delta I}{PqVO}}{j\omega+\dfrac{X}{2S_0}+\dfrac{Y^2}{O}-\dfrac{S_0 Y\alpha g_0\Delta S}{OP\tau_p}+\dfrac{Y\alpha g_0 X\Delta S}{PO}+\dfrac{\Delta S g_0 S_0}{P\tau_p}-\dfrac{X\Delta S g_0}{P}} \qquad \text{(A 68)}$$

Factoring the numerator leaves the equation used in the Matlab code to plot the modulation response

$$\Delta S=\frac{\dfrac{\Delta I\Gamma g_0 S_0}{PqV}\left[1-\dfrac{Y\alpha}{O}\right]}{j\omega+\dfrac{X}{2S_0}+\dfrac{Y^2}{O}-\dfrac{S_0 Y\alpha g_0\Delta S}{OP\tau_p}+\dfrac{Y\alpha g_0 X\Delta S}{PO}+\dfrac{\Delta S g_0 S_0}{P\tau_p}-\dfrac{X\Delta S g_0}{P}} \qquad \text{(A 69)}$$

We know S_0 and ϕ_0 from the Steady state solution ω is the frequency range over which we wish to plot the modulation response ΔI is simply the amplitude of the modulating sine wave and every other term is a constant Hence we can plot the modulation response

Appendix C – Matlab Code

This appendix gives the code used in to simulate the experimental work performed There are three main programs and four functions which are called from these The first program characterises the laser by plotting the PI curve and the modulation response The second program, lets you modulate the laser with simple tones The third program expands on the second one by allowing data to be modulated onto each of the carriers

C.1 – Rate_Equations.m

```
clear


g0 = 1e-12
Nom = 1 4e23
V = 11e-17
tp = 2e-11
tn =  3e-9
OCF = 0 35
B = 0 0000
q = 1 6e-19
alpha = 6 8
Ac = 8e-3
I_bias = 70e-3
deltaf = -11e9
deltaw = 2*pi*deltaf
Si = 0e20
Kc = 2 5e11
if Si == 0
   deltaw = 0
end

h = 6 625e-34
R = 0 32
c = 3e8,
n = 3 63
Ar =  03e-12
lamda = 1550e-9
```

```
f_laser = c/lamda % frequency of the output light
responsivity = 0.6  % Responsivity of the detector

fm1 = 1e7              % Data Modulation rate
bitperiod = 1/fm1  %Data bit period Period = 1/r
numcarriers = 5          % number of subcarriers

%%%%%%%%%%%%%%%%%%%%%%%%%%%%%%%%%%%%%%%%%%%%%%%%%%%%%%%%%%%%%%%%%%%%%%%%%%%%%%%%%
% THIS SECTION GETS THE STEADY STATE VALUES FOR PHASE PHOTON DENSITY AND CARRIER % % %
% DENSITY IT THEN USES THEM TO WORK OUT THE SMALL SIGNAL RESPONSE OF THE LASER WHICH %
  IT PLOTS  THIS IS THE MODULATION RESPONSE
%%%%%%%%%%%%%%%%%%%%%%%%%%%%%%%%%%%%%%%%%%%%%%%%%%%%%%%%%%%%%%%%%%%%%%%%%%%%%%%%%
  the coefficient  for a quartic equation   N0 to determine the steady
% state carrier density
% a_var*X^4 + b_var X^3 + c_var X^2 + d_var*X + e_var = 0
%%%%%%%%%%%%%%%%%%%%%%%%%%%%%%%%%%%%%%%%%%%%%%%%%%%%%%%%%%%%%%%%%%%%%%%%%%%%%%%%%
a_var = OCF^2*V^2*q^2*g0^2*tp^2*(alpha^2 + B^2 - 2*B + 1)
b_var = OCF*V*q*g0*tp*(I_bias*OCF*g0*tn*tp*(alpha^2 - B + 1)
      + V*q*(Nom*OCF*g0*tp*(alpha^2 + (B-1)^2) + alpha^2
        + alpha*2*tp*deltaw -B + 1))
c_var = (I_bias^2*OCF^2*g0^2*tn^2*tp^2*(alpha^2 + 1)
        + 2*I_bias*OCF*V*q*g0*tn*tp*(2*Nom*OCF*g0*tp*(alpha^2 - B + 1) + 2*alpha^2
        + 4*alpha*tp*deltaw - B + 2) + V^2*q^2*(4*Kc^2*Si*g0*tn*tp^2
        + Nom^2*OCF^2*g0^2*tp^2*(alpha^2 + B^2 - 2*B + 1)
        + 2*Nom*OCF*g0*tp*(alpha^2 + 2*alpha*tp*deltaw - B + 1) + alpha^2
        + 4*alpha*tp*deltaw + 4*deltaw^2*tp^2 + 1))
d_var = tn*(I_bias^2*OCF*g0*tn*tp*(Nom*OCF*g0*tp*(alpha^2 + 1) + alpha^2
        + 2*alpha*tp*deltaw + 1) + I_bias*V*q*(2*Kc^2*Si*g0*tn*tp^2
        + Nom^2*OCF^2*g0^2*tp^2*(alpha^2 - B + 1)
        + Nom*OCF*g0*tp*(2*alpha^2 + 4*alpha*tp*deltaw - B + 2)
        + alpha^2 + 4*alpha*tp*deltaw + 4*deltaw^2*tp^2 + 1)
        + 2*Kc^2*Nom*Si*V^2*q^2*g0*tp^2)
e_var = I_bias^2*tn^2*(Nom^2*OCF^2*g0^2*tp^2*(alpha^2 + 1)
        + 2*Nom*OCF*g0*tp*(alpha^2 + 2*alpha*tp*deltaw +1) + alpha^2
        + 4*alpha*tp*deltaw + 4*deltaw^2*tp^2 + 1)
      + 4*I_bias*Kc^2*Nom*Si*V*q*g0*tn^2*tp^2

 Get the roots of the above equation
N0_eq = [a_var -2*b_var c_var -2*d_var e_var]
N0_Roots = roots(N0_eq)
N0 = N0_Roots(4)     %N0  the steady state carrier density

  S0 the steady state photon density  s worked out by rearranging the
% carrier density rate equation
S0 = ((I_bias*tn)- (N0*q*V))/(tn*g0*(N0-Nom)*q*V)

  Injection Ratio
ratio = Si/S0

% Output power is worked out using Photon Density
%Pout = S0 *c /(2*OCF n1*h*f_laser Ar*(1-R)
```

```
%To work out steady state phase Phi0 both equations give same answer but different sign
if Si == 0
   Phi0 = 0
else
  %Phi0 = acos(((S /tp) - (OCF*g0 (N -Nom)*S0))/ (2*Kc*sqrt(S0*Si)))
Phi0 = asin((-alpha/(2*tp) - (deltaw) +
 ((alpha/2)*OCF*g0*(N0-Nom)))/(Kc*sqrt(Si/S0)))
end

% Set up frequency points to plot the frequency response
freq = [10e6 10e6 20e9]
wm = 2*pi*freq

% Using the small signal derivation of the rate equations to get the modulation
%response Modulation response is given by change in photon number with respect to
%change in input current Input current is ac and change in photon density is s1

X = 2*Kc*sqrt(Si*S0)*cos(Phi0)
Y = Kc*sqrt(Si/S0)*sin(Phi0)
O = (j *wm + (X/(2*S0)))
P = (j *wm + (1/tn) + g0*S0)

if Si == 0
s1 = -((Ac/(q*V))*g0*S0*OCF) /(wm ^2 - (wm) *(i*g0*S0) + (wm) *(i/(tn)) - (g0*S0)/tp)
end
if Si > 0
   s1 = (((OCF*Ac*g0*S0) /(P *q*V)) *(1 - Y*alpha /O))       %two line
       /((j *wm)    +    (X/(2*S0))    +    (Y^2 /O)    +    (X*Y*alpha*g0 /(P *O))    -
(S0*Y*alpha*g0 /(P *O*tp)) - (X*g0 /P) + (g0*S0 /(P *tp)))
end

   %% Plot Resonance Freq %%
figure(2)
s = abs(s1)                     %Get absolute values of the change in photon density
logs = 20*log10(s/Ac)      %Get the log of change in photon number with respect to change
                             %in input current (the modulation response)
norms = logs - logs(1)      %Normalise it to the first value
plot(freq *1e-9,norms)       %and plot
axis([0 20 -30 40])
title('Modulation Response')
xlabel('Frequency (GHz)')  ylabel('Response (dB)')
hold on  grid


for I_bias = [0  0001 100e-3] %Each current value to take the power at
a_var = OCF^2*V^2*q^2*g0^2*tp^2*(alpha^2 + B^2 - 2*B + 1)
b_var = OCF*V*q*g0*tp*(I_bias*OCF*g0*tn*tp*(alpha^2 - B + 1)
```

```
      + V*q*(Nom*OCF*g0*tp*(alpha^2 + (B-1)^2) + alpha^2
        + alpha*2*tp*deltaw -B + 1))
c_var = (I_bias^2*OCF^2*g0^2*tn^2*tp^2*(alpha^2 + 1)
        + 2*I_bias*OCF*V*q*g0*tn*tp*(2*Nom*OCF*g0*tp*(alpha^2 - B + 1) + 2*alpha^2
        + 4*alpha*tp*deltaw - B + 2) + V^2*q^2*(4*Kc^2*Si*g0*tn*tp^2
        + Nom^2*OCF^2*g0^2*tp^2*(alpha^2 + B^2 - 2*B + 1)
        + 2*Nom*OCF*g0*tp*(alpha^2 + 2*alpha*tp*deltaw - B + 1) + alpha^2
        + 4*alpha*tp*deltaw + 4*deltaw^2*tp^2 + 1))
d_var = tn*(I_bias^2*OCF*g0*tn*tp*(Nom*OCF*g0*tp*(alpha^2 + 1) + alpha^2
        + 2*alpha*tp*deltaw + 1) + I_bias*V*q*(2*Kc^2*Si*g0*tn*tp^2
        + Nom^2*OCF^2*g0^2*tp^2*(alpha^2 - B + 1)
        + Nom*OCF*g0*tp*(2*alpha^2 + 4*alpha*tp*deltaw - B + 2)
        + alpha^2 + 4*alpha*tp*deltaw + 4*deltaw^2*tp^2 + 1)
        + 2*Kc^2*Nom*Si*V^2*q^2*g0*tp^2)
e_var = I_bias^2*tn^2*(Nom^2*OCF^2*g0^2*tp^2*(alpha^2 + 1)
        + 2*Nom*OCF*g0*tp*(alpha^2 + 2*alpha*tp*deltaw +1) + alpha^2
        + 4*alpha*tp*deltaw + 4*deltaw^2*tp^2 + 1)
      + 4*I_bias*Kc^2*Nom*Si*V*q*g0*tn^2*tp^2

 Get the roots of the above equation
N0_eq = [a_var -2*b_var c_var -2*d_var e_var]
N0_Roots = roots(N0_eq)
N0 = N0_Roots(4)      N0, the steady state carrier density

% S0 the steady state photon density is worked out by rearranging the
% carrier density rate equation
S0 = ((I_bias*tn)- (N0*q*V))/(tn*g0*(N0-Nom)*q*V)

%From the photon density the power can be obtained and then plotted
Pout = S0 *c /(2*OCF*n)*h*f_laser*Ar*(1-R)
   figure(100)
   plot(I_bias*1000,Pout*1000 '[illegible]')
   axis([0 100 0 16])
   title('Plot of [illegible] vs I Curve')
   xlabel('[illegible] Current (mA)') ylabel('[illegible] Power (mW)')
   grid  hold on
end
```

C.2 – Tones.m

```
% This Program models the transmission of a multi tone signal over
% optical fibre. The laser is modelled by solving the laser rate
% equations using the ODE-45 function in Matlab

clear all    % clears all variables

tic          % starts timer Program usually takes about 5-6 mins to run

% defines the global variables
global Ar Nom OCF tp B q V numcarriers spacing moding_sig input_signal
sample_number span fc1 Ac I_bias tn g0 x fm1 TFinal Fs numbits f Tex bitsequence Ts
filtered_moding_sig bitvalue deltaw alpha Si Kc f

%% Laser Parameters %%
g0 = 1e-12          % Differential gain coeff
Nom = 1 4e23        % Transparency density (m-3)
V = 11e-17          % Volume of active layer
tp = 2e-11          % Photon lifetime (s)
tn =  3e-9          % Carrier recombination lifetime
OCF = 0 35          % Mode confinement factor
B = 0 0000          % Beta, spontaneous emission ratio
q = 1 6e-19         % Charge of electron
alpha = 6 8         % Linewidth Enhancement Factor
Ac = 20e-3          % Amplitude of carriers
I_bias = 70e-3      % Bias Current
deltaf = -11e9      % Frequency Detuning
deltaw = 2*pi*deltaf    % Convert frequency to radians
Si = 0          % Injection level (Injected photon density)
Kc = 2 5e11         % Injected light coupling coefficient
if Si == 0
   deltaw = 0       % if injection is off then no detuning in the phase equation
end

h = 6 625e-34       % Planck constant
R = 0 32            % Reflectivity of cavity
c = 3e8             % speed of light
n = 3 63            % Refractive index
Ar =  03e-12        % Area of the active region
lamda = 1550e-9     % wavelength of output light
f_laser = c/lamda   % frequency of the output light
responsivity = 0 6  % Responsivity of the detector

% THIS SECTION GETS THE STEADY STATE VALUES FOR PHASE PHOTON DENSITY, CARRIER DENSITY
% IT THEN USES THEM TO WORK OUT THE SMALL SIGNAL RESPONSE OF THE LASER WHICH IT PLOTS
% THIS IS THE MODULATION RESPONSE
```

```
% the coefficients for a quartic equation in N0 to determine the steady
% state carrier density
% a_var*N0^4 - 2*b_var*N0^3 + c_var*N0^2 - 2*d_var*N0 + e_var = 0
% [illegible]
a_var = OCF^2*V^2*q^2*g0^2*tp^2*(alpha^2 + B^2 - 2*B + 1)
b_var = OCF*V*q*g0*tp*(I_bias*OCF*g0*tn*tp*(alpha^2 - B + 1)
   + V*q*(Nom*OCF*g0*tp*(alpha^2 + (B-1)^2) + alpha^2
   + alpha*2*tp*deltaw -B + 1))
c_var = (I_bias^2*OCF^2*g0^2*tn^2*tp^2*(alpha^2 + 1)
   + 2*I_bias*OCF*V*q*g0*tn*tp*(2*Nom*OCF*g0*tp*(alpha^2 - B + 1) + 2*alpha^2
   + 4*alpha*tp*deltaw - B + 2) + V^2*q^2*(4*Kc^2*Si*g0*tn*tp^2
   + Nom^2*OCF^2*g0^2*tp^2*(alpha^2 + B^2 - 2*B + 1)
   + 2*Nom*OCF*g0*tp*(alpha^2 + 2*alpha*tp*deltaw - B + 1) + alpha^2
   + 4*alpha*tp*deltaw + 4*deltaw^2*tp^2 + 1))
d_var = tn*(I_bias^2*OCF*g0*tn*tp*(Nom*OCF*g0*tp*(alpha^2 + 1) + alpha^2
   + 2*alpha*tp*deltaw + 1) + I_bias*V*q*(2*Kc^2*Si*g0*tn*tp^2
   + Nom^2*OCF^2*g0^2*tp^2*(alpha^2 - B + 1)
   + Nom*OCF*g0*tp*(2*alpha^2 + 4*alpha*tp*deltaw - B + 2)
   + alpha^2 + 4*alpha*tp*deltaw + 4*deltaw^2*tp^2 + 1)
   + 2*Kc^2*Nom*Si*V^2*q^2*g0*tp^2)
e_var = I_bias^2*tn^2*(Nom^2*OCF^2*g0^2*tp^2*(alpha^2 + 1)
   + 2*Nom*OCF*g0*tp*(alpha^2 + 2*alpha*tp*deltaw +1) + alpha^2
   + 4*alpha*tp*deltaw + 4*deltaw^2*tp^2 + 1)
   + 4*I_bias*Kc^2*Nom*Si*V*q*g0*tn^2*tp^2

% for the roots of the above equation
N0_eq = [a_var -2*b_var c_var -2*d_var e_var]
N0_Roots = roots(N0_eq)
N0 = N0_Roots(4)    %N0  the steady state carrier density

% S0 the steady state photon density is worked out by rearranging the
% carrier density rate equation
S0 = ((I_bias*tn)- (N0*q*V))/(tn*g0*(N0-Nom)*q*V)

% Injection Ratio
ratio = Si/S0

% To work out steady state phase  Phi0  both equations give same answer
% but different sign
if Si == 0
   Phi0 = 0
else
% Phi0 = acos(((B)/tp) - (OCF*g0*(N0-Nom)*S0))/(2*Kc*sqrt(S0*Si));
Phi0 = asin((-alpha/(2*tp)-(deltaw)+((alpha/2)*OCF*g0*(N0-Nom)))/(Kc*sqrt(Si/S0)))
end

% Variable coefficients
numcarriers = 2

fc1 = 6e9               % Frequency of 1st carrier (Hz)
spacing = 0             % Carrier spacing        defined later on
```

```
span = 150e6

Fs = 20e9
TFinal = 200e-9
Ts = 1/Fs

spacing = 0

if numcarriers > 1
   spacing = span /(numcarriers - 1)
end

input_signal = 0


tspan = [0 Ts TFinal]
y0 = [Phi0 S0 N0]
[t,p] = ode45(              ,tspan,y0)


for x = 1 1 numcarriers
    fc(x) = fc1 + ((x-1) * spacing)
    carrier_sig( ,x) = (Ac * cos(2*pi*fc(x)*t))
    input_signal = input_signal + carrier_sig( , x)
end

I = I_bias + input_signal

Phi = p( ,1)
S = p( ,2)
N = p( ,3)

Pout = S *c/(2*OCF*n)*h*f_laser*Ar*(1-R)


i = 32768*16
g = i/2
freq = Fs*(0 g)/i
```

```
FPin = fft(I,1)                    Getting fast Fourier transform of input signal
Fin = FPin * conj(FPin) / 1        remove ... components
Fin(1) = Fin(2)                    % Removes the DC value
LFin = 20*log10(Fin)

FPout = fft(Pout,1)                Fourier transform of output signal
Fout = FPout * conj(FPout) / 1
Fout(1) = Fout(2)
LFout = 20*log10(Fout)

%     Display output
% Plot the input and output ... time and frequency domain

figure
subplot(2,1,1)
plot(t,I)
ylabel('...')
grid
subplot(2,1,2)
plot(t,Pout)
ylabel('Output Power'), xlabel('Time')
grid

figure
subplot(2,1,1)
plot(freq *1e-9,LFin(1:g+1))
ylabel('...')
grid
subplot(2,1,2)
plot(freq *1e-9,LFout(1:g+1))
ylabel('O/P ...'), xlabel('Frequency (GHz)')
grid
```

C.3 – Tones_Ode45.m

```
function dp = Tones_ODE45(t,p)

global Ar Nom OCF tp B q V numcarriers spacing moding_sig input_signal
sample_number
   span fc1 Ac I_bias tn g0 x fm1 TFinal Fs numbits f Tex bitsequence Ts
filtered_moding_sig
    bitvalue deltaw alpha Si Kc f

   input_signal = 0
for x = 1:numcarriers
    fc(x) = fc1 + ((x-1) * spacing)
    carrier_sig(:,x) = (Ac * cos(2*pi*fc(x)*t))
    input_signal = input_signal + carrier_sig(:,x)
end

I = I_bias + input_signal

Phi = p(1)
S = p(2)
N = p(3)

dp = [(alpha/2)*(OCF*g0*(N-Nom) - 1/tp) - (deltaw) - (Kc*sqrt(Si/S)*sin(Phi))
      ((OCF*g0*(N-Nom) - (1/tp))*S) + ((OCF*B*N)/tn) + ((2*Kc)*sqrt(Si*S)*cos(Phi))
      (I/(q*V)) - (g0*(N-Nom)*S) - (N/tn)]
```

C.4 – Data.m

```
clear all

tic

global Ar Nom OCF tp B q V numcarriers spacing moding_sig input_signal
sample_number
   span fcl Ac I_bias tn g0 x fml TFinal Fs numbits f Tex bitsequence Ts
filtered_moding_sig
    bitvalue deltaw alpha Si Kc f

g0 = 1e-12
Nom = 1 4e23
V = 11e-17
tp = 2e-11
tn =  3e-9
OCF = 0 35
B = 0 0000
q = 1 6e-19
alpha = 6 8
Ac = 8e-3
I_bias = 70e-3
deltaf = -11e9
deltaw = 2*pi*deltaf
Si = 35e20
Kc = 2 5e11
if Si == 0
   deltaw  =  0
end

h = 6 625e-34
R = 0 32
c = 3e8
n = 3 63
Ar =  03e-12
lamda = 1550e-9
f_laser = c/lamda,
responsivity = 0 6,

fml = 1e7
```

```
bitperiod = 1/fm1   Data bit period Period = /f
numcarriers = 5            mber of subcarriers

%%%%%%%%%%%%%%%%%%%%%%%%%%%%%%%%%%%%%%%%%%%%%%%%%%%%%%%%%%%%%%%%%%%%%%%%%%%%%%%%
%
  THIS SECTION GETS THE STEADY STATE VALUE FOR PHASE PHOTON DENSITY AND CARRIER
DENSITY
% IT  ALSO USES THEM TO WORK OUT THE SMALL SIGNAL RESPONSE OF THE LASER AND IT PLOTS
% THIS IS THE MODULATION RESPONSE
%%%%%%%%%%%%%%%%%%%%%%%%%%%%%%%%%%%%%%%%%%%%%%%%%%%%%%%%%%%%%%%%%%%%%%%%%%%%%%%%
  the coefficients for a quartic equation in N0 to determine the stead
% state carrier density
  a_var  ^4 + b_var  3 + c_var  2 + d_var  - e_var = 0
%%%%%%%%%%%%%%%%%%%%%%%%%%%%%%%%%%%%%%%%%%%%%%%%%%%%%%%%%%%%%%%%%%%%%%%%%%%%%%%%
a_var = OCF^2*V^2*q^2*g0^2*tp^2*(alpha^2 + B^2 - 2*B + 1)
b_var = OCF*V*q*g0*tp*(I_bias*OCF*g0*tn*tp*(alpha^2 - B + 1)
      + V*q*(Nom*OCF*g0*tp*(alpha^2 + (B-1)^2) + alpha^2
        + alpha*2*tp*deltaw -B + 1))
c_var = (I_bias^2*OCF^2*g0^2*tn^2*tp^2*(alpha^2 + 1)
        + 2*I_bias*OCF*V*q*g0*tn*tp*(2*Nom*OCF*g0*tp*(alpha^2 - B + 1) + 2*alpha^2
        + 4*alpha*tp*deltaw - B + 2) + V^2*q^2*(4*Kc^2*Si*g0*tn*tp^2
        + Nom^2*OCF^2*g0^2*tp^2*(alpha^2 + B^2 - 2*B + 1)
        + 2*Nom*OCF*g0*tp*(alpha^2 + 2*alpha*tp*deltaw - B + 1) + alpha^2
        + 4*alpha*tp*deltaw + 4*deltaw^2*tp^2 + 1))
d_var = tn*(I_bias^2*OCF*g0*tn*tp*(Nom*OCF*g0*tp*(alpha^2 + 1) + alpha^2
        + 2*alpha*tp*deltaw + 1) + I_bias*V*q*(2*Kc^2*Si*g0*tn*tp^2
        + Nom^2*OCF^2*g0^2*tp^2*(alpha^2 - B + 1)
        + Nom*OCF*g0*tp*(2*alpha^2 + 4*alpha*tp*deltaw - B + 2)
        + alpha^2 + 4*alpha*tp*deltaw + 4*deltaw^2*tp^2 + 1)
        + 2*Kc^2*Nom*Si*V^2*q^2*g0*tp^2)
e_var = I_bias^2*tn^2*(Nom^2*OCF^2*g0^2*tp^2*(alpha^2 + 1)
        + 2*Nom*OCF*g0*tp*(alpha^2 + 2*alpha*tp*deltaw +1) + alpha^2
        + 4*alpha*tp*deltaw + 4*deltaw^2*tp^2 + 1)
      + 4*I_bias*Kc^2*Nom*Si*V*q*g0*tn^2*tp^2

%Get the roots of the above equation
N0_eq = [a_var -2*b_var c_var -2*d_var e_var]
N0_Roots = roots(N0_eq)
N0 = N0_Roots(4)     N0  the steady state carrier density

% S0 the steady state photon density is worked out by rearraging the
  carrier density rate equation
S0 = ((I_bias*tn)- (N0*q*V))/(tn*g0*(N0-Nom)*q*V)

% Injection Ratio
ratio = Si/S0

  Output power is worked out using Photon Density
%Pout    S0 *c /(2*OCF*n)*h*f_laser*Ar*(1-R)

% To work out steady state phase Phi0, both equations give same answer but
```

```
% different sign
if S1 == 0
   Phi0 = 0
else
  Phi0 = acos(((S0/tp) - (OCF g0*(N0-Nom) S0))/(2 Kc*sqrt(S0*S1)))
Phi0     =     asin((-alpha/(2*tp)     -     (deltaw)     +     ((alpha/2)*OCF*g0*(N0-
Nom)))/(Kc*sqrt(S1/S0)))
end

  Set up frequency points to plot the frequency response
freq = [10e6 10e6 20e9]
wm = 2*pi*freq

  Using the small signal derivation of the rate equations to get the modulation
%response Modulation response is given as change in photon number with respect to
change in input current input current is Ac and change in photon density is s1

X = 2*Kc*sqrt(S1*S0)*cos(Phi0)
Y = Kc*sqrt(S1/S0)*sin(Phi0)
O = (j *wm + (X/(2*S0)))
P = (j *wm + (1/tn) + g0*S0)

if S1 == 0
s1 = -((Ac/(q*V))*g0*S0*OCF) /(wm ^2 - (wm) *(i*g0*S0) + (wm) *(i/(tn)) - (g0*S0)/tp)
end
if S1 > 0
   s1 = (((OCF*Ac*g0*S0) /(P *q*V)) *(1 - Y*alpha /O))      %top line
      /((j *wm)     +     (X/(2*S0))     +     (Y^2 /O)     +     (X*Y*alpha*g0 /(P *O))     -
(S0*Y*alpha*g0 /(P *O*tp))
      - (X*g0 /P) + (g0*S0 /(P *tp)))
end

   %%%% Plot Resonance Frequency %%%%
figure(2)
s = abs(s1)                  Get absolute values of the change in photon density
logs = 20*log10(s/Ac)    %Get the log of change in photon number with respect to chang
                              in input current (The modulation response)
norms = logs - logs(1)     %Normalise it to the first value
plot(freq *1e-9,norms)      and plot
axis([0 20 -30 40])
title('Modulation Response')
xlabel('Frequency (GHz)')  ylabel('Response (dB)')
hold on  grid

  THIS SECTION IS WHERE THE DATA CHANNELS WHICH MODULATE THE LASER ARE SET UP AND
% MODULATED ONTO THE LASER
```

```
%  %
% Ire data patturn c n be fi ed
   %

bitsequence = [0 1 1 0 0 1 0 0 1 0 0 0 1 1 1 0 1 1 0 1 0 1 1 1 0 1 0 1 1 1 0 0
               0 1 1 0 0 1 0 0 1 0 0 0 1 1 1 0 1 1 0 1 0 1 1 1 0 1 0 1 1 1 0 0
               0 1 1 0 0 1 0 0 1 0 0 0 1 1 1 0 1 1 0 1 0 1 1 1 0 1 0 1 1 1 0 0
               0 1 1 0 0 1 0 0 1 0 0 0 1 1 1 0 1 1 0 1 0 1 1 1 0 1 0 1 1 1 0 0
               0 1 1 0 0 1 0 0 1 0 0 0 1 1 1 0 1 1 0 1 0 1 1 1 0 1 0 1 1 1 0 0]
numbits = size(bitsequence,2)
%  %
                  c   andom

% %
%nu bits = 32
%bitsequence = Random_Bit_Allocator(fm1, numbits, numcarriers)

fc1 = 6 01e9         Frequency of 1st carr er (Hz)
spacing = 0        % Ca  ier spacing      defined late  on
span = 80e6          Freq Span occupied by combined carriers

Fs = 20e9          % Sampling Frequency
TFinal = numbits*bitperiod  % time for full pattern
Ts = 1/Fs          % time interval

channel_BW =  7*fm1    Filter Bandwid

  loise parameters
k = 1 3807e-23
T = 295
M = 1
F = 1
Imp = 50
numsamples = (TFinal*Fs) + 1

% Set up thermal noise
thermal_noise = (sqrt((4*k*T*channel_BW)/Imp)*randn(numsamples 1))

  Set up carrier spacing depending on number of carriers and the total span they
o cupy
if numcarriers > 1
   spacing = span /(numcarriers - 1)  % spacing between successive carriers in System
end

  Puts the bit pattern into bitslots for modulation
moding_sig = 0
moding_sig = Bit_Allocator(bitsequence  fm1, numcarriers, Fs, 0, TFinal)

% Sets up a low pass filter and filters the data pattern
[b,a] = cheby2(5,70, 003),
for x = 1 1 numcarriers
```

```
filtered_moding_sig(x  ) = filtfilt(b  a  moding_sig(x, ))   ~ Filtration of Received
Current signal
end

Calls the rear r Da a_ODE'5 and begins taking time varying values of photon dens
ca rier densi y and phase using the value of I below as the modulating current

tspan = [0 Ts TFinal]          time span with sampling freq
y0 = [Phi0 S0 N0]   initial cond (steady state values from above
[t p] = ode45( D  _OF 4  ,tspan,y0)

input_signal = 0
for x = 1 1 numcarriers
fc(x) = fc1 + ((x-1) * spacing)      sets the carrier freque cies
~ This line upconverts the data signal to the carrier frequency
moded_sig( ,x) = modulate((filtered_moding_sig(x, ) ),fc(x),Fs, am')
% moded_sig( ,x) = (filtered_moding_sig(    ')')  * (Ac * cos(2*pi*fc(x)*t)')
  Both lines above do exact same - multipl ing data by a sine wave gives ASK
% This models the electrical power coupler for each carrier
input_signal = input_signal + moded_sig( ,x)
end

  Bias the
I = I_bias + input_signal

 Pa e alues o Phase Photon Density and Carrier Density b  fr  OD  5
Phi = p( ,1)
S = p( ,2)
N = p( ,3)

~ Convert Photon Density to Optical Power in watts
Pout = S *c/(2*OCF*n)*h*f_laser*Ar*(1-R)

  Next 3 lines mod l the variable attenuator used in the BER measurements
atten = 25
ratio = 10^(atten/10)
Pout = Pout/ratio

Power = 10*log10(mean(Pout*1000))     Average Power

 Calculate Frequency Response

  No of  oints for Fourier Transform

i = 32768*16,
g = i/2
freq = Fs*(0 g)/i    Important half of 'F' a s
```

```
FPin = fft(I,i)                      %Getting fourier transform of input signal
Fin = FPin * conj(FPin) / i    % Remove complex components
Fin(1) = Fin(2)                      %Removes the DC value
LFin = 20*log10(Fin)              %Puts into log scale

FPout = fft(Pout,i)                  %Fourier transform of output signal
Fout = FPout * conj(FPout) / i
Fout(1) = Fout(2)
LFout = 20*log10(Fout)

% Used to work out the ACLR, not a very good method as only works with 5 carriers
% from ... to ...
lower = mean(LFout(154920 157040))
upper = mean(LFout(160170 162290))
undesired = max(lower,upper)
desired = mean(LFout(157540 159660))
ACLR = undesired-desired

% Display output
% Plot the input to and output from the laser in the time and frequency domains

figure
subplot(2,1,1)
plot(t,I)
ylabel(  ip t   )
grid
subplot(2,1,2)
plot(t Pout)
ylabel( Output Power )  xlabel( Time')
grid

figure
subplot(2,1,1)
plot(freq *1e-9,LFin(1 g+1))
ylabel( I/P Freq Resp (dB) )
grid
subplot(2,1,2)
plot(freq *1e-9,LFout(1 g+1))
ylabel( O/P Freq Resp (dB)')  xlabel('Frequency (GHz)')
grid

%This line models the detector

I_received = (Pout  * responsivity)


for x = 1 1 numcarriers                    %For each Carrier
downconvert = demod(I_received, fc(x)  Fs,  a ')    Downconvert back to baseband
 These 3 lines simply remove some spurious values introduced in the downconversion
```

```
downconvert(2) = downconvert(3)
downconvert(1) = downconvert(2)
downconvert(length(downconvert)-2) = downconvert(length(downconvert)-3)
downconvert(length(downconvert)-1) = downconvert(length(downconvert)-2)
downconvert(length(downconvert)) = downconvert(length(downconvert)-1)

[b,a] = cheby2(5,70, 003)
Rx_Data_signal = filtfilt(b, a, downconvert)+thermal_noise


mod_interest = filtered_moding_sig(x, )
figure
subplot (2 1,1)
plot(t, mod_interest)
ylabel(            )
grid
subplot (2,1,2)
plot(t, Rx_Data_signal)
ylabel(            )
xlabel(            )
grid


interval = bitperiod * Fs
figure
title (     )
ylabel(     )
xlabel(     )
hold on

x_values = -0 5 1/interval 1 5

HI_values = 0
LO_values = 0

for z = 1 numbits
   y_lower = (z-1) * interval + 1
   y_higher = y_lower + interval

  start = y_lower - (interval/2)
  finish = y_higher + (interval/2),
  if  (start > 0) & (finish < (numbits * interval))
    plot (x_values, Rx_Data_signal(start finish))
```

```
    end

Mean_Rx_Signal = mean(Rx_Data_signal)    Gets an average to work out the
                                         threshold for the BER

      If the average bit value is greater than the threshold then take it as a 1
    % Otherwise take it as a zero
     if  (mean(Rx_Data_signal(y_lower y_higher)) > Mean_Rx_Signal)
          bit value is HI
       HI_values = [HI_values Rx_Data_signal(y_lower +
               floor(interval/4) y_higher - floor(interval/4))]
     else
          bit value is LO
       LO_values = [LO_values Rx_Data_signal(y_lower +
               floor(interval/4) y_higher - floor(interval/4))]
     end
end
    Works out means and standard deviations to work out threshold value
     according to the equation
     mean_HI = mean(HI_values)
     mean_LO = mean(LO_values)
     sigma_HI = std(HI_values)
    sigma_LO = std(LO_values)

    Thresh_Lev = ((sigma_LO*mean_HI) + (sigma_HI*mean_LO))/(sigma_LO + sigma_HI)

    % Uses the equation for BER to work it out for each channel
    BER(x) = 0 25 * (erfc((mean_HI - Thresh_Lev)/(sqrt(2)*sigma_HI)) +
       erfc((Thresh_Lev - mean_LO)/(sqrt(2)*sigma_LO)))
end
BER   Prints out the Bit Error Rates

toc   Ends the timer
```

C.5 – Data_Ode45.m

```
function dp = Data_ODE45(t,p)

global Ar Nom OCF tp B q V numcarriers spacing moding_sig input_signal
sample_number span fc1 Ac I_bias tn g0 x fm1 TFinal Fs numbits f Tex bitsequence
Ts filtered_moding_sig bitvalue deltaw alpha Si Kc f

input_signal = 0
sample_number = floor(t/Ts)
bitvalue = filtered_moding_sig(  sample_number+1)

for x = 1 1 numcarriers
    fc(x) = fc1 + ((x-1) * spacing)
    carrier_value( ,x) = ((bitvalue(x  )) * (Ac * cos(2*pi*fc(x)*t)))
    input_signal = input_signal + carrier_value( ,x)
end

I = I_bias + input_signal

Phi = p(1)
S = p(2)
N = p(3)

dp = [(alpha/2)*(OCF*g0*(N-Nom) - 1/tp) - (deltaw) - (Kc*sqrt(Si/S)*sin(Phi))
      ((OCF*g0*(N-Nom) - (1/tp))*S) + ((OCF*B*N)/tn) + ((2*Kc)*sqrt(Si*S)*cos(Phi))
      (I/(q*V)) - (g0*(N-Nom)*S) - (N/tn)]
```

C.6 – Random_Bit_Allocator.m

```
function [x,n] = Random_Bit_Allocator(mod_rate  num_bits, num_channels)

bitperiod = (1/mod_rate)

x = rand(num_bits  num_channels)

for j = 1 1 num_channels
    for i = 1 1 num_bits-1
      if x(i, j) >= 0 5
         x(i, j) = 1
      else
         x(i, j) = 0
       end
   end
    x(num_bits, j) = 0
end
x  =  x'
```

C.7 – Bit_Allocator

```
function [x,n] = Bit_Allocator(bitseq  mod_rate, num_channels, F_sample
   t_init, t_final)

bitperiod = (1/mod_rate)

numbits = size(bitseq,2)

nmin = t_init*F_sample
nmax = t_final*F_sample

x = zeros(num_channels, nmax+1)

n_lower = 0
n_higher = 0
bit_interval = floor(bitperiod*F_sample)

for i = 1 1 num_channels
    for j = 1 1 numbits
        bitvalue = bitseq(i, j)
        n_lower = nmin + (j-1)*bit_interval
        n_higher = n_lower + bit_interval
        x(i, n_lower+1 n_higher+1) = bitvalue
    end
end
```

Appendix D – List of Publications

Refereed Journals

1) F Smyth, L P Barry, "Overcoming Distortion Limitations in Hybrid Radio/Photonic Systems for the Distribution of WCDMA Signals", *Springer Journal of Electrical Engineering*, Volume 85, Issue 4, September 2003

2) F Smyth, L P Barry, "Overcoming Laser Diode Nonlinearity Issues in Multi-Channel Radio over Fiber Systems", *Elsevier Optics Communications,* Volume 231/1-6, pp 217-225

Refereed Conferences

1) F Smyth, L P Barry, "Effects of Laser Diode Nonlinearities in Hybrid Fiber/Radio Systems", *SPIE's Regional Meeting on Optoelectronics, Photonics and Imaging, Opto-Ireland*, September 2002